$NO_{X\ (x=1,2)}$ reactivity of Co(II) and Ni(II) complexes with N-donor and O-donor ligands

A Dissertation submitted to the
Indian Institute of Technology Guwahati as
Partial fulfillment for the Degree of
Doctor of Philosophy in Chemistry

Submitted by

Somnath Ghosh
(Roll No. 11612210)

Supervisor

Prof. Biplab Mondal

Department of Chemistry
Indian Institute of Technology Guwahati

October, 2016

Dedicated to My Family

(Baba, Maa, Mita and my little Drishti)

Statement

I hereby declare that this thesis entitled "**$NO_{X\ (x=1,2)}$ reactivity of Co(II) and Ni(II) complexes with N-donor and O-donor ligands** " is the outcome of research work carried out by me under the supervision of Prof. Biplab Mondal, in the Department of Chemistry, Indian Institute of Technology Guwahati, India.

In keeping with the general practice of reporting scientific observations, due acknowledgements have been made whenever work described here has been based on the findings of other investigators.

October, 2016 **Somnath Ghosh**

भारतीय प्रौद्योगिकी संस्थान गुवाहाटी
INDIAN INSTITUTE OF TECHNOLOGY GUWAHATI
North Guwahati, Assam – 781039, India

Prof. Biplab Mondal
Department of Chemistry

Phone : + 91-361-258-2317
Fax: + 91-361-258-2349
E-mail: biplab@iitg.ernet.in

Certificate

This is to certify that **Mr. Somnath Ghosh** has been working under my supervision since July, 2011 as a regular Ph. D. student in the Department of Chemistry, Indian Institute of Technology Guwahati. I am forwarding his thesis entitled "**$NO_{X\ (x=1,2)}$ reactivity of Co(II) and Ni(II) complexes with N-donor and O-donor ligands**" being submitted for the Ph. D. degree.

I certify that he has fulfilled all the requirements according to the rules of this Institute regarding the investigations embodied in his thesis and this work has not been submitted elsewhere for a degree.

October, 2016 **Biplab Mondal**

Acknowledgement

I would like to thank all those people who made my thesis possible:

First and foremost I would like to express my sincerest gratitude to my supervisor, Prof. Biplab Mondal, for his whole hearted co-operation and guidance in carrying out my research works meant for doctoral degree of mine. Whenever I have got myself trapped in a fix with acute problems, being cordial enough, he has intellectually solved the same then and there. His inspiration towards accomplishment of works which remains engraved in my mind as a part and parcel of it will stand me in good stead for my whole life. I have technical knowhow of scientific works only from him. I shall be ever-grateful to him.

I am also thankful to my doctoral committee Chairman and members Prof. Gopal Das, Prof. Parameswar Krishnan Iyer and Dr. A. S. Achalkumar for their encouragement, insightful comments and suggestions.

I would like to acknowledge my gratitude to the Central Instrument Facility (CIF) and the department of chemistry for providing instrument facilities. I would like to thank other faculty members of department of Chemistry for their kind help in carrying out this work. I am also thankful to all the staff members of Chemistry department, for their friendly and cooperative nature and IIT Guwahati for the financial support.

I would like to acknowledge Dr. Kumar Vanka, Physical and Materials Chemistry Division, National Chemical Laboratory, Pune, India for carrying out theoretical studies in my research.

I would like to thank my present labmates Soumen, Kuldeep, Baishakhi, Dibyajyoti Da and specially my year mate Hemanta for their support and help during the tough situations as well as for making a pleasant environment in the laboratory to work. My sincere thanks to my lab seniors, Dr. Moushumi Sarma, Dr. Pankaj Kumar, Dr. Apurba

Kalita, Dr. Aswini Kalita, Dr. Vikash kumar and Dr. Kanhu Charan Rout for their immense help and support in my research works.

I thank my PhD batchmates DK, Sujoy da, Samir, Prasenjit, Julfikar, Saugata, Sourav, Pakhi, Sujit, Kobirul, Subhasis, Barun, Utpal, Hari and incredible juniors like Shilaj, Uday, Subhadip, Subhankar, Nilotpal, Ganesh, Buddha, Keshab, Surajit, Soumendra, Subhra, Utsab and Prakash for all the fun we have had in the last five years.

I wish to thank my respected teachers for extraordinary teaching, insightful ideas and advice.

I would like to express my impression from the core of my heart to my family for their love, continuous inspiration and support. Without their support it is not possible for me to pave the way of my research. In a nutshell their contribution to my life is beyond measure. Finally, I would like to thank all others who are associated with my work directly or indirectly at IIT Guwahati for their help.

Somnath Ghosh

Contents

Synopsis

The thesis entitled, "**NO_x (x=1,2) reactivity of Co(II) and Ni(II) complexes with N-donor and O-donor ligands**" is divided into five chapters.

Chapter 1: Introduction

Nitric oxide (NO) gained increasing attention since it's discovery to play the key roles in many fundamental biochemical and biophysical processes including blood pressure control, neurotransmission, and immune response etc.[1,2] The Nobel prize (1998) in Physiology and Medicine was awarded to Furchgott, Ignarro, and Murad for their discoveries of the role of NO as a signalling molecule in the cardiovascular system.[3-5] It is also known that NO imbalance causes various disease states and these observations have stimulated an extensive research activity into the chemistry, biology and pharmacology.[6,7] Transition metal nitrosyl complexes have attracted considerable interest for (i) the versatility of metal-NO bonding,[8,9] (ii) their importance to serve as a NO delivery reagent to biological targets,[10] (iii) the ability of certain transition metal complexes in promoting NO disproportionation to form N_2O and metal nitrite *via* a metal-nitrosyl intermediate[11] and (iv) interactions of NO with heme/non-heme proteins resulting in physiologically relevant M-NO bonds.[12] In this direction, the best characterized example is the ferro-heme enzyme, soluble guanylyl cyclise (sGC).[13] Formation of a nitrosyl complex with Fe(II) leads to labilization of a *trans* axial (proximal) histidine ligand in the protein backbone, and the resulting change in the protein conformation is believed to activate the enzyme for catalytic formation of the secondary messenger cyclic-guanylyl monophosphate (cGMP) from guanylyl triphosphate (GTP).[14] In cytochrome c oxidase, the NO mediated reduction of Cu(II) to Cu(I) is presumed to play the key role in regulating the electron transport activity of this protein.[15]

NO is also known to involve in the generation of powerful secondary nitrating and/or oxidizing agents, like NO_2 and peroxynitrite ($ONOO^-$).[16] As a strong lipophilic oxidant, NO_2 can trigger lipid auto-oxidation and oxidative nitration of tyrosine.[17-19] In various disease states such as neurodegenerative conditions, cardiovascular disorders, diabetes, and Alzheimer's disease, protein tyrosine nitration has been observed and being used as diagnostic biomarker.[20-30] In biological systems, NO_2 can be generated *via* several mechanisms such as oxidation of NO by O_2, decomposition of $ONOO^-$, and oxidation of nitrite (NO_2^-) by hydrogen peroxide (H_2O_2) in presence of peroxidases.[31-33] These reactions are known to be modulated /catalyzed by metallo-proteins, mostly iron or copper. Thus, transition metal ion induced activation of NO_2 has become a fascinating field of research.

The present thesis originates from our interest to study the binding to and activation of $NO_{x\ (x\ =\ 1\ and\ 2)}$ by transition metal ions. Amongst the first row transition metal ions, iron and copper have been studied well towards NO binding and activation. However, nickel and cobalt have not been studied to that extent, though both of these are known to exhibit interesting activity towards NO. In this context, as a continuation to our study, first two chapters of this thesis deal with NO reactivity of Co(II) and Ni(II) centers. Successively, the redox behaviour of the coordinated NO and it's disproportionation to N_2O have been studied. In the next two chapters, relatively less explored reactivity of NO_2 with Ni(II) complexes have been discussed. In these cases, reduction of Ni(II) center by NO_2 and oxo transfer reactions from NO_2 to the metal coordinated nitrite (NO_2^-) ion have been observed.

Chapter 2: Nitric oxide reactivity of Co(II) complexes: Formation of {CoNO}^{8} and their reactivity

Reactivity of NO with the complexes of Co(II) ions have not been studied so extensively as iron or cooper, perhaps because of its less involvement in biological systems. However, cobalt-nitrosyls are interesting for its several unique reactions: for instance, cobalt dinitrosyls nitrosylate alkene double bonds to result in corresponding *bis*-nitroso compounds; they catalyse the disproportionation of NO which is industrially important.

This chapter deals with NO reactivity of two Co(II) complexes of N_2O_2 type ligands. Two ligands **L1** and **L2,** were prepared by the general reaction of 3,5-di-*tert*-butyl-2-hydroxybenzaldehyde with corresponding amines. Co(II) complexes, **2.1** and **2.2** were prepared by the reaction of $Co(OAc)_2{\cdot}4H_2O$ with the corresponding ligand. These complexes were characterized by various spectroscopic techniques as well as by single crystal X-ray structure determination. The ORTEP diagrams are shown in the figure 1. In both the cases, the central metal ion, Co(II) is coordinated with two N_{imine} and two $O_{phenoxide}$ donor atoms almost in a square planer geometry, resulting in neutral complexes.

Upon addition of NO to the dry and degassed THF solution of the complexes **2.1** and **2.2**, a distinct color change from red to greenish brown was observed. This was monitored by UV-visible spectroscopy. The absorption bands at 877 and 716 nm of complexes **2.1** and **2.2**, respectively disappeared after addition of NO (Figure 2).

After purging NO, the respective reaction mixtures were kept in freezer for two days to afford X-ray quality crystals of the corresponding {CoNO}^{8} complexes, **2.3** and **2.4**. The ORTEP diagrams are shown in figure 3.

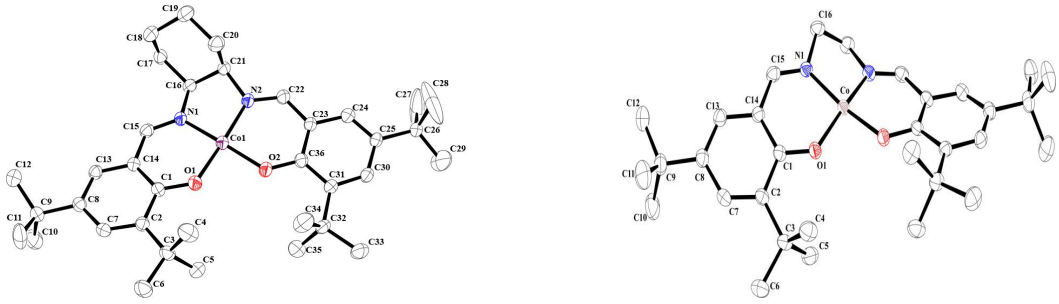

(a) **(b)**

Figure 1. ORTEP diagrams of complexes **2.1 (a)** and **2.2 (b)** (50% thermal ellipsoid plot; H-atoms are removed for clarity).

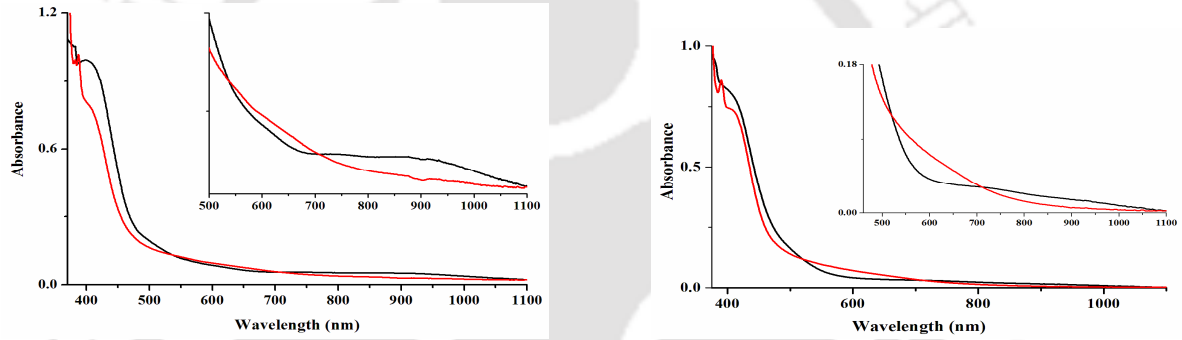

(a) **(b)**

Figure 2. **(a)** UV-visible spectra of complexes **2.1** (black) and **2.3** (red); **(b)** UV-visible spectra of complexes **2.2** (black) and **2.4** (red) in dry THF.

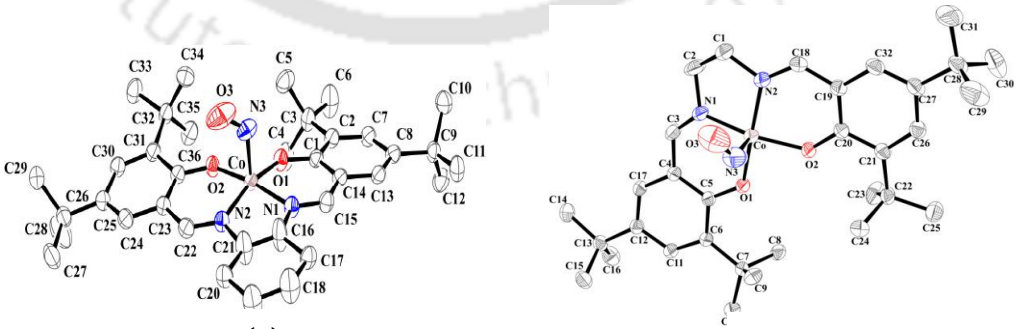

(a) **(b)**

Figure 3. ORTEP diagrams of complexes **2.3 (a)** and **2.4 (b)** (50% thermal ellipsoid plot; H-atoms are removed for clarity).

In both the complexes, the central metal ion is in penta-coordinated in a square pyramidal geometry with the nitrosyl group in the axial position. In complex **2.3**, the Co–N_{NO} bond length is 1.871Å and N–O bond is 1.079 Å. The Co-N-O angle is 125.6º. In the case of complex **2.4**, NO group is coordinated to the metal in a bent fashion with an angle of 126.5º. The Co-N_{NO} bond length is 1.799Å. The bent $\{CoNO\}^8$ description can be envisaged as Co^{III}–NO^- species. The nitrosyl complexes, **2.3** and **2.4** displayed the coordinated nitrosyl stretching frequency at 1651 cm^{-1} and 1650 cm^{-1}, respectively, in FT-IR spectra.

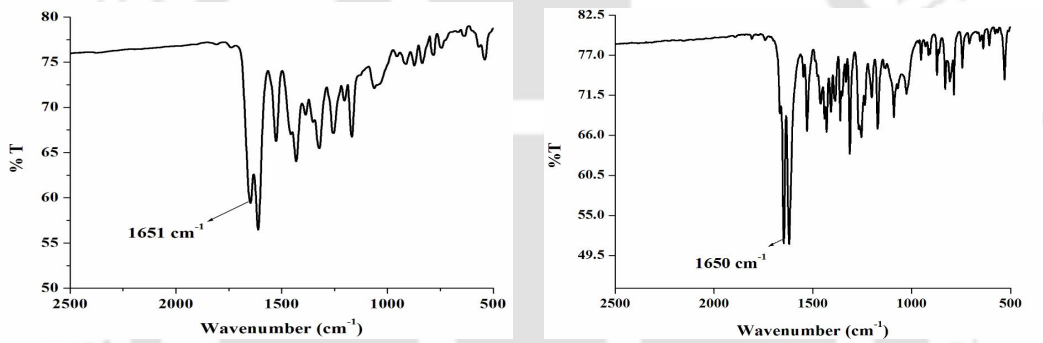

(a) **(b)**

Figure 4. FT-IR spectra of complex **2.3 (a)** and **2.4 (b)** in KBr.

Complexes **2.3** and **2.4** in THF solution were subjected to react with KO_2 at -80 °C to result in the formation of corresponding peroxynitrite ($ONOO^-$) ions as transient intermediate. Thermal instability and reactive nature of the $ONOO^-$ ions precluded their isolation and spectral characterization. Their formation was supported by the characteristic oxidative dimerization reaction of 2,4-di-*tert*butylphenol to result in 2,2′-dihydroxy-3,3′,5,5′-tetra-*tert*-butylbiphenol (~30%) (Scheme 1). Further, isolation of corresponding nitrate complexes, **2.5** and **2.6**, respectively, as the isomerization products suggests the formation of the intermediate (Scheme 1).

The nitrate complexes were characterized by elemental analyses and spectroscopic

techniques. Even after several attempts, X-ray quality crystals were not obtained.

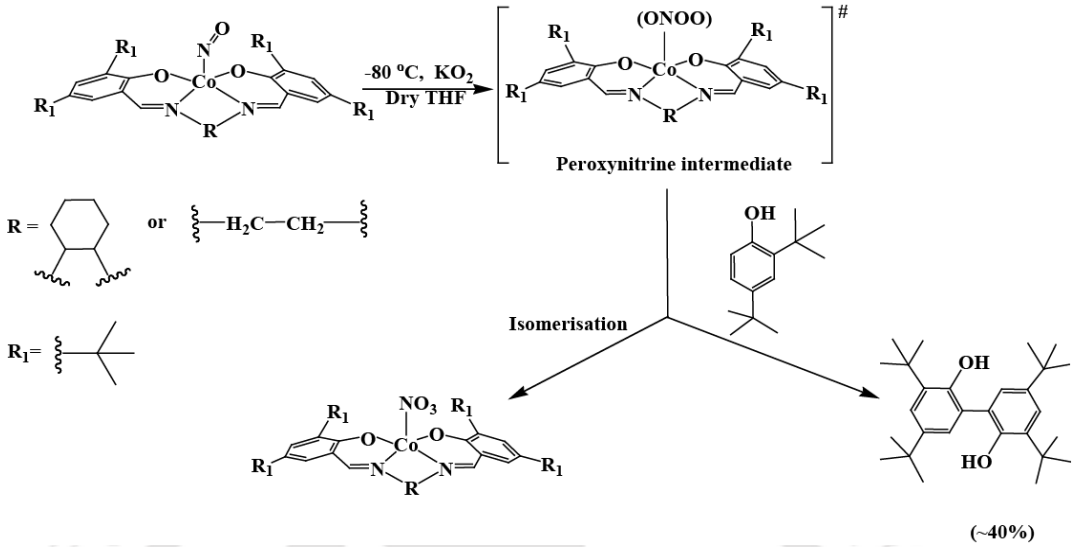

Scheme 1

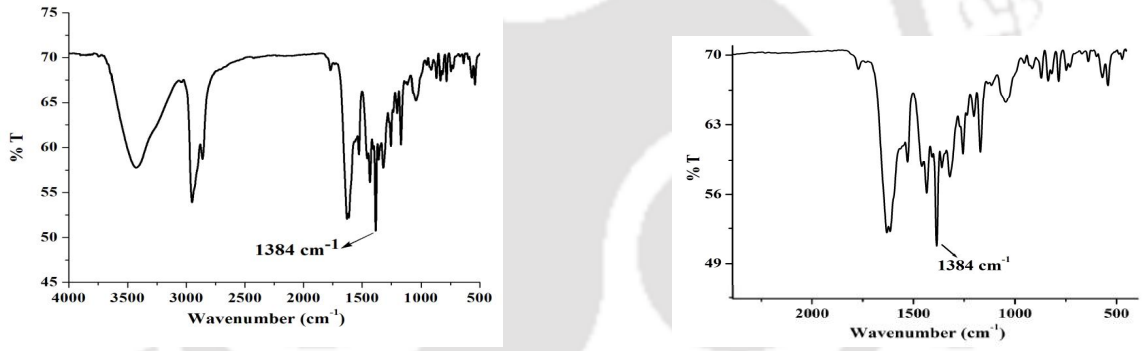

(a) **(b)**

Figure 5. FT-IR spectra of complex **2.5 (a)** and **2.6 (b)** in KBr.

It would be worth mentioning here that the {CoNO}^{8} complexes did not react with dioxygen.

Chapter 3: Nitric oxide reactivity of Ni(II) complex: Reductive nitrosylation of Ni(II) followed by release of nitrous oxide

This chapter describes the NO reactivity of a Ni(II) complex, **3.1** of ligand **L3** {**L3** = *bis*(2-ethyl-4-methylimidazol-5-yl)methane}. The ligand, **L3** was synthesized by following an earlier reported procedure.[34] The Ni(II) complex, **3.1** was prepared by stirring a mixture of

nickel(II) chloride hexahydrate with two equivalent of ligand, **L3** in methanol. It was characterized by various spectroscopic analyses, as well as by single crystal X-ray structure determination (Figure 6).

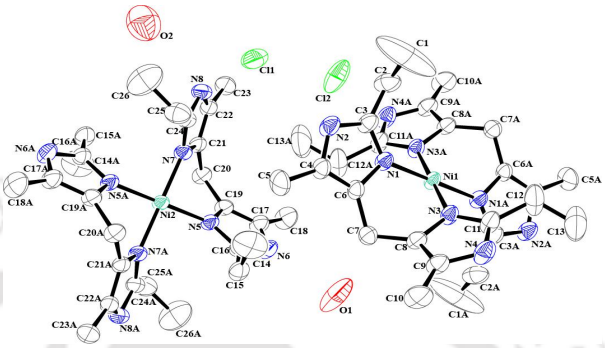

Figure 6. ORTEP diagram of complex **3.1** (50% thermal ellipsoid plot, H-atoms are omitted for clarity).

Addition of equivalent amount of NO in the degassed methanol solution of complex **3.1** at -80 °C displayed a shift in the *d-d* band from 636 nm to 610 nm (Figure 7). The shift in λ_{max} and change in intensity of the *d-d* band is attributed to the formation of corresponding Ni(I) intermediate (Scheme 2).

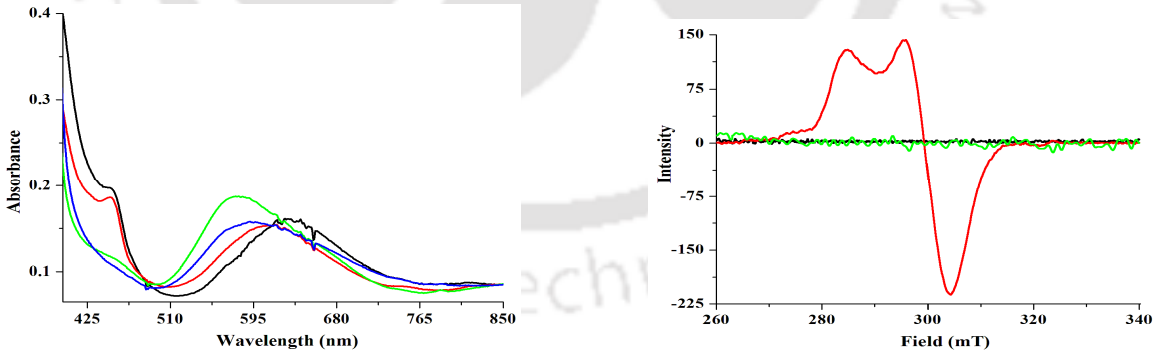

(a) **(b)**

Figure 7. **(a)** UV-visible spectra of complex **3.1** (black), after addition of stoichiometric amount of NO (red), $\{NiNO\}^{10}$ intermediate (green) and complex **3.2** (blue) in methanol at - 80 °C. **(b)** X-band EPR spectra of complex **3.1**(black), Ni(I) species (red) and complex **3.2** (green) in methanol at 77K.

The reduction of Ni(II) center to Ni(I) by NO was also evident from the X-band EPR studies. The diamagnetic Ni(II) center, in presence of equivalent amount of NO displayed EPR signals corresponding to Ni(I) ($g_{\parallel}$, 2.29; $g_{\perp}$, 2.17) (Figure 7).

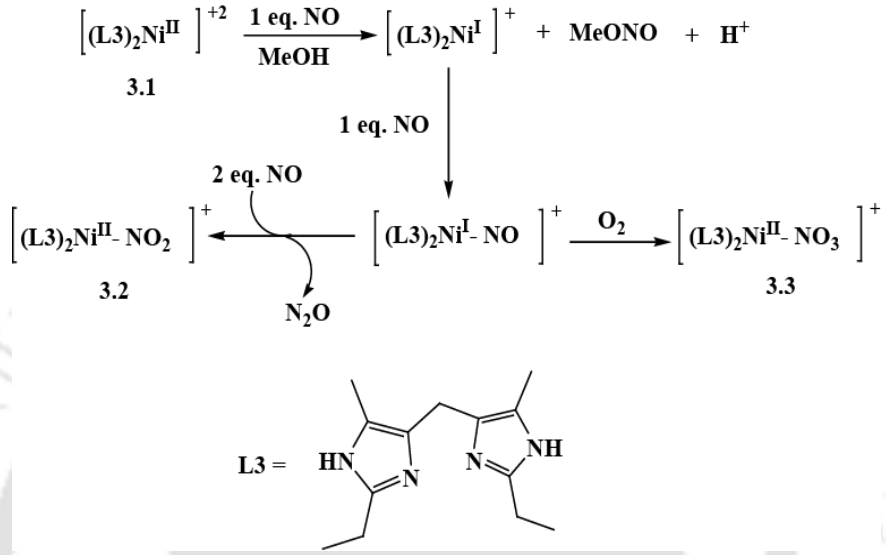

Scheme 2

Another equivalent of NO resulted in the corresponding Ni(I)-nitrosyl intermediate having $\{NiNO\}^{10}$ configuration (Scheme 2). This has been monitored by UV-visible, solution FT-IR and EPR spectroscopic studies. In UV-visible study a shift of the *d-d* band from 610 nm to 578 nm was observed (Figure 7). In the FT-IR spectrum of the methanol solution of complex **3.1**, addition of two equivalent of NO resulted in the appearance of a new band at 1668 cm^{-1}, assignable to the υ_{NO} corresponding $\{NiNO\}^{10}$ intermediate (Figure 8). The intermediate was found to be thermally unstable and highly sensitive towards air and moisture.

In presence of excess NO, the intensity of 578 nm band of $\{NiNO\}^{10}$ was found to decay indicating the decomposition of the intermediate. This finally led to the formation of corresponding Ni(II)-nitrito complex (**3.2**) (Figure 9) and nitrous oxide (N_2O) (Scheme 2). The nitrito complex, **3.2** was isolated and characterized by various spectroscopic

techniques. Single crystal X-ray structure revealed that Ni(II) center is coordinated to two ligand moieties and a (η^2-O,O)-nitrito group (Figure 9). The formation of N_2O was confirmed by GC-mass analysis (Figure 9). This was further supported by the FT-IR monitoring of the reaction mixture which showed the appearance of a stretching frequency at 2230 cm^{-1} assignable to N_2O (Figure 8).

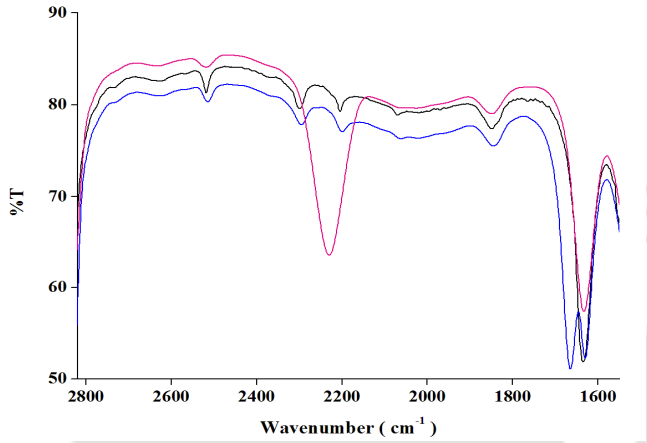

Figure 8. FT-IR spectra of complex **3.1**(black), after immediate (blue) and 30 minutes (pink) of addition of excess NO in methanol at room temperature.

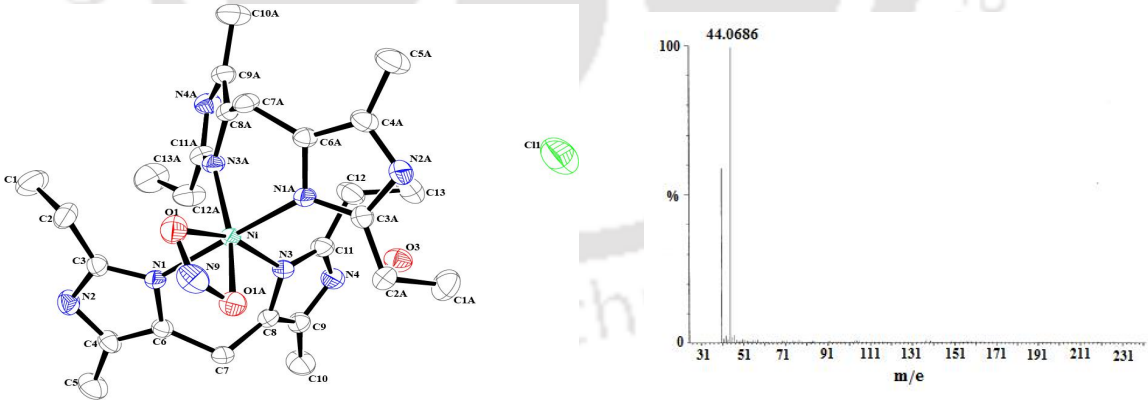

(a) **(b)**

Figure 9. **(a)** ORTEP diagram of complex **3.2** (50% thermal ellipsoid plot, H-atoms are omitted for clarity). **(b)** GC-mass spectra of N_2O, gas taken from the head space of the reaction mixture.

The $\{NiNO\}^{10}$ intermediate was found to decompose to the corresponding nitrato complex (**3.3**) in presence of oxygen (Scheme 2). The perspective ORTEP view of complex **3.3** is shown in figure 10.

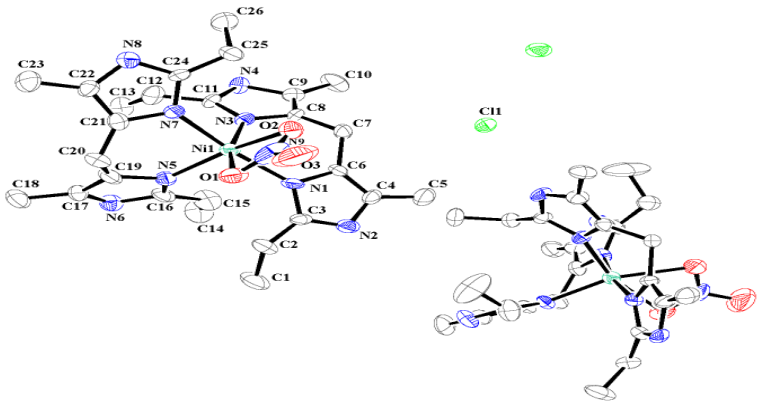

Figure 10. ORTEP diagram of complex **3.3** (50% thermal ellipsoid plot, H-atoms are omitted for clarity).

It would be worth mentioning here that the NO reactivity of complex **3.1** was found to be anion dependent. Complexes with non-coordinated anions react with NO leading to the similar reaction. However, in case of coordinated anions like acetate, benzoate, the complexes were found unreactive towards NO. This is perhaps because of the relative change of redox potentials. For complex **3.1** the Ni^{II}/Ni^{I} reduction potential is -1.05 V versus Ag/Ag^{+} reference electrode; on the other hand, in acetate and benzoate complexes this potential appeared at -1.52 V and -1.56 V, respectively. The redox potentials for complexes with acetate or benzoate anions, match well with the NO_2/NO_2^{+} potential. The next chapter originated from our interest to study the NO_2 reactivity of Ni(II) complexes of ligand **L3** with acetate and benzoate anions.

Chapter 4: Nitrogen dioxide reactivity of Ni(II) complex : Activation of NO_2 leading to the reduction of Ni(II) center

In continuation to the observations of chapter **3**, two Ni(II) complexes **4.1** and **4.2** were prepared by using ligand **L3** having acetate and benzoate as counter anions, respectively. These complexes were characterized by FT-IR spectroscopy, UV-visible spectroscopy and elemental analysis. The single crystal X-ray structure determination revealed that complex **4.2** is in the octahedral geometry, where four N atoms of two ligands (**L3**) and two O atoms from the coordinated benzoate moiety (Figure 11) satisfied the coordination requirements. Even after several attempts, X-ray quality single crystal for complex **4.1** was not obtained.

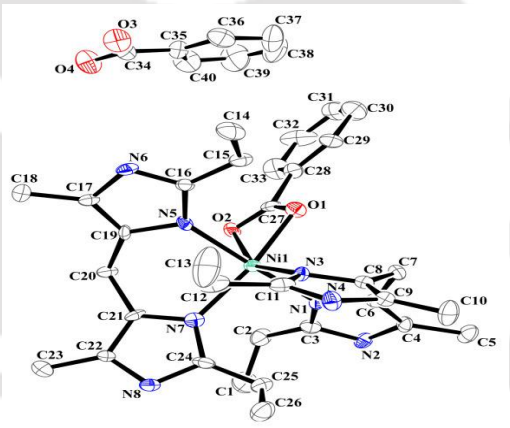

Figure 11. ORTEP diagram of complex **4.2** (50% thermal ellipsoid plot, H- atoms are omitted for clarity).

As mentioned in chapter **3**, complexes **4.1** and **4.2** in dry and degassed methanol solution did not react with NO (Figure 12). However, when NO_2 was purged to the dry and degased methanol solution of complex **4.1**, a blue shift was observed from 598 nm to 588 nm in UV-visible spectrum (Figure 13a). This reaction mixture was found to be EPR silent. This is attributed to the weak coordination of NO_2 to the central metal ion. In presence of

stoichiometric amount of water, the 588 nm band was shifted to 582 nm (Figure 13a). The resulting reaction mixture became EPR active (Figure 14). These observations are attributed to the reduction of Ni(II) to Ni(I) with concomitant formation of nitrato (NO_3^-) species (Scheme 3). In case of complex **4.2**, similar results were observed (Figure 13b).

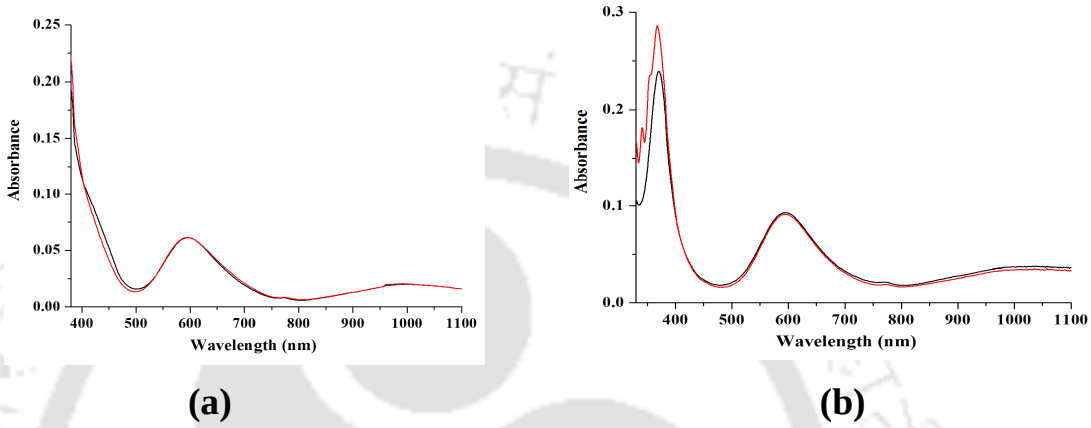

(a) **(b)**

Figure 12. UV-visible spectra of complexes **4.1 (a)** and **4.2 (b)** before (black) and after (red) purging NO in dry methanol at room temperature.

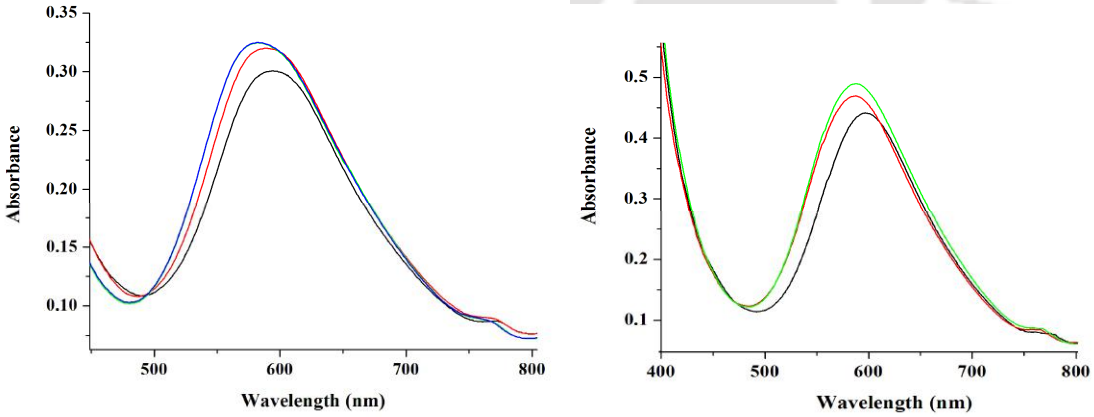

(a) **(b)**

Figure 13. UV-visible spectra **(a)** complex **4.1**(black), after purging NO_2 (red) and after addition of water (blue); **(b)** complex **4.2** (black), after purging NO_2 (red) and after addition of water (green) in methanol at room temperature.

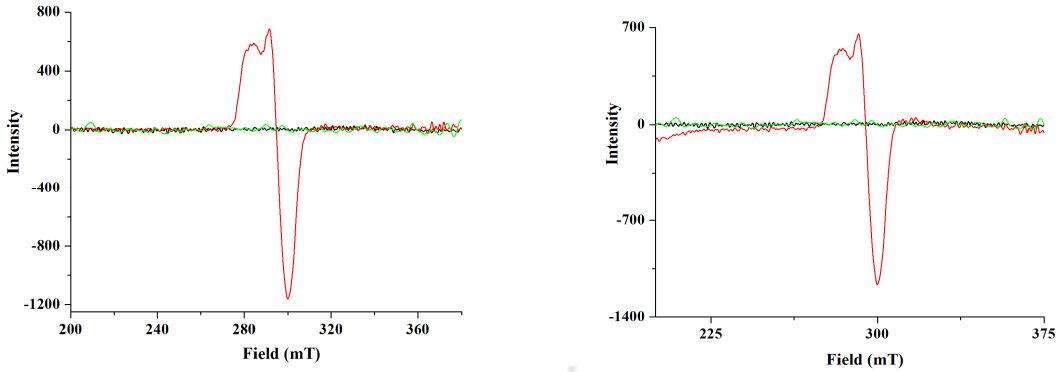

(a) **(b)**

Figure 14. X-band EPR spectra **(a)** complex **4.1** (black), after purging NO_2 (green) and after addition of water (red); (b) complex **4.2** (black), after purging NO_2 (green) and after addition of water (red) in methanol at 77K.

While both the reaction mixtures were kept in freezer for 3- 4 days, crystals of complex **4.3** were obtained. Structure determination revealed the formation of corresponding Ni(I)-nitrato complex, **4.3** (Figure 15a). The presence of Ni(I) ion in complex **4.3** was confirmed by X-band EPR study also (Figure 15b).

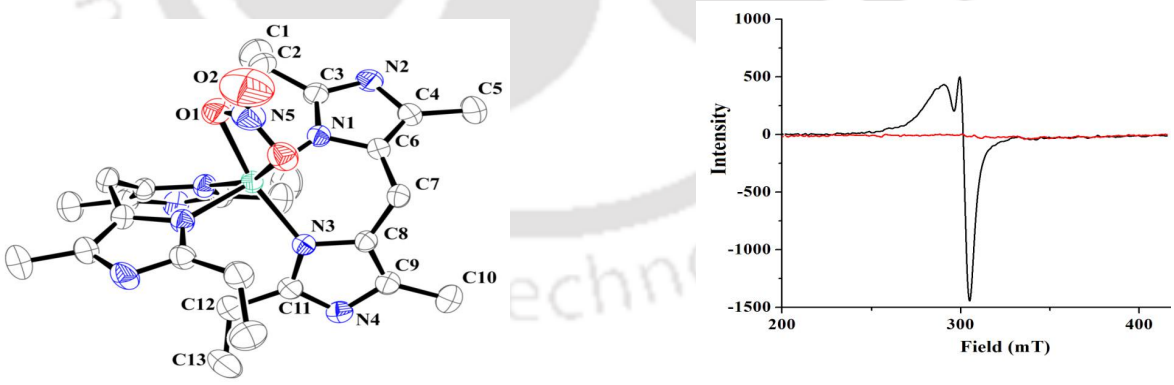

(a) **(b)**

Figure 15. **(a)** ORTEP diagram of complex **4.3** (50% thermal ellipsoid plot, H- atoms are omitted for clarity), **(b)** X-band EPR spectra of complexes **4.1** (red), **4.3** (black) in dry methanol at room temperature.

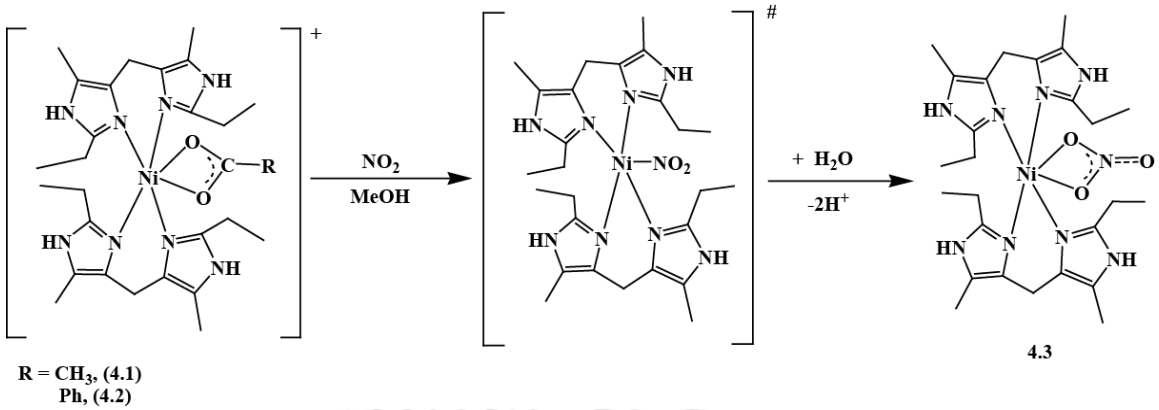

Scheme 3

Chapter 5: NO_2 reactivity of a Ni(II) complex: Oxo transfer reaction from NO_2 to NO_2^-

The ligand, **L4** {**L4** = 5,5,7,12,12,14-hexamethyl-1,4,8,11-tetraazacyclotetradecane} was prepared by using the procedure described by Curtis *et al*.[35] Mononuclear complex **5.1**, [Ni(L4)$(CH_3COO)_2$], was prepared by refluxing a mixture of nickel(II) acetate tetrahydrate with equivalent quantity of **L4** in methanol. The formation of the complex was unambiguously established by various spectroscopic analyses as well as by X-ray single crystal structure determination. The perspective ORTEP view of complex **5.1** is shown in figure 16. The crystal structure revealed an octahedral geometry around Ni(II) center in the mononuclear unit. The four N-atoms from the ligand are coordinated to the metal ion forming a square plane. Two acetate anions are coordinated to the metal centre from the axial positions to balance the charge of the metal ion and to complete the octahedral geometry around the Ni(II) center. In methanol, complex **5.1** displayed *d-d* bands at 960, 574 and 464 nm occurred from three spin-allowed transitions, $^3A_{2g}$ - $^3T_{2g}(F)$, $^3A_{2g}$ - $^3T_{1g}(F)$, and $^3A_{2g}$ - $^3T_{1g}(P)$, respectively of octahedral Ni^{2+}. 362 nm band is assignable to the ligand to metal (LMCT) charge transfer.[36]

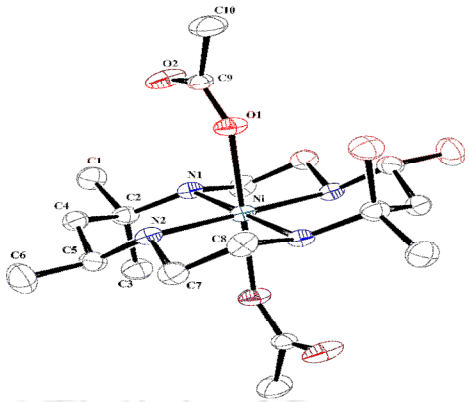

Figure 16. The ORTEP diagram of complex **5.1** (30% thermal ellipsoid; H-atoms are omitted for clarity).

Addition of equivalent amount of NO_2 to the dry and degassed methanol solution of complex **5.1** resulted in the shift of 464 nm to 434 nm (Figure 17). EPR study of the frozen reaction mixture (at 77 K) revealed the presence of Ni(I) species (Figure 17, Eq. 1). The axial nature of the spectrum indicates the existence of Ni(I) (d^9) in a square planar environment with d_z^2 ground state.[37] Calculated values of $g_\perp$ and $g_\parallel$ are 2.22 and 2.03, respectively.

$$\mathbf{(L4)Ni^{II}(OAc)_2 + NO_2 \xrightarrow{MeOH} [(L4)Ni^{I}]^+ + 2AcO^- + H^+ + MeONO_2} \quad \text{-----(Eq. 1)}$$

It should be noted that the electrochemically generated Ni(I) complex of ligand **L4** was also studied earlier by EPR spectroscopy.[37] The spectroscopic evidence obtained in the present study is in very good agreement with the earlier reported results. Thus, it is logical to believe that in this step of reaction Ni(II) center of complex **5.1** has undergone reduction by NO_2 to form $[(L4)Ni]^+$ complex. GC-mass analyses of the reaction mixture revealed the formation of methyl nitrate (CH_3ONO_2) in this step. This is attributed to the formation of NO_2^+ during the reduction of Ni(II) by NO_2 followed by its immediate reaction with methanol to form methyl nitrate. The unstable nature of Ni(I) complex could not allow to isolate or structurally characterize.

Upon addition of further equivalent of NO_2, the absorption band at 434 nm was shifted to 455 nm (Figure 17). This is attributed to the formation of corresponding [Ni^{I}-NO_2] complex, which can be considered as [Ni^{II}-NO_2^-]. The EPR signal of Ni(I) intermediate was also disappeared. When the reaction mixture was allowed to stand at room temperature for 3-4 days, two types of crystals, violet and purple, appeared almost in equal proportion (Scheme 4). Structural characterization revealed that the violet crystals are of complex **5.1** and the purple one is of [(L4)Ni(NO_2)$_2$], complex **5.2**. The ORTEP diagram of complex **5.2** is shown in figure 18. A η^1-O coordination mode of two nitrito moieties to the Ni^{II} center was observed.

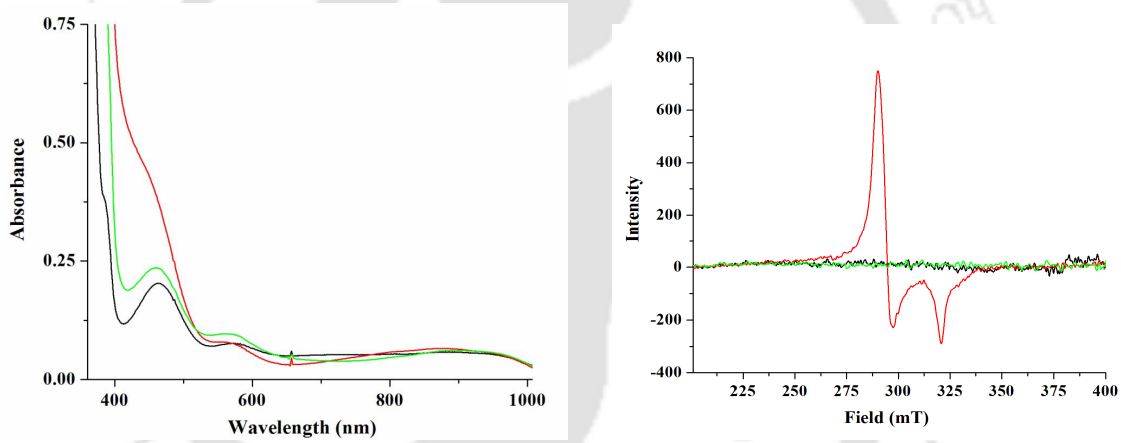

(a) **(b)**

Figure 17. **(a)** UV-visible spectra of complex **5.1**(black), after addition of one (red) and two (green) equivalent/s of NO_2 in dry methanol at room temperature, **(b)** X-band EPR of complex **5.1** (black), after purging one (red) and two (green) equivalent/s amount of NO_2 in methanol at 77 K.

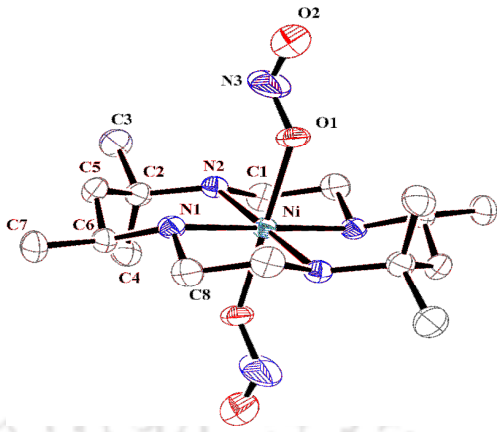

Figure 18. The ORTEP diagram of complex **5.2** (30% thermal ellipsoid; H-atoms are omitted for clarity).

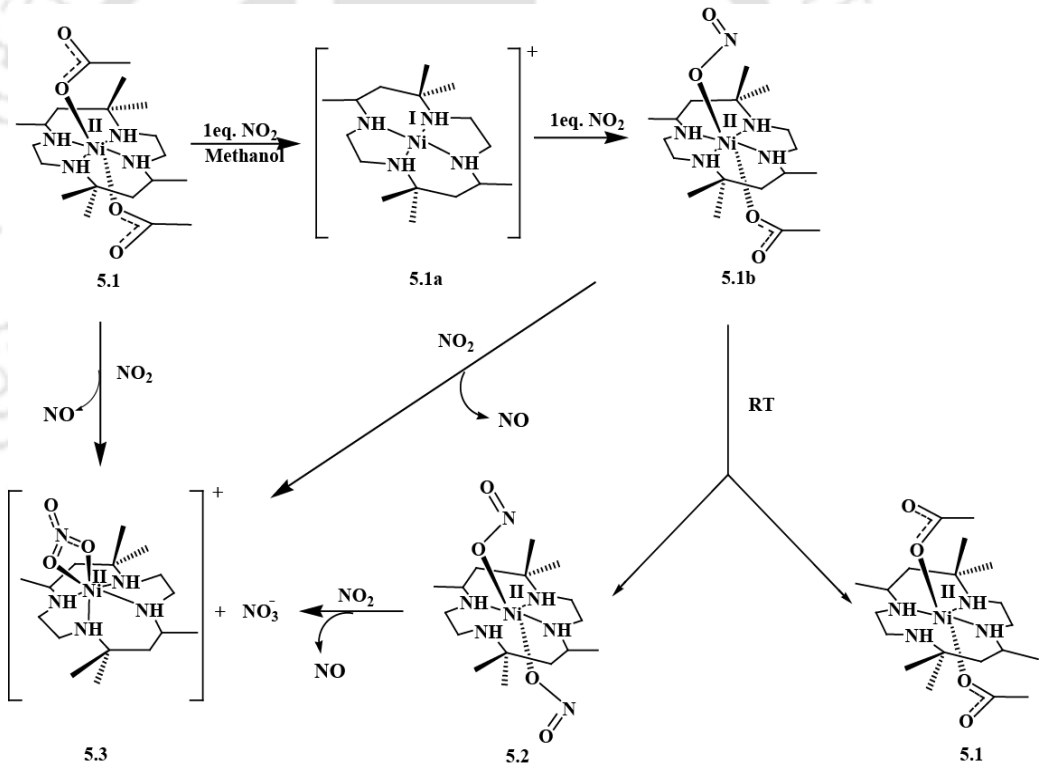

Scheme 4

The crystallization of complexes **5.1** and **5.2**, from the reaction mixture suggests the formation of [(L4)Ni(NO_2)(CH_3COO)], **5.1b**, as intermediate upon addition of equivalent amount of NO_2 gas in the solution of $[(L4)Ni]^+$ species. Allowing it to crystallize out, it

dissociated into complexes **5.1**, [(L4)Ni($CH_3COO)_2$] and **5.2**, [(L4)Ni($NO_2)_2$] owing to the lesser stability of **5.1b** compared to those (Scheme 4).

When the reaction mixture containing **5.1b** was subjected to addition of further equivalent NO_2, there was no appreciable change in the *d-d* absorption bands in UV-visible spectrum. However, in FT-IR spectrum (Figure 19), stretching at 1272 cm^{-1} assigned to nitrito group was disappeared and a new intense stretching band at 1384 cm^{-1} assignable to nitrato group was appeared. Structural characterization revealed the formation of corresponding Ni(II) nitrato complex **5.3** in the reaction. The ORTEP diagram of complex **5.3** is shown in figure 19.

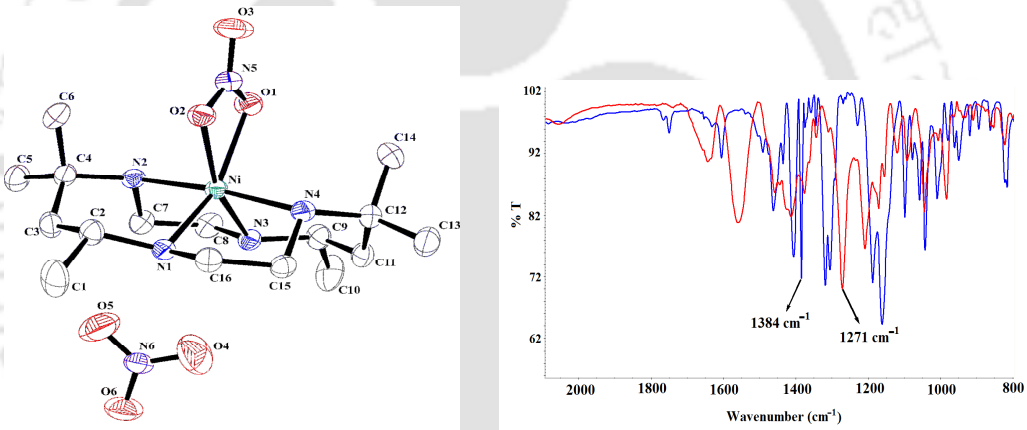

(a) **(b)**

Figure 19. **(a)** The ORTEP diagram of complex **5.3** (30% thermal ellipsoid; H-atoms are omitted for clarity), **(b)** FT-IR spectra of complexes **5.2** (red) and **5. 3** (blue) in KBr pellet.

Second nitrate ion is not coordinated to the metal ion. The formation of complex **5.3** is perhaps because of the less stability of corresponding [(L4)Ni(NO_3)(OAc)]. The peak observed at *m/z* 404.215 in mass spectrometry is assignable to $[\{Ni^{II}(L4)(NO_3)\}]^+$. Expected and observed fragmentations in mass spectroscopy matched well (Figure 20).

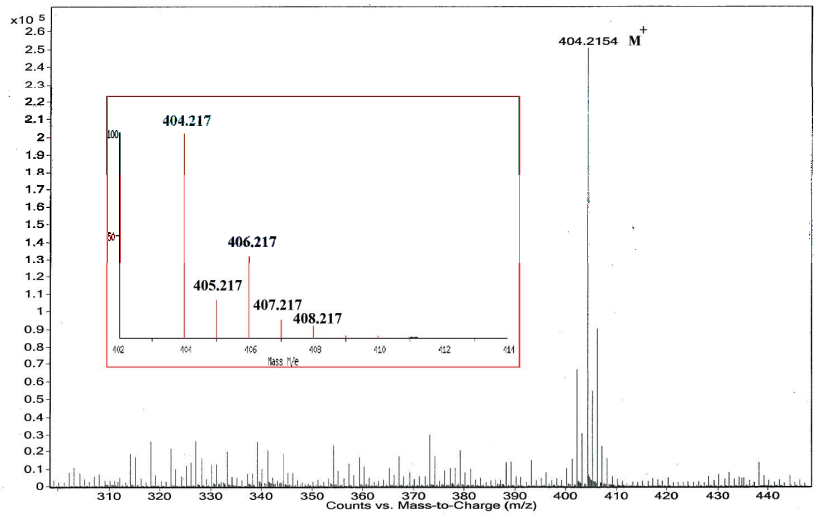

Figure 20. ESI mass spectrum of complex **5.3** in methanol (Inset: simulated spectrum).

Thus, addition of NO_2 in methanol solution of intermediate complex **5.1b** afforded an oxo transfer resulting in the corresponding nitrate complex **5.3**. NO is expected to form as side product in the reaction and was confirmed by GC-MS as well by spin trapping using iron(II)diethyldithiocarbamato complex.

It would be worth to mention here that purging NO_2 to the methanol solution of complex **5.2** also afforded complex **5.3**. On the other hand addition of excess NO_2 in methanol solution of complex **5.1** resulted in complex **5.3** as the final product with the release of NO. The reaction of intermediate complex **5.1b** with NO_2 leading to the conversion of O-nitrito to O-nitrato complex can be envisaged to follow pathway of oxo transfer as was observed in earlier reports (Scheme 5).[38-40] ESI-mass experiment studies with scrambled $NO_2^{16/18}$ was found to result in two equal intensity mass signals for $[Ni(L4)(^{16}O_2N^{18}O)]^+$ (406.223) and $[Ni(L4)(N^{16}O_3)]^+$ (404.222) shown in figure 21. On the other hand, addition of $^{15}NO_2$ to the solution of **5.1b** was found to release ^{15}NO. These suggest that the oxo transfer takes place from free NO_2 to the coordinated nitrito group. In case of earlier reported examples involving Fe(II)(TPP), Mn(II)(TPP) and Cu(II) complex of 4,6-di-*tert*-

butyl-2-((2-picolyl(isopropyl)amino)methyl)phenol the oxo transfer was found to follow the similar mechanistic pathway.

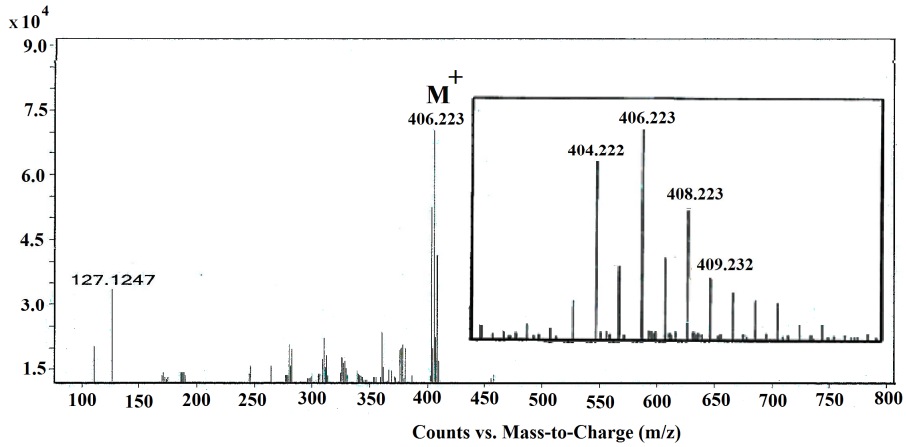

Figure 21. ESI mass spectrum of complex **5.3** with $^{18}ONO_2$ as anion in methanol.

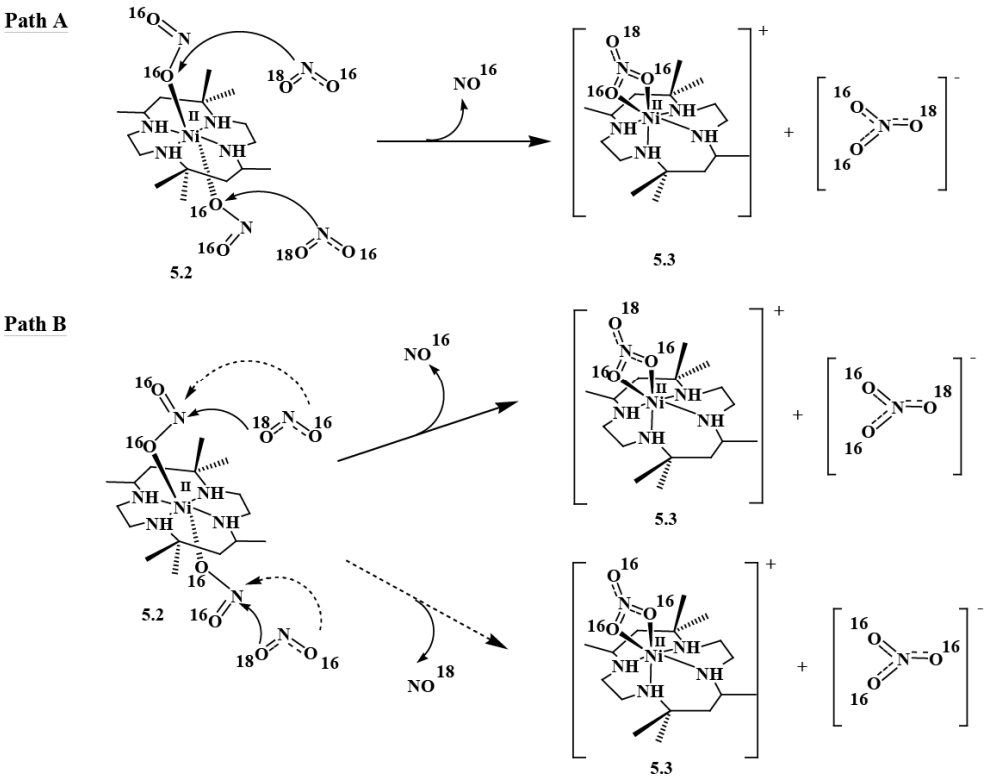

Scheme 5

References

(1) Moncada, S.; Palmer, R. M. J.; Higgs, E. A. *Pharmacol. Rev.* **1991**, *43*, 109.

(2) Culotta, E.; Koshland, D. *Science* **1992**, *258*, 1862.

(3) Furchgott, R. F. *Angew. Chem. Int. Ed.* **1999**, *38*, 1870.

(4) Ignarro, L. J. *Angew. Chem. Int. Ed.* **1999**, *38*, 1882.

(5) Murad, F. *Angew. Chem. Int. Ed.* **1999**, *38*, 1856.

(6) *Nitric Oxide: Biology and Pathobiology*; Ignarro, L. J., Ed.; Academic Press: San Diego, **2000**.

(7) *Nitric Oxide and Infection*; Fang, F. C., Ed.; Kluwer Academic/ Plenum Publishers: New York, **1999**.

(8) *(a)* Ford, P. C.; Bourassa, J.; Lee, K. B.; Lorkovic, I.; Boggs, S.; Kudo, S.; Laverman, L. *Coord. Chem. Rev.* **1998**, *171*, 185. (b) Ford, P. C.; Lorkovic, I. M. *Chem. Rev.* **2002**, *102*, 993. (c) Butler, A. R.; Megson, I. L. *Chem. Rev.* **2002**, *102*, 1155.

(9) (a) Hayton, T. W.; Legzdins, P.; Sharp, W. B. *Chem. Rev.* **2002**, *102*, 935. (b) Hsu, I. J.; Hsieh, C. H.; Ke, S. C.; Chiang, K.-A.; Lee, J.- M.; Chen, J. M.; Jang, L. Y.; Lee, G. H.; Wang, Y.; Liaw, W. F. *J. Am. Chem. Soc.* **2007**, *129*, 1151.

(10) (a) Cheng, L.; Richter-Addo, G. B. *Binding and Activation of Nitric Oxide by Metalloporphyrins and Heme*. In *The Porphyrin Handbook*; Guilard, R., Smith, L., Kadish, K. M., Eds.; Academic Press: New York, 2000; Vol. *4*, Chapter 33. (b) Afshar, R. K.; Patra, A. K.; Mascharak, P. K. *J. Inorg. Biochem.* **2005**, *99*, 1458.

(11) Averill, B. A. *Chem. Rev.* **1996**, *96*, 2951.

(12) Richter-Addo, G. B.; Legzdins, P. *Metal Nitrosyls*; Oxford University: New York, **1992**.

(13) (a) Kim, S.; Deinum, G.; Gardner, M. T.; Marletta, M. A.; Babcock, G. T. *J. Am. Chem. Soc.* **1996**, *118*, 8769. (b) Burstyn, J. N.; Yu, A. E.; Dierks, E. A.; Hawkins, B. K.; Dawson, J. H. *Biochemistry* **1995**, *34*, 5896.

(14) Torres, J.; Svinstunenko, D.; Karlsson, B.; Cooper, C. E.; Wilson, M. T. *J. Am. Chem. Soc.* **2002**, *124*, 963.

(15) Cooper, C. E.; Torres, J.; Sharpe, M. A.; Wilson, M. T. *FEBS Lett.* **1997**, *414*, 281.

(16) (a) Schopfer, M. P.; Mondal, B.; Lee, D.-H.; Sarjeant, A. A. N.; Karlin, K. D. *J. Am. Chem. Soc*. **2009**, *131*, 11304. (b) Maiti, D.; Lee, D.-H.; Sarjeant, A. A. N.; Pau, M. Y. M.; Solomon, E. I.; Gaoutchenova, K.; Sundermeyer, J.; Karlin, K. D. *J. Am. Chem. Soc*. **2008**, *130*, 6700. (c) Park, G. A.; Deepalatha, S.; Simona, C. P.; Lee, D.-H.; Mondal, B.; Sarjeant, A. A. N.; Rio, D. Del.; Pau, M. Y. M.; Solomon, E. I.; Karlin, K. D. *J. Biol. Inorg. Chem.* **2009**, *14*, 1301. (d) Kumar, V.; Kalita, A.; Mondal, B. *Dalton Trans*. **2013**, *42*, 16264.

(17) Nagano, T.; Yoshimura, T. *Chem. Rev.* **2002**, *102*, 1235.

(18) Cosby, K.; Partovi, K. S.; Crawford, J. H.; Patel, R. P.; Reiter, C. D.; Martyr, S.; Yanq, B. K.; Waclawiw, M. A.; Zalos, G.; Xu, X.; Huang, K. T.; Shields, H.; Kim-Shapiro, D. B.; Schechter, A. N.; Cannon, R. O.; Gladvin, M. T. *Nat. Med.* **2003**, *9*, 1498.

(19) Kirsch, M.; Korth, H. G.; Sustmann, R.; de Groot, H. *Biol. Chem.* **2002**, *383*, 389.

(20) Beckman, J. S. *Arch. Biochem. Biophys.* **2009**, *484*, 114.

(21) Ischiropoulos, H. *Arch. Biochem. Biophys.* **2009**, *484*, 117.

(22) Ferrer-Sueta, G.; Radi, R. *ACS Chem. Biol.* **2009**, *4*, 161.

(23) Abello, N.; Kerstjens, H. A. M.; Postma, D. S.; Bischoff, R. *J. Proteome Res.* **2009**, *8*, 3222.

(24) Radi, R. *Proc. Natl. Acad. Sci. U.S.A.* **2004**, *101*, 4003.

(25) Ischiropoulos, H. *Arch. Biochem. Biophys.* **1998**, *356*, 1.

(26) Reynolds, M. R.; Berry, R. W.; Binder, L. I. *Biochemistry* **2007**, *46*, 7325.

(27) Ascenzi, P.; di Masi, A.; Sciorati, C.; Clementi, E. *BioFactors* **2010**, *36*, 264.

(28) Reyes, J. F.; Reynolds, M. R.; Horowitz, P. M.; Fu, Y. F.; Guillozet- Bongaarts, A. L.; Berry, R.; Binder, L. I. *Neurobiol. Dis.* **2008**, *31*, 198.

(29) Wattanapitayakul, S. K.; Weinstein, D. M.; Holycross, B. J.; Bauer, J. A. *FASEB J.* **2000**, *14*, 271.

(30) Cruthirds, D. L.; Novak, L.; Akhi, K. M.; Sanders, P. W.; Thompson, J. A.; MacMillan-Crow, L. A. *Arch. Biochem. Biophys.* **2003**, *412*, 27.

(31) Olbregts, J. *Int. J. Chem. Kinet.* **1985**, *17*, 835.

(32) Su, J.; Groves, J. T. *J. Am. Chem. Soc.* **2009**, *131*, 12979.

(33) Bian, K.; Gao, Z. H.; Weisbrodt, N.; Murad, F. *Proc. Natl. Acad. Sci. U.S.A.* **2003**, *100*, 5712.

(34) Kalita, A.; Kumar, P.; Deka, R. C.; Mondal, B. *Chem. Commun*. **2012**, *48*, 1551.

(35) Hay, R. W.; Lawrance, A. G.; Curtis, N. F. *J. Chem. Soc., Perkin Trans.* **1975**, *1*, 59.

(36) (a) Jorgensen, C. K.; *Inorganic Complexes*, pp. 54, Academic Press: New York, **1963**. (b) Lever, A. B. P. (ed.) *Inorganic Electronic Spectroscopy*, pp 507 and 738, Elsevier, Amsterdam, **1984**.

(37) (a) Hathaway, B. J.; Billing, D. E. *Coord. Chem. Rev.* **1970**, *5*, 143. (b) Gagne, R. R.; Ingle, D. M. *Inorg. Chem.* **1981**, *20*, 420. (c) Nag, K.; Chakravorty, A. *Coord. Chem. Rev.* **1980**, *33*, 87. (d) Ansell, C. W. G.; Lewis, J.; Raithby, P. R.; Ramsden,

J. N.; Shroder, M. *Chem. Commun.* **1982**, 546. (e) Suh, M. P.; Oh, K. Y.; Lee, J. W.; Bae, Y. Y. *J. Am. Chem. Soc.* **1996**, *118*, 777.

(38) (a) Kurtikyan, T. S.; Hayrapetyan, V. A.; Mehrabyan, M. M.; Ford, P. C. *Inorg. Chem.* **2014**, *53*, 11948. (b) Kurtikyan, T. S.; Ford, P. C. *Angew. Chem., Int. Ed.* **2006**, *45*, 492.

(39) Kurtikyan, T. S.; Hovhannisyan, A. A.; Gulyan, G. M.; Ford, P. C. *Inorg. Chem.* **2007**, *46*, 7024.

(40) Gogoi, K.; Deka, H.; Kumar, V.; Mondal, B. *Inorg. Chem*. **2015**, *54*, 4799.

Chapter 1

Introduction

1.1 General aspects of nitric oxide

Amongst all other oxides of nitrogen, nitric oxide (NO) has attracted enormous attention after its discovery to play the key roles in many fundamental biochemical and biophysical process including blood pressure control, neurotransmission, immune response etc.[1] It is also known that NO imbalance causes various disease states and these observations have stimulated an extensive research in the chemistry, biology and pharmacology of NO.[2] Transition-metal nitrosyl complexes have attracted considerable interest for (i) their versatile bonding properties between metal and NO; and electronic structures,[3,4] (ii) the metal nitrosyl complexes being employed to serve as a NO delivery reagent to biological targets,[5] (iii) the ability of certain transition-metal complexes promoting NO disproportionation to form N_2O and metal nitrite *via* a metal nitrosyl intermediate[6] and (iv) interactions of NO and heme/nonheme proteins resulting in physiologically relevant M-NO bonds.[7] In this direction, the best characterized example is the ferro-heme enzyme, soluble guanylyl cyclise (sGC).[8] Formation of a nitrosyl complex with Fe(II) leads to labilization of a *trans* axial (proximal) histidine ligand in the protein backbone, and the resulting change in the protein conformation is believed to activate the enzyme for catalytic formation of the secondary messenger cyclic-guanylyl monophosphate (cGMP) from guanylyl triphosphate (GTP).[9] In cytochrome c-oxidase, the NO mediated reduction of Cu(II) to Cu(I) is presumed to play the key role in regulating the electron transport activity of this protein.[10]

On the other way NO is also known to involve in the generation of powerful secondary nitrating and/or oxidizing agents, like NO_2 and peroxynitrite.[11] Thus, interaction of NO with transition metal complexes and their redox behaviour is always an interesting field of research from coordination as well as bioinorganic chemistry perspective.

Our laboratory has been actively involved in studying the binding and activation of NO/NO_2 with/by transition metal ions. Biological relevance of copper ion makes it attractive for those studies. For instance: in recent reports of the reaction of NO with $[Cu(TEAEA)(CH_3CN)]^{2+}$, and $[Cu(TIAEA)(CH_3CN)]^{2+}$, {TEAEA = *tris*(2-ethylaminoethyl)amine; TIAEA = *tris*(2-isopropylaminoethyl)amine} complexes, reduction of copper(II) center has been reported to proceed through the formation of a thermally unstable $[Cu^{II}\text{-NO}]$ intermediate (Scheme 1.1).[12]

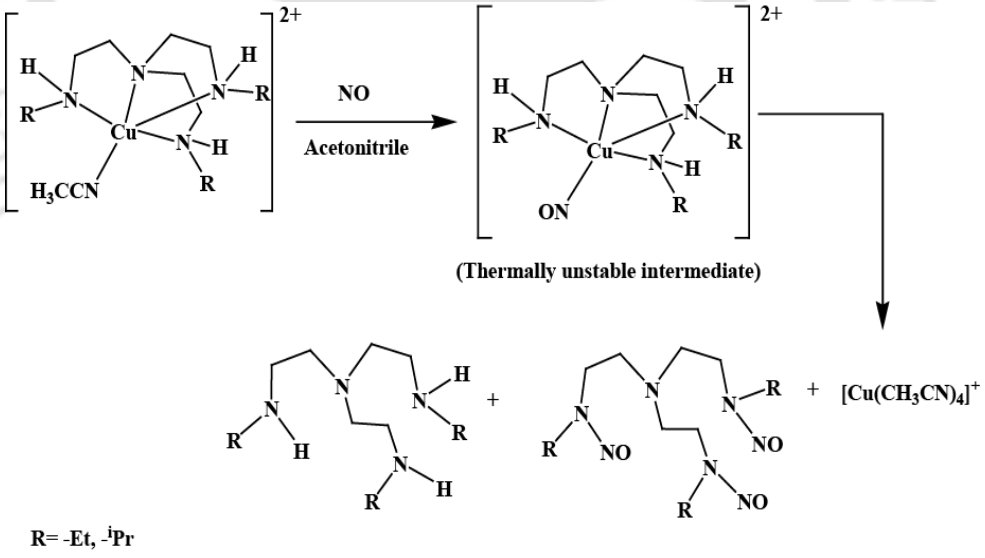

Scheme 1.1

Spectral evidences of the formation of $[Cu^{II}\text{-NO}]$ intermediate have been reported in the reaction of NO with $[Cu(TAEA)(CH_3CN)]^{2+}$, **1.1;** $[Cu(PYMEA)_2]^{2+}$, **1.2** and $[Cu(BAEA)(CH_3CN)]^{2+}$, **1.3** {TAEA = *tris*(2- aminoethyl)amine; PYMEA = pyridine-2-

methylamine and BAEA = *bis*(2-aminoethyl)amine}complexes. In the FT-IR spectra of the acetonitrile solutions of complexes **1.1**, **1.2** and **1.3** after addition of NO a new intense and sharp band was found to appear at ~1650 , 1642 and 1635 cm^{-1} respectively. These were assigned as the stretching of NO (ν_{NO}) coordinated to the Cu(II) center. These were found to disappear with time, indicating the unstable nature of the intermediate.[13]

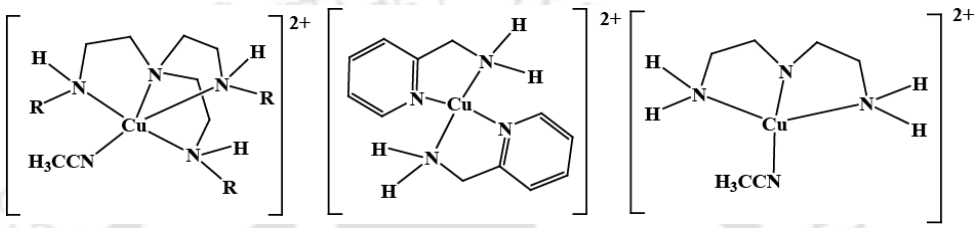

(a) (b) (c)

Figure 1.1. Copper complexes (a) **1.1**, (b) **1.2** and (c) **1.3**.

In another case we have reported a Cu(II) complex of a bi-dentate ligand, *bis*(2-ethyl-4-methyl-imidazol-5yl)methane upon reaction with NO gas formed the corresponding Cu(II)-nitrosyl complex. That nitrosyl complex on reaction with water afforded the corresponding Cu(I)-nitrite complex. This is the first example of structurally characterized Cu(I)-(η^2-O,O) nitrite complex with N-donor ligand (Scheme 1.2).[14]

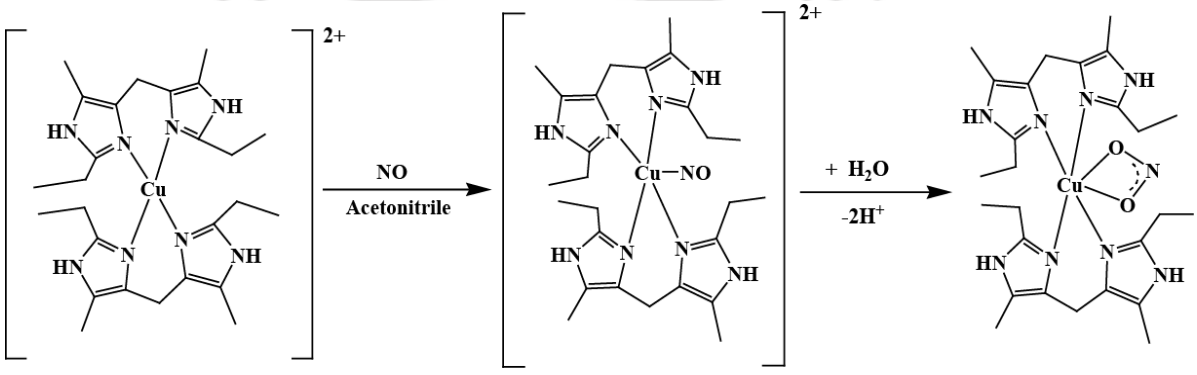

Scheme 1.2

In literature, most of the examples of metal nitrosyls include iron and copper owing to their biological relevance. Other first row transition metal ions have not been explored that much though some of them show interesting reactivity towards NO. For example, cobalt dinitrosyls nitrosylate alkene double bonds to result in corresponding *bis*-nitroso compounds;[15] they catalyse the disproportionation of NO which is industrially important.[15] Heme-cobalt systems have been studied more in comparison to the non-heme systems.[16] A few representative examples for non-heme are as follows:

1.2 Cobalt nitrosyls

Sacconi's group reported structurally characterized Co-NO complexes using the tripod like ligands *tris*(2-diphenylphosphinoethyl)amine, and *tris*(2-diphenylarsinoethyl)amine, having the donor atom sets NP_3 and NAs_3 respectively.[17] The metal nitrosyl complexes with the formula [Co(NO)L]X; {L = NP_3, NAs_3; X = I, NO_3, BF_4, BPh_4} had been characterized by X-ray crystallography. The geometry of the cobalt complexes are tetrahedral in nature complex **1.4** ($[Co(NO)NP_3]^+$).

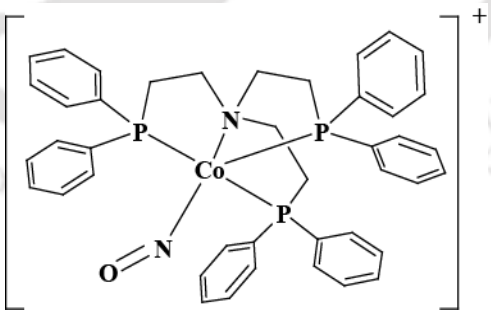

Figure 1.2. Cobalt complex **1.4**.

Later Crimmin *et al*. reported a number of four and five coordinated $\{Co(NO)_2\}^{10}$ complexes by salt-metathesis reactions of $[(TMEDA)Co(NO)_2][BPh_4]$ {TMEDA= N^1,N^1,N^2,N^2-tetramethylethane-1,2-diamine} with various mono-anionic ligands, along

with their reaction with alkenes (Scheme 1.3).[18] These four coordinated complexes are thermally robust and readily isolable species, while five coordinate complexes are thermally unstable transient intermediates, readily undergo dissociation of an NO ligand.[18] These latter complexes were trapped by alkenes to form the corresponding metal dinitrosoalkane complexes.

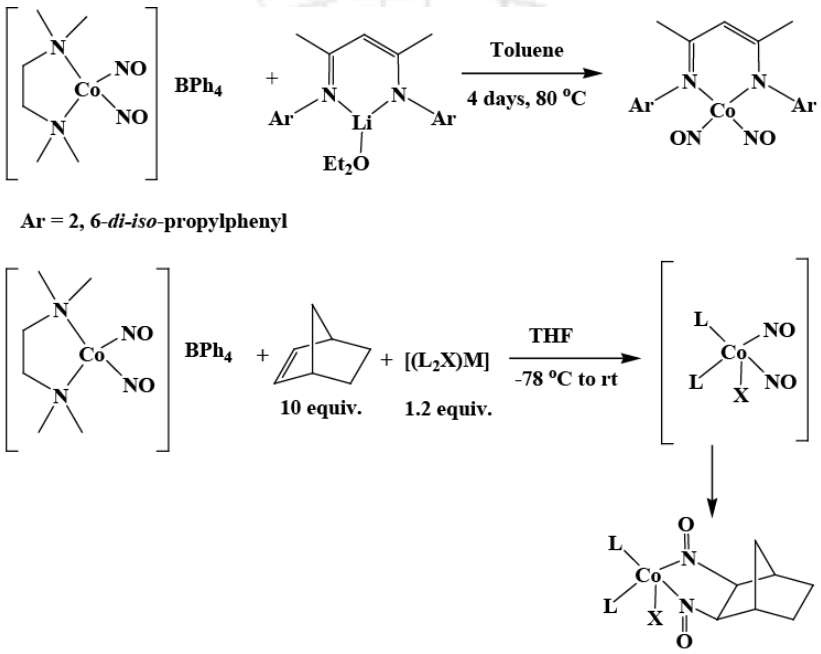

Scheme 1.3

H_2DATI-4, {5-(dimethylamino)-*N*-(((E)-7-((4-((E)-7-(((5-(dimethylamino)naphthalen-1-yl)sulfonyl)imino)cyclohepta-1,3,5-trien-1-yl)amino)butyl)imino)cyclohepta-1,3,5-trien-1-yl)naphthalene-1-sulfonamide}, was reported as a transition metal based fluorogenic sensor, showing a positive fluorescent signal in response to NO through the formation of transition metal nitrosyl complex. The fluorescence of the ligand was quenched by Co^{II}, in absence of NO; however, in presence of NO one portion of the fluorescent ligand gets detached from the quenching environment and turns the fluorescence "on". (Scheme 1.4)[19]

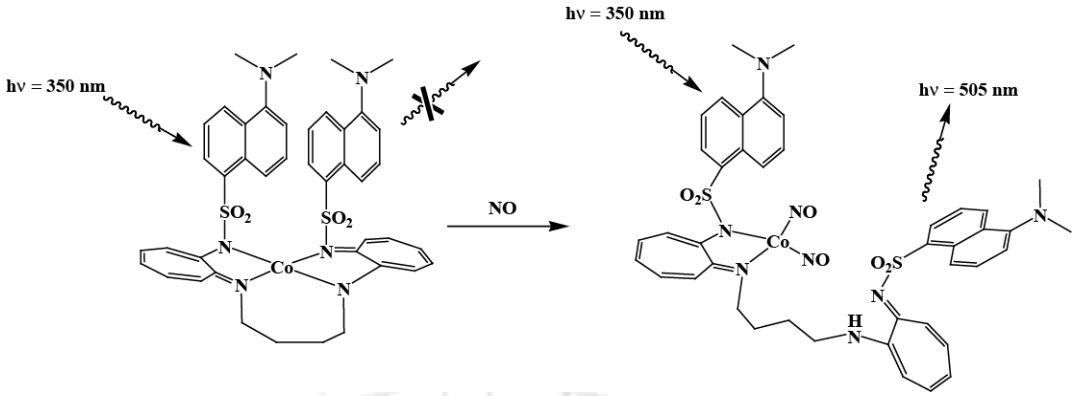

Scheme 1.4

Tropocoronand family of ligands are known to modulated the physical and chemical properties of their transition metal ion complexes with the change of the macrocyclic ring size and flexibility. Lipard's group showed the influence of tetraazamacrocyclic tropocornand (TC) ligands on the NO reactivity of their Co(II) complexes. They had found that [Co(TC-3,3)], [Co(TC-4,4)] and [Co(TC-5,5)] react with NO and preferentially form $\{CoNO\}^8$ species **1.5**, **1.6** and **1.7** respectively, whereas exposure of [Co(TC-6,6)] to NO results in cobalt nitrite complex through the formation of $\{Co(NO)_2\}^{10}$ intermediate **1.8**.[20]

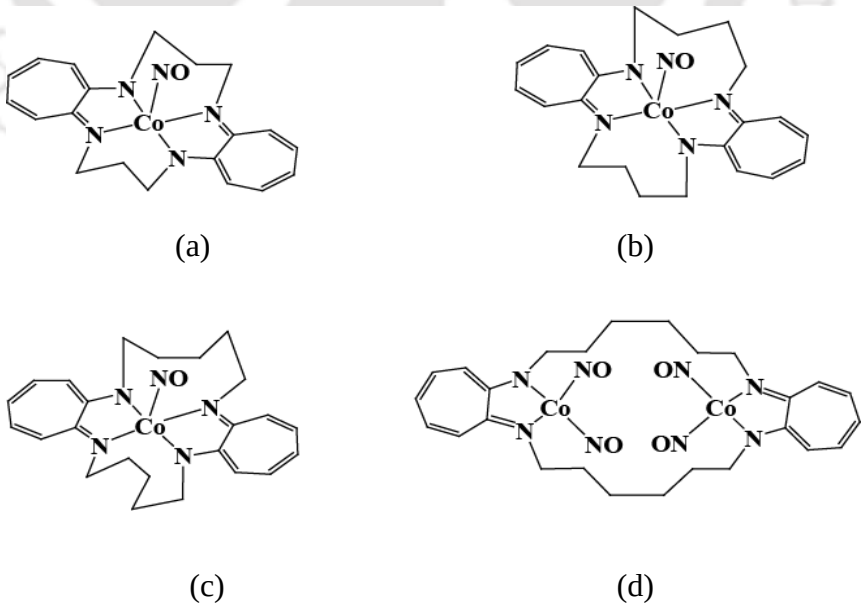

Figure 1.3. Cobalt nitrosyl complexes (a) **1.5**, (b) **1.6**, (c) **1.7** and (d) **1.8**.

The redox chemistry of NO to its reduced analogues such as nitroxyl (HNO/NO^-), has not been extensively studied, due to its rapid dimerization and dehydration of HNO to N_2O and H_2O. Recently, Harrop *et al* reported an example of proton-induced reactivity of NO^- from a $\{CoNO\}^8$ complex with {(*N*^{1}*E*, *N*^{2}*E*)-*N*^{1},*N*^{2}-*bis*((1H-pyrrol-2-yl)methylene)-4,5-dichloro-benzene-1,2-diamine}.[21] Reaction of $\{CoNO\}^8$ complex of this ligand with H^+ reported to generate the HNO donating intermediate towards HNO targets such as Fe(II)-heme, PPh_3 (Scheme 1.5). On the other hand the HNO donating intermediate ultimately leads to the formation of the Co-dinitrosyl complex in the absence of an HNO target (Scheme 1.6).[21]

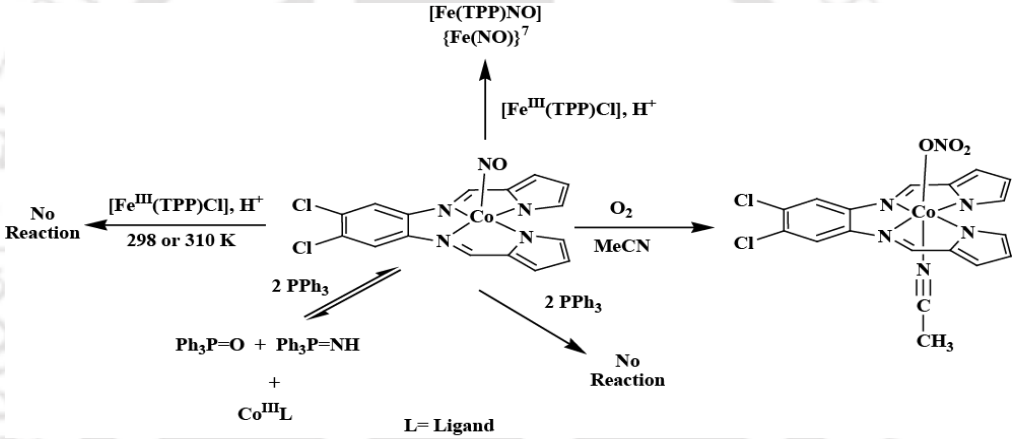

Scheme 1.5

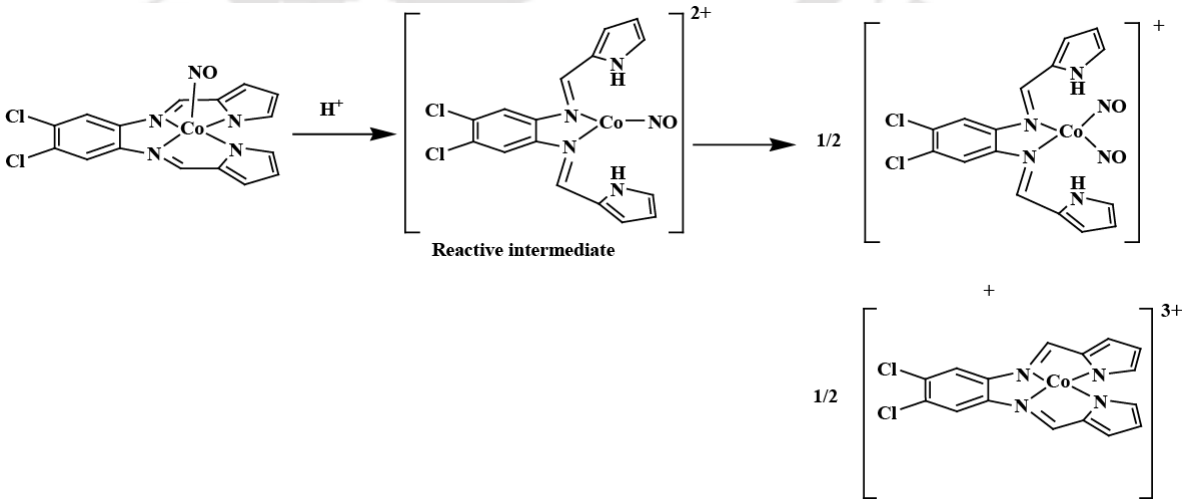

Scheme 1.6

Tomson *et al*. reported an example of antiferromagnetically coupled Co(II)-NO^- species. They prepared the novel $\{CoNO\}^9$ species $Tp^*Co(NO)$ {Tp^* = hydro-*tris*(3,5-Me_2-pyrazolyl)borate} by the reaction of $[(TMDA)Co(NO)_2](BPh_4)$ and KTp^*(Scheme 1.7).[22]

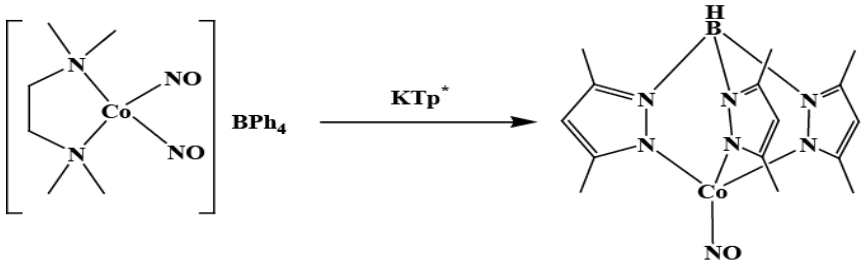

Scheme 1.7

Nam's group recently reported the reaction of Co(III)-nitrosyl complexes with superoxide ended to yield Co(II)-nitrite complexes *via* the putative formation of peroxynitrite intermediate (Scheme 1.8).[23]

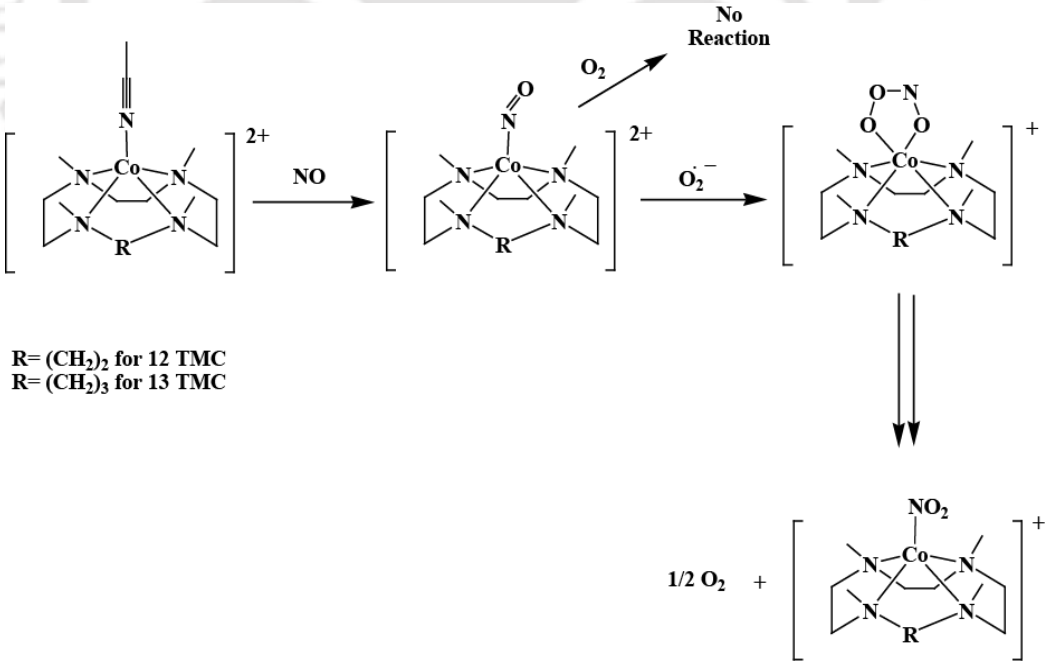

Scheme 1.8

1.3 Nickel nitrosyls

Example of cationic nickel nitrosyls complexes (**1.9**, **1.10**) with aliphatic triphosphines have been reported by Meek's group in early seventy.[24]

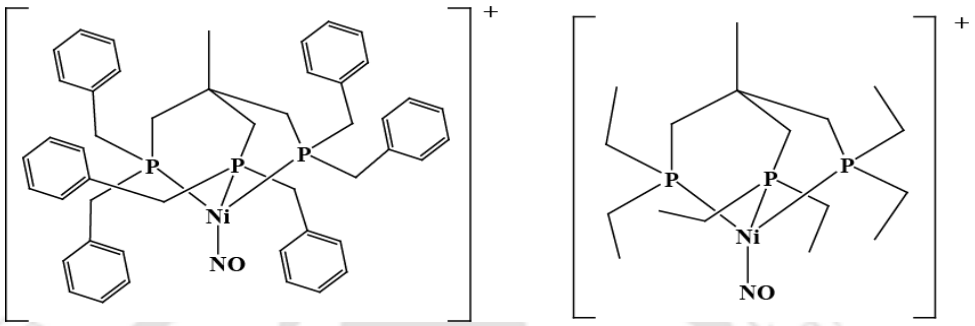

(a) (b)

Figure 1.4. Nickel nitrosyl complexes (a) **1.9** and (b) **1.10**.

Metalloenzymes of the category [nFe-nS] (n=2 or 4) can be activated by NO in biological as well as model systems, being motivated from this activation phenomena nickel complexes of similar category were prepared and their reactivity have studied (Scheme 1.9).[25] These includes the examples of anionic complexes (**1.11**, **1.12**) containing {Ni(NO)}[10].

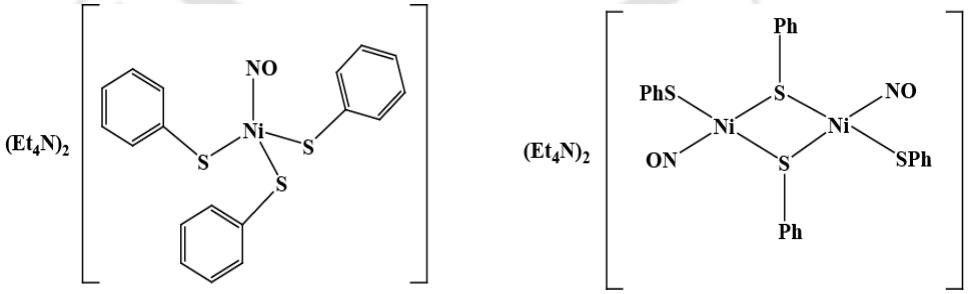

(a) (b)

Figure 1.5. Anionic nickel nitrosyl complexes (a) **1.11** and (b) **1.12**.

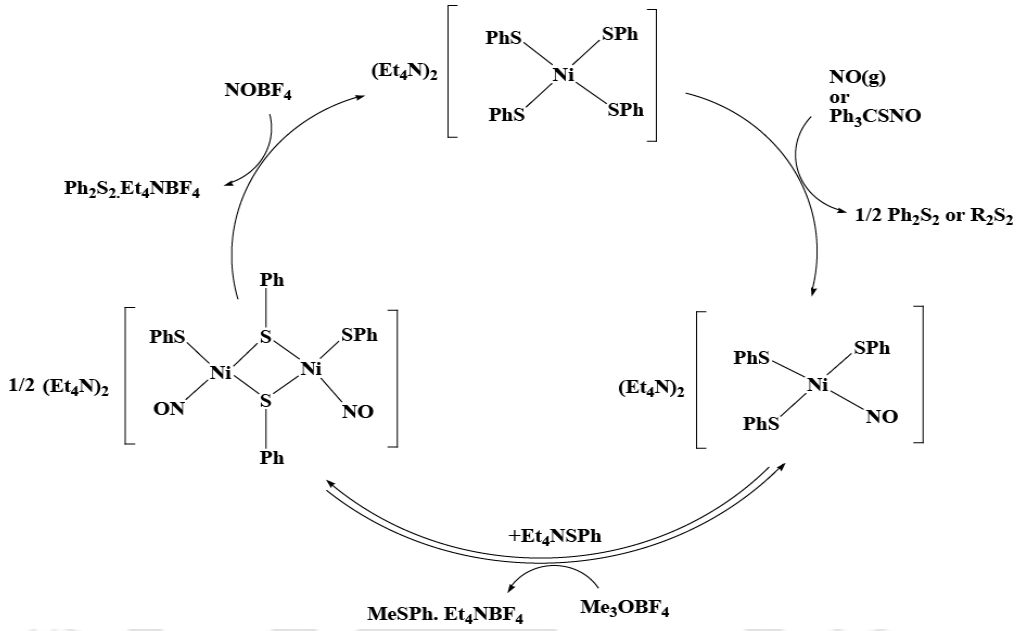

Scheme 1.9

It would be worth mentioning that most of the nickel nitrosyls are tetrahedral and transition metal nitrosyls with coordination number of three are rare. Warren's group reported three coordinated *β*-diketiminato nickel nitrosyl complexes from Ni(I)-lutidine and Ni(II)-alkyl precursors (Scheme 1.10, 1.11).[26]

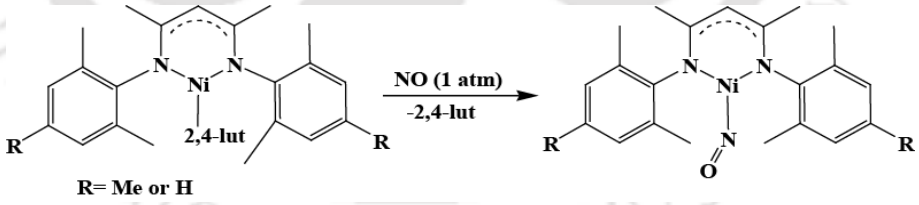

Scheme 1.10

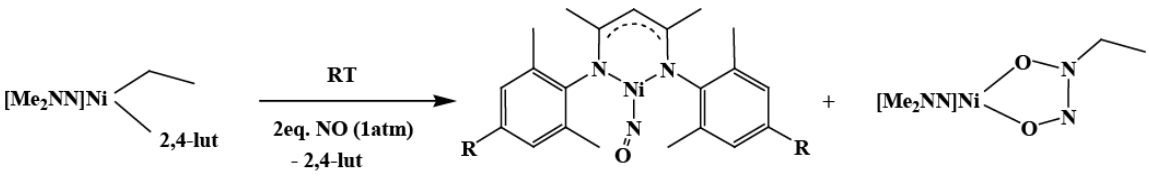

Scheme 1.11

In continuation of that tri-coordinated N-heterocyclic carbene nickel nitrosyl complexes

were also reported by same group (**1.13**, **1.14**, **1.15** and Scheme 1.12).[26]

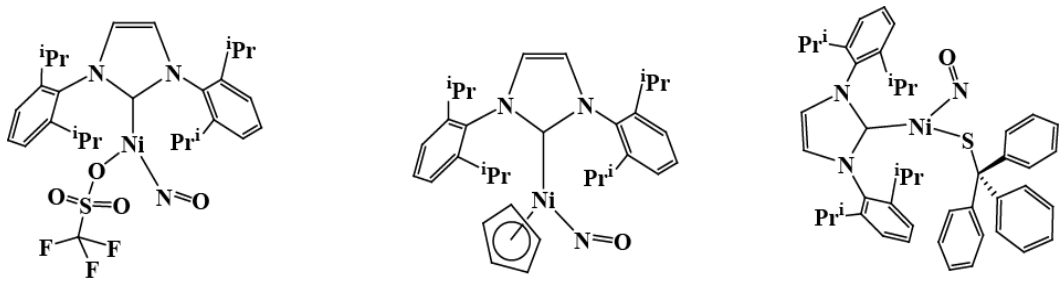

(a) (b) (c)

Figure 1.6. Tri-coordinated nickel nitrosyl complexes (a) **1.13**, (b) **1.14** and (c) **1.15**.

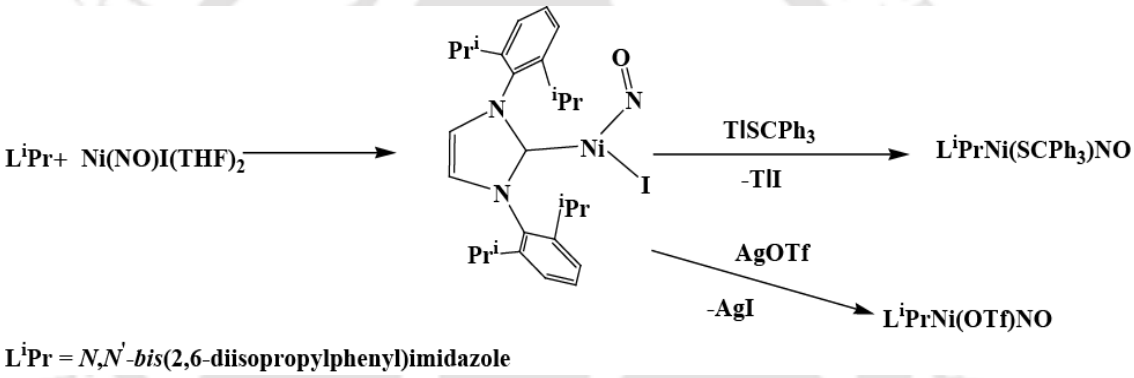

Scheme 1.12

A cationic nickel nitrosyl complex $[Ni(NO)(CH_3NO_2)][PF_6]$ was reported by Hayton's group (Scheme 1.13).[27]

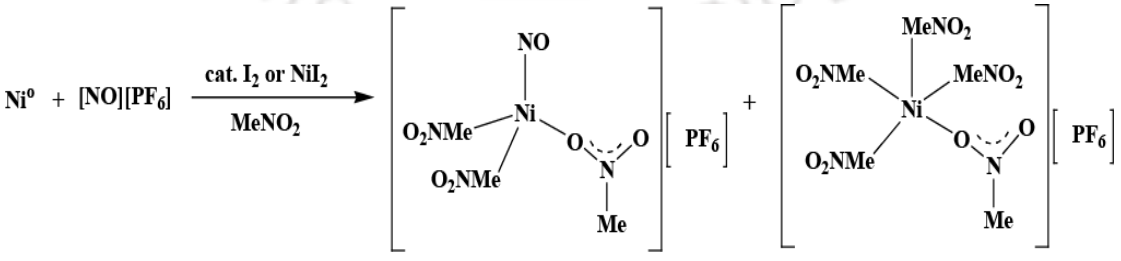

Scheme 1.13

Nitromethane as a ligand, remains weakly coordinated to the metal centre, and hence has easily been displaced by a variety of donors, such as Et_2O, CH_3CN etc. (**1.16**, **1.17**).

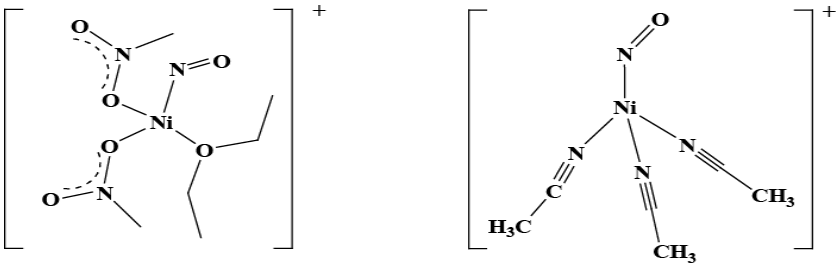

(a) (b)

Figure 1.7. Cationic-nickel nitrosyl complexes (a) **1.16** and (b) **1.17**.

Another report showed the NO release from nickel nitrosyl complex induced by one electron oxidation.[28] The reaction of nitrosyl complex with $AgPF_6$ or $[NO][PF_6]$ in acetonitrile results in the formation of Ni(II) complex and the release of NO as gas (Scheme 1.14). The oxidation of the nitrosyl complex with TEMPO (2,2,6,6-tetramethylpiperridine-1-oxyl) generates NO through the cleavage of Ni–NO bond (Scheme 1.15).

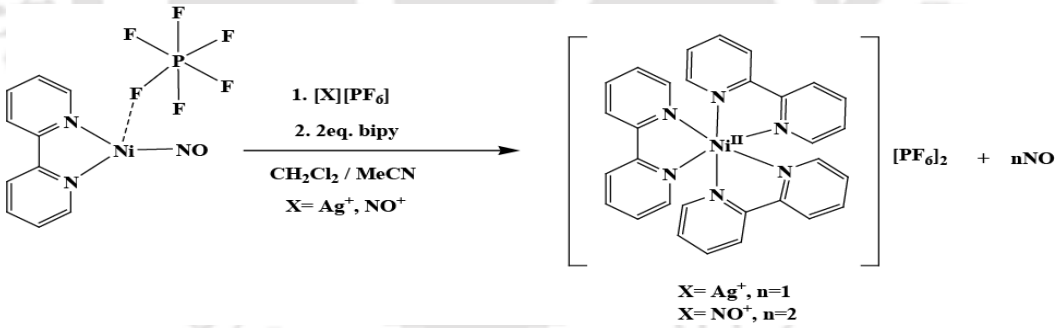

Scheme 1.14

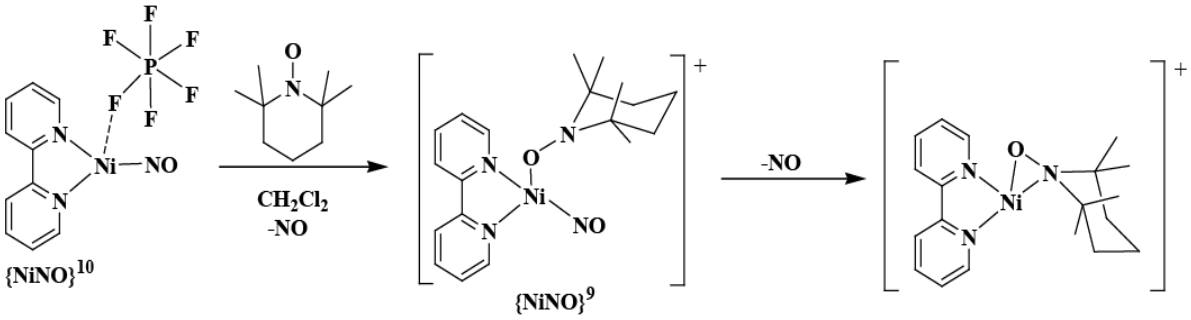

Scheme 1.15

The very nitrosyl complex resulted in the formation of the *cis*-$[N_2O_2]^{2-}$ as intermediate, in presence of excess NO, this then releases N_2O.[29] The plausible reaction pathway and the involved redox couples were investigated in details. [29]

1.4 A brief discussion of nitrogen dioxide and its reactivity

In contrast to NO, NO_2 is known as a strong lipophilic oxidant and can trigger lipid auto-oxidation and oxidative nitration of aromatic amino acids, particularly tyrosine.[30,31] In numerous diseases including neurodegenerative conditions, cardiovascular disorders, diabetes, Alzheimer's disease and protein tyrosine nitration have been observed.[32-36]

In biological system, *via* several mechanisms NO_2 can be generated, including the oxidation of NO by O_2, the decomposition of $ONOO^-$, and the oxidation of nitrite (NO_2^-) by hydrogen peroxide (H_2O_2) in presence of peroxidases.[37, 38]

Groves *et al*. had reported that metMb-PN (Fe^{III}-$OONO^-$) formed, decomposes to nitrate and NO_2 (Scheme 1.16).[39]

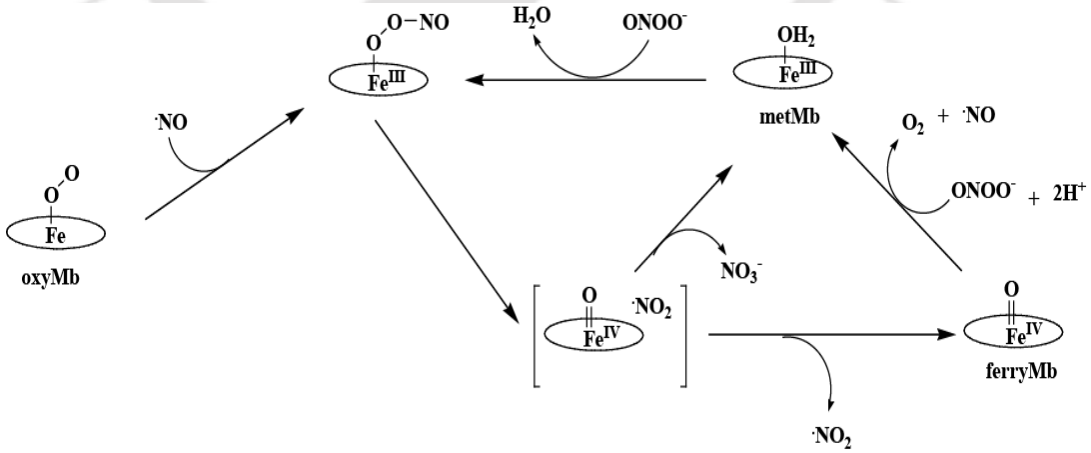

Scheme 1.16

Recently it has been established that activation of various heme peroxidases (MPO/LPO)

by H_2O_2 can promote the oxidation of NO_2^- to the formation of NO_2 as intermediate that is capable of nitrating aromatic substrates and proteins (Scheme 1.17).[40]

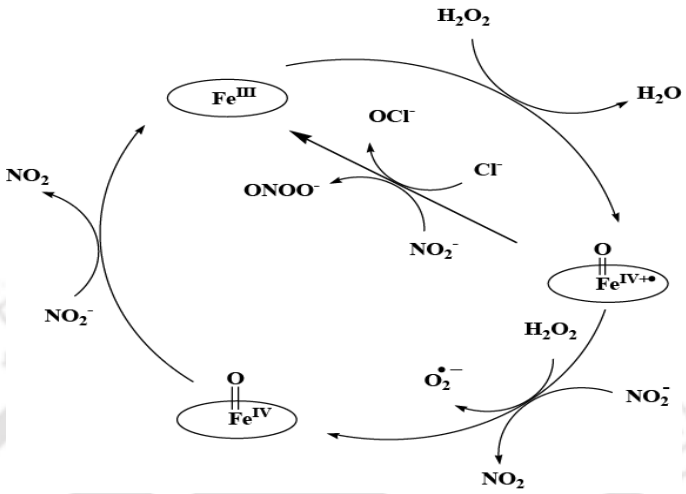

Scheme 1.17

Grault *et al*. reported tyrosine nitration catalysed by cupric ion through a Fenton-like catalytic pathway which eventually lead to the formation of NO_2 and tyrosyl radical (Scheme 1.18).[40]

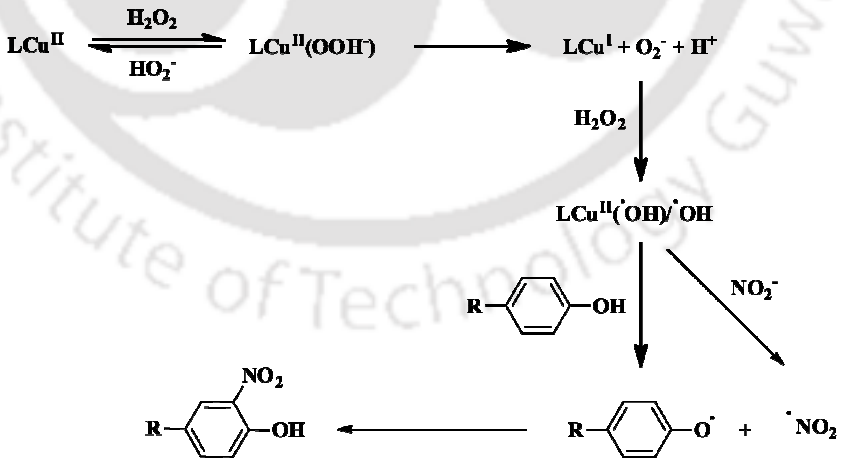

Scheme 1.18

Recently, Huang *et al*. reported the example of metal based highly selective NO_2 sensor. Ni(II)-complex of dithiocarbamate ligands derived from the *ortho* and *para* isomers of

sulforhodamine B fluorophores had been exemplified to sense NO_2 selectively (Scheme 1.19).[41]

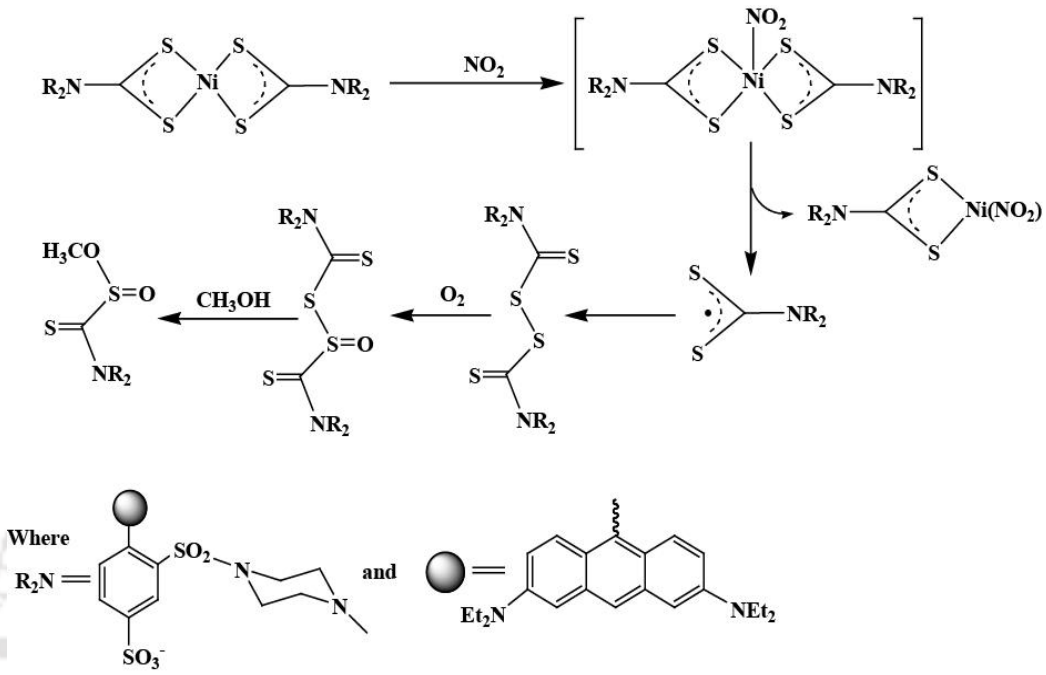

Scheme 1.19

Recently, our group reported the NO_2 reactivity of Cu(II) complexes **1.18** and **1.19**, with ligands {2,4-di-*tert*-butyl-6-(((2-dimethylamino)ethyl)(isopropyl)amino)methyl)phenol} and {6,6'-(((2-(dimethylamino)ethyl)azanediyl)*bis*(methylene))*bis*(2,4-di-*tert*-butyl phenol)} respectively. Both the complexes show the phenol ring nitration induced by the unprecendented reduction of Cu(II) centre by NO_2 (Scheme 1.20).[42]

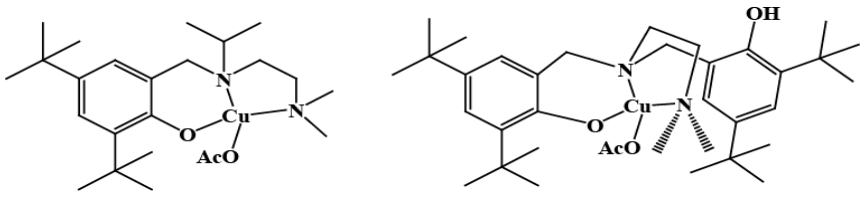

(a) (b)

Figure 1.8. Copper complexes (a) **1.18** and (b) **1.19**.

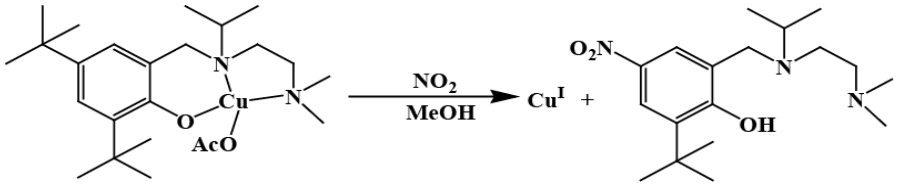

Scheme 1.20

Cu(II) complexes of two fluorophoric ligands, {2-{[anthracene-9-ylmethyl-(2-dimethylamino-ethyl)-amino]-methyl}-4,6-di-*tert*-butyl-phenol} and {5-dimethylamino-naphthalene-1-sulfonic acid (3,5-di-*tert*-butyl-2-hydroxy-benzyl)-(2-dimethylamino-ethyl)-amide}, respectively, had been utilized for fluorometric sensing of NO_2. The quenched fluorescence of the ligands in the complexes found to restore upon reaction with NO_2 (Scheme 1.21).[43]

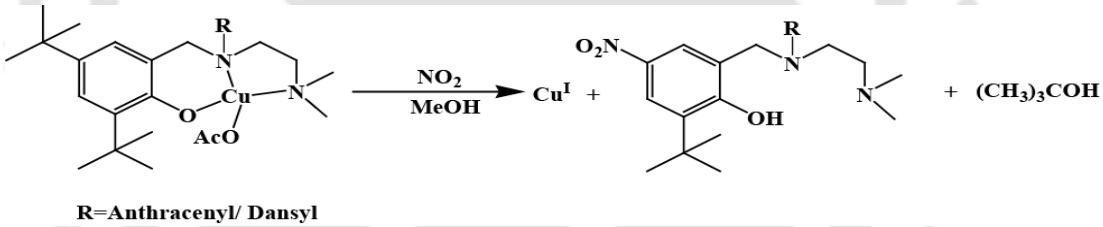

Scheme 1.21

The NO_2 reactivity of Cu(II) complexes of N_2O_2 type ligands {6,6'-(((pyridin-2-ylmethyl) azanediyl)-*bis*(methylene))*bis*(2,4-di-*tert*-butylpheno)} and {2,4-di-*tert*-butyl-6-(((3-(*tert*-butyl)-2-hydroxy-5-methylbenzyl)(pyridin-2-yl-ethyl)amino)methyl)phenol)} reported to result nitration at phenol ring. But spectroscopic studies suggest that the reaction poceeds through a phenoxyl radical complex formation not through the reduction of Cu(II) centre (Scheme 1.22).[44]

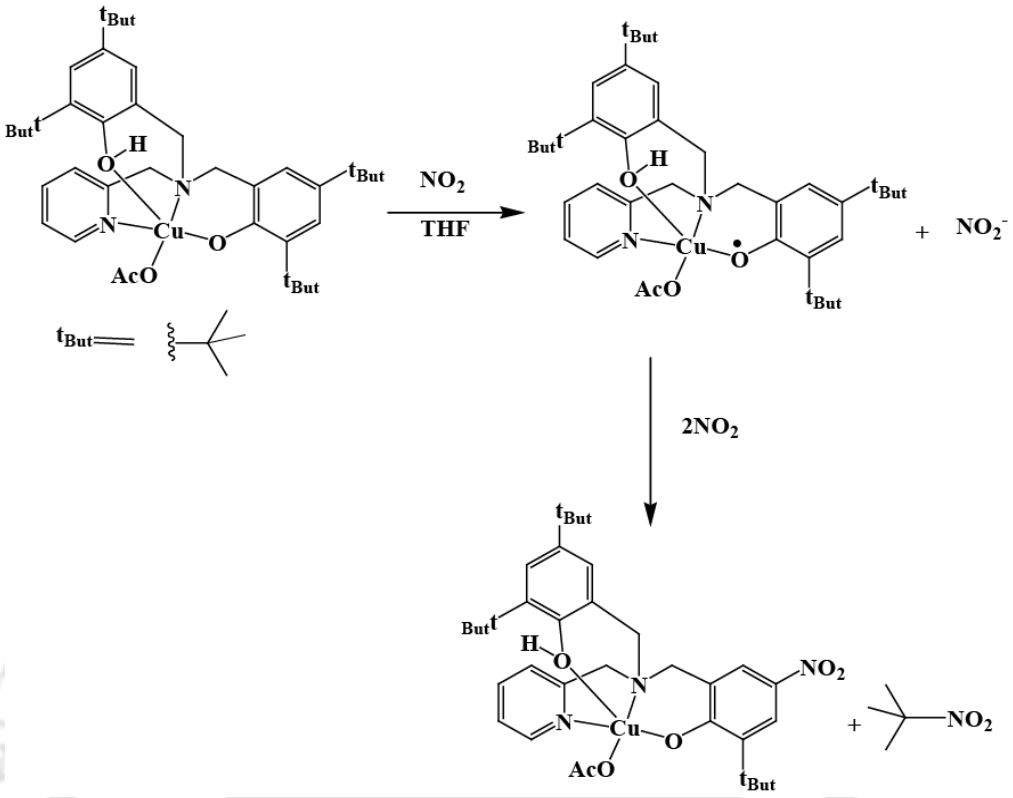

Scheme 1.22

Oxo transfer from NO_2 to coordinated nitrito group in a Cu(II) complex reported recently. Cu(II) complex of {4,6-di-*tert*-butyl-2-((2-picolyl(isopropyl) amino) methyl)-phenol} reacted with equivalent amount of NO_2 leading to the reduction of Cu(II), with simultaneous nitration at the phenol ring of the ligand. That resulted in the *in situ* formation of intermediate Cu(I) complex of the nitrated ligand. Further addition of NO_2, Cu(I) center simultiniously oxidised and resulted in corresponding Cu(II)-O-nitrito complex formation. Subsequent addition of NO_2 lead to an oxo transfer reaction resulting in the formation of O-nitrato complex, with concomitant release of NO. (Scheme 1.23).[45]

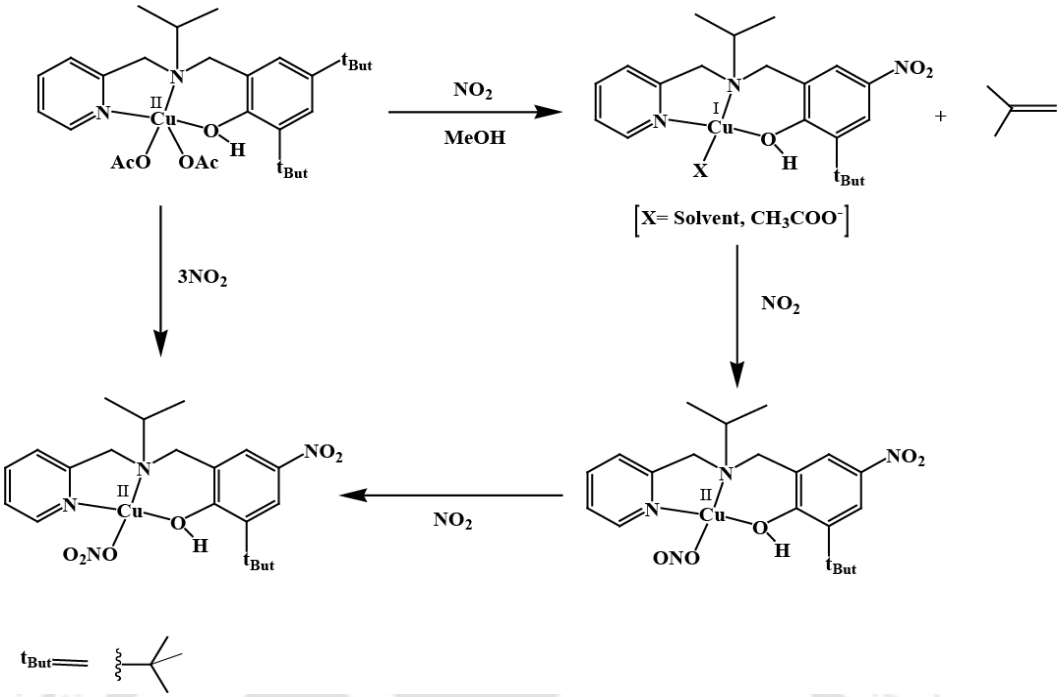

Scheme 1.23

The present thesis originates from our interest to understand the basic chemistry involved in the binding to and activation of NO_x (x = 1 and 2) by transition metal ions. Amongst the first row transition metal ions, iron and copper have been studied well towards NO binding and activation. However, nickel and cobalt have not been studied to that extent, though both of these are known to exhibit interesting activity towards NO. In this context, as a continuation of our study, first two chapters of this thesis deals with NO reactivity of Co(II) and Ni(II) centers. Successively, the redox behaviour of the coordinated NO and its disproportionation to N_2O have been studied. In the next two chapters, relatively less explored reactivity of NO_2 with Ni(II) complexes have been discussed. In these cases, reduction of Ni(II) center by NO_2 and oxo transfer reactions from NO_2 to the metal coordinated nitrite (NO_2^-) ion have been observed.

1.5 References

(1) (a) Moncada, S.; Palmer, R. M. J.; Higgs, E. A. *Pharmacol. Rev.* **1991**, *43*, 109. (b) Culotta, E.; Koshland, D. *Science* **1992**, *258*, 1862. (c) Furchgott, R. F. *Angew. Chem. Int. Ed.* **1999**, *38*, 1870. (d) Ignarro, L. J. *Angew. Chem. Int. Ed.* **1999**, *38*, 1882. (e) Murad, F. *Angew. Chem. Int. Ed.* **1999**, *38*, 1856.

(2) *Nitric Oxide: Biology and Pathobiology*; Ignarro, L. J., Ed.; Academic Press: San Diego, **2000**.

(3) (a) Ford, P. C.; Bourassa, J.; Lee, K. B.; Lorkovic, I.; Boggs, S.; Kudo, S.; Laverman, L. *Coord. Chem. Rev.* **1998**, *171*, 185. (b) Ford, P. C.; Lorkovic, I. M. *Chem. Rev.* **2002**, *102*, 993. (c) Butler, A. R.; Megson, I. L. *Chem. Rev.* **2002**, *102*, 1155.

(4) (a) Hayton, T. W.; Legzdins, P.; Sharp, W. B. *Chem. Rev.* **2002**, *102*, 935. (b) Hsu, I.-J.; Hsieh, C. H.; Ke, S. C.; Chiang, K.-A.; Lee, J.- M.; Chen, J.-M.; Jang, L.-Y.; Lee, G.-H.; Wang, Y.; Liaw, W.-F. *J. Am. Chem. Soc.* **2007**, *129*, 1151.

(5) (a) Cheng, L.; Richter-Addo, G. B. *Binding and Activation of Nitric Oxide by Metalloporphyrins and Heme*; Academic Press: New York, **2000**; Vol. *4*, Chapter 33. (b) Afshar, R. K.; Patra, A. K.; Mascharak, P. K. *J. Inorg. Biochem.* **2005**, *99*, 1458.

(6) Averill, B. A. *Chem. Rev.* **1996**, *96*, 2951.

(7) Richter-Addo, G. B.; Legzdins, P. *Metal Nitrosyls*; Oxford University: New York, **1992**.

(8) (a) Kim, S.; Deinum, G.; Gardner, M. T.; Marletta, M. A.; Babcock, G. T. *J. Am. Chem. Soc.* **1996**, *118*, 8769. (b) Burstyn, J. N.; Yu, A. E.; Dierks, E. A.; Hawkins, B. K.; Dawson, J. H. *Biochemistry* **1995**, *34*, 5896.

(9) Torres, J.; Svinstunenko, D.; Karlsson, B.; Cooper, C. E.; Wilson, M. T. *J. Am. Chem. Soc.* **2002**, *124*, 963.

(10) Cooper, C. E.; Torres, J.; Sharpe, M. A.; Wilson, M. T. *FEBS Lett.* **1997**, *414*, 281.

(11) (a) Schopfer, M. P.; Mondal, B.; Lee, D.-H.; Sarjeant, A. A. N.; Karlin, K. D. *J. Am. Chem. Soc.* **2009**, *131*, 11304. (b) Maiti, D.; Lee, D.-H.; Sarjeant, A. A. N.; Pau, M. Y. M.; Solomon, E. I.; Gaoutchenova, K.; Sundermeyer, J.; Karlin, K. D. *J. Am. Chem. Soc.* **2008**, *130*, 6700. (c) Park, G. A.; Deepalatha, S.; Simona, C. P.; Lee, D.-H.; Mondal, B.; Sarjeant, A. A. N.; Rio, D. Del.; Pau, M. Y. M.; Solomon, E. I.; Karlin, K. D. *J. Biol. Inorg. Chem.* **2009**, *14*, 1301. (d) Kumar, V.; Kalita, A.; Mondal, B. *Dalton Trans.* **2013**, *42*, 16264.

(12) Sarma, M.; Kalita, A.; Kumar, P.; Singh, A.; Mondal, B. *J. Am. Chem. Soc.* **2010**, *132*, 7846.

(13) (a) Sarma, M.; Singh, A.; Mondal, B. *Inorg. Chim. Acta* **2010**, *363*, 63. (b) Sarma, M.; Mondal, B. *Inorg. Chem.* **2011**, *50*, 3206.

(14) Kalita, A.; Kumar, P.; Deka, R. C.; Mondal, B. *Chem. Commun.* **2012**, *48*, 1551.

(15) (a) Brunner, H. *J. Organomet. Chem.* **1968**, *12*, 517. (b) Brunner, H.; Loskot, S. *Angew. Chem. Int. Ed.* **1971**, *10*, 515. (c) Weiner, W. P.; White, M. A.; Bergman, R. G. *J. Am. Chem. Soc.* **1981**, *103*, 3612. (d) Becker, N. P.; Bergman, R. G. *J. Am. Chem. Soc.* **1983**, *105*, 2985. (e) Becker, P. N.; Bergman, R. G. *Organometallics* **1983**, *2*, 787. (f) Weiner, W. P.; Hollander, F. J.; Bergman, R. G. *J. Am. Chem. Soc.* **1984**, *106*, 7462.

(16) (a) Richter-Addo, G. B.; Hodge, S. J.; Yi, G.-B.; Khan, M. A.; Ma, T.; Caemelbecke, E. V.; Guo, N.; Kadish, K. M. *Inorg. Chem.* **1996**, *35*, 6530. (b) Zhu,

X-Q.; Li, Q.; Hao, W-F.; Cheng, J-P. *J. Am. Chem. Soc*. **2002**, *124*, 9887. (c) Chuang, C-H.; Liaw, W-F.; Hung, C-H. *Angew. Chem. Int. Ed*. **2016**, *55*, 5190.

(17) Vaira, M. D. I.; Ghilardi, C. A.; Sacconi, L. *Inorg. Chem.***1975**, *15*, 1555.

(18) Crimmin, M. R.; Roseburgh, L. E.; Tomson, N. C.; Weyhermuller, T.; Bergman, R. G.; Toste, F. D.; Wieghardt, K. *J. Organomet. Chem.* **2011**, *696*, 3974.

(19) (a) Franz, K. J.; Singh, N.; Lipard, S. J. *Angew. Chem. Int. Ed*. **2000**, *39*, 2120. (b) Franz, K. J.; Singh, N.; Spingler, B.; Lipard, S. J. *Inorg. Chem.* **2000**, *39*, 4081.

(20) (a) Franz, K. J.; Doerrer, L. H.; Spingler, B.; Lipard, S. J. *Inorg. Chem.* **2001**, *40*, 3774. (b) Kozhukh, J.; Lipard, S. J. *J. Am. Chem. Soc.* **2012**, *134*, 11120.

(21) Rhine, M. A.; Rodrigues, A. V.; Urbauer, R. J. B.; Urbauer, J. L.; Stemmler, T. L.; Harrop, T. C. *J . Am. Chem. Soc.* **2014**, *136*, 12560.

(22) Tomson, N. C.; Crimmin, M. R.; Petrenko, T.; Roseburgh, L. E.; Sproules, S.; Boyd, W. C.; Bergman, R. G.; DeBeer, S.; Toste, F. D.; Wieghardt, K. *J. Am. Chem. Soc*. **2011**, *133*, 18785.

(23) Kumar, P.; Lee, Y. M.; Park, Y. J.; Siegler, M. A.; Karlin, K. D.; Nam, W. *J. Am. Chem. Soc*. **2015**, *137*, 4284.

(24) Berglund, D.; Meek, D. W. *Inorg. Chem.* **1972**, *11*, 1493.

(25) Tennyson, A. G.; Dhar, S.; Lipard, S. J. *J. Am. Chem. Soc*. **2008**, *130*, 9780.

(26) (a) Puiu, S. C.; Warren, T. H. *Organometallics* **2003**, *22*, 3974. (b) Varonka, M. S.; Warren, T. H. *Organometallics* **2010**, *29*, 717.

(27) Wright, A. M.; Wu, G.; Hayton, T. W. *Inorg. Chem.* **2011**, *50*, 11746.

(28) Wright, A. M.; Zaman, W. H.; Wu, G.; Hayton, T. W. *Inorg. Chem.* **2013**, *52*, 3207.

(29) (a) Wright, A. M.; Wu, G.; Hayton, T. W. *J. Am. Chem. Soc.* **2012**, *134*, 9930. (b) Wright, A. M.; Zaman, W. H.; Wu, G.; Hayton, T. W. *Inorg. Chem.* **2014**, *53*, 3108.

(30) Cosby, K.; Partovi, K. S.; Crawford, J. H.; Patel, R. P.; Reiter, C. D.; Martyr, S.; Yanq, B. K.; Waclawiw, M. A.; Zalos, G.; Xu, X.; Huang, K. T.; Shields, H.; Kim-Shapiro, D. B.; Schechter, A. N.; Cannon, R. O.; Gladvin, M. T. *Nat. Med.* **2003**, *9*, 1498.

(31) Kirsch, M.; Korth, H. G.; Sustmann, R.; de Groot, H. *Biol. Chem.* **2002**, *383*, 389.

(32) Ferrer-Sueta, G.; Radi, R. *ACS Chem. Biol.* **2009**, *4*, 161.

(33) Abello, N.; Kerstjens, H. A. M.; Postma, D. S.; Bischoff, R. *J. Proteome Res.* **2009**, *8*, 3222.

(34) Radi, R. *Proc. Natl. Acad. Sci. U.S.A.* **2004**, *101*, 4003.

(35) Reynolds, M. R.; Berry, R. W.; Binder, L. I. *Biochemistry* **2007**, *46*, 7325.

(36) Wattanapitayakul, S. K.; Weinstein, D. M.; Holycross, B. J.; Bauer, J. A. *FASEB J.* **2000**, *14*, 271.

(37) Su, J.; Groves, J. T. *J. Am. Chem. Soc.* **2009**, *131*, 12979.

(38) Bian, K.; Gao, Z. H.; Weisbrodt, N.; Murad, F. *Proc. Natl. Acad. Sci. U.S.A.* **2003**, *100*, 5712.

(39) Bourassa, J. L.; Ives, E. P.; Marqueling, A. L.; Shimanovich, R.; Groves, J. T. *J. Am. Chem. Soc.* **2001**, *123*, 5142.

(40) (a) Vliet, A. V.; Eiserich, J. P.; Halliwell, B.; Cross, C. E. *J. Biol. Chem.* **1997**, *272*, 7617. (b) Qiao, L.; Lu, Y.; Liu, Baohong.; Grault, H. H. *J. Am. Chem. Soc.* **2011**, *133*, 19823.

(41) Yan, Y.; Krishnakumar, S.; Yu, H.; Ramishetti, S.; Deng, L. W.; Wang, S.; Huang, L.; Huang, D. *J. Am. Chem. Soc*. **2013**, *135*, 5312.

(42) Kumar, V.; Kalita, A.; Mondal, B. *Dalton Trans.* **2013**, *42*, 16264.

(43) Kumar, V.; Mondal, B. *RSC Adv.* **2014**, *4*, 61944.

(44) Kumar, V.; Ghosh, S.; Saini, A. K.; Mobin, S. M.; Mondal, B. *Dalton Trans.* **2015**, *44*, 19909.

(45) Gogoi, K.; Deka, H.; Kumar, V.; Mondal, B. *Inorg. Chem.* **2015**, *54*, 4799.

Chapter 2

Nitric oxide reactivity of Co(II) complexes: Formation of $\{CoNO\}^8$ and their reactivity

Abstract

Two cobalt complexes, **2.1** and **2.2**, of ligands **L1** and **L2** {**L1** = 6,6'-((1E,1'E)-(((1R,2R)-cyclohexane-1,2-diyl)*bis*(azanylylidene))*bis*(methanylylidene))*bis*(2,4-di-*tert*-butylphenol) ; **L2** = 6,6'-((1E,1'E)-(ethane-1,2-diyl)bis (azanylylidene))*bis*(methanylylidene))*bis*(2,4-di-*tert*-butylphenol)}, respectively, have been synthesized and characterized structurally. Purging of NO gas into the THF solution of complexes **2.1** and **2.2** resulted in the corresponding nitrosyl complexes, **2.3** and **2.4**, respectively, having $\{CoNO\}^8$ configuration. Structural characterization revealed the presence of bent nitrosyl in both the complexes. Addition of superoxide, O_2^-, into the THF solution of **2.3** and **2.4** afforded nitrato (NO_3^-) complexes, **2.5** and **2.6**, respectively, *via* putative formation of corresponding peroxynitrite intermediates.

2.1 Introduction

Reactivity of nitric oxide (NO) with transition metal ions has been the subject of continuous research since NO is discovered to play the fundamental roles in various biophysical processes.[1] Most of the reactivity of NO in biological systems are attributed to its interaction with the metallo-proteins, mostly iorn and copper.[2] NO induces oxidative damage to DNA, lipids, proteins etc. when produced in higher concentration.[3] Being radical in nature, it produces secondary reactive nitrogen species (RNS) such as nitrogen dioxide (NO_2), peroxynitrite ($ONOO^-$) in presence of other oxidants (O_2, H_2O_2 or O_2^-) and/or transition metal ions.[4] Tyrosine nitration is known to occur by ($ONOO^-$) or NO_2 and is used as a diagnostic biomarker for several disease states as it can alter protein functions.[5] However, there are certain metallo-enzymes, such as nitric oxide deoxygenases (NOD) in biological systems to control the level of NO. In NODs, the Fe(III)-superoxide species reacts with NO to result in the biological benign nitrate (NO_3^-) ion. This reaction is believed to proceed through the formation of metal-peroxynitrite intermediate.[6] Transition metal ions are known to play important roles in generation, stabilization, activation for substrate oxidation and thermal isomerization of $ONOO^-$.[7] Extensive studies have been done in this direction with heme-proteins and their models.[8] Recently, the examples involving other transition metal ions in generation and reactivity of $ONOO^-$ are reported though limited. For instance, Clarkson and Basolo reported that a Co-nitrosyl complex reacts with O_2 to result in corresponding nitrite (NO_2^-) product.[9] Similarly, Cu-NO complex reacts with O_2 to result in Cu-peroxynitrite intermediate which decomposes to NO_2^-.[10] Nam and co-workers reported that the reaction of non-heme Cr(IV)-peroxo and Cr^{III}-superoxo complexes with NO lead to the formation of a presumed Cr(III)-peroxynitrite intermediate.[11] We have reported that Cu-NO complexes react with H_2O_2 to

form copper-nitrato complex *via* the thermal decomposition of a presumed Cu-peroxynitrite as intermediate.[12] Recently, Nam and co-workers reported Co(III)-nitrosyl complexes of 12 and 13 membered N-tetramethylated cyclam ligands, [(12-TMC)$Co^{III}(NO)]^{2+}$ and [(13-TMC)$Co^{III}(NO)]^{2+}$ [12-TMC = 1,4,7,10-tetramethyl-1,4,7,10-tetraazacyclododecane] react with superoxide ion to result in corresponding Co(II)-nitrite and O_2 *via* a presumed Co(III)-peroxynitrite intermediate.[13] Hence, the transition metal ion mediated reactions of NO with O_2 or other reactive oxygen species (O_2^{2-} or O_2^-) is of potential interest from the NOD point of view.

This chapter describes synthesis and structure of two cobalt-nitrosyl complexes of **L1** and **L2** {**L1** = 6,6'-((1E,1'E)-(((1R,2R)-cyclohexane-1,2-diyl)*bis*(azanylylidene))*bis*(methanylylidene))*bis*(2,4-di-*tert*-butylphenol), **L2** = 6,6'-((1E,1'E)-(ethane-1,2-diyl)*bis*(azanylylidene))*bis*(methanylylidene))*bis*(2,4-di-*tert*-butylphenol)} ligands and their reactivity with superoxide ion to afford corresponding nitrate complexes *via* Co(III)-peroxynitrite intermediate.

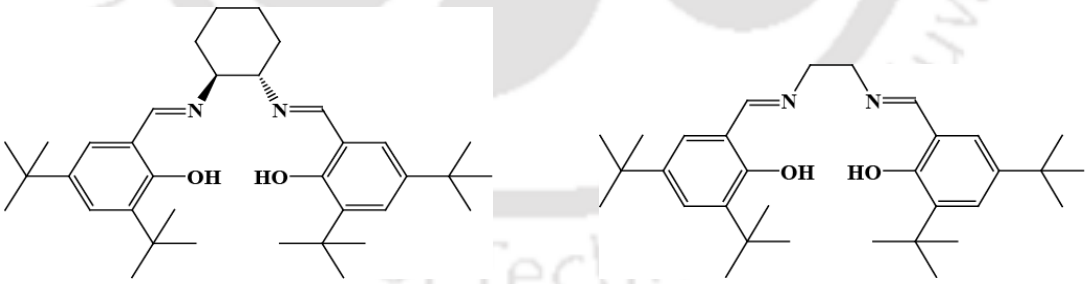

(a) (b)

Figure 2.1. Ligands used for the present study (a) **L1** and (b) **L2**.

2.2 Results and Discussion

The ligands were prepared by following the earlier literature report.[14] Corresponding diamines were allowed to react with 3,5-di-*tert*-butyl-2-hydroxybenzaldehyde in ethanol.

They were recrystallized from hot ethanol. Elemental and spectroscopic analyses confirmed the formation of the ligands (Experimental Section). The complexes, **2.1** and **2.2** were synthesized by stirring a solution of cobalt(II) acetate tetrahydrate with **L1** and **L2**, respectively, in methanol.[15] Single crystal X-ray structure has been determined for both the complexes. ORTEP diagrams are shown in figure 2.2. Crystallographic data are given in table 2.1. Structural characterization revealed that Co(II) ion is coordinated by two N_{imine} and two O_{phenol} atoms from the respective ligands in an overall distorted square planar geometry. The average Co–N_{imine} and Co–$O_{phenolato}$ distances are 1.856 and 1.847 Å, respectively, in complex **2.1**. In the case of complex **2.2**, these distances are 1.848 and 1.845 Å, respectively. These are within the range found in earlier reported examples.[16] The phenol moieties of the ligands are coordinated to the metal ion as phenolate and thereby neutralizing the overall charge of the metal ions.

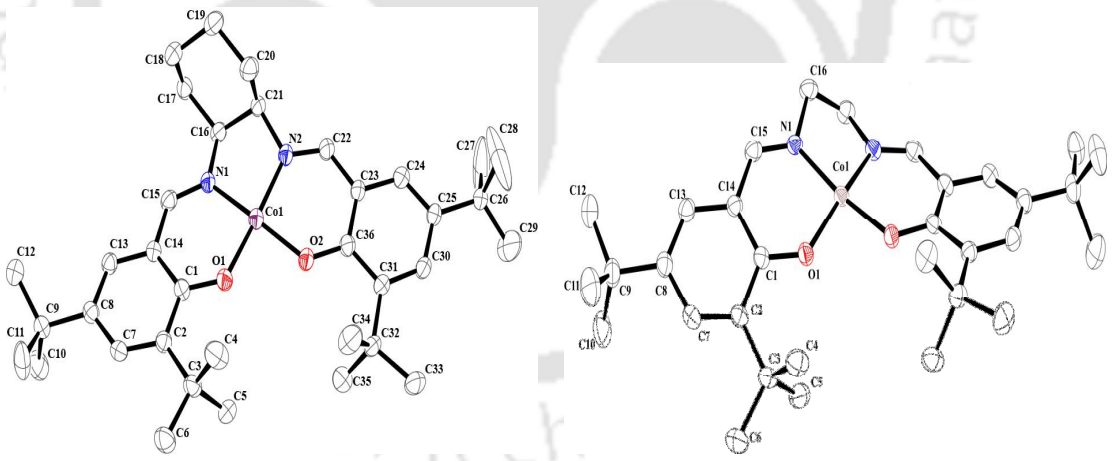

(a) (b)

Figure 2.2. ORTEP diagrams of complexes (a) **2.1** and (b) **2.2** (50% thermal ellipsoid plot, H-atoms are omitted for clarity).

Table 2.1. Crystallographic data of complexes **2.1**, **2.2**, **2.3** and **2.4**.

	2.1	**2.2**	**2.3**	**2.4**
Formule	$C_{36}H_{52}CoN_2O_2$	$C_{32}H_{46}CoN_2O_2$	C_{44} H_{68} Co N_3 O_5	C_{32} H_{46} Co N_3 O_3
Mol. wt.	603.73	549.64	777.94	579.65
Crystal system	orthorhombic	orthorhombic	monoclinic	monoclinic
Space group	Pccn	Pbcn	I2/c	P2(1)/c
Temperature/ K	296(2)	296(2)	296(2)	296(2)
Wavelength/ Å	0.71073	0.710 73	0.710 73	0.710 73
a/Å	21.0570(16)	26.7490(14)	33.5265(20)	15.141(3)
b/Å	26.980(3)	11.0089(4)	10.2466(6)	19.113(3)
c/Å	11.8069(10)	10.3143(5)	28.366(2)	11.689(2)
α/deg	90.00	90.00	90.00	90.00
β/deg	90.00	90.00	115.702(8)	105.886(6)
γ/deg	90.00	90.00	90.00	90.00
V/Å^3	6707.8(10)	3037.3(2)	8780.5(9)	3253.4(10)
Z	8	4	8	4
density/Mg·m^{-3}	1.196	1.202	1.177	1.183
Abs. coeff./mm^{-1}	0.544	0.594	0.435	0.561
Abs. correction	none	multi-scan	multi-scan	multi-scan
F(000)	2600	1180	3360	1240
Total no. of reflections	5626	2670	7936	5610
Reflections, $I > 2\sigma(I)$	3140	1994	5247	3783
Max. 2θ/deg	25.00	25.00	25.25	25.00
Ranges (*h*, *k*, *l*)	$-13 \le h \le 23$	$-31 \le h \le 29$	$-40 \le h \le 40$	$-18 \le h \le 16$
	$-30 \le k \le 27$	$-13 \le k \le 12$	$-12 \le k \le 10$	$-22 \le k \le 22$
	$-14 \le l \le 12$	$-12 \le l \le 7$	$-21 \le l \le 34$	$-13 \le l \le 13$
Complete to 2θ (%)	95.4	99.9	99.8	98.1
Refinement method	full-matrix least-squares on F^2	full-matrix least-squares on F^2	full-matrix least-squares on F^2	full-matrix least-squares on F^2
GOF (F^2)	1.196	1.044	1.182	1.045
R indices [$I > 2\sigma(I)$]	0.0758	0.0396	0.0730	0.0550
R indices (all data)	0.1270	0.0635	0.1116	0.0903

Table 2.2. Selected bond lengths (Å).

	2.1	**2.2**	**2.3**	**2.4**
Co(1)-O(1)	1.843(3)	1.845(18)	1.867(3)	1.904(2)
Co(1)-O(2)	1.851(3)	-	1.879(3)	1.878(2)
Co(1)-N(1)	1.866(3)	1.848(2)	1.879(3)	1.881(3)
Co(1)-N(2)	1.847(3)	-	1.892(3)	1.879(3)
Co(1)-N(3)	-	-	1.804(4)	1.799(4)
C(1)-O(1)	1.323(4)	1.315(3)	1.314(5)	1.318(4)
N(1)-C(15)	1.296(5)	1.293(4)	1.289(5)	1.295(5)
N(1)-C(16)	1.499(5)	1.481(3)	1.478(5)	1.487(5)

Table 2.3. Selected bond angles (º).

	2.1	**2.2**	**2.3**	**2.4**
O(1)-Co(1)-N(1)	93.75(13)	93.38(9)	93.80(13)	92.71(12)
O(1)-Co(1)-O(2)	88.27(12)	-	84.92(12)	86.78(10)
N(2)-Co(1)-O(2)	93.11(13)	-	93.15(13)	92.30(12)
O(1)-Co(1)-N(2)	173.68(13)	-	169.64(15)	167.79(12)
O(3)- N(3)- Co(1)	-	-	126.3(5)	126.50(4)
N(2)- Co(1)- N(1)	85.81(15)	-	84.78(14)	84.08(13)
O(2)-Co(1)-N(1)	171.23(13)	-	161.41(14)	160.37(13)
C(1)-O(1)-Co(1)	130.0(3)	129.23(17)	128.1(2)	127.50(2)
O(1)-C(1)-C(14)	121.9(4)	121.7(2)	122.7(3)	122.70(3)
C(1)-C(14)- C(15)	121.9(4)	121.9(3)	121.4(4)	121.70(3)

Nitric Oxide reactivity

Purging of excess NO into the dry and degassed solutions of complexes **2.1** and **2.2** in THF at room temperature under Ar atmosphere resulted in the formation of complexes **2.3** and **2.4**, respectively. The color of the solutions changed to greenish brown from deep red in course of the reaction indicating the complete conversion of complexes **2.1** and **2.2** to **2.3** and **2.4**, respectively (Scheme 2.1). In UV-visible spectroscopy, the absorption bands at 401 nm (ε/ $M^{-1}cm^{-1}$, 1980) and 866 nm (ε/ $M^{-1}cm^{-1}$, 31) of complex **2.1** were diminished

upon addition of NO (Figure 2.3). In case of complex **2.2**, the bands at 406 nm (ε/ $M^{-1}cm^{-1}$, 1640) and 711 nm (ε/ $M^{-1}cm^{-1}$, 45) were found to behave similarly (Figure 2.3).

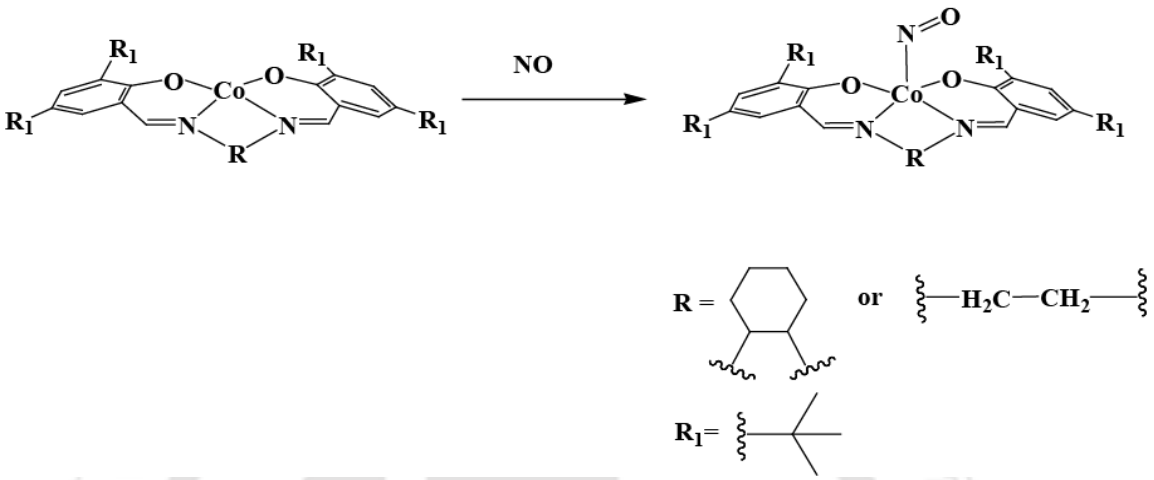

Scheme 2.1

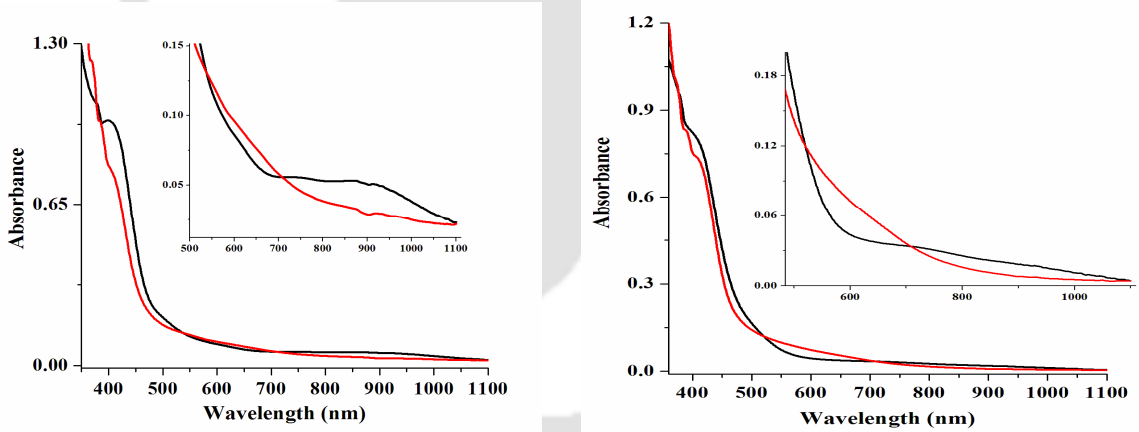

(a) (b)

Figure 2.3. UV-visible spectra of complexes (a) **2.1** (black), after addition of NO (red), (b) **2.2** (black), after addition of NO (red) in dry THF at room temperature.

FT-IR studies of the isolated solid complexes **2.3** and **2.4** showed a moderately strong stretching frequency at 1651 and 1650 cm^{-1}, respectively, assignable to the coordinated NO stretching (Figures 2.4).[13,17] These stretching frequencies were found to shift to ~1618 cm^{-1}

upon labeling by ^{15}NO. In case of $[(12\text{-TMC})Co(NO)]^{2+}$ and $[(13\text{-TMC})Co(NO)]^{2+}$, these nitrosyl stretching frequencies were appeared at 1712 and 1716 cm^{-1} in solution FT-IR spectroscopy.[13] In electron paramagnetic resonance spectroscopy, complexes **2.3** and **2.4** were found to be silent in THF solution at room temperature as well as at 77K (Figure 2.5). These observations are in well agreement with the existence of trivalent cobalt center and thus, the nitrosyl complexes can be designated as $[Co^{III}\text{-}NO^{-}]$ or $\{CoNO\}^{8}$ configuration. In the cases of Co(III)-nitrosyls with 12- and 13-TMC ligands also were reported to be EPR silent owing to the $\{CoNO\}^{8}$ descriptions. [13,17]

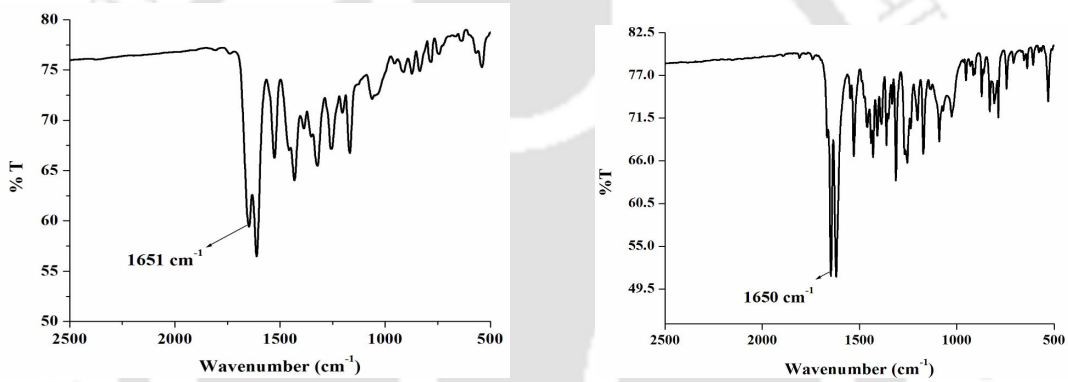

(a) (b)

Figure 2.4. FT-IR spectra of complexes (a) **2.3** and (b) **2.4** in KBr.

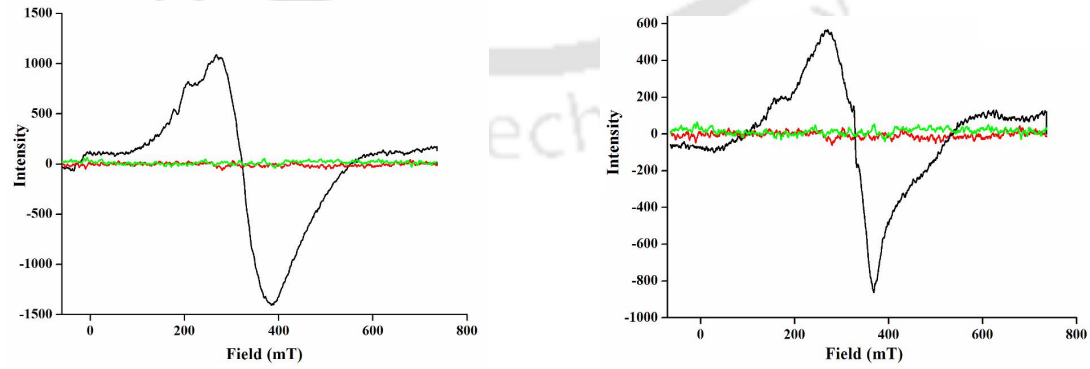

(a) (b)

Figure 2.5. X-band EPR spectra of complexes (a) **2.1** (black), **2.3** (red) and **2.5** (green); (b) **2.2** (black), **2.4** (red) and **2.6** (green) in THF at room temperature.

ESI mass spectra of complexes **2.3** and **2.4** displayed peaks assignable to the $[CoL]^+$ fragments (Figure 2.6 and 2.7). This is attributed to the facile loss of the NO group as axial ligand under reaction condition. This was observed earlier with cobalt nitrosyls of porphyrin ligands.[18]

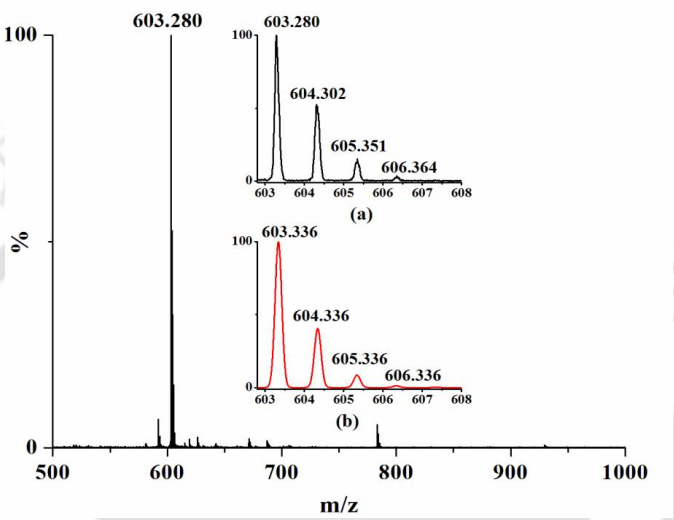

Figure 2.6. ESI-mass spectra of complex **2.3** with isotopic distribution (a) experimental and (b) simulated [**L1Co**] $^+$ in methanol.

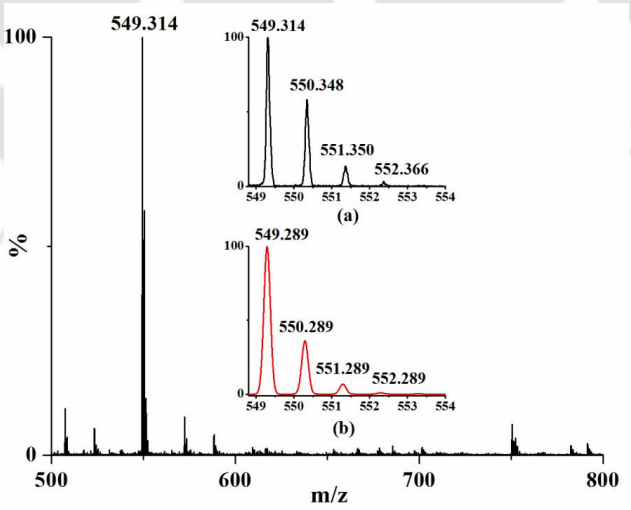

Figure 2.7. ESI-mass spectra of complex **2.4** with isotopic distribution (a) experimental and (b) simulated [**L2Co**] $^+$ in methanol.

Further, these complexes have been characterized by single crystal X-ray structure determination. ORTEP diagrams of complexes **2.3** and **2.4** are shown in figure 2.8. The NO group was coordinated to the central metal ion, cobalt from the axial position in both the cases offering a square pyramid structure.

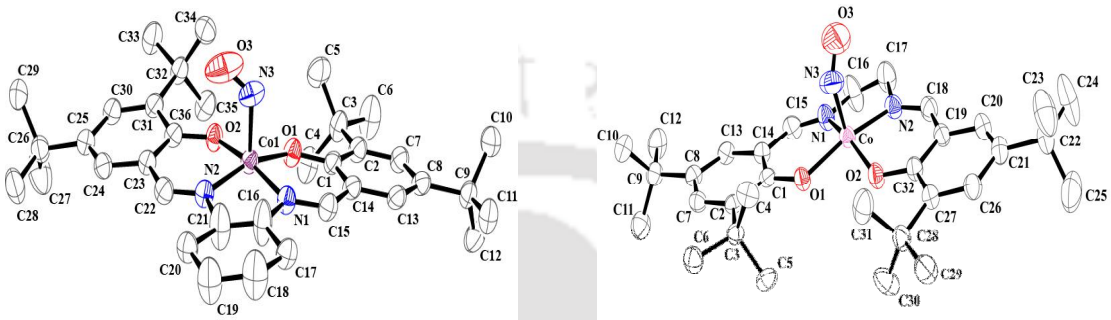

(a) (b)

Figure 2.8. ORTEP diagrams of complexes (a) **2.3** and (b) **2.4** (50% thermal ellipsoid Hydrogen atoms are omitted for clarity).

The Co–N_{NO} distances are 1.803 and 1.799Å in cases of complexes **2.3** and **2.4** respectively. The average N–O distance of coordinated NO moiety is 1.119 Å. In cases of $[(12\text{-TMC})Co(NO)]^{2+}$ and $[(13\text{-TMC})Co(NO)]^{2+}$, the N-O bond lengths were 1.155 and 1.159 Å respectively.[13] The Co-N-O angles are 126.3° and 126.5° respectively in complexes **2.3** and **2.4** suggest a large bending of the metal nitrosyl unit. For $[(12\text{-TMC})Co(NO)]^{2+}$ and $[(13\text{-TMC})Co(NO)]^{2+}$, the Co-N-O angles were reported as 128.50° and 124.4° respectively. The values in the present cases are very much in agreement with the earlier reported Co(III)-nitrosyl complexes. The bending nature is also consistent with the NO^- description.[13]

Reactivity of $\{CoNO\}^8$ with superoxide (O_2^-)

It was reported earlier that cobalt-nitrosyls react with molecular O_2 leading to formation of

corresponding nitrite complexes.[9] However, complexes **2.3** and **2.4** were found to be not reactive towards O_2. Similar observation was reported with Co(III)-nitrosyls, [(12-TMC)Co(NO)]$^{2+}$ and [(13-TMC)Co(NO)]$^{2+}$.[13] In those cases it was speculated that NO did not undergo dissociation in the complexes which is required for the dioxygen reactivity.[13] However, addition of potassium superoxide in presence of 18-crown-6 in dry THF solution of complexes **2.3** and **2.4** afforded a change in color. In the UV-visible spectroscopy, a new absorption band at 675 nm (ε/ $M^{-1}cm^{-1}$, 115) and 665 nm (ε/ $M^{-1}cm^{-1}$, 95) for complexes **2.3** and **2.4**, respectively, was observed (Figure 2.9).

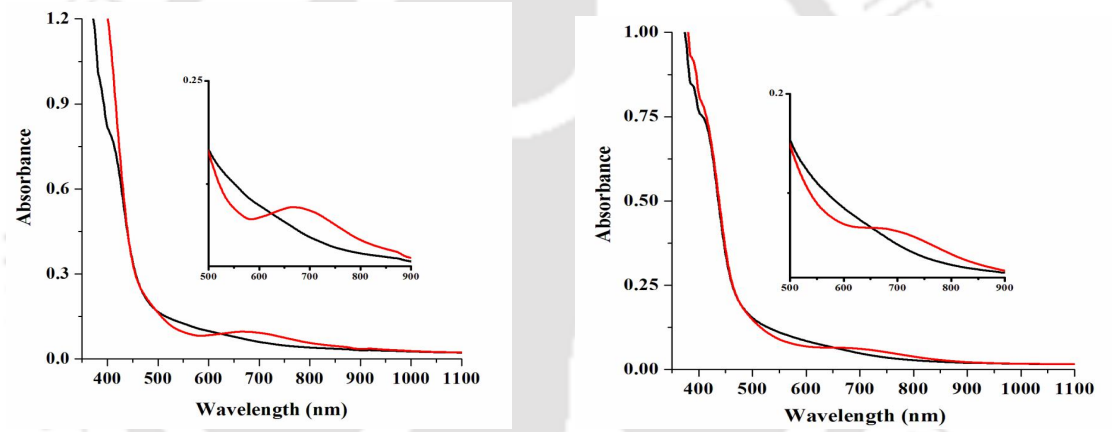

(a) (b)

Figure 2.9. UV-visible spectra of complexes (a) **2.3** (black), after addition of KO_2 (red) (**2.5)** and (b) **2.4** (black), after addition of KO_2 (red) (**2.6)** in dry THF at room temperature.

These are attributed to the formation of corresponding Co(III)-nitrato complexes, **2.5** and **2.6**, respectively. These complexes were isolated and characterized by various spectral analyses and microanalysis (Experimental Section and Figure 2.10). However, even after several attempts X-ray quality crystals were not obtained. When the reaction were carried out in presence of external substrate like 2,4-di-*tert*-butylphenol, formation of corresponding bisphenol as product (~ 40% yield) was observed (Scheme 2.2 and

Experimental Section). This is also in accord with the formation of presumed Co-peroxynitrite intermediate.[13]

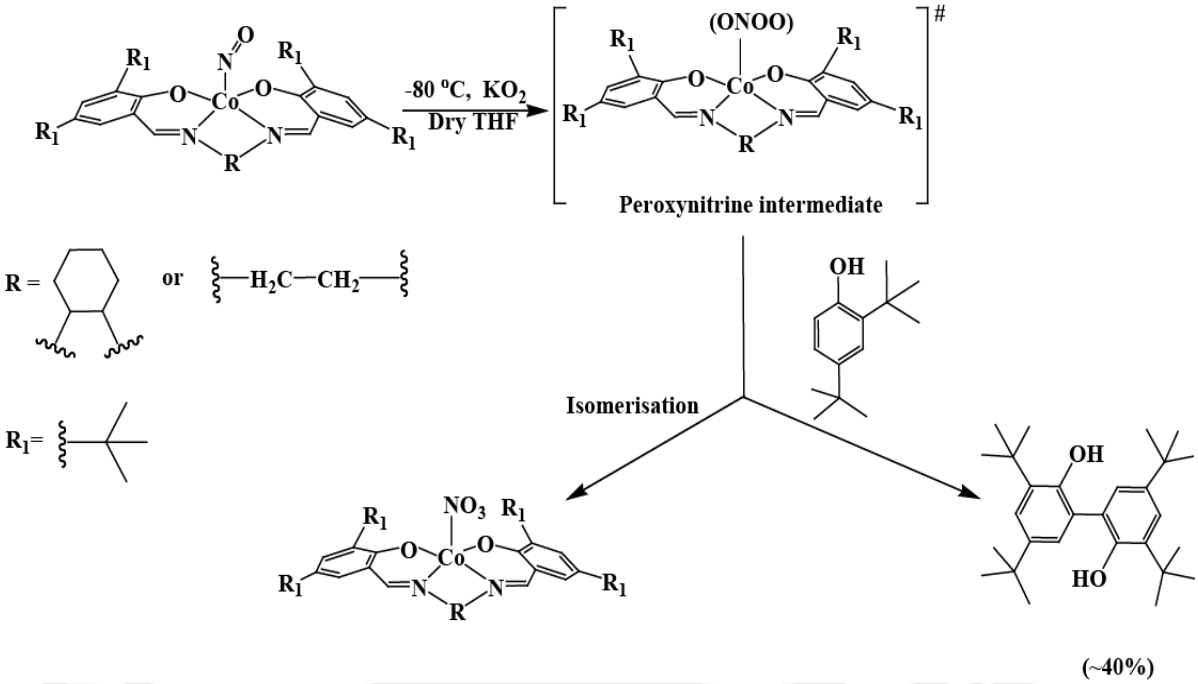

Scheme 2.2

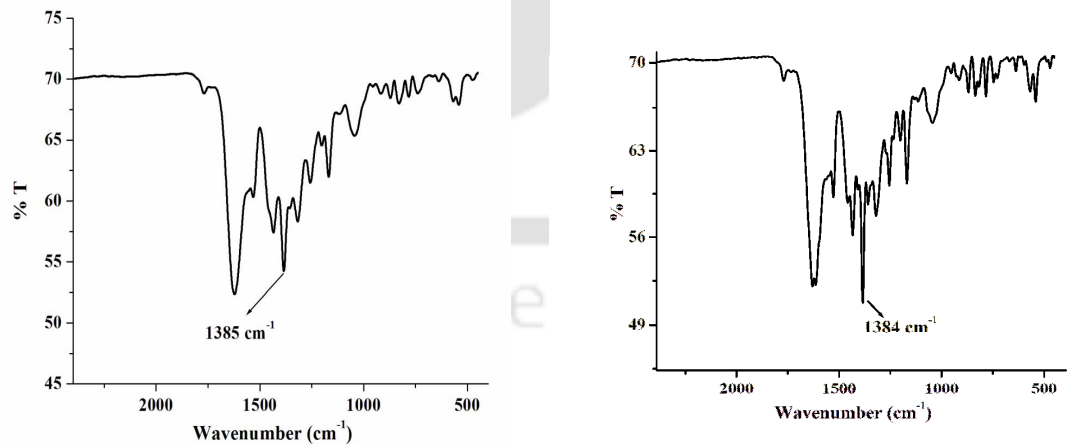

(a) (b)

Figure 2.10. FT-IR spectrum of complexes (a) **2.5** and (b) **2.6** in KBr.

2.3 Experimental Section

2.3.1 Materials and Methods

All reagents and solvents of reagent grade were purchased from commercial sources and used as received except specified. ^{15}NO was purchased from Icon Isotopes. Deoxygenation of the solvent and solutions was effected by repeated vacuum/purge cycles or bubbling with nitrogen or argon for 30 minutes. NO gas was used from a cylinder after purification using standard procedure. The dilution of NO was effected with argon gas using Environics Series 4040 computerized gas dilution system. UV-visible spectra were recorded on Agilent HP 8454 dioad arrey UV-visible spectrophotometer. FT-IR spectra of the solid samples were taken on a Perkin Elmer spectrophotometer with samples prepared as KBr pellets. Solution electrical conductivity was measured using a Systronic 305 conductivity bridge. ^{1}H-NMR and ^{13}C-NMR spectra were recorded respectively in 400 MHz and 100MHz Varian FT spectrometer. Chemical shifts (ppm) were referenced either with an internal standard (Me_4Si) or to the residual solvent peaks. The X-band Electron Paramagnetic Resonance (EPR) spectra were recorded on a JES-FA200 ESR spectrometer, at room temperature or at 77 K with microwave power, 0.998 mW; microwave frequency, 9.14 GHz and modulation amplitude, 2. Elemental analyses were obtained from a Perkin Elmer Series II Analyzer. The magnetic moment of complexes was measured on a Cambridge Magnetic Balance. Single crystals were grown by slow diffusion followed by slow evaporation technique. The intensity data were collected using a Bruker SMART APEX-II CCD diffractometer, equipped with a fine focus 1.75 kW sealed tube MoK_α radiation (λ = 0.71073 Å) at 273(3) K, with increasing ω (width of 0.3° per frame) at a scan speed of 3 s/frame. The SMART software was used for data acquisition.[19] Data integration and reduction were undertaken with SAINT and XPREP software.[20] Structures

were solved by direct methods using SHELXS-97 and refined with full-matrix least squares on F^2 using SHELXL-97.[21] Structural illustrations have been drawn with ORTEP-3 for Windows.[22]

2.3.2 Syntheses

(a) Ligand L1

The imine ligand, **L1** was reported earlier.[14] **L1** was synthesized by condensation of *trans*-1,2-cyclohexanediamine (1.14 g, 10 mmol) in the presence of 2 equivalent of 2,4-di-*tert*-butyl salicylaldehyde (4.68 g, 20 mmol) in 20 ml ethanol solution at room temperature. The reaction mixture was allowed to stir for 4 h. A yellow colored solid was precipitated out. It was filtered off and washed with cold ethanol. After washing the solid was dried in air and kept in desiccators for overnight. Yield: 4.81 g (88%). Elemental analyses for $C_{36}H_{54}N_2O_2$, Calcd(%): C, 79.07; H, 9.95; N, 5.12. Found (%): C, 78.95; H, 9.98; N, 5.24. FT-IR (in KBr): 3436, 2961, 1630, 1468, 1438, 1270, 1173, 878, 828, 772, 644 cm^{-1}. ^{1}H-NMR (400 MHz, $CDCl_3$): δ_{ppm}, 13.68 (2H), 8.29 (2H), 7.30 (2H), 6.97 (2H), 3.35 (2H), 1.96 (2H), 1.89 (2H), 1.71 (2H), 1.45 (2H), 1.41 (18H), 1.23 (18H). ^{13}C-NMR (100 MHz, $CDCl_3$): δ_{ppm}, 166.0, 158.2, 140.1, 136.5, 126.9, 126.2, 118.0, 72.6, 35.1, 34.2, 33.5, 31.6, 29.6, 24.6.

(b) Ligand L2

The reported imine ligand **L2** was also prepared following the same procedure as for **L1**. To the solution of ethylenediamine (0.6 g, 10 mmol) in 10 ml ethanol, 20 ml ethanol solution of 2,4-di-*tert*-butyl salicylaldehyde (4.68 g, 20 mmol) was added drop wise at room temperature. The reaction mixture was allowed to stir for 4 h till yellow colored

precipitate formed. It was filtered off and washed with cold ethanol. After washing the solid was dried in air and kept in desiccators for overnight. Yield: 4.1g (83%). Elemental analyses for $C_{32}H_{48}N_2O_2$,.Calcd. (%): C, 78.00; H, 9.82; N, 5.69. Found (%): C, 77.95; H, 9.79; N, 5.78. FT-IR (in KBr): 2961, 2869, 1629, 1481, 1466, 1439, 1361, 1270, 1253, 1041, 879, 839, 830, 773, 729, 710, 645 cm^{-1}. ^{1}H-NMR (400 MHz, $CDCl_3$): 13.62 (1H), 8.38 (1H), 7.36 (1H), 7.06 (1H), 3.92 (1H), 1.41 (9H), 1.23 (9H). ^{13}C-NMR (100 MHz, $CDCl_3$): δ_{ppm}, 167.8, 158.2, 140.3, 136.8, 127.2, 126.3, 118.0, 59.8, 34.3, 31.7, 29.6.

(c) Complex 2.1

Complex **2.1** was prepared by following the reported procedure with some modifications.[15] Cobalt(II) acetate tetrahydrate (1.25 g, 5 mmol) was taken in a 50 ml round bottom flask, dissolved in 10 ml of MeOH. To this, a solution of ligand **L1** (2.73 g, 5 mmol) in hot methanol (25 ml) was added and stirred for 3 h. A red colored precipitate was formed, it was filtered off and washed several time by cold methanol. After washing the solid was dried in air and then kept in desiccators for overnight. Finally it was recrystallized from THF solution to obtain red crystals. Yield: 2.11 g (70%). Elemental analyses for $C_{36}H_{52}N_2O_2Co$, Calcd(%): C, 71.62; H, 8.68; N, 4.64. Found (%): C, 71.67; H, 8.69; N, 4.71. FT-IR(in KBr): 3435, 2950, 1595, 1526, 1462, 1423, 1320, 1254, 1175, 870, 786, 543 cm^{-1}. UV-visible (THF): 401 nm (ε/ $M^{-1}cm^{-1}$, 1980) and 866 nm (ε/ $M^{-1}cm^{-1}$, 31). Molar conductance: 40 S cm^2 mol^{-1} (in THF), observed magnetic moment: 1.52 BM.

(d) Complex 2.2

Complex **2.2** was prepared following the same procedure as complex **2.1**, with cobalt(II) acetate tetrahydrate (1.25 g, 5 mmol) and ligand **L2** (2.46 g, 5 mmol) dissolved in 20 ml hot methanol. The solid complex **2.2** was recrystallized from THF solution at room

temperature. Yield: 1.77g (72%). Elemental analyses for $C_{32}H_{46}N_2O_2Co$, Calcd(%): C, 69.92; H, 8.44; N, 5.10. Found (%): C, 69.80; H, 8.41; N, 5.16. FT-IR (in KBr): 3433, 2952, 1598, 1528, 1462, 1439, 1254, 1175, 872, 786 cm^{-1}. UV-visible (THF): 406 nm (ε/ $M^{-1}cm^{-1}$, 1640) and 711 nm (ε/ $M^{-1}cm^{-1}$, 45). Molar conductance: 38 S cm^2 mol^{-1} (in THF), observed magnetic moment: 1.55 BM.

(e) Complex 2.3

In 20 ml of dry and degassed THF solution of complex **2.1** (201 mg), freshly purified NO was bubbled in excess till the deep red color of the solution became greenish brown. The reaction mixture was kept at room temperature for crystallization. Yield: 180 mg (85%). Elemental analyses for $C_{36}H_{52}N_3O_3Co$, Calcd(%): C, 68.23; H, 8.27; N, 6.63. Found (%): C, 68.18; H, 8.25; N, 6.82. FT-IR (in KBr): 2952, 1651, 1610, 1430, 1324, 1255, 1170, 785, 541 cm^{-1}. Molar conductance: 45 S cm^2 mol^{-1} (in THF).

(f) Complex 2.4

In 20 ml of dry and degassed THF solution of complex **2.2** (250 mg), freshly purified NO was bubbled till greenish brown color was appeared. The reaction mixture was kept at room temperature for crystallization. Yield: 230 mg (88%). Elemental analyses for $C_{32}H_{46}N_3O_3Co$, Calcd(%): C, 66.31; H, 8.00; N, 7.25. Found (%): C, 66.24; H, 8.02; N, 7.34. FT-IR (in KBr): 2955, 1649, 1620, 1529, 1430, 1313, 1172, 1090, 744, 530 cm^{-1}. Molar conductance: 42 S cm^2 mol^{-1} (in THF).

(g) Complex 2.5

Complex **2.5** was prepared by the reaction of freshly prepared nitrosyl complex **2.3** and KO_2. The freshly prepared complex **2.3** was obtained by purging NO in 20 ml of dry and

degassed THF solution of complex **2.1** (180 mg). After that the excess NO was removed by vaccum/purging Ar. Then the nitrosyl complex **2.3** was reacted with 2 equivalent of KO_2 in presence of 18-crown-6 (5 equivalent) in dry THF at -80 °C. A color change was observed to deep brown due to the formation of complex **2.5**. The volume of the reaction mixture was reduced to 5ml using vaccum and layered with hexane. The whole mixture was kept in freezer for 24 h. A dark brown precipitate was obtained; it was filtered off and washed with hexane for several times. The solid mass was kept at desiccators for overnight. Yield: 114 mg (~ 61%). Elemental analyses for $C_{36}H_{52}N_3O_5Co$, Calcd(%): C, 64.95; H, 7.87; N, 6.31. Found (%): C, 64.89; H, 7.88; N, 6.46. FT-IR (in KBr): 3432, 2951, 1631, 1612, 1433, 1384, 1255, 1169, 1045, 570 cm^{-1}. UV-visible (THF): 675 nm (ε/ $M^{-1}cm^{-1}$, 115). Molar conductance: 32 S cm^2 mol^{-1} (in THF).

(h) Complex 2.6

Complex **2.6** was prepared from freshly prepared complex **2.4**, (150 mg) and 2 equivalent of KO_2 in presence of 18-crown-6 (5 equivalent) in dry THF at -80°C. The volume of the reaction mixture was reduced to 5 ml using vaccum and layered with hexane. The reaction mixture was kept in freeze for 24 h. The dark brown precipitate was filtered off and washed with hexane for several times. The solid mass was kept at desiccators for overnight. Yield: 102 mg (~ 64%). Elemental analyses for $C_{32}H_{46}N_3O_5Co$, Calcd(%): C, 62.84; H, 7.58; N, 6.87. Found (%): C, 62.77; H, 7.69; N, 6.88. FT-IR (in KBr): 1630, 1613, 1434, 1384, 1359, 1321, 1255, 1170, 1046, 834, 784, 540 cm^{-1}. UV-visible: 665 nm (ε/ $M^{-1}cm^{-1}$, 95). Molar conductance: 35 S cm^2 mol^{-1} (in THF).

(i) Reaction of complex 2.3 and 2.4 with superoxide in presence of 2,4-di-*tert*-butylphenol : Isolation 2,2′-dihydroxy-3,3′,5,5′-tetra-*tert*-butylbiphenol

In 20 ml THF solution of freshly prepared complex **2.3** (0.633 g, 1 mmol), a solution of 2, 4-di-*tert*-butyl phenol (DTBP) (1.24 g, 6 mmol in 5 ml dry THF), was added and the mixture was cooled to -80 ºC. To that KO_2/18-crown-6 (~1 eq.) was added, and the mixture was stirred for 20 min. After that, it was warmed to room temperature and dried under reduce pressure. The solid mass was then subjected to column chromatography using silica gel column to obtain pure 2,2′-dihydroxy-3,3′,5,5′-tetra-*tert*-butylbiphenol. Yield: 0.164 g (~40%). ^{1}H-NMR (400 MHz, $CDCl_3$) δ_{ppm}: 7.39 (2H), 7.12 (2H), 5.23 (2H), 1.45(18H) and 1.32 (18H). ^{13}C-NMR (100 MHz, $CDCl_3$) δ_{ppm}: 150.0, 143.2, 136.5, 125.5, 125.0, 122.6, 35.4, 34.7, 31.9 and 29.9. Mass (m/z): Calcd: 410.32, Found: 409.32 (M-1).

Using same procedure 2,2′-dihydroxy-3,3′,5,5′-tetra-*tert*-butylbiphenol was also obtained from freshly prepared complex **2.4**, and it was also characterized by ^{1}H-NMR, ^{13}C-NMR as well as by ESI- mass spectrometry.

2.4 Conclusion

Two cobalt(II) complexes, **2.1** and **2.2**, of tetradentate N,O-donor ligands have been synthesized. Reactions of these complexes with NO gas in THF afforded the corresponding Co(III)-nitrosyls having $\{CoNO\}^{8}$ configuration. These complexes were found unreactive towards dioxygen. However, their reaction with superoxide ion resulted in the formation of corresponding cobalt(III)-nitrate complexes through the presumed formation of cobalt-peroxynitrite intermediates. The intermediates led to the oxidative formation of corresponding *bis*-phenol in presence of 2,4-di-*tert*-butylphenol. This also suggests the formation of peroxynitrite intermediate.

2.5 References

(1) (a) Ignarro, J. E. *Nitric Oxide: Biology and Pathobiology*; Academic Press: San Diego, CA, **2000**. (b) Richter-Addo, G. B.; Legzdins, P.; Burstyn, J. *Chem. Rev.* **2002**, *102*, 857. (c) Wasser, I. M.; de Vries, S.; Moenne-Loccoz, P.; Schröder, I.; Karlin, K. D. *Chem. Rev.* **2002**, *102*, 1201. (d) Møller, J. K. S.; Skibsted, L. H. *Chem. Rev*. **2002**, *102*, 1167.

(2) (a) Doyle, M. P.; Hoekstra, J. W. *J. Inorg. Biochem*. **1981**, *14*, 351. (b) Cooper, C. E.; Torres, J.; Sharpe, M. A.; Wilson, M. T. *FEBS Lett*. **1997**, *414*, 281. (c) Tocheva, E. I.; Rosell, F. I.; Mauk, A. G.; Murphy, M. E. P. *Science* **2004**, *304*, 867.

(3) (a) Radi, R. *Proc. Natl. Acad. Sci. U.S.A.* **2004**, *101*, 4003. (b) Kalyanaraman, B. *Proc. Natl. Acad. Sci. U.S.A.* **2004**, *101*, 11527. (c) Dedon, P. C.; Tannenbaum, S. Arch, R. *Biochem. Biophys*. **2004**, *423*, 12. (d) Goldstein, S.; Lind, J.; Merényi, G. *Chem. Rev*. **2005**, *105*, 2457. (e) Pacher, P.; Beckman, J. S.; Liaudet, L. *Physiol. Rev*. **2007**, *87*, 315.

(4) (a) Ford, P. C.; Wink, D. A.; Stanbury, D. M. *FEBS Lett*. **1993**, *326*, 1. (b) Tran, N. G.; Kalyvas, H.; Skodje, K. M.; Hayashi, T.; Moënne-Loccoz, P.; Callan, P. E.; Shearer, J.; Kirschenbaum, L. J.; Kim, E. *J. Am. Chem. Soc*. **2011**, *133*, 1184. (c) Blough, N. V.; Zafiriou, O. C. *Inorg. Chem.* **1985**, *24*, 3502. (d) Nauser, T.; Koppenol, W. H. *J. Phys. Chem. A*. **2002**, *106*, 4084. (e) Qiao, L.; Lu, Y.; Liu, B.; Girault, H. H. *J. Am. Chem. Soc.* **2011**, *133*, 19823. (f) Speelman, A. L.; Lehnert, N. *Acc. Chem. Res*. **2014**, *47*, 1106. (g) Fry, N. L.; Mascharak, P. K. *Acc. Chem. Res*. **2011**, *44*, 289.

(5) (a) Shishehbor, M. H.; Aviles, R. J.; Brennan, M. L.; Fu, X. M.; Goormastic, M.; Pearce, G. L.; Gokce, N.; Keaney, J. F.; Penn, M. S.; Sprecher, D. L.; Vita, J. A.; Hazen, S. L. *J. Am. Med. Assoc.* **2003**, *289*, 1675. (b) Good, P. F.; Werner, P.; Hsu, A.; Olanow, C. W.; Perl, D. P. *Am. J. Pathol.* **1996**, *149*, 21. (c) Danielson, S. R.; Held, J. M.; Schilling, B.; Oo. M.; Gibson, B. W.; Andersen, J. K. *Anal. Chem.* **2009**, *81*, 7823.

(6) (a) Gardner, P. R.; Gardner, A. M.; Martin, L. A.; Salzman, A. L. *Proc. Natl. Acad. Sci. U.S.A.* **1998**, *95*, 10378. (b) Ford, P. C.; Lorkovic, I. M. *Chem. Rev.* **2002**, *102*, 993. (c) Schopfer, M. P.; Mondal, B.; Lee, D. H.; Sarjeant, A. A. N.; Karlin, K. D. *J. Am. Chem. Soc*. **2009**, *131*, 11304.

(7) (a) Wick, P. K.; Kissner, R.; Koppenol, W. H. *Helv. Chim. Acta* **2000**, *83*, 748. (b) Roncaroli, F.; Videla, M.; Slep, L. D.; Olabe, J. A. *Coord. Chem. Rev*. **2007**, *251*, 1903. (c) Maiti, D.; Lee, D.-H.; Sarjeant, A. A. N; Pau, M. Y. M.; Solomon, E. I.; Gaoutchenova, K.; Sundermeyer, J.; Karlin, K. D. *J. Am. Chem. Soc*. **2008**, *130*, 6700. (d) Goodwin, J. A.; Coor, J. L.; Kavanagh, D. F.; Sabbagh, M.; Howard, J. W.; Adamec, J. R.; Parmley, D. J.; Tarsis, E. M.; Kurtikyan, T. S.; Hovhannisyan, A. A.; Desrochers, P. J.; Standard, J. M. *Inorg. Chem*. **2008**, *47*, 7852. (e) Kurtikyan, T. S.; Ford, P. C. *Chem. Commun*. **2010**, *46*, 8570. (f) Kurtikyan, T. S.; Eksuzyan, S. R.; Goodwin, J. A.; Hovhannisyan, G. S. *Inorg. Chem*. **2013**, *52*, 12046. (g) Herold, S.; Koppenol, W. H. *Coord. Chem. Rev*. **2005**, *249*, 499.

(8) (a) Tran, N. G.; Kalyvas, H.; Skodje, K. M.; Hayashi, T.; Loccoz, P. M.; Callan, P. E.; Shearer, J.; Kirschenbaum, L. J.; Kim, E. *J. Am. Chem. Soc*. **2011**, *133*, 1184. (b) Geletii, Y. V.; Bailey, A. J.; Boring, E. A.; Hill, C. L. *Chem. Commun*. **2001**, 1700. (c) Pellei, M.; Lobbia, G. G.; Santini, C.; Spagna, R.; Camalli, M.; Fedeli,

D.; Falcioni, G. *Dalton Trans*. **2004**, 2822. (d) Kohnen, S.; Halusiak, E.; Mouithys-Mickalad, A.; Deby-Dupont, G.; Deby, C.; Hans, P.; Lamy, M.; Noels. *Nitric Oxide* **2005**, *12*, 252.

(9) (a) Clarkson, S. G.; Basolo, F. *J. Chem. Soc. Chem. Commun*. **1972**, *119*, 670. (b) Clarkson, S. G.; Basolo, F. *Inorg. Chem*. **1973**, *12*, 1528. (c) Subedi, H.; Brasch, N. E. *Inorg. Chem*. **2013**, *52*, 11608. (d) Frech, C. M.; Blacque, O.; Schmalle, H. W.; Berke, H. *Dalton Trans*. **2006**, 4590.

(10) Park, G. Y.; Deepalatha, S.; Puiu, S. C.; Lee, D.-H.; Mondal, B.; Sarjeant, A. A. N; del Rio, D.; Pau, M. Y. M.; Solomon, E. I.; Karlin, K. D. *J. Biol. Inorg. Chem*. **2009**, *14*, 1301.

(11) (a) Yokoyama, A.; Han, J. E.; Cho, J.; Kubo, M.; Ogura, T.; Siegler, M. A.; Karlin, K. D.; Nam, W. *J. Am. Chem. Soc*. **2012**, *134*, 15269. (b) Yokoyama, A.; Cho, K.-B.; Karlin, K. D.; Nam, W. *J. Am. Chem. Soc*. **2013**, *135*, 14900.

(12) (a) Kalita, A.; Kumar, P.; Mondal, B. *Chem. Commun*. **2012**, *48*, 4636. (b) Kalita, A.; Deka, R. C.; Mondal, B. *Inorg.Chem*. **2013**, *52*, 10897.

(13) Kumar, P.; Lee, Y. M.; Park, Y. J.; Siegler, M. A.; Karlin, K. D.; Nam, W. *J. Am. Chem. Soc*. **2015**, *137*, 4284.

(14) (a) Chiang, L.; Herasymchuk, K.; Thomas, F.; Storr, T. *Inorg. Chem*. **2015**, *54*, 5970. (b) Rotthaus, O.; Thomas, F.; Jarjayes, O.; Philouze, C.; Saint-Aman, E.; Pierre, J.-L. *Chem. Eur. J*. **2006**, *12*, 6953.

(15) Kochem, A.; Kanso, H.; Baptiste, B.; Arora, H.; Philouze, C.; Jarjayes, O.; Vezin, H.; Luneau, D.; Orio, M.; Thomas, F. *Inorg. Chem*. **2012**, *51*, 10557.

(16) (a) Clarke, R. M.; Hazin, K.; Thompson, J. R.; Savard, D.; Prosser, K. E.; Storr, T. *Inorg. Chem*. **2016**, *55*, 762. (b) Deiasi, R.; Holt, S. L.; Post, A. *Inorg. Chem*. **1971**, *10*, 1498.

(17) (a) Enemark, J. H.; Feltham, R. D. *Coord. Chem. Rev*. **1974**, *5*, 686. (b) Richter-Addo, G. B.; Legzdins, P. *Metal Nitrosyls*; Oxford University Press: New York, **1992**. (c) McCleverty, J. A. *Chem. Rev*. **2004**, *104*, 403. (d) Berto, T. C.; Speelman, A. L.; Zheng, S.; Lehnert, N. *Coord. Chem. Rev*. **2013**, *257*, 244.

(18) Richter-Addo, G. B.; Hodge, S. J.; Yi, G.-B.; Khan, M. A.; Ma, T.; Caemelbeck, E. V.; Huo, N.; Kadish, K. M. *Inorg. Chem*. **1996**, *35*, 6530.

(19) SMART, SAINT and XPREP, Siemens Analytical X-ray Instruments Inc., Madison, Wisconsin, USA, **1995**.

(20) Sheldrick, G. M.; SADABS: software for Empirical Absorption Correction, University of Gottingen, Institut fur Anorganische Chemieder Universitat, Tammanstrasse 4, D-3400 Gottingen, Germany, **1999**.

(21) Sheldrick, G. M. SHELXS-97, University of Gottingen, Germany, **1997**.

(22) Farrugia, L. J. ORTEP-3 for Windows - a Version of ORTEP-III with a Graphical User Interface (GUI). *J. Appl. Crystallogr*. **1997**, *30*, 565.

Chapter 3

Nitric oxide reactivity of Ni(II) complex: Reductive nitrosylation of nickel(II) followed by release of nitrous oxide

Abstract

Ni(II) complex of ligand **L3** (**L3** = *bis*(2-ethyl-4-methylimidazol-5-yl)methane) in methanol solution reacts with equivalent amount of NO to result in corresponding Ni(I) complex. Addition of further equivalent of NO affords Ni(I)-nitrosyl intermediate with $\{NiNO\}^{10}$ configuration. This nitrosyl intermediate on subsequent reactions with additional NO, results in the release of N_2O and formation of Ni(II)-nitrito complex. Crystallographic characterization of the nitrito complex reveals a symmetric η^2-O,O-nitrito bonding to the metal ion. This study demonstrates the reductive nitrosylation of a Ni(II) center followed by the release of N_2O in presence of excess NO.

3.1 Introduction

Transition metal ions induced activation of nitric oxide (NO), has attracted enormous research interest as various biological and physiological reactivity which are attributed to the formation of nitrosyl complexes of metallo-proteins, mostly iron or copper-proteins. [1-3] In this regard, the iron-nitrosyls have been studied extensively, both in protein and model systems.[3] Ferriheme proteins are reported to undergo reduction in aqueous media in the presence of NO.[4,5] The corresponding ferrous protein then reacts with excess of NO to form stable ferroheme nitrosyl.[6-8]

The reduction of Cu(II) centers in cytochrome *c*-oxidase and laccase, to Cu(I) by NO is known for a long time.[9-12] In model systems, it has been exemplified by a number of Cu(II) complexes in recent years.[13-23]

Mn(III) complex $[Mn(PaPy_2Q)(OH)]ClO_4$ ($PaPy_2QH$ = N,N-*bis*(2-pyridylmethyl)amine-N-ethyl-2-quinoline-2-carboxamide) was found to react with excess NO to afford the nitrosyl complex $[Mn(PaPy_2Q)(NO)]ClO_4$ *via* reductive nitrosylation.[24] Another example demonstrated that addition of NO to the acetonitrile solution of $[(Mn(PaPy_3))_2(\mu\text{-}O)](ClO_4)_2$ ($PaPy_3$ = the anion of the designed ligand N,N-*bis*(2-pyridylmethyl)amine-N-ethyl-2-pyridine-2-carboxamide) results in the $\{MnNO\}^6$ nitrosyl $[Mn(PaPy_3)(NO)](ClO_4)$ *via* reductive nitrosylation.[25]

Ni(II) in different ligand environment are known to undergo reduction to Ni(I) either by electrochemical procedure or by reducing agents.[26-28] However, reduction of Ni(II) center by NO leading to subsequent nitrosylation to form $\{NiNO\}^{10}$ complexes have not been explored extensively. Hayton's group reported the examples of $\{NiNO\}^{10}$ and their reactivity; but, in all the examples nickel(I)-nitrosyl complexes have been utilized. [29-30]

This chapter describes a Ni(II) complex, **3.1** of ligand **L3** {**L3** = *bis*(2-ethyl-4-methylimidazol-5-yl)methane}. The ligand framework has been chosen as it offers structural flexibility and an accessible reduction potential for the transition metal ions due to its π-acceptor property. In methanol solution of complex **3.1** upon addition of NO undergoes reductive nitrosylation to result in $\{NiNO\}^{10}$ complex. This, in presence of excess NO releases N_2O with the formation of corresponding Ni(II)-nitrito complex, **3.2**.

3.2 Results and Discussion

The ligand, **L3** was synthesized by following an earlier reported procedure.[31] The Ni(II) complex, **3.1** was prepared by stirring a mixture of nickel(II) chloride hexahydrate with two equivalent of ligand, **L3** in methanol. The microanalytical data of complex **3.1** shows good agreement with the calculated values (Experimental Section). It was characterized by various spectroscopic analyses, as well (Experimental Section). The single crystal X-ray structure of complex **3.1** was determined. The crystallographic data, important bond angles and distances are listed in tables 3.1, 3.2 and 3.3, respectively. The ORTEP view of the complex **3.1** is shown in figure 3.1. The crystal structure reveals that Ni(II) center is coordinated by two ligand units in a distorted square planar geometry. The average Ni-N distance is found 1.893 Å, which is within the range of analogous reported complexes.[32] The average N-Ni-N bite angle is ~ 90.0°.

The complex **3.1** in dry methanol solution displays absorption bands at 636 nm (ε/ $M^{-1}cm^{-1}$, 25) and 398 nm (ε/ $M^{-1}cm^{-1}$, 240) in the UV-visible spectrum along with other intra-ligand transitions in lower wavelengths (Figure 3.2) (Appendix II). The band centred at 636 nm is assigned to the *d-d* transition for Ni(II) center.

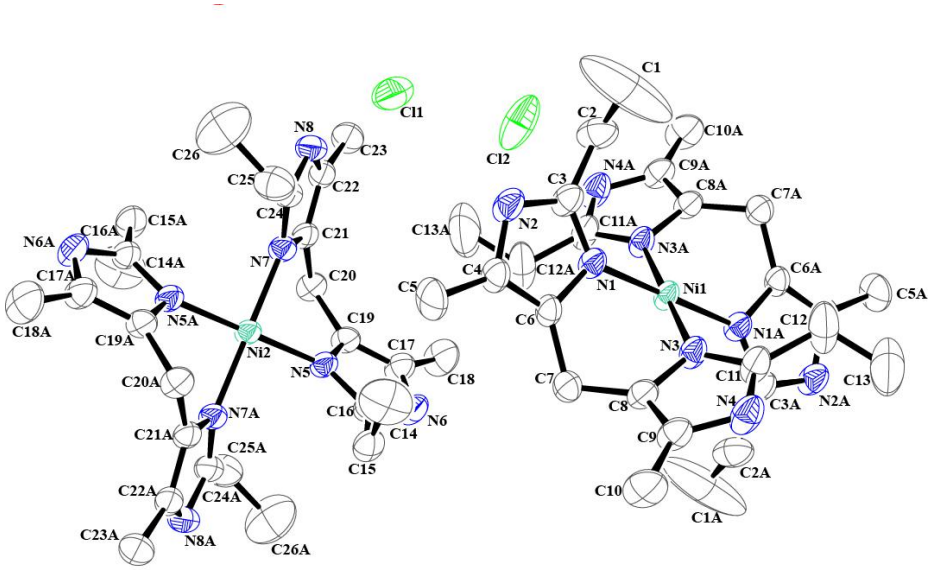

Figure 3.1. ORTEP diagram of complex **3.1** (50% thermal ellipsoid plot, H-atoms are omitted for clarity).

The cyclic voltammogram of complex **3.1** was recorded in methanol using TBAP supporting electrolyte in a three electrode configuration with a saturated Ag/Ag+ reference, glassy carbon working and Pt auxiliary electrodes. A quasi-reversible reduction at −1.05 V was observed in the voltammogram (Appendix II). These are attributed to the Ni(II)/Ni(I) reduction. In the same setup, the NO/NO^+ couple appeared at 1.15 V (Appendix II).

Addition of equivalent amount of NO in the degassed methanol solution of complex **3.1** at -80 °C displays a shift in the *d-d* band from 636 nm to 578 nm (Figure 3.2). The shift in λ_{max} and change in intensity of the *d-d* band is attributed to the formation of corresponding Ni(I)-complex (Scheme 3.1). The reduction of Ni(II) center to Ni(I) by NO was also suggested from the X-band EPR studies. The diamagnetic Ni(II) center, upon addition of

equivalent amount of NO displays EPR signals corresponding to Ni(I) ($g_{\parallel}$, 2.29; $g_{\perp}$, 2.17) (Figure 3.3).[33]

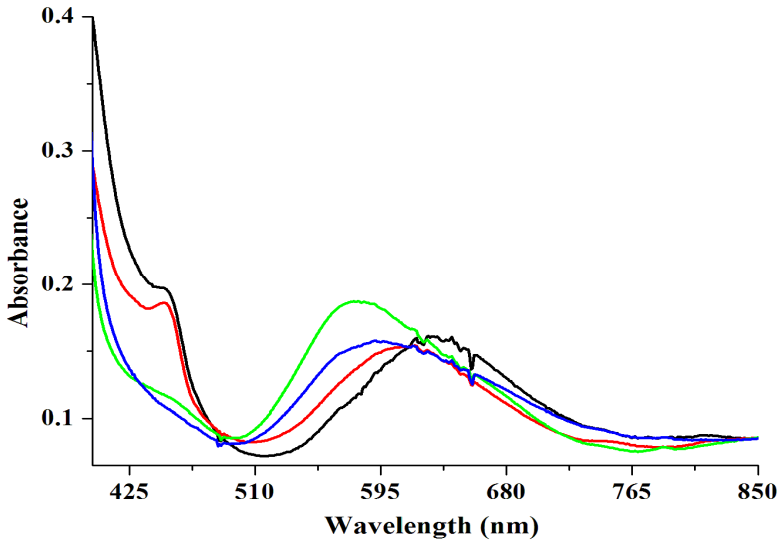

Figure 3.2. UV-visible spectra of complex **3.1** (black), after addition of stoichiometric amount of NO (red), {NiNO}^{10} intermediate (green) and complex **3.2** (blue) in methanol at - 80 °C.

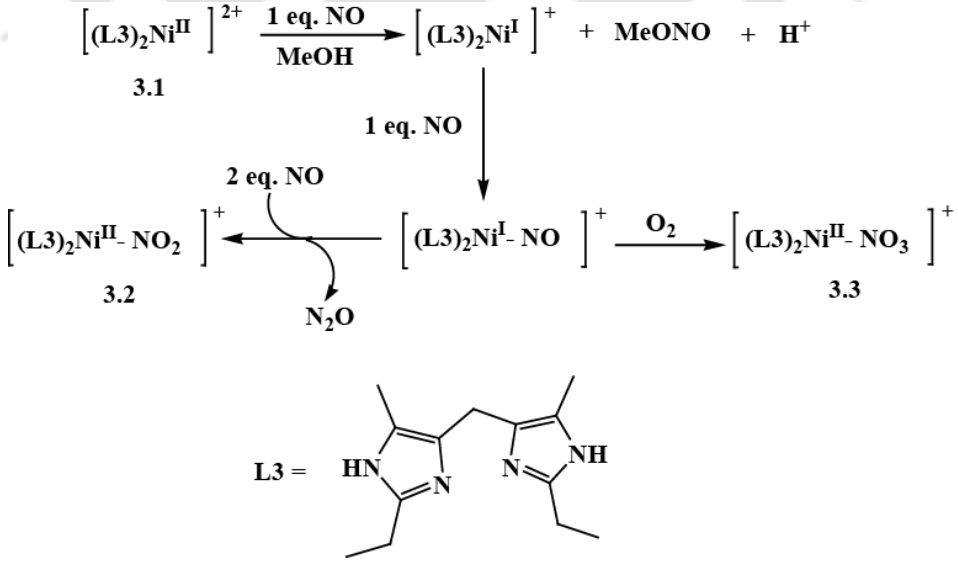

Scheme 3.1

The EPR spectra of electrochemically generated Ni(I) complexes reported earlier. For instance, Ni(I) complex of 5,5,7,12,12,14-hexamethyl-1,4,8,11-tetraazacyclotetradecane also displayed axial EPR spectrum.[33b] Double integration using Cu(II) sulphate pentahydrate as a standard for d^9 electronic configuration revealed the presence of ~ 80% Ni(I) in solution (Appendix II). On the other hand, the appearance of methyl nitrite in the GC-mass spectrum of the reaction mixture also suggested the formation of NO^+ ion during the reaction (Appendix II). That was found to be thermally unstable and highly sensitive towards air and moisture which preclude it's isolation and further characterization. Addition of one more equivalent of NO resulted in the corresponding Ni(I)-nitrosyl intermediate with $\{NiNO\}^{10}$ configuration (Scheme 3.1). That was monitored by UV-visible, solution FT-IR, NMR and EPR spectroscopic studies. The intermediate is found to be thermally unstable and highly sensitive towards air and moisture, too.

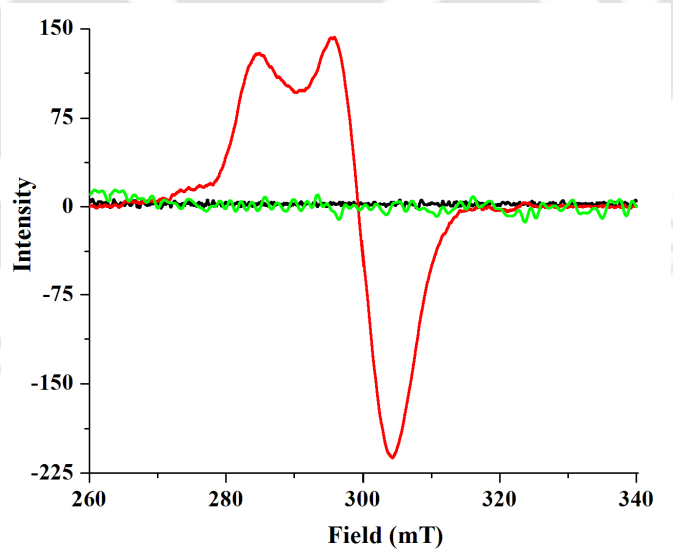

Figure 3.3. X-band EPR spectra of complex **3.1** (black), Ni(I) species (red) and complex **3.2** (green) in methanol at 77 K.

It is to be noted that though there was not much change in the position of *d-d* absorption

band of Ni(I) species and {NiNO}^{10} , the shoulder observed near ~460 nm on case of Ni(I) intermediate was found to disappear after addition of NO (Figure 3.2). In the FT-IR spectrum of the methanol solution of complex **3.1**, addition of two equivalent of NO resulted in the appearance of a new band at 1668 cm^{-1} (Figure 3.4), assignable to the υ_{NO} of corresponding {NiNO}^{10} intermediate. ^{15}NO labelling showed a shift of this frequency to 1636 cm^{-1} (Appendix II). This frequency is actually at the low end of values reported for nickel nitrosyl complexes (ranging from 1568 cm^{-1} to 1915 cm^{-1}).[34,35] The nitrosyl stretching frequency was reported to appear at 1869 and 1868 cm^{-1} in cases of [Ni(NO)(bpy)](PF_6) and [Ni(NO)(bpy)(μ-S_2Ph_2)](PF_6), respectively, in dichloromethane solution.[29]

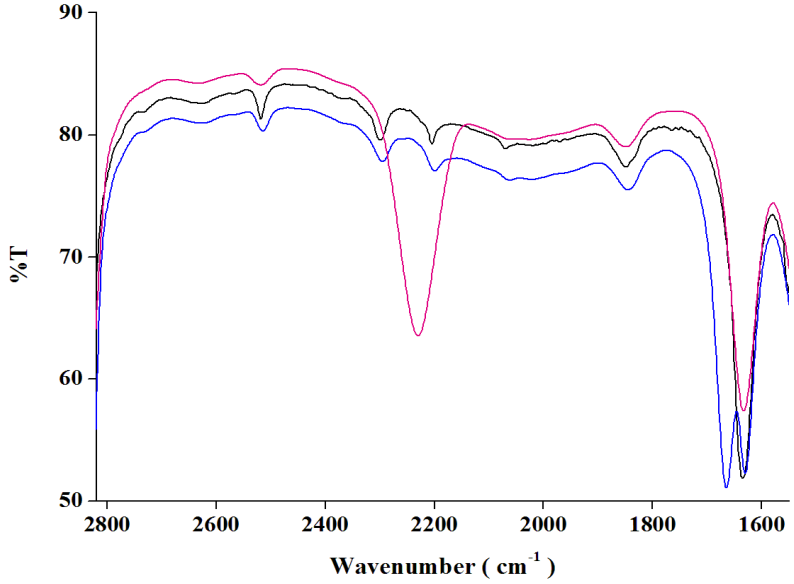

Figure 3.4. FT-IR spectra of complex **3.1** (black), after immediate addition of NO (blue); and after 30 minutes of addition of excess NO (pink; formation of N_2O is indicated by 2230 cm^{-1}) in methanol at room temperature.

It is known that the geometry around the central metal ion also dictates the IR stretching

frequency of metal nitrosyls. For instance, [Ni(NO)(bpy)](PF_6), the nitrosyl stretching appears at 1869 cm^{-1} in CH_2Cl_2, whereas at 1567 cm^{-1} in case of [Ni(NO)$(bpy)_2$](PF_6); on the other hand, for [Ni(NO)(bpy)](PF_6) in acetonitrile solution, it appears at 1828 cm^{-1} owing to the solvent coordination to the metal ion.[30] In addition, linear nitrosyls are known to have higher stretching frequency compared to that in bent geometry.[36]

ESI mass spectral studies showed peak at 584.28 suggesting the formation of $[(L3)_2Ni(NO)(MeOH)]^+$ (Figure 3.5). The fragmentation pattern matches very well with the simulated spectrum suggesting a correct assignment (Figure 3.5). In X-band EPR studies, the $\{NiNO\}^{10}$ intermediate appeared to be silent owing to the anti-ferromagnetic coupling of spins of the paramagnetic Ni(I) and NO resulting in S = 0 spin state (Figure 3.3).

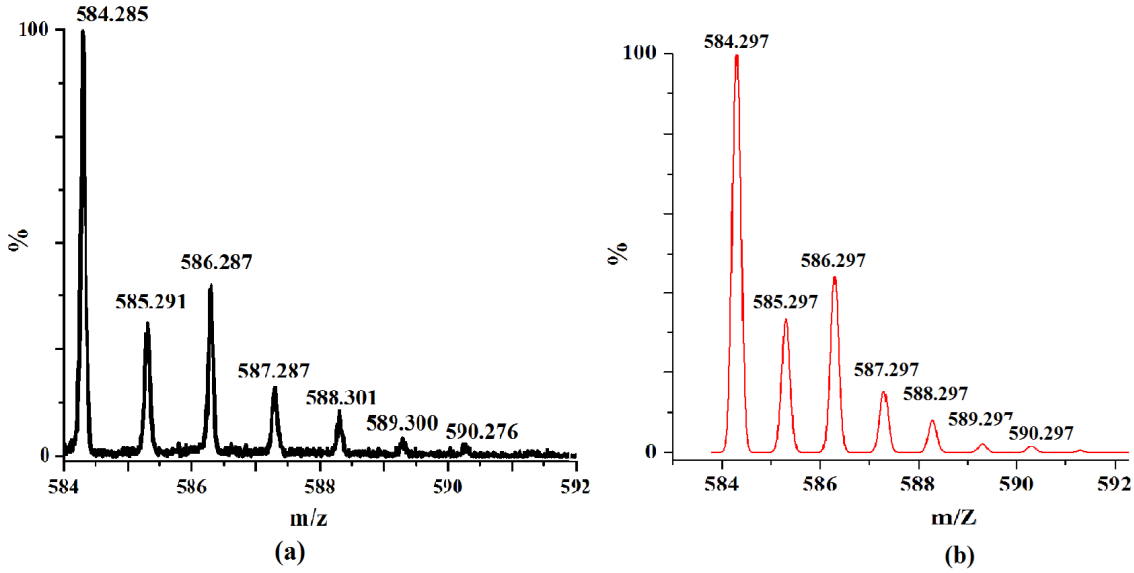

Figure 3.5. ESI-mass spectra of $[(L3)_2Ni(NO)(CH_3OH)]^+$ with isotopic distribution (a) experimental and (b) simulated in methanol.

In ^{1}H-NMR study, the broad signals of Ni(I) species became sharp and well resolved suggesting the formation of diamagnetic $\{NiNO\}^{10}$ (Figure 3.6 and appendix II). The

proposed {NiNO}[10] intermediate shown in scheme 3.1 was also investigated through quantum chemical calculations employing density functional theory (DFT). The calculations were carried out using the Turbomole 6.0 suite of programs. [37] Geometry optimizations were performed using the Perdew, Burke, and Ernzerhof density functional (PBE). [38] The electronic configuration of the atoms was described by a triple-ζ basis set augmented by a polarization function (Turbomole basis set TZVP).[39] The resolution of identity (ri), along with the multipole accelerated resolution of identity (mari) approximations were employed for an accurate and efficient treatment of the electronic Coulomb term in the density functional calculations.[40,41] Furthermore, the solvent effects were incorporated in the COSMO model, with ε = 32.7 for methanol. [42] The DFT optimized structure of the proposed intermediate (Scheme 3.1) is shown in figure 3.7 below.

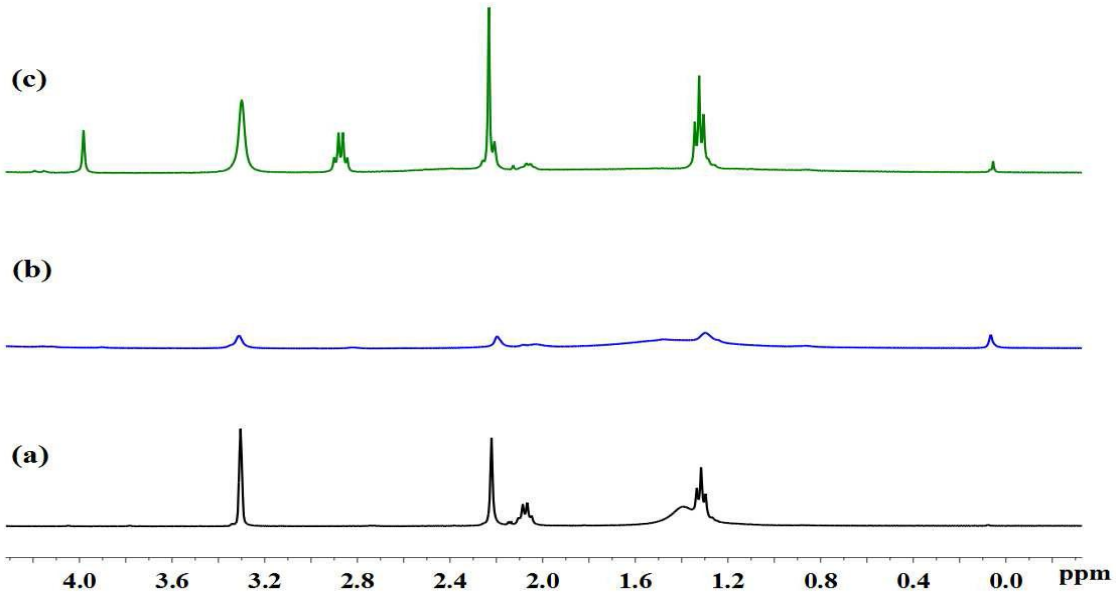

Figure 3.6. ^{1}H-NMR spectra of complex **3.1** (a), after purging one (b) and two (c) equivalent of NO in complex **3.1** in CD_3OD.

As shown in figure 3.7, the $\{NiNO\}^{10}$ intermediate has a square based pyramidal geometry where the NO is coordinated to nickel. It was observed that methanol does not bind to the nickel centre but remains in close proximity by forming a hydrogen bond with the nitrogen of NO, as shown in figure 3.7; the NO stretching frequency calculated with PBE/TZVP was found to be 1534.3 cm^{-1}, which is lower by 135 cm^{-1} with respect to the experimentally observed frequency for the NO stretch. It is to be noted that the stretching frequencies obtained from DFT calculations normally differ with experiments by 150-200 cm^{-1}, as has been seen from previous reports.[43-46] Hence, the value can be deemed to be acceptable.

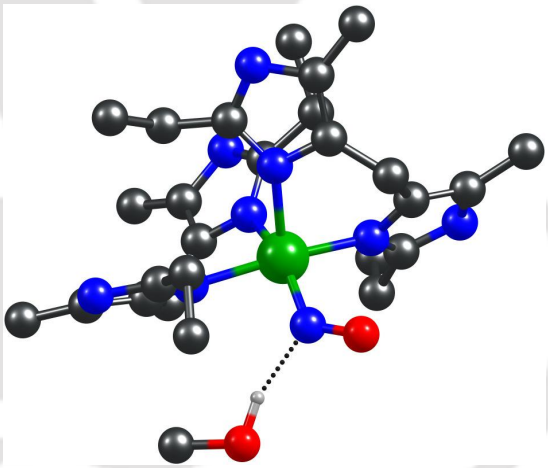

Figure 3.7. The optimized structure corresponding to the proposed intermediate; the color scheme is as follows: nickel: green, carbon: black, oxygen: red, nitrogen: blue and hydrogen: white; only the methanol hydrogen is shown in the structure, the rest of the hydrogen atoms have been removed for the purpose of clarity.

In this regard, it is also noted that several other possible structures for the intermediate have been looked into computationally. This includes octahedral complexes having chlorine coordinated to the nickel centre, square planar complexes where one of the ligand is mono coordinated, and a trigonal geometry where both the ligands are mono coordinated. These possible structures have been shown in the appendix II. It was found

that none of the other structures were (a) optimizing to form stable minima or (b) comparable in stability (i.e. they were found to be energetically less stable) to the proposed intermediate structure. This provides further indication of the validity of the proposed intermediate complex.

Furthermore, the UV-visible spectrum for the intermediate $\{NiNO\}^{10}$ complex in methanol has been calculated with TD-DFT calculations at PBE/TZVP level of theory, with solvent corrections included. The intermediate complex shows three absorption bands: (i) at 428 nm with oscillator strength of 0.0035, (ii) at 521 nm with oscillator strength of 0.0036 and at 580 nm with oscillator strength of 0.0055. Therefore, the calculations indicate that the strong absorption band at 580 nm which is in agreement with the experimentally observed λ_{max} of 578 nm (Figure 3.2). Thus, the current computational investigations suggest that the intermediate formed is indeed the square based pyramidal geometry where the NO is coordinated to Ni(I) center, with a methanol solvent molecule hydrogen bonded to the nitrosyl nitrogen, as shown in the optimized structure in figure 3.7.

In presence of excess NO, the intensity of 578 nm band of $\{NiNO\}^{10}$ was found to decay indicating the decomposition of the intermediate (Figure 3.2). This finally lead to the formation of corresponding Ni(II)-nitrito complex (**3.2**) and nitrous oxide (N_2O) (Scheme 3.1). The final nitrito complex, **3.2** was isolated and characterized by various spectroscopic techniques (Experimental Section). It behaves as 1:1 electrolyte in solution (Experimental Section). Single crystal X-ray structure reveals that a Ni(II) center is coordinated to two ligand moieties and a (η^2-O,O)-nitrito group (Figure 3.8). The crystallographic data, selected bond distances and angles are listed in tables 3.1, 3.2 and 3.3, respectively.

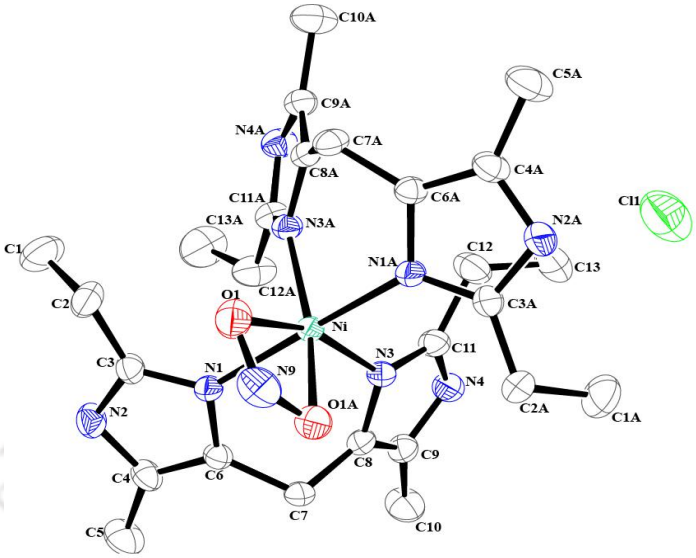

Figure 3.8. ORTEP diagram of complex **3.2** (50% thermal ellipsoid plot, H-atoms are omitted for clarity).

The average Ni–N distances (2.078 Å) are found to bit longer compared to that in complex **3.1**, perhaps because of difference in geometry. The average N–O distance of the coordinated nitrito group is 1.268 Å and the Ni–O distance is 2.124 Å.

Table 3.1. Crystallographic data for complexes **3.1**, **3.2** and **3.3**

	3.1	**3.2**	**3.3**
Formulae	C_{26} H_{40} Cl_2 N_8 Ni O_2	C_{26} H_{40} Cl N_9 Ni O_4	C_{52} H_{82} Cl_2 N_{18} Ni_2 O
Mol. wt.	626.25	636.81	1259.68
Crystal system	Triclinic	Monoclinic	Monoclinic
Space group	P -1	P 2/c	P 21
Temperature /K	296(2)	296(2)	296(2)
Wavelength /Å	0.71073	0.71073	0.71073
a /Å	10.8432(9)	9.4536(3)	9.7243(4)
b /Å	11.2496(10)	9.3089(3)	33.0698(17)
c /Å	14.2270(12)	18.4419(7)	9.7619(5)
α/°	85.227(4)	90.00	90.00
β/°	77.009(4)	91.025(2)	97.492(3)
γ/°	73.307(4)	90.00	90.00
V/ $Å^3$	1619.4(2)	1622.68(10)	3112.4(3)
Z	2	2	2

Density/Mgm^{-3}	1.284	1.303	1.342
Abs. Coeff. /mm^{-1}	0.799	0.725	0.753
Abs. correction	None	None	None
F(000)	660	672	1328
Total no. of reflections	7786	2828	9833
Reflections, $I > 2\sigma(I)$	6432	2406	6257
Max. 2θ/°	28.25	25.00	25.00
Ranges (h, k, l)	-14≤ h ≤14 -14≤ k ≤13 -18≤ l ≤ 17	-11≤ h ≤10 -11≤ k ≤10 -21≤ l ≤ 21	-11≤ h ≤11 -37≤ k ≤39 -11≤ l ≤ 11
Complete to 2θ (%)	97.2	99.0	98.3
Refinement method	Full-matrix least-squares on F^2	Full-matrix least-squares on F^2	Full-matrix least-squares on F^2
Goof (F^2)	1.062	1.076	1.047
R indices [$I > 2\sigma(I)$]	0.0482	0.0615	0.0761
R indices (all data)	0.1510	0.0679	0.1294

Table 3.2. Selected bond lengths (Å).

	3.1	**3.2**	**3.3**
Ni(1)-N(1)	1.895(3)	2.077(4)	2.050(1)
Ni(1)-N(3)	1.890(3)	2.079(4)	2.070(1)
Ni(1)-O(1)	-	2.214(4)	2.290(1)
O(1)-N(9)	-	1.268(5)	1.220(2)
N(1)-C(3)	1.337(5)	1.326(6)	1.360(2)
N(1)-C(6)	1.397(6)	1.392(6)	1.410(2)
N(2)-C(3)	1.351(7)	1.343(7)	1.340(2)
N(2)-C(4)	1.378(7)	1.374(7)	1.430(2)

Table 3.3. Selected bond angles (°).

	3.1	**3.2**	**3.3**
N(1)-Ni(1)-N(3)	86.70 (1)	89.10(1)	90.90(4)
N(1)-Ni(1)-N(1A)	180.00(1)	171.30(2)	-
N(1)-Ni(1)-N(3A)	93.30(1)	96.80(2)	-
N(3)-Ni(1)-N(3A)	180.00(1)	94.20(2)	-
N(1)-Ni(1)-N(7)	-	-	98.50(4)
O(1)-Ni(1)-N(1)	-	86.20(1)	158.70(4)
O(1)-Ni(1)-N(3)	-	104.50(1)	86.60(4)
Ni(1)-O(1)-N(9)	-	95.40(4)	89.40(8)
O(1)-N(9)-O(1A)	-	112.40(5)	-

The formation of N_2O in the reaction was confirmed by GC-mass spectral analysis of the head space gas of the reaction vessel (Appendix II). This was further confirmed by the FT-IR monitoring of the reaction mixture which shows the appearance of a stretching frequency at 2230 cm^{-1} assignable to N_2O (Figure 3.4). Recently, Hayton *et al*. reported the isolation of a nickel nitrosyl, $[Ni(NO)(bipy)_2](PF_6)$, which forms N_2O on standing *via* a *cis*-$[N_2O_2]^{2-}$ intermediate. For that case the N_2O stretching frequency appears at 2228 cm^{-1}.[29,30]

The formation of N_2O from NO can occur either by HNO disproportionation or by hyponitrite intermediate formation.[47] One proposed mechanism involves the initial formation of a *cis*-dinitrosyl complex followed by the coupling of the two nitrosyl groups and subsequent reduction to form hyponitrite, $(N_2O_2)^{2-}$ intermediate.[47,48] This on reaction with H^+ results H_2O and N_2O. Solid state thermal decomposition study of various metal-nitrosyls reveal that $[M(NO)_2]$ motif actually plays an important role in homogeneous solution phase reduction of NO to N_2O for transition metal ions like Rh, Ir, Ru, Fe and Pt.[49,50]

On the other hand, the bent nitrosyl ligands are known to be the subject of electrophilic attack at the nitrogen lone pair.[47,51] There are several examples reported on the electrophilic attack of free NO on a metal bound nitrosyl ligand.[47,51] For instance, $[Co(NO)(NH_3)_5]^{2+}$ is known to react with free NO to generate asymmetric hyponitrie bridged dimer.[51b] Troggler *et al*. also has suggested that the electrophilic attack of the free NO on that coordinated to the transition metal will result in a hyponitrite complex. [47] This decomposes to yield N_2O and water. The proposed mechanistic cycle of nitric oxide reductase activity of cytochrome *c*-oxidase, it is believed that initial binding of NO to the reduced heme centre results a bent nitrosyl (ν_{NO}, 1610 cm^{-1}).[52] In subsequent steps, nitrogen-nitrogen bond formation was suggested through the reaction of a second nitrosyl group bound to the copper centre of CcO.[52]

It would be worth to mention that mononuclear copper(I)-nitrosyl complexes were found to promote NO disproportionation with the formation of Cu(II)-nitrito complexes.[53] For instance, Cu(I) complexes of *bis*-(phenyl) substituted *tris*-(pyrazole)-hydroborate and 1,4-diisopropyl-7,2-pyridylmethyl-1,4,7-triazacyclononane were reported to catalyze the disproportionation under excess NO condition to result in N_2O and corresponding Cu(II)-NO_2^- complexes.[54] Notably, the X-ray crystallography characterization of the corresponding nitrito complexes revealed a symmetric η^2-O,O-nitrite binding to the metal ions. Mechanistic studies suggested an electrophilic attack of a second NO molecule to the initially formed Cu-NO complex to result in $Cu(NO)_2$ species; which in subsequent N-N coupling and O-atom transfer gives N_2O and nitrito complex of Cu(II) ion.

The $\{NiNO\}^{10}$ intermediate was found to decompose to the corresponding nitrato complex (**3.3**) in presence of oxygen (Scheme 3.1). Iron-nitrosyls in heme models and copper-

nitrosyls are known to react with oxygen to afford peroxynitrite ($ONOO^-$) which then isomerise to the corresponding nitrato complexes.[55] The decomposition product, complex **3.3** has been isolated as solid and characterized structurally. The perspective ORTEP view of complex **3.3** is shown in figure 3.9.

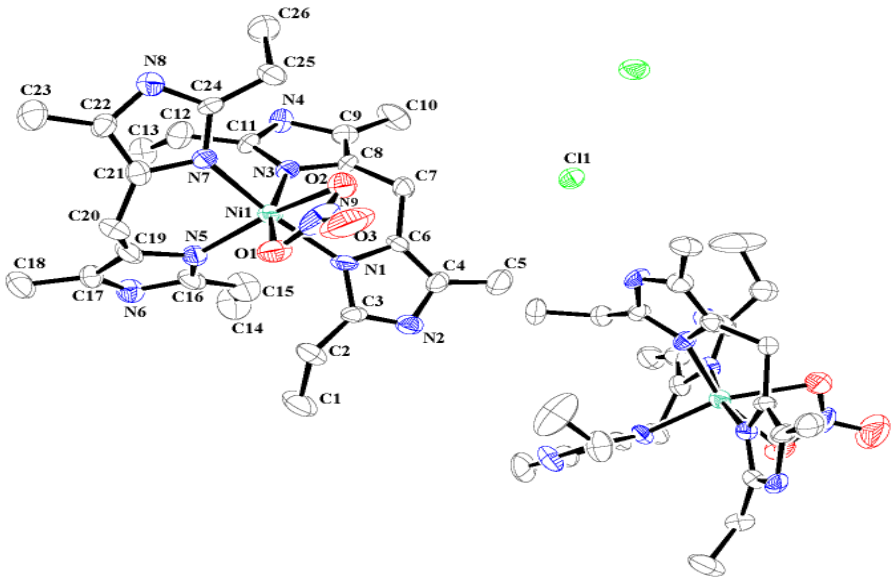

Figure 3.9. ORTEP diagram of complex **3.3** (50% thermal ellipsoid plot, H-atoms is omitted for clarity).

Single crystal X-ray structure suggests that the Ni(II) center is coordinated to two ligand moieties and a (η^2-O,O)-nitrato group (Figure 3.9). The crystallographic data, selected bond distances and angles are listed in tables 3.1, 3.2 and 3.3, respectively. The average Ni–N distances (2.06 Å) are shorter in comparison to complex **3.2** but longer with respect to complex **3.1**. The average N–O distance of the coordinated nitrato group is 1.22 Å and the Ni–O distance is 2.29 Å.

3.3 Experimental Section

3.3.1 Materials and Methods

All reagents and solvents were purchased from commercial sources and were of reagent grade. HPLC grade methanol was used and dried using standard protocol. ^{15}NO was purchased from Icon Isotopes. Deoxygenation of the solvent and solutions were effected by repeated vacuum/purge cycles or bubbling with nitrogen or argon for 30 minutes. NO was used from cylinder after purification by passing through KOH and P_2O_5 column. Further purification was done following reported methods of fractional distillation. Stoichiometric amount of NO was added to the sample using a Hamilton gas tight syringe after diluting with argon gas. The required dilution of NO was effected with argon gas using Environics Series 4040 computerized gas dilution system. UV-visible spectra were recorded on Agilent HP 8453 UV-visible spectrophotometer. FT-IR spectra were taken on a Perkin-Elmer spectrophotometer with either sample prepared as KBr pellets or in solution in a potassium bromide cell. Solution electrical conductivity was checked using a Systronic 305 conductivity bridge. ^{1}H-NMR and ^{13}C-NMR spectra were obtained with a 400 MHz Varian FT spectrometer. Chemical shifts (ppm) were referenced either with an internal standard (Me_4Si) for organic compounds or to the residual solvent peaks. The X-band Electron Paramagnetic Resonance (EPR) spectra were recorded on a JES-FA200 ESR spectrometer, at room temperature and 77K with microwave power, 0.998 mW; microwave frequency, 9.14 GHz and modulation amplitude, 2. The magnetic moment of complexes are measured on a Cambridge Magnetic Balance. Mass spectra of the compounds were recorded in a Waters Q-Tof Premier and Aquity instrument. Elemental analyses were obtained from a Perkin Elmer Series II Analyzer.

Single crystals were grown by slow diffusion followed by slow evaporation technique. The intensity data were collected using a Bruker SMART APEX-II CCD diffractometer, equipped with a fine focus 1.75 kW sealed tube MoKa radiation (λ = 0.71073 Å) at 273(3) K, with increasing ω (width of 0.3° per frame) at a scan speed of 3s/frame. The SMART software was used for data acquisition.[56] Data integration and reduction was undertaken with SAINT and XPREP software.[57] Structures were solved by direct methods using SHELXS-97 and refined with full-matrix least squares on F^2 using SHELXL-97.[58] Structural illustrations have been drawn with ORTEP-3 for Windows.[59]

3.3.2 Syntheses

(a) Ligand L3

2-ethyl-4-methyl imidazole (2.2 g; 20 mmol) was taken in a round bottom flask with 50 ml of methanol; to this 0.45 g of (15 mmol) formaldehyde and aqueous solution of 5.1 g (91 mmol) potassium hydroxide was added drop wise. The reaction mixture was stirred for 24 h. at room temperature. A white coloured solid was obtained. It was filtered off and washed with water. After washing the solid was dried in air and then kept in desiccators for overnight. Yield: 1.97g (85%). Elemental analyses for $C_{13}H_{20}N_4$, Calcd(%): C, 67.21; H, 8.68; N, 24.12. Found (%): C, 67.19; H, 8.68; N, 24.02. FT-IR (in KBr): 2964, 2842, 1614, 1529, 1455, 1071 cm^{-1}; ^{1}H-NMR (400 MHz, $CDCl_3$): δ_{ppm}, 3.53 (2H), 2.44 (4H), 1.87 (6H), 1.08 (6H). ^{13}C-NMR (100 MHz, $CDCl_3$): δ_{ppm}, 149.2, 129.1, 127.2, 23.3, 22.6, 13.7, 10.6.

(b) Complex 3.1

Nickel(II) chloride hexahydrate (2.38 g) was taken in a 50 ml round bottom flask,

dissolved in 20 ml of MeOH. To this, a solution of 4.64 g of ligand **L3** in methanol (5 ml) was added and stirred for 1 h. A deep green solution was dried in rotary evaporator to obtain a green solid which upon crystallization gives yellow crystals. Yield: 5.26 g (84%). Elemental analyses for $C_{26}H_{40}Cl_2N_8Ni$, Calcd(%): C, 52.55; H, 6.78; N, 18.86. Found (%): C, 52.61; H, 6.77; N, 18.95. FT-IR(in KBr): 3435, 2980, 1643, 1468, 1432, 1319, 1287, 1089, 816, 591 cm^{-1}. UV–visible (methanol): 398 nm (ε/ $M^{-1}cm^{-1}$, 240) and 636 nm (ε/ $M^{-1}cm^{-1}$, 25). Molar conductance: 239 S cm^2 mol^{-1}(in methanol).

(c) Complex 3.2

In 20 ml of dry and degassed methanol solution of complex **3.1** (180 mg), freshly purified NO was bubbled in excess till the deep color of the solution becomes fade. The reaction mixture was kept at room temperature for crystallization. Yield: 138.5 mg (72%). Elemental analyses for $C_{26}H_{40}ClN_9O_4Ni$, Calcd(%): C, 49.04; H, 6.33; N, 19.79. Found (%): C, 49.11; H, 6.36; N, 19.92. FT-IR (in KBr): 3390, 3174, 3126, 1627, 1530, 1464, 1429, 1322, 1197, 1048, 776 cm^{-1}. UV–visible (methanol): 621 nm (ε/ $M^{-1}cm^{-1}$, 31), 979 nm (ε/ $M^{-1}cm^{-1}$, 12). Molar conductance: 160 S cm^2 mol^{-1} (in methanol), observed magnetic moment: 1.93 BM.

(d) Complex 3.3

To a degassed methanol solution of complex **3.1** (240 mg) at -80 °C, freshly purified NO was bubbled for 30 s. Then the excess of NO gas was removed by using four cycles of vacuum and Ar purging. To this, an excess of dioxygen was added through a gas tight syringe. The reaction mixture was warmed up to room temperature and kept for two days while complex **3.3** was crystallized out. Yield: 128 mg (~52%). Elemental analyses for

$C_{26}H_{40}ClN_9O_5Ni$, Calcd(%): C, 47.84; H, 6.17; N, 19.31. Found(%): C, 47.91; H, 6.16; N, 19.40. FT-IR (in KBr): 3168, 3127, 3126, 1625, 1531, 1464, 1429, 1384, 1333, 1222, 1053, 839, 752, 620 cm^{-1}. UV–visible (methanol): 600 nm (ε/ $M^{-1}cm^{-1}$, 41), 987 nm (ε/ $M^{-1}cm^{-1}$, 15). Molar conductance: 176 S cm^2 mol^{-1} (in methanol), observed magnetic moment: 1.84 BM.

(e) *In-situ* generation of Ni(I) and Ni(I)-NO intermediates:

Complex **3.1** (200 mg) was dissolved in 20 ml of dry methanol in a 50 ml Schlenk flask and then the solution was degassed by bubbling argon for 1 h. The solution was then cooled to -80 °C and equivalent amount of NO gas was purged into the solution using a gas tight Hamilton syringe. The color of the solution became light indicating the formation of Ni(I) intermediate. The reaction mixture was transferred into EPR and NMR tube using gas tight Hamilton syringe and the spectra were recorded.

Similar procedure was followed for generating $\{NiNO\}^{10}$ where two equivalent of NO was added to result in a blue solution.

3.4 Conclusion

In conclusion, the Ni(II) complex of *bis*(2-ethyl-4-methylimidazol-5-yl)methane, **3.1** in methanol solution reacts with NO to result in reductive nitrosylation leading to the formation of corresponding $\{NiNO\}^{10}$ intermediate. This intermediate on subsequent reactions with additional NO, results in the release of N_2O and formation of Ni(II)-nitrito complex. The crystallographic characterization of the nitrito complex reveals a symmetric η^2-O,O-nitrito bonding to the metal ion as observed in cases of iron, manganese and copper complexes.

3.5 References

(1) (a) *Nitric Oxide: Biology and Pathobiology*; Ignarro, L. J., ed.; Academic Press: San Diego, CA, **2000**. (b) Martin, C. T.; Morse, R. H.; Kanne, R. M.; Gray, H. B.; Malmstrom, B. G.; Chan, S. I. *Biochemistry* **1981**, *20*, 5147.

(2) (a) Cooper, C. E.; Torres, J.; Sharpe, M. A.; Wilson, M. T. FEBS *Lett*. **1997**, *414*, 281.(b) Studbauer, G.; Giuffre, P.; Sarti, P. *J. Biol. Chem*. **1999**, *274*, 28128. (c) McCleverty, J. A. *Chem. Rev*. **2004**, *104*, 403. (d) Arikawa, Y.; Onishi, M. *Coord. Chem. Rev*. **2012**, *256*, 468.

(3) (a) Patra, A. K.; Rose, M. J.; Olmstead, M. M.; Mascharak, P. K.; *J. Am. Chem. Soc*. **2004**, *126*, 4780. (b) Patra, A. K.; Afshar, R. K.; Rowland, J. M.; Olmstead, M. M.; Mascharak, P. K. *Angew. Chem., Int. Ed*. **2003**, *42*, 4517. (c) Patra, A. K.; Rowland, J. M.; Marlin, D. S.; Bill, E.; Olmstead M. M.; Mascharak, P. K. *Inorg. Chem*. **2003**, *42*, 6812.

(4) (a) Chien, J. C. W. *J. Am. Chem. Soc*. **1969**, *91*, 2166. (b) Wayland, B. B.; Olson, L. W. *J. Am. Chem. Soc*. **1974**, *96*, 6037.

(5) (a) Hoshino, M.; Maeda, M.; Konishi, R.; Seki, H.; Ford, P. C. *J. Am. Chem. Soc*. **1996**, *118*, 5702. (b) Hoshino, M.; Ozawa, K.; Seki, H.; Ford, P. C. *J. Am. Chem. Soc*. **1993**, *115*, 9568. (c) Lehnert, N.; Praneeth, V. K. K.; Paulat, F. *J. Comput. Chem*. **2006**, *27*, 1338.

(6) (a) Fernandez, B. O.; Ford, P. C. *J. Am. Chem. Soc*. **2003**, *125*, 10510. (b) Fernandez, B. O.; Lorkovic, I. M.; Ford, P. C. *Inorg. Chem*. **2004**, *43*, 5393.

(7) (a) Ellison, M. K.; Scheidt, W. R. *J. Am. Chem. Soc*. **1999**, *121*, 5210. (b) Linder, D. P.; Rodgers, K. R.; Banister, J.; Wyllie, G. R. A.; Ellison, M. K.; Scheidt, W. R. *J. Am. Chem. Soc*. **2004**, *126*, 14136.

(8) (a) Lim, M. D.; Lorkovic, I. M.; Ford, P. C. *J. Inorg. Biochem.* **2005**, *99*, 151. (b) Shamir, D.; Zilbermann, I.; Maimon, E.; Gellerman, G.; Cohen, H.; Meyerstein, D. *Eur. J. Inorg. Chem.* **2007**, 5029.

(9) Gorren, A. C. F.; de Boer, E.; Wever, R. *Biochem. Biophys. Acta* **1987**, *916*, 38.

(10) Torres, J.; Cooper, C. E.; Wilson, M. T. *J. Biol. Chem*. **1998**, *273*, 8756.

(11) (a) Torres, J.; Svistunenko, D.; Karlsson, B.; Cooper, C. E.; Wilson, M. T. *J. Am. Chem. Soc.* **2002**, *124*, 963. (b) Brown, G. C. *Biochim. Biophys. Acta* **2001**, *1504*, 46.

(12) (a) Torres, J.; Sharpe, M. A.; Rosquist, A.; Cooper, C. E.; Wilson, M. T. *FEBS Lett.* **2000**, *475*, 263. (b) Wijma, H. J.; Canters, G. W.; de Vries, S.; Verbeet, M. P. *Biochem.* **2004**, *43*, 10467.

(13) Miranda, K. M.; Bu, X.; Lorkovic, I. M.; Ford, P. C. *Inorg. Chem.* **1997**, *36*, 4838.

(14) (a) Lorkovic, I. M.; Miranda, K. M.; Lee, B.; Bernhard, S.; Schoonover, J. R.; Ford, P. C. *J. Am. Chem. Soc*. **1998**, *120*, 11674. (b) Lorkovic, I. M.; Ford, P. C. *Inorg. Chem*. **1999**, *38*, 1467.

(15) (a) Lorkovic, I. M.; Ford, P. C. *J. Am. Chem. Soc.* **2000**, *122*, 6516. (b) Laverman, L. E.; Wanat, A.; Oszajca, J.; Stochel, G.; Ford, P. C.; van Eldik, R. *J. Am. Chem. Soc*. **2001**, *123*, 285.

(16) (a) Laverman, L. E.; Ford, P. C. *J. Am. Chem. Soc.* **2001**, *123*, 11614. (b) Kurtikyan, T. S.; Martirosyan, G. G.; Lorkovic, I. M.; Ford, P. C. *J. Am. Chem. Soc*. **2002**, *124*, 10124.

(17) (a) Lim, M. D.; Lorkovic, I. M.; Wedeking, K.; Zanella, A. W.; Works, C. F.; Massick, S. M.; Ford, P. C. *J. Am. Chem. Soc*. **2002**, *124*, 9737. (b) Patterson, J. C.; Lorkovic, I. M.; Ford, P. C. *Inorg. Chem.* **2003**, *42*, 4902.

(18) (a) Ford, P. C. *Pure App. Chem.* **2004**, *76*, 335. (b) Martirosyan, G. G.; Azizyan, A. S.; Kurtikyan, T. S.; Ford, P. C. *Chem. Commun*. **2004**, 1488.

(19) (a) Kurtikyan, T. S.; Gulyan, G. M.; Martirosyan, G. G.; Lim, M. D.; Ford, P. C. *J. Am. Chem. Soc*. **2005**, *127*, 6216. (b) Ford, P. C.; Fernandez, B. O.; Lim, M. D. *Chem. Rev*. **2005**, *105*, 2439.

(20) (a) Gow, A. J.; Luchsinger, B. P.; Pawloski, J. R.; Singel, D. J.; Stamler, J. S. *Proc. Nat. Acad. Sci. U.S.A.* **1999**, *96*, 9027. (b) Luchsinger, B. P.; Rich, E. N.; Gow, A. J.; Williams, E. M.; Stamler, J. S.; Singel, D. J. *Proc. Nat. Acad. Sci. U.S.A.* **2003**, *100*, 461.

(21) (a) Gladwin, M. T.; Lancaster, J. R. Jr.; Freeman, B. A.; Schechter, A. N. *Nature Med.* **2003**, *9*, 496. (b) Han, T. H.; Fukuto, J. M.; Liao, J. C. *Nitric Oxide Bio. Chem.* **2004**, *10*, 74.

(22) (a) Feelisch, M. S.; Rassaf, T.; Manimneh, S.; Singh, N.; Byran, N. S.; Jourd'Heuil, D.; Kelm, M. *FASEB J.* **2002**, *16*, 1775. (b) Bryan, N. S.; Rassaf, T.; Maloney, R. E.; Rodriguez, C. M.; Saijo, F.; Rodriguez, J. R.; Feelisch, M. *Proc. Nat. Acad. Sci., U.S.A.* **2004**, *101*, 4308.

(23) (a) Rassaf, T.; Feelisch, M.; Kelm, M. *Free Rad. Bio. Med.* **2004**, *36*, 413. (b) Bryan, N. S.; Fernandez, B. O.; Bauer, S. M.; Garcia-Saura, M. F.; Milsom, Alexandra B.; Rassaf, T.; Maloney, R. E.; Bharti, A.; Rodriguez, J.; Feelisch, M. *Nat. Chem. Biol.* **2005**, *1*, 290.

(24) Eroy-Reveles, A. A.; Leung, Y.; Beavers, C. M.; Olmstead, M. M.; Mascharak, P. K. *J. Am. Chem. Soc*. **2008**, *130*, 4447.

(25) Ghosh, K.; Eroy-Reveles, A. A.; Olmstead, M. M.; Mascharak, P. K. *Inorg. Chem.* **2005**, *44*, 8469.

(26) (a) Halcrow, M. A.; Christou, G. *Chem. Rev.* **1994**, *94*, 2421. (b) Signor, L.; Knuppe, C.; Hug, R.; Schweizer, B.; Pfaltz, A.; Jaun, B. *Chem. Eur. J.* **2000**, *6*, 3508.

(27) (a) Ozaki, S.; Matsushita, H.; Ohmori, H. *J. Chem. Soc., Perkin Trans. 1* **1993**, 649. (b) Campbell, C. J.; Rusling, J. F.; Bruckner, C. *J. Am. Chem. Soc.* **2000**, *122*, 6679.

(28) (a) Kryatov, S. V.; Mohanraj, B. S.; Tarasov, V. V.; Kryatova, O. P.; Rybak-Akimova, E. V.; Nuthakki, B.; Rusling, J. F.; Staples, R. J.; Nazarenko, A. Y. *Inorg. Chem.* **2002**, *41*, 923. (b) James, T. L.; Cai, L.; Muetterties, M. C.; Holm, R. H. *Inorg. Chem.* **1996**, *35*, 4148.

(29) (a) Wright, A. M.; Wu, G.; Hayton, T. W. *J. Am. Chem. Soc.* **2012**, *134*, 9930. (b) Wright, A. M.; Zaman, H. T.; Wu, G.; Hayton, T. W. *Inorg. Chem.* **2014**, *53*, 3108.

(30) (a) Wright, A. M.; Zaman, H. T.; Wu, G.; Hayton, T. W. *Inorg. Chem.* **2013**, *52*, 3207. (b) Wright, A. M.; Wu, G.; Hayton, T. W. *Inorg. Chem.* **2011**, *50*, 11746.

(31) Kalita, A.; Kumar, P.; Deka, R. C.; Mondal, B. *Chem. Commun.* **2012**, *48*, 1551.

(32) (a) Butcher, R. J.; Sinn, E. *Inorg. Chem.* **1977**, *16*, 2334. (b) Ohtsu, H.; Tanaka, K.; *Inorg. Chem.* **2004**, *43*, 3024.

(33) (a) Kryatov, S. V.; Mohanraj, B. S.; Tarasov, V. V.; Kryatova, O. P.; Rybak-Akimova, E. V.; Nuthakki, B.; Rusling, J. F.; Staples, R. J.; Nazarenko, A. Y. *Inorg. Chem.* **2002**, *41*, 923. (b) Hathaway B. J.; Billing, D. E. *Coord. Chem. Rev.* **1970**, *5*, 143. (c) Gagne, R. R.; Ingle, D. M. *Inorg. Chem.* **1981**, *20*, 420. (d) Nag K.; Chakravorty, A. *Coord. Chem. Rev.* **1980**, *33*, 87. (e) Ansell, C. W. G.; Lewis, J.; Raithby, P. R.; Ramsden, J. N.; Shröder, M. *J. Chem. Soc. Chem. Commun.*

1982, 546 (f) Suh, M. P.; Oh, K. Y.; Lee, J. W.; Bae, Y. Y. *J. Am. Chem. Soc.* **1996**, *118*, 777.

(34) Feltham, R. D.; Carriel, J. T. *Inorg. Chem.* **1964**, *3*, 121.

(35) (a) Landry, V. K.; Parkin, G. *Polyhedron* **2007**, *26*, 4751. (b) Del, Z. A.; Mezzetti, A.; Novelli, V.; Rigo, P.; Lanfranchi, M.; Tiripicchio, A. *Dalton Trans*. **1990**, 1035. (c) Fullmer, B. C.; Pink, M.; Fan, H.; Yang, X.; Baik, M.-H.; Caulton, K. G. *Inorg. Chem.* **2008**, *47*, 3888. (d) Tennyson, A. G.; Dhar, S.; Lippard, S. J. *J. Am. Chem. Soc*. **2008**, *130*, 15087. (e) Varonka, M. S.; Warren, T. H. *Organometallics* **2010**, *29*, 717.

(36) Legzdins, P.; Richter-Addo, G. B. *Metal Nitrosyls*, Oxford University Press: New York, **1992**.

(37) Ahlrichs, R.; Baer, M.; Haeser, M.; Horn, H.; Koelmel, C. *Chem. Phys. Lett.* **1989**, *162*, 165.

(38) Perdew, J. P.; Burke, K.; Ernzerhof, M. *Physical Review Letters* **1996**, *77*, 3865.

(39) Weigend, F. *Phys. Chem. Chem. Phys.* **2002**, *4*, 4285.

(40) Eichkorn, K.; Treutler, O.; Oehm, H.; Haeser, M.; Ahlrichs, R. *Chem. Phys. Lett.* **1995**, *240*, 283.

(41) Sierka, M.; Hogekamp, A.; Ahlrichs, R. *J. Chem. Phys.* **2003**, *118*, 9136.

(42) Klamt, A. *J. Phys. Chem.* **1995**, *99*, 2224.

(43) Sundaraganesan, N.; Kalaichelvan, S.; Meganathan, C.; Joshua, B. D.; Cornard, J. *Spect. Acta Part A* **2008**, *71*, 898.

(44) Karabacak, M.; Kurt, M. *Spect. Acta Part A: Molecular and Biomolecular Spectroscopy* **2008**, *71*, 876.

(45) Karabacak, M.; Karagaz, D.; Kurt, M. *J. Mol. Struct.* **2008**, *892*, 25.

(46) Fan, L.; Ziegler, T. *J. Chem.Phys.* **1992**, *96*, 9005.

(47) MacNeil, J. H.; Berseth, P. A.; Bruner, E. L.; Perkins, T. L.; Wadia, Y.; Westwood, G.; Trogler, W. C. *J. Am. Chem. Soc*. **1997**, *119*, 1668.

(48) Eisenberg, R.; Hendricksen, D. E. *Adv. Catal*. **1979**, *28*, 79.

(49) (a) Hendriksen, D. E.; Meyer, C. D.; Eisenberg, R. *Inorg. Chem.* **1977**, *16*, 970. (b) Haymore, B. L.; Ibers, J. A. *J. Am. Chem. Soc.* **1974**, *96*, 3325.

(50) (a) Pearsall, K. A.; Bonner, F. T. *Inorg. Chem.* **1982**, *21*, 1978. (b) Bhaduri, S.; Johnson, B. F. G.; Savory, C. J.; Segal, J. A.; Walter, R. H. *J. Chem. Soc*., *Chem. Commun.* **1974**, 809.

(51) (a) Gwost, D.; Caulton, K. G. *Inorg. Chem.* **1974**, *13*, 414. (b) Hoskins, B. F.; Whillans, F. D.; Dale, D. H.; Hodgkin, D. C. *Chem. Commun.* **1969**, *69*.

(52) (a) Zhao, X.-J.; Sampath, V.; Caughey, W. S. *Biochem. Biophys. Res. Commun.* **1994**, *204*, 537. (b) Brudwig, G. W.; Stevens, T. H.; Chan, S. I. *Biochemistry* **1980**, *19*, 5275.

(53) Schneider, J. L.; Carrier, S. M.; Ruggiero, C. E.; Young, J. V. E.; Tolman, W. B. *J. Am. Chem. Soc.* **1998**, *120*, 11408.

(54) Ruggiero, C. E.; Carrier, S. M.; Antholine, W. E.; Whittaker, J. W.; Cramer, C. J.; Tolman, W. B. *J. Am. Chem. Soc*. **1993**, *115*, 11285.

(55) (a) Park, G. A.; Deepalatha, S.; Puiu, S. C.; Lee, D.-H.; Mondal, B.; Sarjeant, A. A. N.; del Rio, D.; Pau, M. Y. M.; Solomon, E. D.; Karlin, K. D. *J. Biol. Inorg. Chem.* **2009**, *14*, 1301. (b) Goldstein, S.; Lind, J.; Merenyi, G. *Chem. Rev.* **2005**, *105*, 2457. (c) Herold, S.; Koppenol, W. H. *Coord. Chem. Rev.* **2005**, *249*, 499.

(56) SMART, SAINT and XPREP, Siemens Analytical X-ray Instruments Inc., Madison, Wisconsin, USA, **1995**.

(57) Sheldrick, G. M. SADABS: Software for Empirical Absorption Correction, University of Gottingen, Institut fur Anorganische Chemieder Universitat, Tammanstrasse 4, D-3400 Gottingen, Germany, **1999**.

(58) Sheldrick, G. M. SHELXS-97, University of Gottingen, Germany, **1997**.

(59) Farrugia, L. J. *J. Appl. Crystallogr*. **1997**, *30*, 565.

Chapter 4

Nitrogen dioxide reactivity of Ni(II) complex: Activation of NO_2 leading to the reduction of Ni-center

Abstract

Ni(II) complexes, **4.1** and **4.2**, of ligand **L3** {**L3** = *bis*(2-ethyl-4-methylimidazol-5-yl)methane} having acetate and benzoate counter anions, respectively, have been prepared. Complex **4.2** has been characterized structurally. The complexes in methanol solution did not react with NO. However, addition of NO_2 gas into the methanol solution of the complexes followed by stoichiometric amount of water resulted in the formation of corresponding Ni(I)-nitrate complex, **4.3**. The reduction was evidenced by UV-visible and EPR spectroscopic analyses. Finally, formation of complex **4.3** was confirmed by its single crystal structure determination.

4.1 Introduction

Reactive nitrogen species (RNS) constitute a major class of oxidizing agent in biological systems.[1] At low or moderate concentration, they behave as messenger for signal transduction; whereas at high concentration they induce oxidative stress.[2] Tyrosine nitration induced by RNS has attracted a considerable interest of chemists and biochemists as it can alter the protein function as well as can be used as a biomarker of several disease states such as Alzheimar's and Perkinson's diseases.[3] In biosystems, tyrosine nitration occurs either through peroxynitrite ($ONOO^-$) or nitrogen dioxide (NO_2).[4] $ONOO^-$ forms in diffusion controlled reaction between superoxide and nitric oxide (NO).[5] NO_2 can be generated by the reaction of NO with oxygen, decomposition of peroxynitrite or by the oxidation of nitrite (NO_2^-) by hydrogen peroxide (H_2O_2) in presence of peroxidases.[6]

Transition metal ions are known to favor the generation of radicals and thus causing the oxidative damage of proteins, lipids and nucleic acids. For example, known examples of tyrosine nitration involving Cu(II) ion have been shown to promote the oxidation of NO_2^- to NO_2 in addition to the principal role of scavenging superoxide to form H_2O_2 and oxygen.[7,8] On the other hand, NO_2, a widely accepted nitrating agent for tyrosine, induces nitration through radical mechanism.[9] Nitronium ion (NO_2^+) is known as the key nitrating agent in nitration reaction generally produced at pH < 0 in concentrated mixture of nitric and sulphuric acid.[10] Transition metal ions like iron and copper can also catalyze two electron oxidation of $ONOO^-$ leading to a heterolytic O–O bond cleavage and thus generating a species with similar reactivity like NO_2^+.[10] The formation of NO_2^+ from NO_2 in its reaction with Cu(II) is reported recently from our group.[11] In aqueous medium at pH 7, the NO_2^+/NO_2 potential was found to be 1.6 (±0.2)V relative to NHE.[12] A little lower value (1.51V) for the same couple was reported based on the concentration of NO_2^+ in the

mixture of concentrated nitric and sulphuric acid.[11]

On the other hand, Ni(II) in different ligand environment are known to undergo reduction to Ni(I) either by electrochemical procedure or by reducing agents.[13-15] In previous chapter NO induced reduction of Ni(II) chloride complex of *bis*(2-ethyl-4-methylimidazol-5-yl)methane ligand leading to the reductive nitrosylation to yield {NiNO}^{10} complex was reported recently. In this case, it has been observed that the counter anion plays an important role (Chapter **3**). The complex with chloride anion reacts with NO, whereas the same with acetate or benzoate does not. However, they react with NO_2 and lead to the reduction of Ni(II) center which has not been explored yet.

Thus, in continuation to our study of NO_x reactivity of transition metal ions, specially to understand the role of counter anion in controlling the overall behaviour of the metal ions towards NO_x, Ni(II) complexes of ligand **L3 (L3** = *bis*(2-ethyl-4-methylimidazol-5-yl)methane) having acetate and benzoate counter anions have been prepared.

4.2 Results and Discussion

The preparation of the ligand, **L3** was done by following earlier reported procedure and is described in chapter **3**.[16] The Ni(II) complex, **4.1** was synthesized by stirring a mixture of nickel(II) acetate tetrahydrate with two equivalent of ligand, **L3** in methanol. Micro-analyses of complex **4.1** showed good agreement with the calculated values (Experimental Section). UV-Visible, FT-IR, ESI-mass studies confirm the formation of the complex un-ambiguously. Even after several attempts we could not grow the X-ray quality single crystals of complex **4.1**. Then the counter anion was changed to benzoate to prepare complex **4.2**. Same experimental protocol was used to prepare complex **4.2** as in the case of **4.1**. The formation of the complex was authenticated by various spectroscopic analyses

as well as by single crystal X-ray structure determination (Experimental Section). The crystallographic data, important bond angles and distances are listed in tables 4.1, 4.2 and 4.3, respectively. The ORTEP diagram of complex **4.2** is shown in figure 4.1. Ni(II) center is coordinated by two ligand units and a benzoate moiety in a η^2-fashion resulting in a distorted octahedral geometry. The average Ni–N distance is found 2.094 Å, which is within the range of analogous reported complexes.[17] The average N-Ni-N bite angle is ~ 88.65°. It should be noted that Ni(II) complex of the same ligand with chloride anion is square planar with Ni–N distances of 1.893 Å and N-Ni-N angle of ~ 90.00° (Chapter **3**).

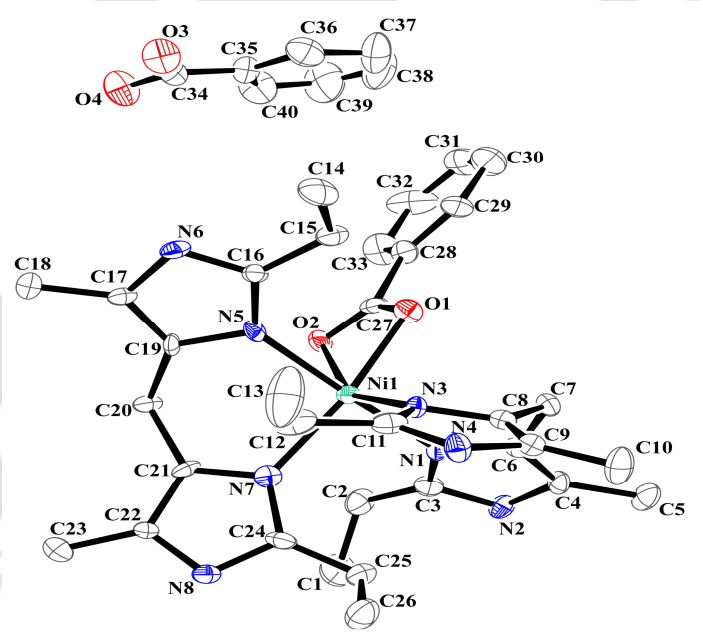

Figure 4.1. ORTEP diagram of complex **4.2** (50% thermal ellipsoid plot, H atoms are omitted for clarity).

Table 4.1. Crystallographic data for complexes **4.2** and **4.3**.

	4.2	**4.3**
Formulae	$C_{41}H_{54}NiN_8O_5$	$C_{26}H_{40}NiN_9O_7$
Mol. wt.	797.63	649.38
Crystal system	orthorhombic	monoclinic
Space group	*P* 21 21 21	*P*2/c
Temperature/ K	296(2)	296(2)
Wavelength/ Å	0.71073	0.710 73
a/Å	9.7388(4)	9.4763(12)
b/Å	17.4592(7)	9.3789(11)
c/Å	24.3745(10)	18.4290(2)
α/deg	90.00	90.00
β/deg	90.00	91.087(6)
γ/deg	90.00	90.00
V/Å^3	4144.4(3)	1637.60(3)
Z	4	2
density/Mg·m^{-3}	1.278	1.317
Abs. coeff./mm^{-1}	0.521	0.647
Abs. correction	multi-scan	none
F(000)	1696	686
Total no. of reflections	6396	2787
Reflections, $I > 2\sigma(I)$	4763	2431
Max. 2θ/deg	25.00	25.00
Ranges (*h*, *k*, *l*)	$-11 \le h \le 8$ $-16 \le k \le 20$ $-28 \le l \le 24$	$-11 \le h \le 10$ $-10 \le k \le 10$ $-21 \le l \le 19$
Complete to 2θ (%)	99.5	96.8
Refinement method	full-matrix least-squares on F^2	full-matrix least-squares on F^2
GOF (F^2)	0.951	0.924
R indices [$I > 2\sigma(I)$]	0.0623	0.0539
R indices (all data)	0.1018	0.0578

Table 4.2. Selected bond lengths (Å).

	4.2	**4.3**
Ni(1)-N(1)	2.097(7)	2.076(3)
Ni(1)-N(3)	2.090(7)	2.079(3)
Ni(1)-O(1)	2.062(5)	2.216(3)
Ni(1)- O(2)	2.488(7)	-
O(1)-N(5)	-	1.249(4)
N(1)-C(3)	1.320(1)	1.328(4)
N(1)-C(6)	1.370(1)	1.390(4)
N(2)-C(3)	1.3615)	1.337(4)
N(2)-C(4)	1.380(1)	1.377(5)

Table 4.3. Selected bond angles (°).

	4.2	**4.3**
N(1)-Ni(1)-N(3)	89.20(2)	89.30(8)
N(1)-Ni(1)-N(3A)	-	96.95(10)
N(1)-Ni(1)-N(5)	88.10(3)	-
O(1)-Ni(1)-N(1)	86.90(3)	86.10(7)
O(1)-Ni(1)-N(3)	97.00(3)	160.80(8)
Ni(1)-O(1)-N(5)	-	93.90(2)
O(1)-N(5)-O(1A)	-	115.30(4)

Complex **4.1** in dry methanol solution absorbs at 595 nm (ε/mol^{-1}cm^{-1}, 22) and 371 nm (ε/mol^{-1}cm^{-1}, 198) nm in the UV-visible spectrum (Figure 4.2 and Appendix III). In case of complex **4.2**, these absorption bands appear at 600 nm (ε/mol^{-1}cm^{-1}, 25) and 368 nm (ε/mol^{-1}cm^{-1}, 178) nm (Figure 4.2 and Appendix III). Intra-ligand transitions were observed in the lower wavelengths. The bands at 595 and 600 nm for complexes **4.1** and **4.2,** respectively, assigned as the *d-d* transitions. Similar spectral features of complexes **4.1** and **4.2** suggested that they have similar coordination environment around the central metal ion. In contrast, complex **3.1** displayed *d-d* transition at 636 nm (Figure 3.2, Chapter **3**).

The cyclic volatmmograms of complexes **4.1** and **4.2** were recorded in methanol using TBAP supporting electrolyte in a three electrode configuration with saturated Ag/Ag^+ reference, glassy carbon working and Pt auxiliary electrodes. An irreversible reduction at –1.52 V and –1.56 V was observed in the voltammograms of complexes **4.1** and **4.2**, respectively (Appendix III). These are assignable to the Ni(II)/Ni(I) reduction potential. In the same setup, the NO/NO^+ couple appeared at 1.15 V (Appendix II, Chapter **3**).[18]

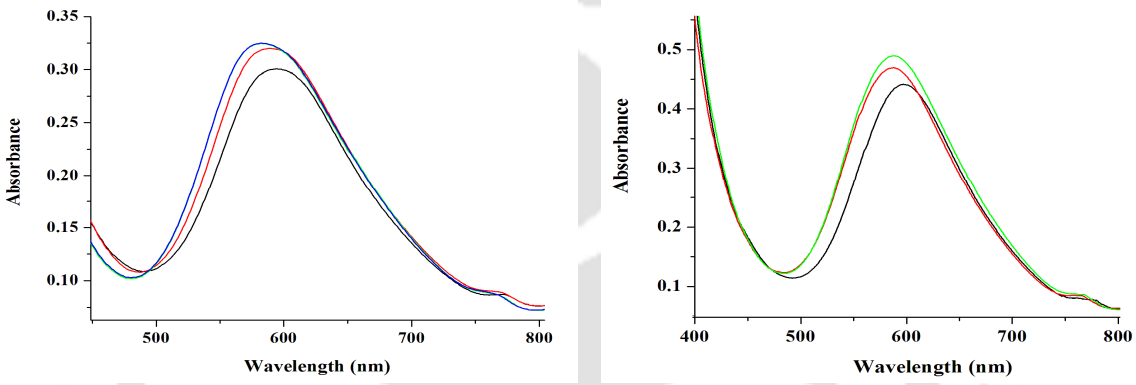

(a) (b)

Figure 4.2. UV-visible spectra (a) complex **4.1**(black), after purging NO_2 (red) and after addition of water (blue); (b) complex **4.2** (black), after purging NO_2 (red) and after addition of water (green) in methanol at room temperature.

Interestingly, for complex **3.1**, the Ni(II)/Ni(I) reduction potential appeared at -1.05 V in the same condition (Chapter **3**). The difference in reduction potential is attributed to the counter anion present in the complexes. In case of complex **3.1**, the single crystal X-ray structure revealed that the Cl^- ion is not coordinated to the central metal ion whereas in case of complex **4.2**, the benzoate unit is coordinated to the Ni(II) center in a η^2 fashion resulting a distorted octahedral geometry around the metal ion. This resulted in the shift of reduction potential to ~0.50 V.

Addition of equivalent amount of NO in the degassed methanol solution of complex **3.1** at -80 °C resulted in a shift of the *d-d* band from 636 nm to 578 nm (Chapter **3**, Figure 3.2) which is attributed to the formation of corresponding Ni(I)- complex (Chapter **3**, Scheme 3.1). As mentioned earlier, complexes **4.1** and **4.2** in dry and degassed methanol solution did not react with NO. However, when NO_2 was purged to the dry and degassed methanol solution of complex **4.1**, a blue shift was observed from 598 nm to 588 nm in UV-visible spectrum (Figure 4.2). This reaction mixture was found to be EPR silent. This is attributed to the weak coordination of NO_2 to the central metal ion. In presence of stoichiometric amount of water, the 588 nm band was shifted to 582 nm (Figure 4.2). In case of complex **4.2**, the *d-d* band was shifted to 590 nm after addition of NO_2 which was further moved to 581 nm upon addition of stoichiometric amount of H_2O (Figure 4.2). The resulting reaction mixtures became EPR active (Figure 4.3). These observations are attributed to the reduction of Ni(II) to Ni(I) with concomitant formation of nitrato (NO_3^-) species (Scheme 4.1). The existence of Ni(I) (d^9 configuration; $g_{\parallel}$, 2.18; $g_{\perp}$, 2.27) was also suggested by the axial nature of the EPR spectrum (Figure 4.3).[19,20] The EPR spectra of electrochemically generated Ni(I) complex of 5,5,7,12,12,14-hexamethyl-1,4,8,11-tetraazacyclotetradecane also reported to display axial EPR spectrum.[20]

While both the reaction mixtures were kept in freezer for 3- 4 days, microcrystals of complex **4.3** were obtained. FT-IR studies revealed the presence of nitrato (~1380 cm^{-1}) group in complex, **4.3** (Figure 4.3).[21] X-band EPR study in dry methanol solution at room temperature suggested the presence of Ni(I) center in the complex (Appendix III).

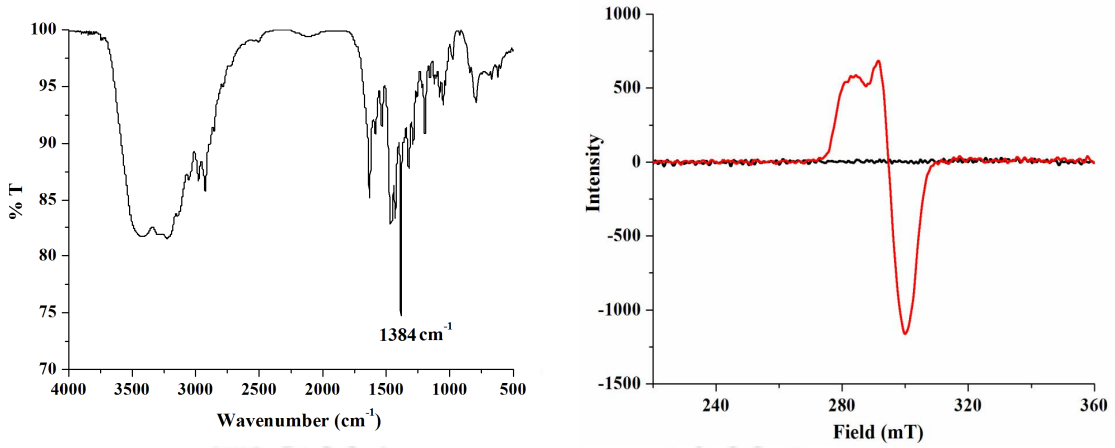

(a) (b)

Figure 4.3. (a) FT-IR spectrum of complex **4.3** in KBr, (b) X-band EPR spectra of complexes **4.2** (black), after addition of NO_2 and stoichiometric amount of H_2O (red) in dry methanol at 77 K.

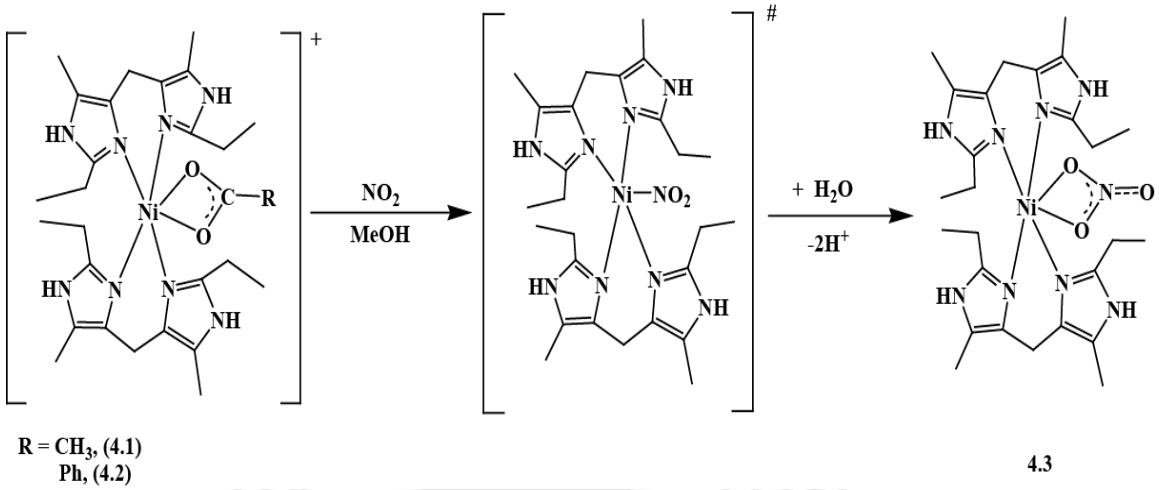

Scheme 4.1

Further, single crystal X-ray structure determination confirmed the formulation of complex **4.3** as a Ni(I)-nitrato complex of the ligand **L3**. The ORTEP diagram is shown in figure 4.4. The crystallographic data important bond lengths and angles are listed in tables 4.1, 4.2 and 4.3, respectively.

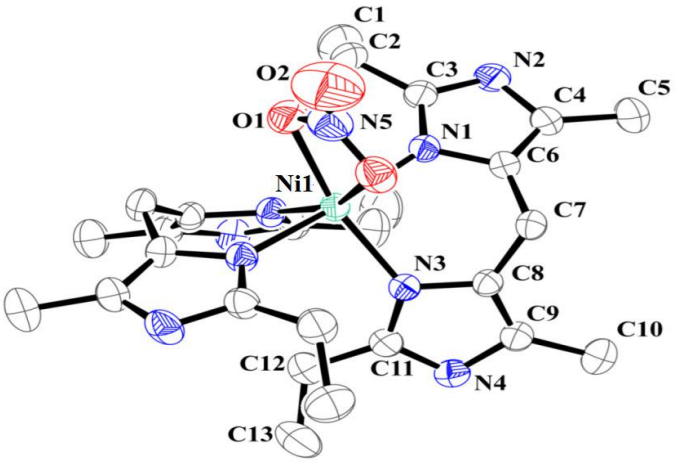

Figure 4.4. ORTEP diagram of complex **4.3** (50% thermal ellipsoid plot, H atoms are omitted for clarity)

Structure determination revealed that the Ni(I) center is coordinated with four N-donor atoms from two ligand units and two O-atoms from the nitrate moiety in η^2 fashion. This resulted in a distorted octahedral geometry around the central metal ion. The Ni–N bond lengths are in the order of ~2.076 Å and the average N-Ni-N angle is 93.12°. The difference in bond length from complex **4.2** is attributed to the change of oxidation number of the central metal ion.

4.3 Experimental Section

4.3.1 Materials and Methods

All reagents and solvents of reagent grade were purchased from commercial sources and used as received except specified. Deoxygenation of the solvent and solutions was effected by repeated vacuum/purge cycles or bubbling with nitrogen or argon for 30 min. NO_2 was used from cylinder after purification using reported methods.[22] The dilution of NO_2 was effected with argon gas using Environics Series 4040 computerized gas dilution system. UV–visible spectra were recorded on a PerkinElmer Lambda 25 UV–visible

spectrophotometer. FT-IR spectra of the solid samples were taken on a PerkinElmer spectrophotometer with samples prepared as KBr pellets. Solution electrical conductivity was measured using a Systronic 305 conductivity bridge. ^{1}H NMR spectra were recorded in a 400 MHz Varian FT spectrometer. Chemical shifts (ppm) were referenced either with an internal standard (Me_4Si) or to the residual solvent peaks. The X-band EPR spectra were recorded on a JES-FA200 ESR spectrometer, at room temperature or at 77 K with microwave power of 0.998 mW, microwave frequency of 9.14 GHz, and modulation amplitude of 2. Elemental analyses were obtained from a PerkinElmer Series II Analyzer. The magnetic moment of complexes was measured on a Cambridge Magnetic Balance.

Single crystals were grown by slow diffusion followed by slow evaporation technique. The intensity data were collected using a Bruker SMART APEX-II CCD diffractometer, equipped with a fine focus 1.75 kW sealed tube Mo Kα radiation (λ = 0.710 73 Å) at 273(3) K, with increasing ω (width of 0.3° per frame) at a scan speed of three seconds per frame. The SMART software was used for data acquisition.[23] Data integration and reduction were undertaken with SAINT and XPREP software.[24] Structures were solved by direct methods using SHELXS-97 and refined with full-matrix least-squares on F^2 using SHELXL-97.[25] Structural illustrations were drawn with ORTEP-3 for Windows.[26]

4.3.2 Syntheses

(a) Complex 4.1

Nickel(II) acetate tetrahydrate (2.48 g, 10 mmol) was taken in a 50 ml round bottom flask, dissolved in 20 ml of methanol. To this, a solution of 4.64 g (20 mmol) of ligand **L3** in methanol (10 ml) was added and stirred for 1 h. to result in a bluish solution. The solution was layered with diethyl ether and kept in freezer for overnight to get blue precipitate of

complex **4.1**. Yield: 5.13 g (80%). Elemental analyses for $C_{30}H_{46}N_8O_4Ni$, Calcd(%): C, 56.17; H, 7.23; N, 17.47. Found(%): C, 56.22; H, 7.19; N, 17.43. FT-IR (in KBr): 2978, 1633, 1569, 1463, 1422, 1328, 1293, 1047, 932, 665, 620 cm^{-1}. UV–visible (methanol): 595 nm (ε/ $M^{-1}cm^{-1}$, 22). Molar conductance: 148 S cm^2 mol^{-1} (in methanol), observed magnetic moment: 1.98 BM.

(b) Complex 4.2

In 20 ml methanol solution of complex **4.1** (3.2 g, 5 mmol), 1.58 g (11 mmol) of sodium benzoate in water (5 ml) was added and stirred for 2 h. Color of the solution changed from a light blue to a dark blue. After removing the solvent in rotary evaporator, the solid was washed with cold water to remove excess sodium benzoate and sodium acetate. Then it was dissolved in methanol, and kept at room temperature; after ten days blue crystals were obtained. Yield: 2.8 g (75%). Elemental analyses for $C_{40}H_{50}N_8O_4Ni$, Calcd(%): C, 62.75; H, 6.58; N, 14.74. Found(%): C, 62.70; H, 6.62; N, 14.68. FT-IR (in KBr): 3192, 2969, 1632, 1593, 1544, 1460, 1407, 1365, 1048, 853, 720, 678 cm^{-1}. UV–visible (methanol): 600 nm (ε/ $M^{-1}cm^{-1}$, 25). Molar conductance: 139 S cm^2 mol^{-1} (in methanol), observed magnetic moment: 2.11 BM.

(c) Complex 4.3

In 20 ml of dry and degassed methanol solution of complex **4.1** (160 mg), NO_2 was bubbled and few drops of water was added, the color of the solution became fade. The capped reaction mixture was kept at −40°C for crystallization for several days to get blue color crystal of complex **4.3**. Yield: 102.4 mg (70%). Elemental analyses for $C_{26}H_{40}N_9O_3Ni$, Calcd(%): C, 53.35; H, 6.89; N, 21.54. Found(%): C, 53.38; H, 6.85; N, 21.65. FT-IR (in KBr): 3424, 3224, 2923, 1632, 1530, 1458, 1427, 1384, 1322, 1196, 788

cm^{-1}. UV–visible (methanol): 582 nm (ε/ $M^{-1}cm^{-1}$, 36). Molar conductance: 70 S cm^2 mol^{-1} (in methanol), observed magnetic moment: 1.26 BM. X-band EPR: $g_{\parallel}$, 2.16, $g_{\perp}$, 2.27

Using same procedure complex **4.3** was also prepared from complex **4.2**.

4.4 Conclusion

In conclusion, Ni(II) complexes, **4.1** and **4.2**, of ligand **L3** having acetate and benzoate counter anions, respectively, were found to be unreactive towards NO. However, addition of NO_2 gas into the methanol solution of the complexes resulted in a blue shift of the visible band in UV-visible spectrum. This is attributed to the weak interaction of the NO_2 with the metal ion. Addition of stoichiometric amount of water into the reaction mixture resulted in the reduction of Ni(II) center to Ni(I) with simultaneous oxidation of NO_2 to NO_3^-. The reduction was evidenced by UV-visible and EPR spectroscopic analyses. This was further confirmed by isolation and structural characterization of corresponding Ni(I)-nitrate complex, **4.3.**

4.5 References

(1) Wiseman, H.; Halliwell, B. *Biochem. J.* **1996**, *313*, 17.

(2) (a) Apel, K.; Hirt, H. *Annu. Rev. Plant Biol.* **2004**, *55*, 373. (b) Radi, R. *Proc. Natl. Acad. Sci. U.S.A.* **2004**, *101*, 4003.

(3) (a) Shishehbor, M. H.; Aviles, R. J.; Brennan, M. L.; Fu, X. M.; Goormastic, M.; Pearce, G. L.; Gokce, N.; Keaney, J. F.; Penn, M. S.; Sprecher, D. L.; Vita, J. A.; Hazen, S. L. *J. Am. Med. Assoc.* **2003**, *289*, 1675. (b) Good, P. F.; Werner, P.; Hsu, A.; Olanow, C. W.; Perl, D. P. *Am. J. Pathol.* **1996**, *149*, 21. (c) Danielson, S. R.; J. Held, M.; Schilling, B.; Oo, M.; Gibson, B. W.; Andersen, J. K. *Anal. Chem.* **2009**, *81*, 7823.

(4) (a) Gunaydin, H.; Houk, K. N. *Chem. Res. Toxicol.* **2009**, *22*, 894. (b) van der Vliet, A.; Eiserich, J. P.; Halliwell, B.; Cross, C. E. *J. Biol. Chem.* **1997**, *272*, 7617.

(5) (a) Goldstein, S.; Lind, J.; Merenyi, G. *Chem. Rev.* **2005**, *105*, 2457. (b) Schopfer, M. P.; Wang, J.; Karlin, K. D. *Inorg. Chem.* **2010**, *49*, 6267. (c) Surmeli, N. B.; Litterman, N. K.; Miller, A. F.; Groves, J. T. *J. Am. Chem. Soc.* **2010**, *132*, 17174.

(6) (a) Olbregts, J. *Int. J. Chem. Kinet.* **1985**, *17*, 835. (b) Su, J.; Groves, J. T. *J. Am. Chem. Soc.* **2009**, *131*, 12979. (c) Bian, B.; Gao, Z. H.; Weisbrodt, N.; Murad, F. *Proc. Natl. Acad. Sci. U.S.A.* **2003**, *100*, 5712.

(7) (a) Thomas, D. D.; Espey, M. G.; Vitek, M. P.; Miranda, K. M.; Wink, D. A. *Proc. Natl. Acad. Sci. U.S.A.* **2002**, *99*, 12691. (b) Gaggelli, E.; Kozlowski, H.; Valensin, D.; Valensin, G. *Chem. Rev.* **2006**, *106*, 1995.

(8) (a) Lu, Y.; Prudent, M.; Qiao, L. A.; Mendez, M. A.; Girault, H. H. *Metallomics* **2010**, *2*, 474. (b) Goss, S. P. A.; Singh, R. J.; Kalyanaraman, B. *J. Biol. Chem.* **1999**, *274*, 28233. (c) Singh, R. J.; Goss, S. P. A.; Joseph, J.; Kalyanaraman, B.

Proc. Natl. Acad. Sci. U.S.A. **1998**, *95*, 12912. (d) Zhang, H.; Joseph, J.; Felix, C.; Kalyanaraman, B. *J. Biol. Chem.* **2000**, *275*, 14038. (e) Bonini, M. G.; Fernandes, D. C.; Augusto, O. *Biochemistry* **2004**, *43*, 344.

(9) Qiao, L.; Lu, Y.; Liu, B.; Girault, H. H. *J. Am. Chem. Soc*. **2011**, *133*, 19823.

(10) Beckman, J. S. *Chem. Res. Toxicol*. **1996**, *9*, 836.

(11) Kumar, V.; Kalita, A.; Mondal, B. *Dalton Trans.* **2013**, *42*, 16264.

(12) (a) Tennyson, A. G.; Lippard, S. J. *Cell* **2011**, *18*, 1211. (b) Koppenol, W. H.; Moreno, J. J.; Pryor, W. A.; Ischiropoulos, H.; Beckman, J. S. *Chem. Res. Toxicol.* **1992**, *5*, 834. (c) Stanbury, D. M. *Adv. Inorg. Chem*. **1989**, *33*, 69.

(13) (a) Halcrow, M. A.; Christou, G. *Chem. Re*v. **1994**, *94*, 2421. (b) Signor, L.; Knuppe, C.; Hug, R.; Schweizer, B.; Pfaltz, A.; Jaun, B. *Chem. Eur. J.* **2000**, *6*, 3508.

(14) (a) Ozaki, S.; Matsushita, H.; Ohmori, H. *J. Chem. Soc., Perkin Trans. 1* **1993**, 649. (b) Campbell, C. J.; Rusling, J. F.; Bruckner, C. *J. Am. Chem. Soc.* **2000**, *122*, 6679.

(15) (a) Kryatov, S. V.; Mohanraj, B. S.; Tarasov, V. V.; Kryatova, O. P.; Rybak-Akimova, E. V.; Nuthakki, B.; Rusling, J. F.; Staples, R. J.; Nazarenko, A. Y. *Inorg. Chem.* **2002**, *41*, 923. (b) James, T. L.; Cai, L.; Muetterties, M. C.; Holm, R. H.; *Inorg. Chem.* **1996**, *35*, 4148.

(16) Kalita, A.; Kumar, P.; Deka, R. C.; Mondal, B. *Chem. Commun*. **2012**, *48*, 1551.

(17) (a) Butcher, R. J.; Sinn, E. *Inorg. Chem*. **1977**, *16*, 2334. (b) Ohtsu, H.; Tanaka, K.; *Inorg. Chem.* **2004**, *43*, 3024.

(18) Ghosh, S.; Deka, H.; Dangat, Y. B.; Saha, S.; Gogoi, K.; Vanka, K.; Mondal, B. *Dalton Trans*. **2016**, *45*, 10200.

(19) (a) Gagne, R. R.; Ingle, D. M. *Inorg. Chem.* **1981**, *20*, 420. (b) Nag, K.; Chakravorty, A. *Coord. Chem. Rev.* **1980**, *33*, 87. (c) Ansell, C. W. G.; Lewis, J.; Raithby, P. R.; Ramsden, J. N.; Shroder, M. *Chem. Commun.* **1982**, 546. (d) Suh, M. P.; Oh, K. Y.; Lee, J. W.; Bae, Y. Y. *J. Am. Chem. Soc.* **1996**, *118*, 777.

(20) Hathaway, B. J.; Billing, D. E. *Coord. Chem. Rev.* **1970**, *5*, 143.

(21) Kalita, A.; Deka, R. C.; Mondal, B. *Inorg.Chem.* **2013**, *52*, 10897.

(22) (a) Kurtikyan, T. S.; Hayrapetyan, V. A.; Mehrabyan, M. M.; Ford, P. C. *Inorg. Chem.* **2014**, *53*, 11948. (b) Kurtikyan, T. S.; Ford, P. C. *Angew. Chem., Int. Ed.* **2006**, *45*, 492. (c) Kurtikyan, T. S.; Hovhannisyan, A. A.; Gulyan, G. M.; Ford, P. C. *Inorg. Chem.* **2007**, *46*, 7024.

(23) SMART, SAINT and XPREP, Siemens Analytical X-ray Instruments Inc., Madison, Wisconsin, USA, **1995**.

(24) G. M. Sheldrick, SADABS: software for Empirical Absorption Correction, University of Gottingen, Institut fur Anorganische Chemieder Universitat, Tammanstrasse 4, D-3400 Gottingen, Germany, **1999**

(25) G. M. Sheldrick, SHELXS-97, University of Gottingen, Germany, **1997**.

(26) Farrugia, L. J. *J. Appl. Crystallogr.* **1997**, *30*, 565.

Chapter 5

Nitrogen dioxide reactivity of a Ni(II) complex: Oxo transfer reaction from NO_2 to NO_2^-

Abstract

Reaction of a Ni(II) complex of ligand **L4** {**L4** = 5,5,7,12,12,14-hexamethyl-1,4,8,11-tetraazacyclotetradecane} (**5.1**) in methanol with equivalent amount of NO_2 resulted in the reduction of Ni(II) to Ni(I). The reduction was confirmed by UV-visible, and EPR spectroscopic studies. The intermediate Ni(I) complex reacted with additional equivalent of NO_2 to form corresponding O-nitrito Ni(II) complex, $[Ni^{II}(L4)(\eta^1\text{-}ONO)_2]$ (**5.2**). Structural characterization confirmed the formation of **(5.2)**. Subsequent equivalent of NO_2 resulted in the oxo transfer from NO_2 to the metal bound nitrito group yielding corresponding O-nitrato complex, $[Ni^{II}(L4)(\eta^2\text{-}ONO_2)]^+$ (**5.3**) with simultaneous release of NO. The release of NO in the reaction was evidenced by spin trapping experiment. Complex **5.3** was isolated and characterized by single crystal X-ray structure determination.

5.1 Introduction

The chemistry of NO_x such as nitric oxide (NO), nitrogen dioxide (NO_2) has been the subject of research interest because of their involvement in diverse biological processes.[1] Activation of NO_2 by transition metal ions has attracted special interest with the aim of understanding the redox transformations between various NO_x complexes.[2,3] For instance, it has been found that the reaction of small amounts of NO_2 with sublimed thin layers of the [Fe(II)-(Por)] complex [Por = *meso*-tetraphenylporphyrinato dianion, TPP, or *meso*-tetra-*p*-tolylporphyrinato dianion, TTP] resulted in the formation of the five-coordinate nitrito complexes [Fe(Por)(η^1-ONO)].[4] Further addition of NO_2 led to the nitrato complex [Fe(Por)(η^2-O_2NO)]. Another study demonstrated the reaction of NO_2 with amorphous layers of Mn(TPP) afforded the corresponding nitrato complex, [Mn(TPP)(η^1-ONO_2)].[5] This reaction was shown to proceed through two distinct steps: (i) initially low NO_2 pressure results in the corresponding O-nitrito complex; (ii) additional NO_2 affords the nitrato analogue with the release of NO. Recently, a Cu(II) complex was found to undergo reduction by NO_2; subsequent addition of NO_2 resulted in corresponding Cu(II)-nitrito intermediate complex.[6] The corresponding intermediate nitrito complex was isolated and structurally characterized. Addition of further equivalent of NO_2 to the methanol solution of the intermediate Cu(II)-nitrito complex lead to oxo transfer from NO_2 to the coordinated nitrito group with a concomitant release of NO.

Nickel(II) centers in various ligand environments are exemplified to be reduced to corresponding Ni(I) by electrochemical reduction or in presence of a reducing agent.[7] However, the reduction of Ni(II) center by NO_2 is not yet reported. To understand the activation of NO_x by transition metal ions, the reactivity of a Ni(II) complex of a macro-

cyclic ligand **L4** (**L4** = 5,5,7,12,12,14-hexamethyl-1,4,8,11-tetraazacyclotetradecane) with NO_2 has been studied.

5.2 Results and Discussion

The ligand, **L4** (**L4** = 5,5,7,12,12,14-hexamethyl-1,4,8,11-tetraazacyclotetradecane) was prepared by using the procedure described earlier (Experimental Section).[8] Complex **5.1**, $[Ni^{II}(L4)(CH_3COO)_2]$, was prepared by refluxing a mixture of nickel(II) acetate tetrahydrate with equivalent quantity of **L4** in methanol (Experimental Section). The formation of the complex was unambiguously established by various spectroscopic analyses as well as by X-ray single crystal structure determination. The perspective ORTEP view of complex **5.1** is shown in figure 5.1. The crystallographic data are given in table 5.1 and other metric parameters are listed in table 5.2 and 5.3. The crystal structure revealed that the four N-atoms of the ligand are coordinated to the metal ion forming a square plane; two acetate anions from the axial positions to completed the octahedral geometry around the Ni(II) center.

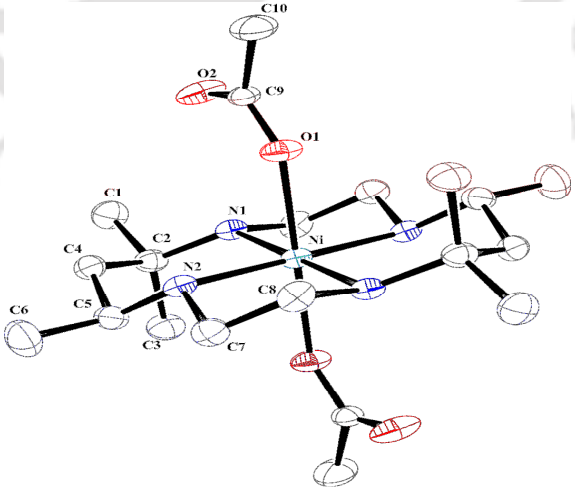

Figure 5.1. The ORTEP diagram of complex **5.1** (50% thermal ellipsoid; H-atoms are omitted for clarity.

The average Ni–N distance was 2.088 Å. The longer Ni–O_{OAc} distance (2.144 Å) suggested that the axial elongation prevails in this structure. Both the acetate ions were bonded in monodentate fashion.

In methanol, complex **5.1** absorbs at 960, 574, 464 and 362 nm along with strong intraligand transitions (Appendix IV). The bands at 960, 574 and 464 nm were assigned as the *d-d* bands occurred from three spin-allowed transitions, $^3A_{2g}$ - $^3T_{2g}(F)$, $^3A_{2g}$ - $^3T_{1g}(F)$, and $^3A_{2g}$ - $^3T_{1g}(P)$, respectively of octahedral Ni^{2+}. 362 nm band was assignable to the ligand to metal (LMCT) charge transfer.[9]

Addition of equivalent amount of NO_2 to the dry and degassed methanol solution of complex **5.1** resulted in the change of color from violet to yellow. In the UV–visible spectrum, 464 nm band was shifted to 434 nm giving a shoulder like band (Figure 5.2). X-band EPR study of the frozen reaction mixture (at 77 K) revealed the presence of Ni(I) species (Eq. 5.1). The axial nature of the spectrum is indicating the existence of Ni(I) (d^9) in a square planar environment with d_z^2 ground state. Calculated values of $g_\perp$ and $g_\parallel$ are 2.22 and 2.03, respectively. The EPR spectral study was repeated in other solvents like acetonitrile and chloroform, also.

$$\mathbf{(L4)Ni^{II}(OAc)_2 + NO_2 \xrightarrow{MeOH} [(L4)Ni^{I}]^+ + 2AcO^- + H^+ + MeONO_2}$$

------- (Eq. 5.1)

In all the cases, same axial spectrum was observed. The electrochemically generated Ni(I) complex of ligand **L4** was also studied earlier by EPR spectroscopy.[10,7e] However, in those cases, solvent and the counter anion (BF_4^-) were different. The spectroscopic evidence obtained in the present study was in very good agreement with the earlier reported results.

Thus, it is logical to believe that in this step of reaction Ni(II) center of complex **5.1** has undergone reduction by NO_2 to form square planar $[L4Ni]^+$ complex. GC-mass analyses of the reaction mixture revealed the formation of methyl nitrate (CH_3ONO_2) in this step (Appendix IV). This was attributed to the formation of NO_2^+ during the reduction of Ni(II) by NO_2 followed by its immediate reaction with methanol to form methyl nitrate. The unstable nature of Ni(I) complex did not allow to isolate or structurally characterize.

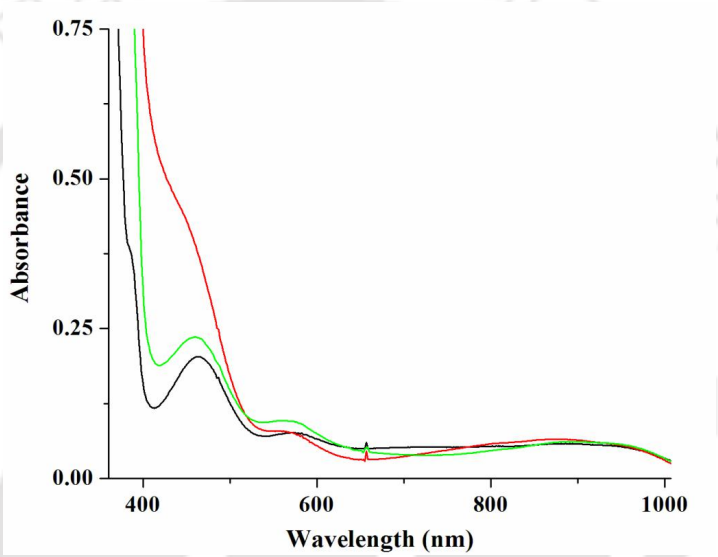

Figure 5.2. UV-visible spectra of complex **5.1** (black), after addition of one equivalent NO_2 (red) and after addition of another equivalent of NO_2 (green).

Upon addition of further equivalent of NO_2, the absorption band at 434 nm was shifted to 455 nm (Figure 5.2). Indicating the formation of corresponding $[Ni^{I}\text{-}NO_2]$ complex, which can be considered as $[Ni^{II}\text{-}NO_2^-]$. The EPR signal of Ni(I) intermediate was also disappeared. When the reaction mixture was allowed to stand at room temperature for 3-4 days, two types of crystals, violet and purple, appeared almost in equal proportion. Structural characterization revealed that the violet crystals are of complex **5.1** and the purple one is of $[(L4)Ni(NO_2)_2]$, complex **5.2**. The ORTEP diagram of complex **5.2** is shown in figure 5.4. A η^1-O coordination mode of two nitrito moiety to the Ni(II) center

was observed. The average Ni–N and Ni–O bond distances were 2.099 and 2.138 Å, respectively. The N–O bond distances in coordinated nitrite were 1.305 and 1.110 Å suggesting it's localized nature.[6]

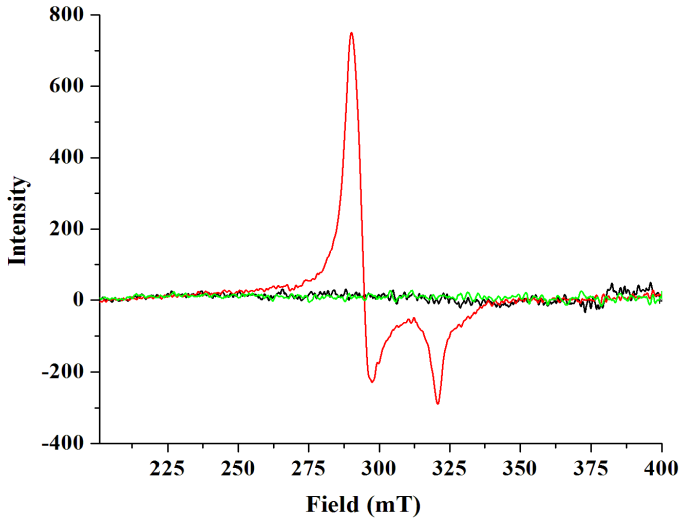

Figure 5.3. X-band EPR of complex **5.1** (black), after purging of equivalent amount of NO_2 (red) and after purging another equivalent of NO_2 (green) in acetonitrile at 77 K.

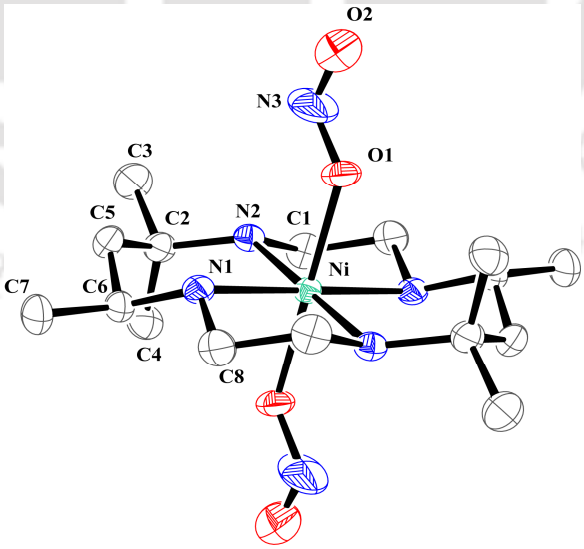

Figure 5.4. The ORTEP diagram of complex **5.2** (50% thermal ellipsoid; H-atoms are omitted for clarity).

Table 5.1. Crystallographic data for complexes **5.1**, **5.2** and **5.3**.

	5.1	**5.2**	**5.3**
Formulae	$C_{20}H_{42}NiN_4O_6$	$C_{16}H_{36}NiN_6O_4$	$C_{16}H_{36}NiN_6O_6$
Mol. wt.	489.25	435.22	467.22
Crystal system	triclinic	monoclinic	monoclinic
Space group	*P*-1	*C2/c*	*P*21/c
Temperature/ K	296(2)	296(2)	296(2)
Wavelength/ Å	0.71073	0.710 73	0.710 73
a/Å	8.3991(8)	12.8596(4)	8.980(2)
b/Å	9.3496(6)	11.6454(4)	18.693(5)
c/Å	9.4079(7)	15.2598(5)	15.499(4)
α/deg	73.619(6)	90.00	90.00
β/deg	81.717(7)	112.077(2)	120.013(14)
γ/deg	68.498(7)	90.00	90.00
V/Å^3	658.78(9)	2117.68(12)	2252.9(10)
Z	1	4	4
density/Mg·m^{-3}	1.233	1.365	1.378
Abs. coeff./mm^{-1}	0.774	0.949	0.904
Abs. correction	multi-scan	none	none
F(000)	262	936	1000
Total no. of reflections	2300	1873	3851
Reflections, $I > 2\sigma(I)$	2118	1538	3064
Max. 2θ/deg	25.00	24.99	25.00
Ranges (*h*, *k*, *l*)	$-9 \le h \le 7$	$-15 \le h \le 15$	$-9 \le h \le 10$
	$-11 \le k \le 10$	$-13 \le k \le 13$	$-22 \le k \le 21$
	$-11 \le l \le 11$	$-18 \le l \le 18$	$-18 \le l \le 18$
Complete to 2θ (%)	99.8	100.0	97.1
Refinement method	full-matrix least-squares on F^2	full-matrix least-squares on F^2	full-matrix least-squares on F^2
GOF (F^2)	1.113	1.056	1.165
R indices [$I > 2\sigma(I)$]	0.0488	0.0496	0.0326
R indices (all data)	0.0444	0.0576	0.0430

Table 5.2. Selected bond lengths (Å).

	5.1	**5.2**	**5.3**
Ni1–N1	2.101(3)	2.099(2)	2.081(2)
Ni1–N2	2.081(2)	2.071(3)	2.133(2)
Ni1–N3	-	-	2.092(2)
Ni1–N4	-	-	2.119(3)
Ni1–O1	2.144(3)	2.138(3)	2.196(2)
Ni1–O2	-	-	2.132(1)
N1–C2	1.500(4)	1.505(4)	1.494(3)
N3–O1	-	1.305(8)	-
N3–O2	-	1.110(1)	-
N5–O1	-	-	1.272(3)
N5–O2	-	-	1.266(3)
N5–O3	-	-	1.226(3)
C9–O1	1.245(5)	-	-
C9–O2	1.241(4)	-	-

Table 5.3. Selected bond angles (˚).

	5.1	**5.2**	**5.3**
N1–Ni1–N2	85.50(1)	94.20(1)	90.86(7)
N1–Ni1–N3	-	-	102.94(8)
N2–Ni1–N3	-	-	85.06(8)
N3–Ni1–N4	-	-	90.31(8)
N2–Ni1–N4	-	-	173.64(8)
N1–Ni1–O1	88.80(1)	90.00(1)	153.79(7)
N2–Ni1–O1	91.90(1)	89.10(1)	88.55(7)
O1–N5–O2	-	-	115.90(2)
O1–N5–O3	-	-	122.60(2)
O1–N3–O2	-	112.50(6)	-
O1–C9–C10	115.80(3)	-	-

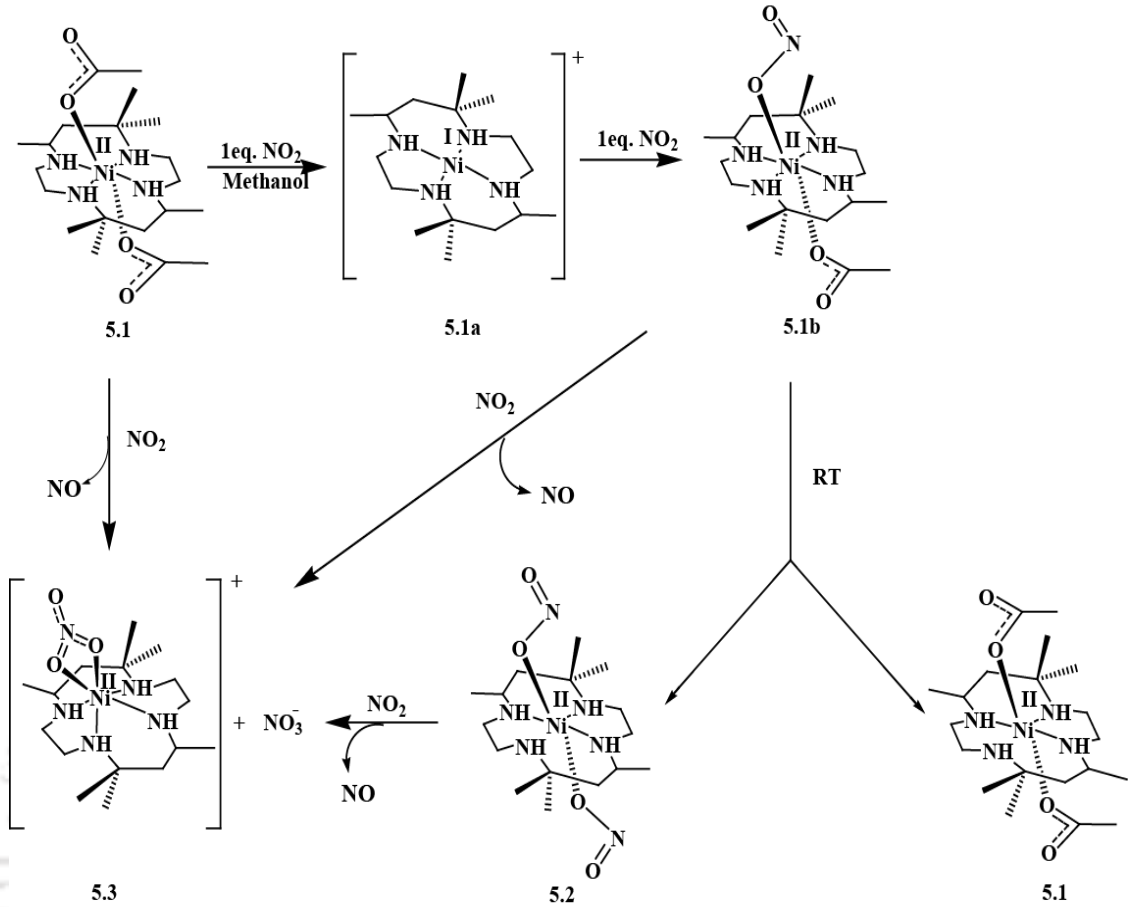

Scheme 5.1

The crystallization of complexes **5.1** and **5.2**, from the reaction mixture suggests the formation of [(L4)Ni(NO_2)(CH_3COO)], **5.1b**, as intermediate complex which during crystallization dissociated into complexes **5.1**, [(L4)Ni($CH_3COO)_2$] and **5.2**, [(L4)Ni($NO_2)_2$] owing to the lesser stability of **5.1b** compared to those. This was further confirmed by carrying out control reactions. In methanol solution of complex **5.1**, addition of equivalent amount of aqueous $NaNO_2$ resulted in the formation of complexes **5.1** and **5.2**, roughly in equal proportion. While an excess of $NaNO_2$ was used, exclusively complex **5.2** was obtained. On the other hand, stirring of a methanol solution of complex **5.2** with equivalent amount of Na(CH_3COO), resulted in the formation of almost equal amounts of complexes **5.1** and **5.2**; but excess Na(CH_3COO) afforded only complex **5.1**.

Complex **5.1b** was never isolated as intermediate in these control experiments presumably because of its less stability compared to complexes **5.1** and **5.2**.

When the reaction mixture containing **5.1b** was subjected to the addition of further equivalent NO_2, there was no appreciable change in the *d-d* absorption bands in UV-visible spectrum. However, in FT-IR spectrum, stretching at 1272 cm^{-1} assigned to nitrito group was disappeared and a new intense stretching band at 1384 cm^{-1} assignable to nitrato group was appeared. Structural characterization revealed the formation of corresponding Ni(II) nitrato complex, **5.3** in the reaction. The ORTEP diagram of complex **5.3** is shown in figure 5.5. In complex **5.3**, one of the nitrate ions is O-coordinated in a η^2 fashion with an average Ni–O distance of 2.164 Å.

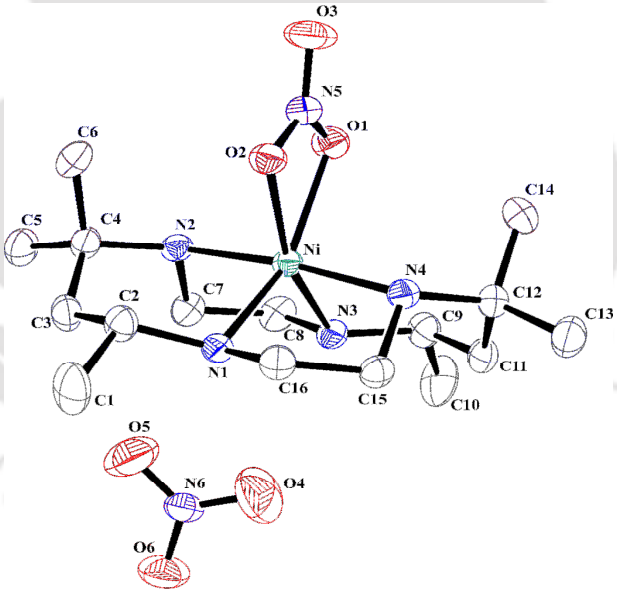

Figure 5.5. The ORTEP diagram of complex **5.3** (50% thermal ellipsoid; H-atoms are omitted for clarity).

Second nitrate ion was not coordinated to the metal ion. The formation of complex **5.3** was attributed to the less stability of corresponding [(L4)Ni(NO_3)(OAc)]. The peak observed at *m*/*z* 404.215 in mass spectrometry was assignable to $[(L4)NiNO_3]^+$. Simulated and

observed isotopic distribution in mass spectroscopy matched well (Appendix IV). Thus, addition of NO_2 in methanol solution of intermediate complex **5.1b** afforded oxo transfer resulting in the corresponding nitrate complex **5.3**. NO was expected to form as side product in the reaction and was confirmed by GC-mass as well by spin trapping using iron(II)diethyldithiocarbamato complex (Appendix IV).[11]

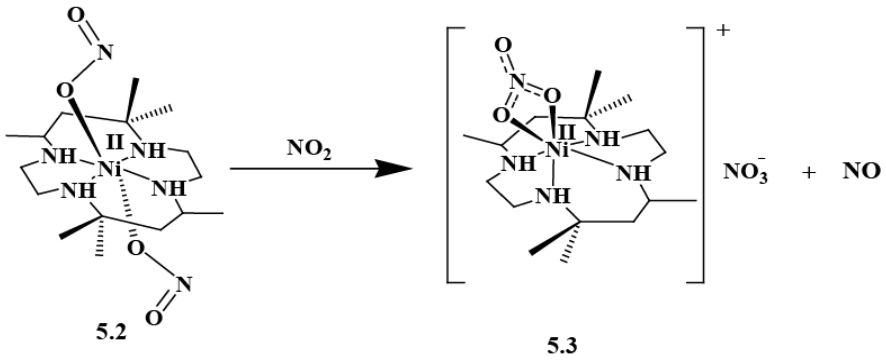

Scheme 5.2

It would be worth to mention here that purging NO_2 to the methanol solution of complex **5.2** also afforded complex **5.3**. On the other hand addition of excess NO_2 in methanol solution of complex **5.1** resulted in complex **5.3** as the final product with release of NO.

Recently, the NO_2 reactivity of a Cu(II) complex of 4,6-di-*tert*-butyl-2-((2-picolyl(isopropyl)amino)methyl)phenol ligand was reported.[6] The Cu(II) center was found to undergo reduction by NO_2 with simultaneous nitration of the phenol ring of the ligand and Cu(I) complex of the nitrated ligand was resulted. The Cu(I) complex in presence of one equivalent of NO_2 gave corresponding Cu(II)-nitrito complex which was characterized structurally. Reaction of the Cu(II)-nitrito complex with NO_2 resulted in the oxo transfer from NO_2 to the coordinated nitrito group to afford corresponding Cu(II)-nitrate and NO. Earlier Kurtikyan *et al*. reported that the reaction of Fe^{II}(TPP) and Mn^{II}(TPP) [TPP =

meso-tetra-*p*-tolylporphyrinato dianion) with NO_2 lead to the corresponding nitrato complex.[4,5] The reaction was proposed to proceed in two steps. Low NO_2 pressure and short reaction time resulted in the NO_2 coordination to the metal ion to afford corresponding O-nitrito complex in the first step. Suslick and Watson also reported this earlier.[12] In the presence of additional NO_2, oxo transfer reaction occured to afford the corresponding η^2-ONO_2 complexes with presumably formation of NO.[4-6]

The present study involving the coordination of NO_2 with Ni(I) intermediate to form [Ni^I-$NO_2 \leftrightarrow Ni^{II}NO_2^-$] followed by its reaction with additional NO_2 to afford corresponding Ni(II)-nitrate was also in good agreement with the proposition made by Kurtikyan *et al*. It is to be noted that unlike the examples of Fe^{II}(TPP) and Mn^{II}(TPP), the intermediate Ni(II)-nitrite was isolated and structurally characterized.[4,5]

The reaction of intermediate complex **5.1b** with NO_2 leading to the conversion of O-nitrito to O- nitrato complex can be envisaged to follow pathway of oxo transfer as was observed in earlier reports.[4-6] (Scheme 5.3).

ESI-mass experiment studies with scrambled NO_2[16/18] was found to result in two equal intensity mass signals for [Ni(L4)($^{16}O_2N^{18}O$)]$^+$ and [Ni(L4)($N^{16}O_3$)]$^+$ (Appendix IV). On the other hand, addition of $^{15}NO_2$ to the solution of **5.1b** was found to release ^{15}NO. Hence an oxo transfer from free NO_2 to the coordinated nitrito group was suggested. In case of earlier reported examples the oxo transfer was found to follow the similar mechanistic pathway.

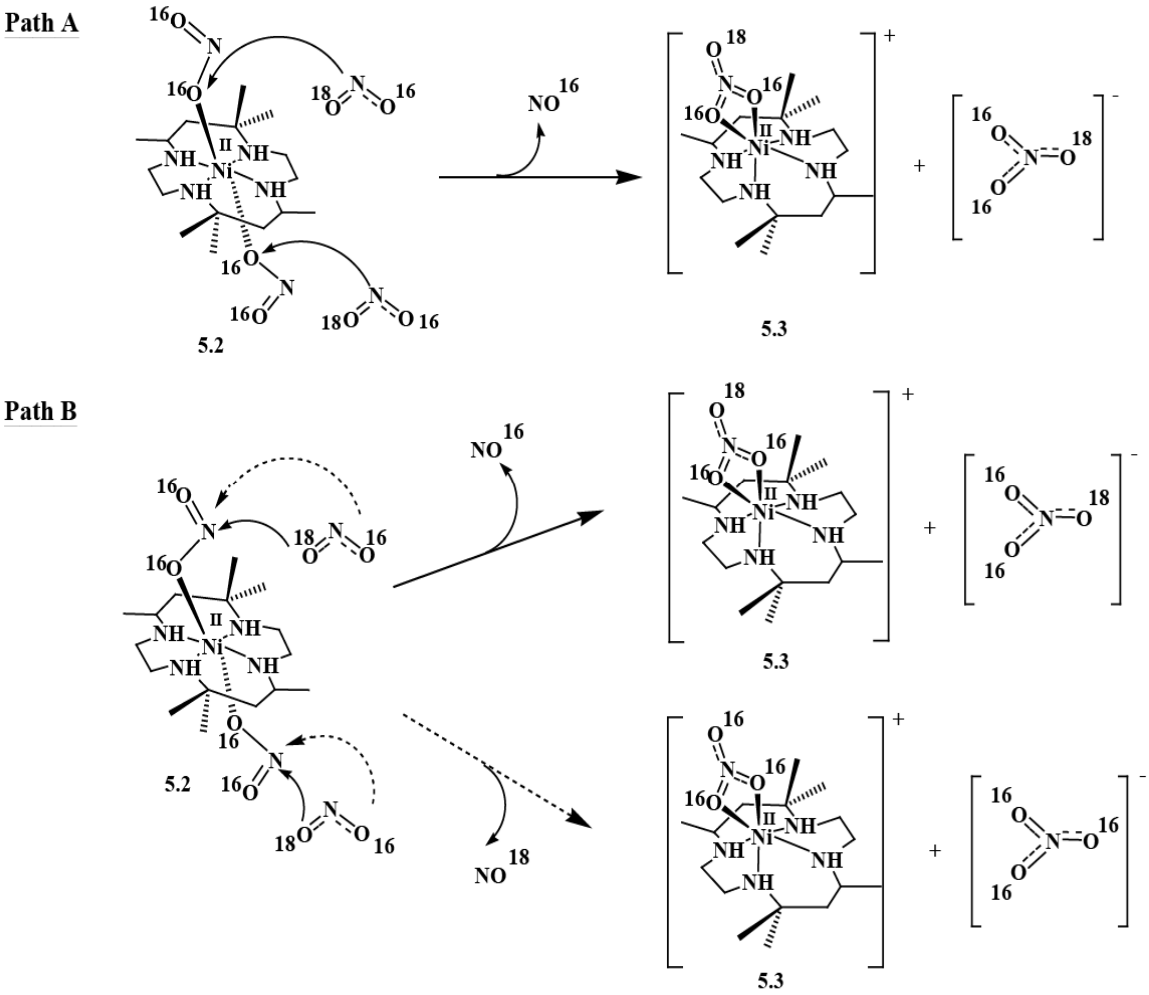

Scheme 5.3

It would be interesting to note that in all the examples including the present work, the NO_2^- binds to the metal ion in mono-dentate fashion. Perhaps, the nitrito binding mode to the metal center is the key in such oxo transfer reactions.

5.3 Experimental Section

5.3.1 Materials and Methods

All reagents and solvents of reagent grade were purchased from commercial sources and used as received except specified. $^{18}O_2$ was purchased from Icon Isotopes. Deoxygenation

of the solvent and solutions was effected by repeated vacuum/purge cycles or bubbling with nitrogen or argon for 30 min. NO_2 was used from cylinder after purification using reported methods.[4,5] ^{18}ONO gas was prepared by the reaction of purified NO with $^{18}O_2$ in an airtight glass chamber fitted with a stoppered outlet at room temperature followed by removal of excess O_2 by passing through O_2 trap. Further purification was done following earlier reported methods of fractional distillation.[4,5] The isotopic enrichment of ^{18}O in $^{16/18}O_2N$ is 50% as measured by GC-mass. The dilution of NO_2 was effected with argon gas using Environics Series 4040 computerized gas dilution system. UV–visible spectra were recorded on Agilent HP 8454 dioad arrey UV-visible spectrophotometer. FT-IR spectra of the solid samples were taken on a PerkinElmer spectrophotometer with samples prepared as KBr pellets. Solution electrical conductivity was measured using a Systronic 305 conductivity bridge. ^1H NMR and ^{13}C-NMR spectra were recorded in 400 MHz and 100MHz Varian FT spectrometer respectively Chemical shifts (ppm) were referenced either with an internal standard (Me_4Si) or to the residual solvent peaks. The X-band EPR spectra were recorded on a JES-FA200 ESR spectrometer, at room temperature or at 77 K with microwave power of 0.998 mW, microwave frequency of 9.14 GHz, and modulation amplitude of 2. Elemental analyses were obtained from a PerkinElmer Series II Analyzer. The magnetic moment of complexes were measured on a Cambridge Magnetic Balance.

Single crystals were grown by slow diffusion followed by slow evaporation technique. The intensity data were collected using a Bruker SMART APEX-II CCD diffractometer, equipped with a fine focus 1.75 kW sealed tube Mo Kα radiation (λ = 0.710 73 Å) at 273(3) K, with increasing ω (width of 0.3° per frame) at a scan speed of three seconds per frame. The SMART software was used for data acquisition.[13] Data integration and reduction were undertaken with SAINT and XPREP software.[14] Structures were solved by

direct methods using SHELXS-97 and refined with full-matrix least-squares on F^2 using SHELXL-97.[15] Structural illustrations were drawn with ORTEP-3 for Windows.[16]

5.3.2 Synthesis

(a) Ligand L4

The macrocyclic ligand **L4** was prepared by using the procedure described earlier.[8] It was characterized by elemental analyses, FT-IR, ^{1}H-NMR, and ^{13}C-NMR spectroscopy. Elemental analyses for $C_{16}H_{36}N_4$, Calcd(%): C, 67.55; H, 12.75; N, 19.69. Found (%): C, 67.59; H, 12.75; N, 19.76. FT-IR (in KBr): 753, 1177, 1372, 1465, 2832, 2923, 2965, 3275 cm^{-1}. ^{1}H NMR (400 MHz, $CDCl_3$): δ_{ppm}, 2.96 (2H), 2.66 (8H), 2.24 (4H), 1.79 (4H), 1.13 (12H), 1.09 (6H). ^{13}C NMR (100 MHz, $CDCl_3$): δ_{ppm}, 53.9, 48.2, 46.4, 45.5, 45.2, 29.7, 28.2, 24.4.

(b) Complex 5.1

To a stirred solution of nickel(II) acetate tetrahydrate, (0.488 g, 2 mmol) in methanol (20 ml) was added a solution of **L4** (0.564 g, 2 mmol) in methanol (20 ml). The reaction mixture was refluxed for 2 h. and then the volume was reduced under vacuum to ~5 ml. A layer of ether (10 m;) was made, and the mixture was kept in freezer over night to obtain the metal complex **5.1** as violet crystalline solid. Yield: 0.84 g (85%). Elemental analysis for $C_{20}H_{42}NiN_4O_4$, Calcd(%): C, 52.08; H, 9.18; N, 12.15; Found(%): C, 52.16; H, 9.17; N, 12.27. FT-IR (in KBr): 3424, 1633, 1562, 1457, 1409, 1167, 1033, 963, 941, 677, 654 cm^{-1}. UV–visible (methanol): 362 nm (ε/ $M^{-1}cm^{-1}$, 24), 464 nm (ε/ $M^{-1}cm^{-1}$, 28), 574 nm (ε/ $M^{-1}cm^{-1}$, 18) and 960 nm (ε/ $M^{-1}cm^{-1}$, 12). The complex **5.1** behaved as non-electrolyte in

methanol solution [Λ_M (S cm^{-1}), 64]. The observed magnetic moment is found to be 2.45 BM.

(c) Complex 5.2

Complex **5.1** (461 mg, 1.0 mmol) was dissolved in dry methanol (20 ml) in a schlenk flask fitted with a rubber septum and degassed using argon gas. To this, two equivalent of NO_2/Ar (1:25 v/v) were added through a gastight syringe fitted in a Schlenk line, and the mixture was stirred for 1/2 h. The volume of the solution was reduced under vacuum to ~5 mL, and a layer of diethyl ether (~10 ml) was made. The mixture was kept in freezer over night to afford complex **5.2** as pink colored solid. Yield: 0.218 g (~50%). Elemental analysis for $C_{16}H_{36}NiN_6O_4$, Calcd(%): C, 44.16; H, 8.34; N, 19.31; Found(%): C, 44.29; H, 8.33; N, 19.42. FT-IR (in KBr): 3421, 2967, 1566, 1377, 1271, 1208, 1044, 852, 821 cm^{-1}. UV–visible (methanol): 355 nm (ε/ $M^{-1}cm^{-1}$, 57), 462 nm (ε/ $M^{-1}cm^{-1}$, 32), 567 nm (ε/ $M^{-1}cm^{-1}$, 19) and 948 nm (ε/ $M^{-1}cm^{-1}$, 14). The complex **5.2** behaved as non-electrolyte in methanol [Λ_M (S cm^{-1}), 40]. The observed magnetic moment is found to be 2.34 BM.

(d) Complex 5.3

To a degassed solution of complex **5.1** (218 mg, 0.5 mmol) in dry methanol (10 ml), excess NO_2 gas was purged for 1 min. The resulting bluish pink solution was dried under vacuum to reduce its volume to ~5 ml. Ether (20 ml) was then added to give blue precipitate of complex **5.3**. Product was further crystallized from methanol solvent. Yield: 168 mg (72%). Elemental analysis for $C_{16}H_{36}NiN_6O_6$, Calcd(%): C, 41.13; H, 7.77; N, 17.99; Found(%): C, 41.18; H, 7.78; N, 18.06. FT-IR (in KBr): 3421, 3232, 2969, 1406, 1384, 1318, 1306, 1161, 1024, 821 cm^{-1}. UV–visible (methanol): 358 nm (ε/ $M^{-1}cm^{-1}$, 50),

459 nm (ε/ $M^{-1}cm^{-1}$, 41), 571 nm (ε/ $M^{-1}cm^{-1}$, 26) and 953 nm (ε/ $M^{-1}cm^{-1}$, 16). The observed magnetic moment is found to be 2.20 BM. Alternatively complex **5.3** can also be prepared by purging NO_2 into the methanol solution of complex **5.2**.

(e) Spin-Trapping experiment to establish the formation of NO

Complex **5.2** (300 mg) was dissolved in dry and degassed acetonitrile in a Schlenk flask attached through a rubber tubing to another flask containing a solution of $[Fe^{II}(dtc)_2]$ [dtc= diethyldithiocarbamato] (100 mg in 20 mL of acetonitrile). Equivalent amount of NO_2 gas (diluted using Ar gas; NO_2:Ar, 1:25 v/v) was purged in the solution of complex **5.2** using a gastight syringe. The mixture was stirred for 10 min. Ar gas was bubbled for 5 min through the reaction mixture to push the gas mixture into the flask containing $[Fe^{II}(dtc)_2]$. X-band EPR spectrum of this solution was then recorded to establish the presence of NO.

5.4 Conclusion

Complex **5.1** $[Ni(L4)(O_2CCH_3)_2]$ reacted with equivalent amount of NO_2 to result in the reduction of Ni(II) to Ni(I). The *in situ* generated Ni(I) intermediate complex reacted with additional equivalent of NO_2 to form corresponding η^1-O-nitrito Ni(II) complex, **5.2**. Subsequent addition of NO_2 lead to the corresponding Ni(II) η^2-O-nitrato complex, **5.3** with concomitant formation of NO. Complexes **5.2** and **5.3** were isolated and structurally characterized. Isotopic labelling experiment revealed that the oxo transfer took place from NO_2 to the coordinated η^1-ONO group. Thus, the present study demonstrated the Ni(II) complex induced conversion of NO_2 to NO_2^-, NO and NO_3^-.

5.5 References

(1) Bascom, R.; Bromberg, P. A.; Costa, D. A.; Devlin, R.; Dockery, D. W.; Frampton, M. W.; Lambert, W.; Samet, J. M.; Peizer, F. E.; Utell, M. *Am. J. Respir. Crit. Care Med*. **1996**, *153*, 3.

(2) (a) Cosby, K.; Partovi, K. S.; Crawford, J. H.; Patel, R. P.; Reiter, C. D.; Martyr, S.; Yang, B. K.; Waclawiw, M. A.; Zalos, G.; Xu, X.; Huang, K. T.; Shields, H.; Kim-Shapiro, D. B.; Schechter, A. N.; Cannon, R. O.; Gladwin, M. T. *Nat. Med*. **2003**, *9*, 1498. (b) Fernandez, B. O.; Bryan, N. S.; Garcia-Saura, M. F.; Bauer, S.; Whitlock, D. R.; Ford, P. C.; Janero, D. R.; Rodriguez, J.; Ashrafian, H. *J. Biol. Chem*. **2008**, *283*, 33927. (c) Luchsinger, B. P.; Rich, E. N.; Yan, Y.; Williams, E. M.; Stamler, J. S.; Singel, D. J. *J. Inorg. Biochem.* **2005**, *99*, 912. (d) Averill, B. A. *Chem. Rev*. **1996**, *96*, 2951. (e) Gladwin, M. T.; Grubina, R.; Doyle, M. P. *Acc. Chem. Res*. **2009**, *42*, 157. (f) Ford, P. C. *Inorg. Chem*. **2010**, *49*, 6226.

(3) (a) Radi, R. *Proc. Natl. Acad. Sci. U.S.A.* **2004**, *101*, 4003. (b) Radi, R. *Acc. Chem. Res*. **2013**, *46*, 550. (c) Surmeli, N. B.; Litterman, N. K.; Miller, A. F.; Groves, J. T. *J. Am. Chem. Soc.* **2010**, *132*, 17174. (d) Olbregts, J. *Int. J. Chem. Kinet.* **1985**, *17*, 835. (e) Su, J.; Groves, J. T. *J. Am. Chem. Soc.* **2009**, *131*, 12979. (f) Bian, K.; Gao, Z. H.; Weisbrodt, N.; Murad, F. *Proc. Natl. Acad. Sci. U.S.A.* **2003**, *100*, 5712.

(4) (a) Kurtikyan, T. S.; Hayrapetyan, V. A.; Mehrabyan, M. M.; Ford, P. C. *Inorg. Chem.* **2014**, *53*, 11948. (b) Kurtikyan, T. S.; Ford, P. C. *Angew. Chem., Int. Ed*. **2006**, *45*, 492.

(5) Kurtikyan, T. S.; Hovhannisyan, A. A.; Gulyan, G. M.; Ford, P. C. *Inorg. Chem*. **2007**, *46*, 7024.

(6) Gogoi, K.; Deka, H.; Kumar, V.; Mondal, B. *Inorg. Chem*. **2015**, *54*, 4799.

(7) (a) Halcrow, M. A.; Christou, G. *Chem. Rev.* **1994**, *94*, 2421. (b) Signor, L.; Knuppe, C.; Hug, R.; Schweizer, B.; Pfaltz, A.; Jaun, B. *Chem. Eur. J.* **2000**, *6*, 3508. (c) Ozaki, S.; Matsushita, H.; Ohmori, H. *J. Chem. Soc., Perkin Trans. 1* **1993**, 649. (d) Campbell, C. J.; Rusling, J. F.; Bruckner, C. *J. Am. Chem. Soc.* **2000**, *122*, 6679. (e) Kryatov, S. V.; Mohanraj, B. S.; Tarasov, V. V.; Kryatova, O. P.; Rybak-Akimova, E. V.; Nuthakki, B.; Rusling, J. F.; Staples, R. J.; Nazarenko, A. Y. *Inorg. Chem.* **2002**, *41*, 923. (f) James, T. L.; Cai, L.; Muetterties, M. C.; Holm, R. H. *Inorg. Chem.* **1996**, *35*, 4148.

(8) Hay, R. W.; Lawrance, A. G.; Curtis, N. F. *J. Chem. Soc., Perkin Trans.* **1975**, *1*, 59.

(9) (a) Jorgensen, C. K.; *Inorganic Complexes*, pp. 54, Academic Press, New York, **1963**. (b) Lever, A. B. P. (ed.) *Inorganic Electronic Spectroscopy*, pp 507 and 738, Elsevier, Amsterdam, **1984**.

(10) (a) Hathaway, B. J.; Billing, D. E. *Coord. Chem. Rev.* **1970**, *5*, 143. (b) Gagne, R. R.; Ingle, D. M. *Inorg. Chem.* **1981**, *20*, 420. (c) Nag, K.; Chakravorty, A. *Coord. Chem. Rev.* **1980**, *33*, 87. (d) Ansell, C. W. G.; Lewis, J.; Raithby, P. R.; Ramsden, J. N.; Shroder, M. *Chem. Commun.* **1982**, 546. (e) Suh, M. P.; Oh, K. Y.; Lee, J. W.; Bae, Y. Y. *J. Am. Chem. Soc.* **1996**, *118*, 777.

(11) Melzer, M. M.; Mossin, S.; Dai, X.; Bartell, A. M.; Kapoor, P.; Meyer, K.; Warren, T. H. *Angew. Chem., Int. Ed*. **2010**, *49*, 904.

(12) Suslick, K. S.; Watson, R. A. *Inorg. Chem.* **1991**, *30*, 912.

(13) *SMART, SAINT, and XPREP;* Siemens Analytical X-ray Instruments Inc.: Madison, WI, **1995**.

(14) Sheldrick, G. M. SADABS, Software for Empirical Absorption Correction; University of Gottingen: Gottingen, Germany, **2003**.

(15) Sheldrick, G. M. SHELXS-97*;* University of Gottingen: Gottingen, Germany, **1997**.

(16) Farrugia, L. J. *J. Appl. Crystallogr*. **1997**, *30*, 565.

Appendix I

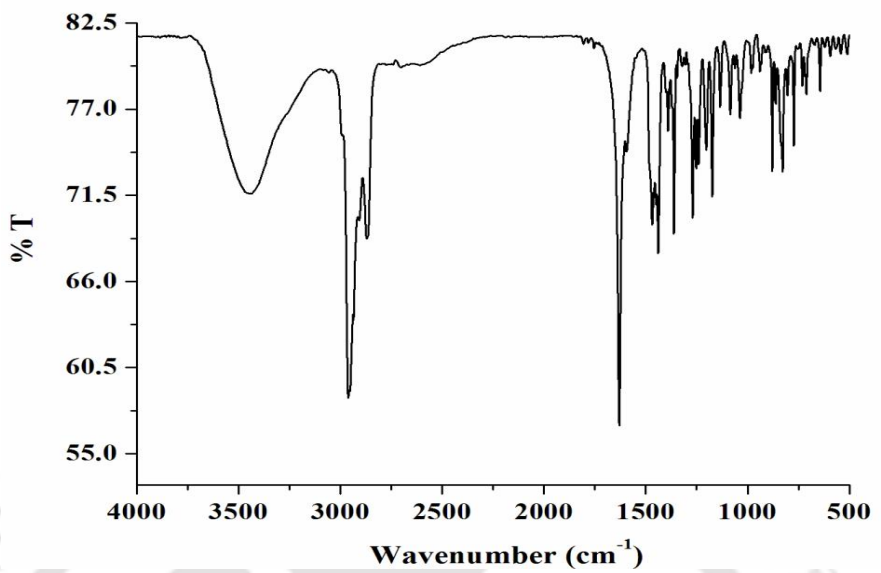

Figure A1.1. FT-IR spectrum of ligand **L1** in KBr.

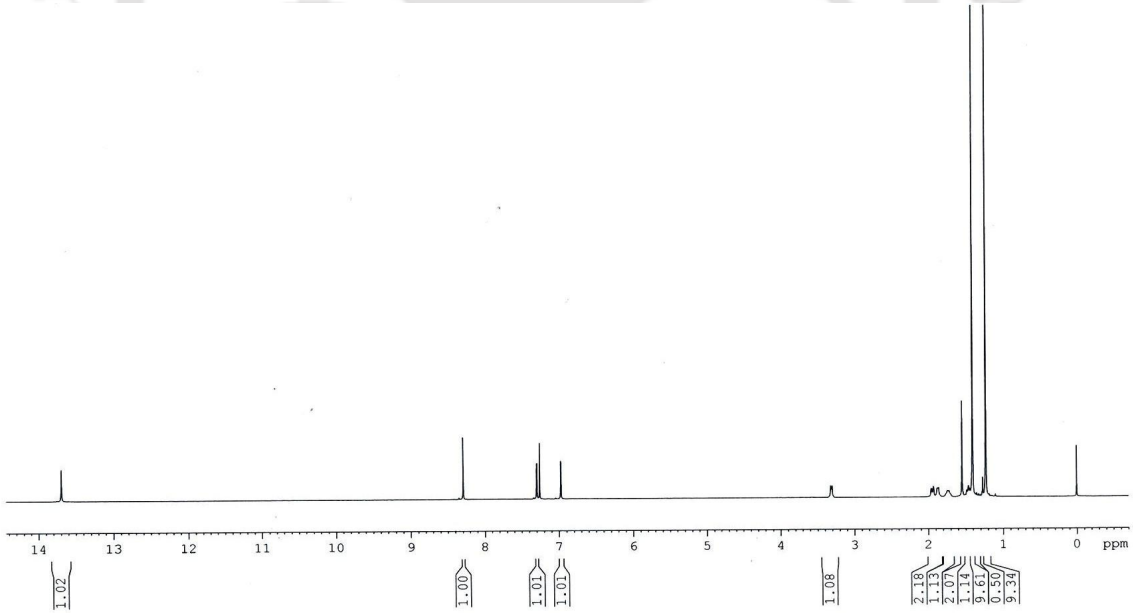

Figure A1.2. ^{1}H-NMR spectrum of ligand **L1** in $CDCl_3$.

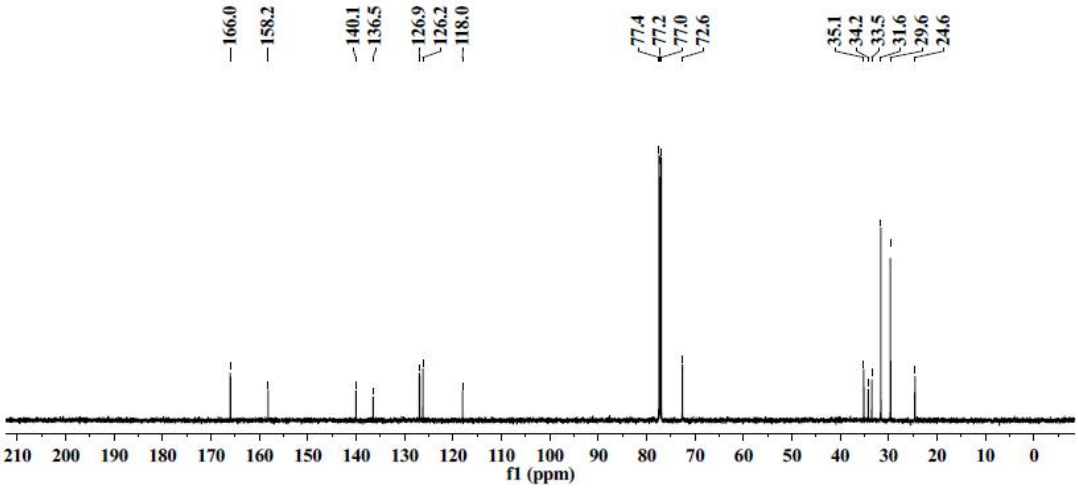

Figure A1.3. ^{13}C-NMR spectrum of ligand **L1** in $CDCl_3$

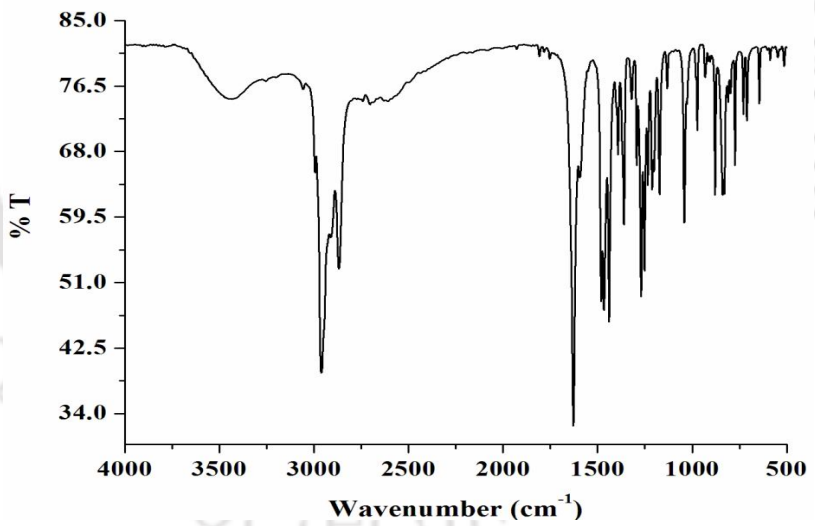

Figure A1.4. FT-IR spectrum of ligand **L2** in KBr.

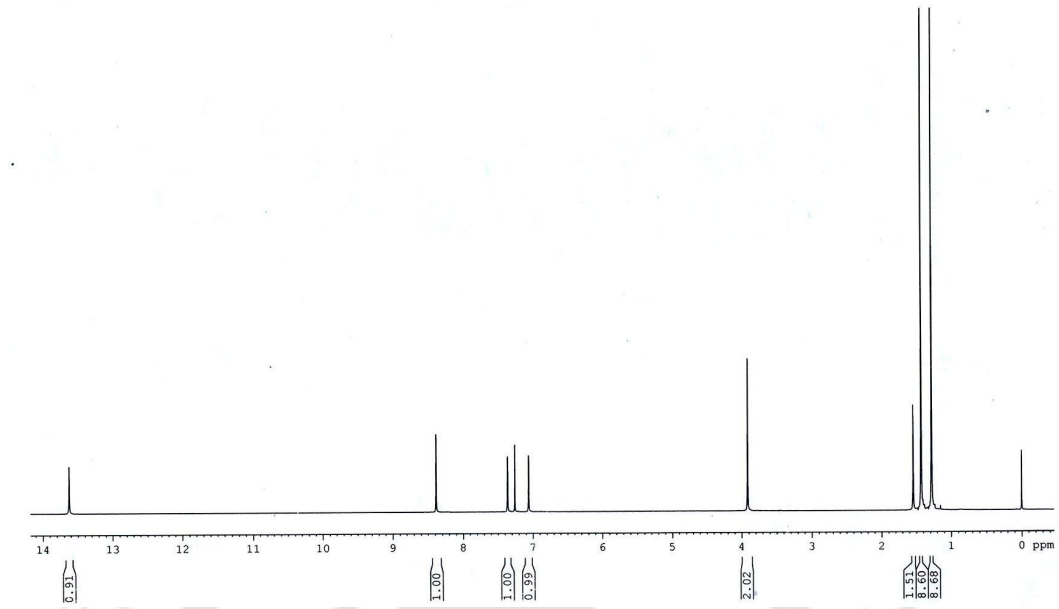

Figure A1.5. ^{1}H-NMR spectrum of ligand **L2** in $CDCl_3$.

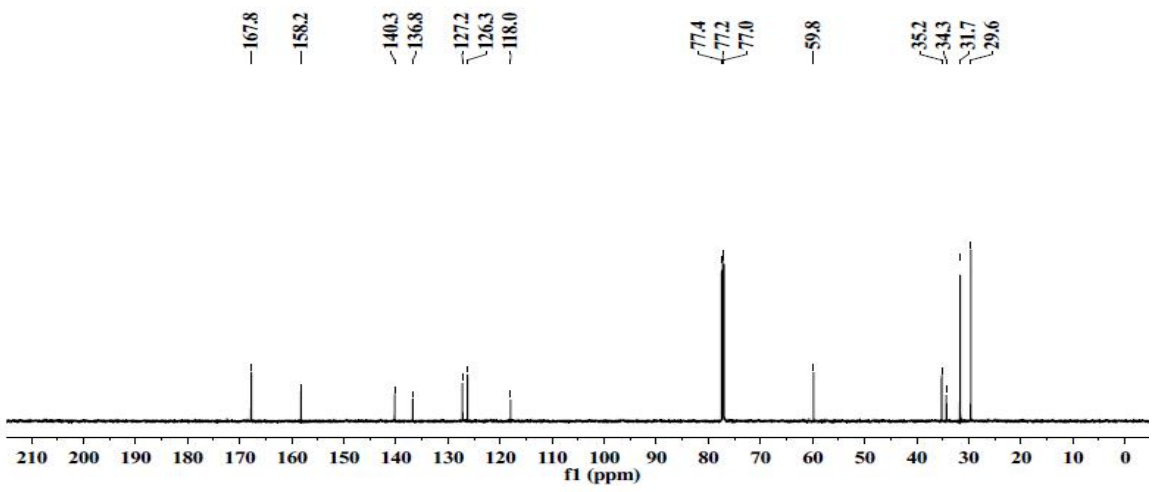

Figure A1.6. ^{13}C-NMR spectrum of ligand **L2** in $CDCl_3$

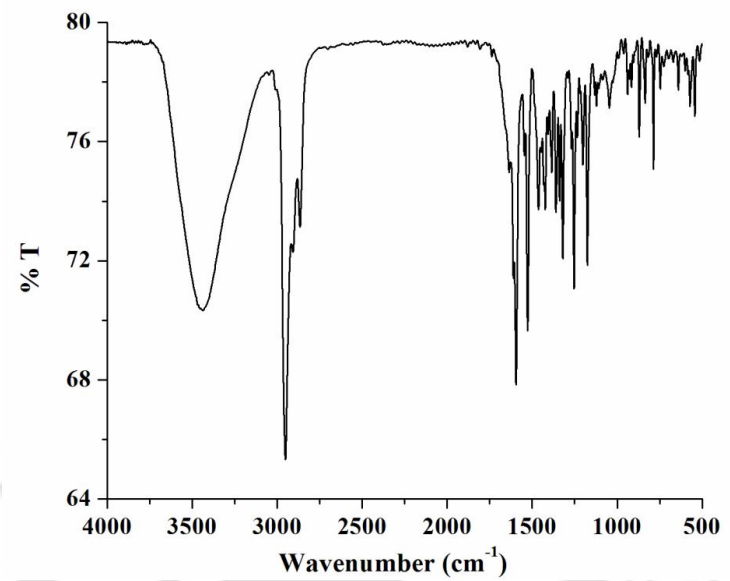

Figure A1.7. FT-IR spectrum of complex **2.1** in KBr.

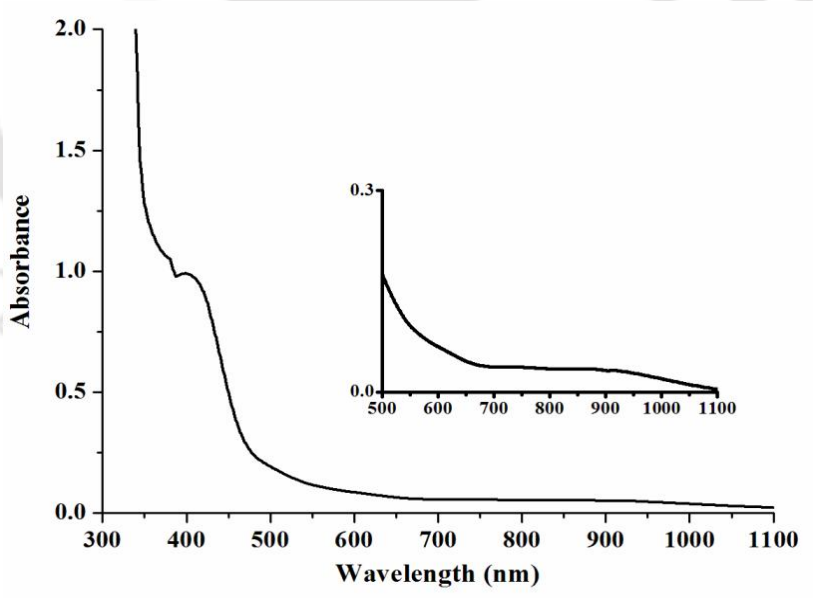

Figure A1.8. UV-visible spectrum of complex **2.1** in dry THF.

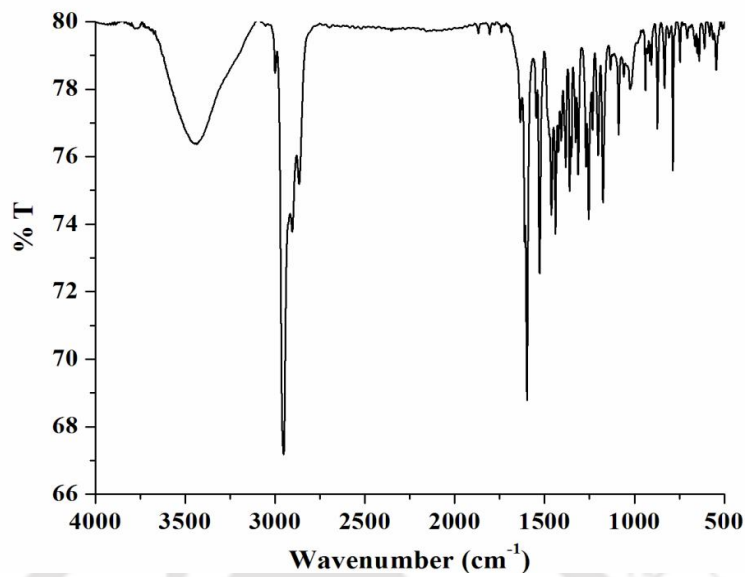

Figure A1.9. FT-IR spectrum of Complex **2.2** in KBr.

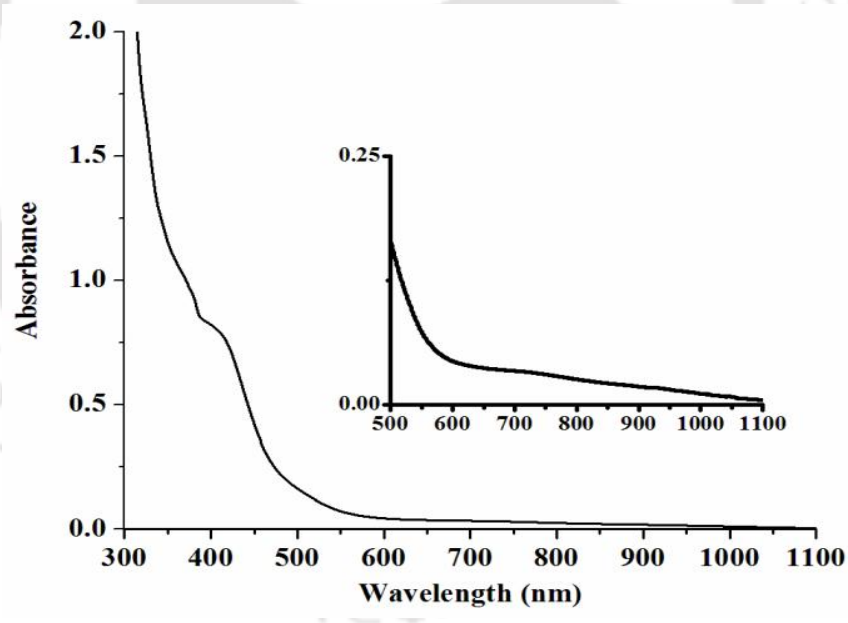

Figure A1.10. UV-visible spectrum of complex **2.2** in dry THF.

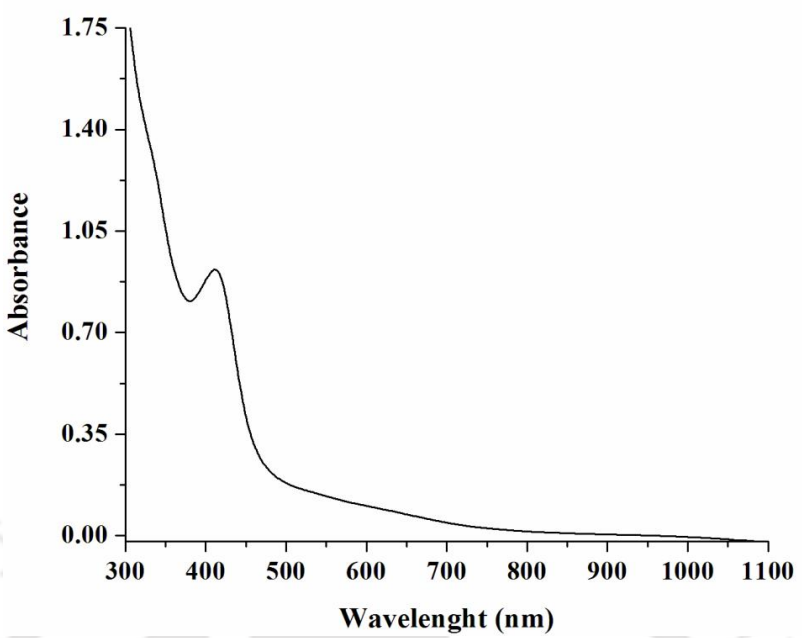

Figure A1.11. UV-visible spectrum of complex **2.3** in dry THF.

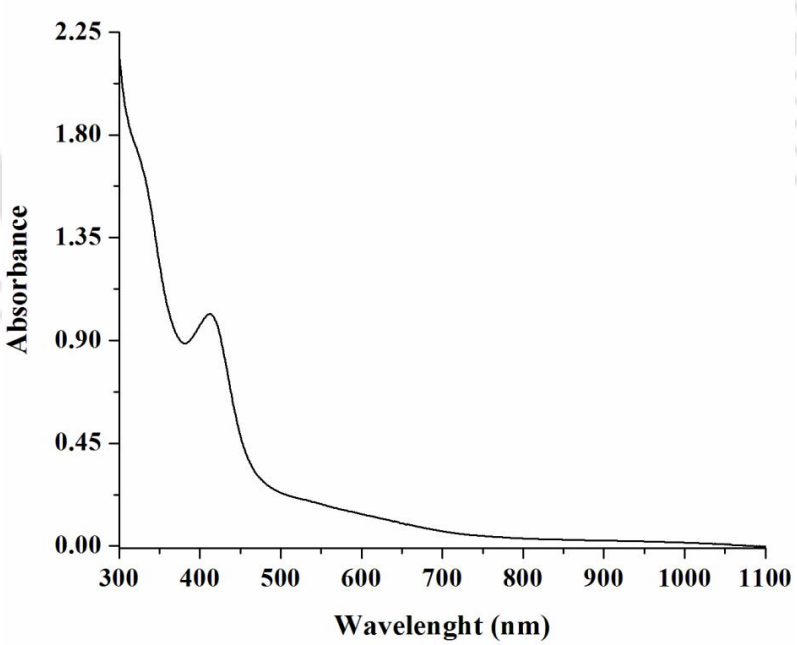

Figure A1.12. UV-visible spectrum of complex **2.4** in dry THF.

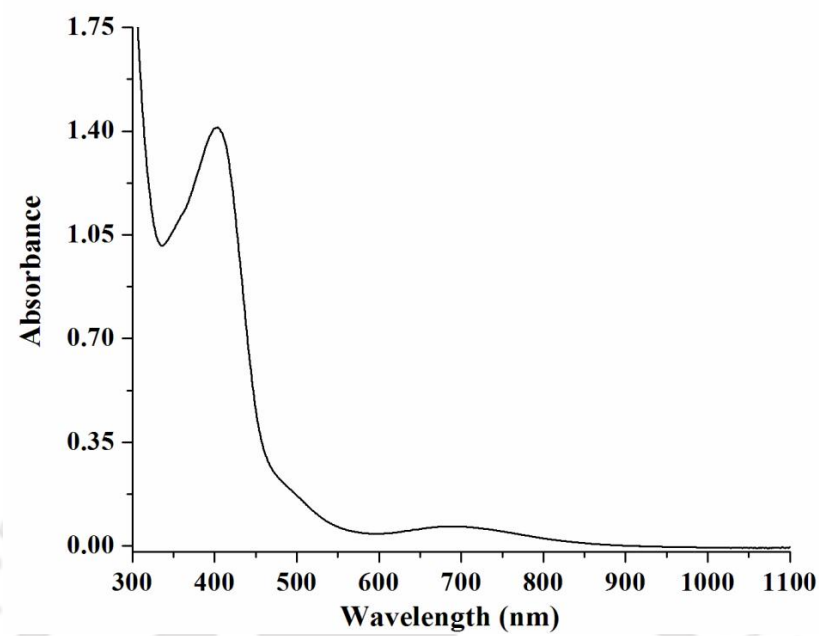

Figure A1.13. UV-visible spectrum of complex **2.5** in dry THF.

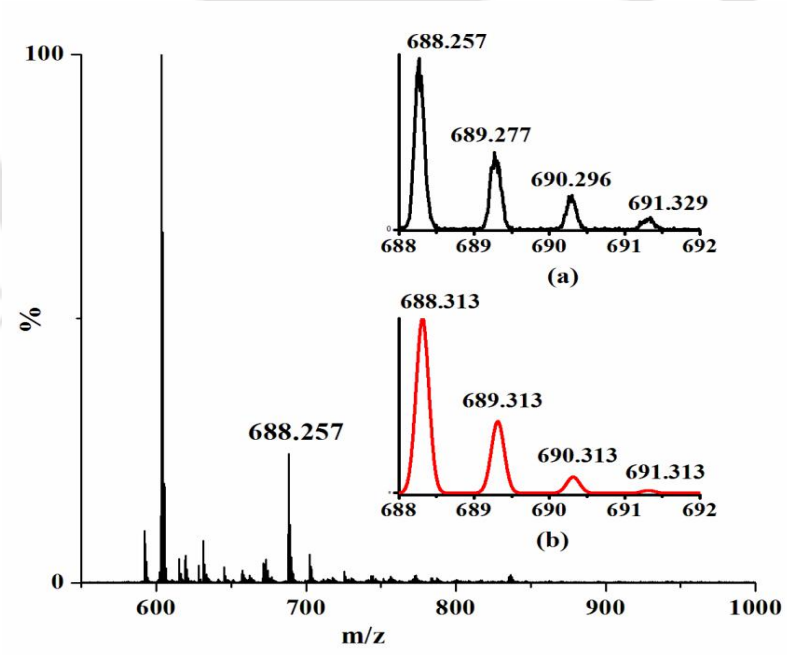

Figure A1.14. ESI-mass spectra of complex **2.5** with isotopic distribution (a) experimental (b) simulated in methanol [(**L1CoNO$_3$**)+**Na**]$^+$.

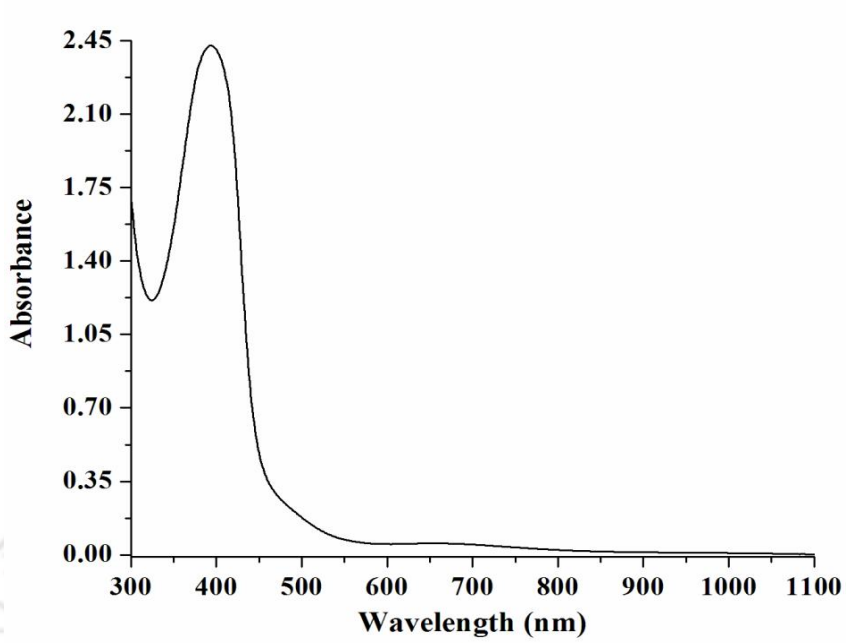

Figure A1.15. UV-visible spectrum of complex **2.6** in dry THF.

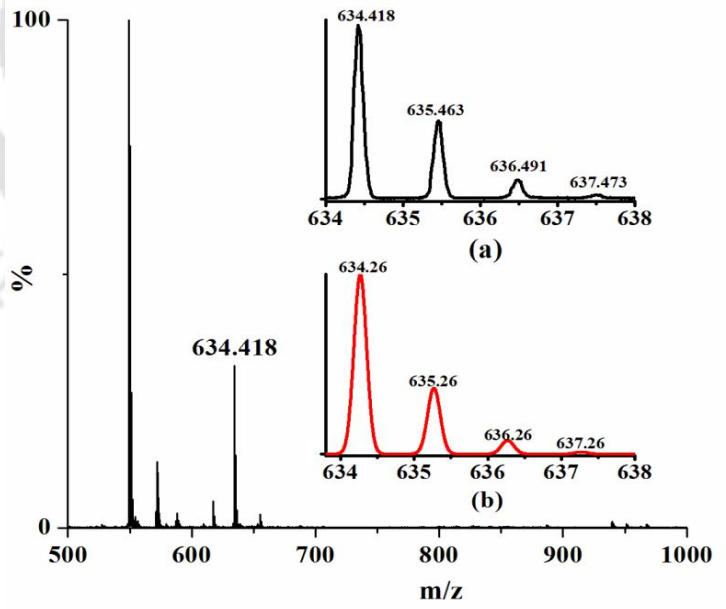

Figure A1.16. ESI-mass spectra of complex **2.6** with isotopic distribution (a) experimental (b) simulated in methanol [(**L2CoNO**$_3$)+**Na**]$^+$.

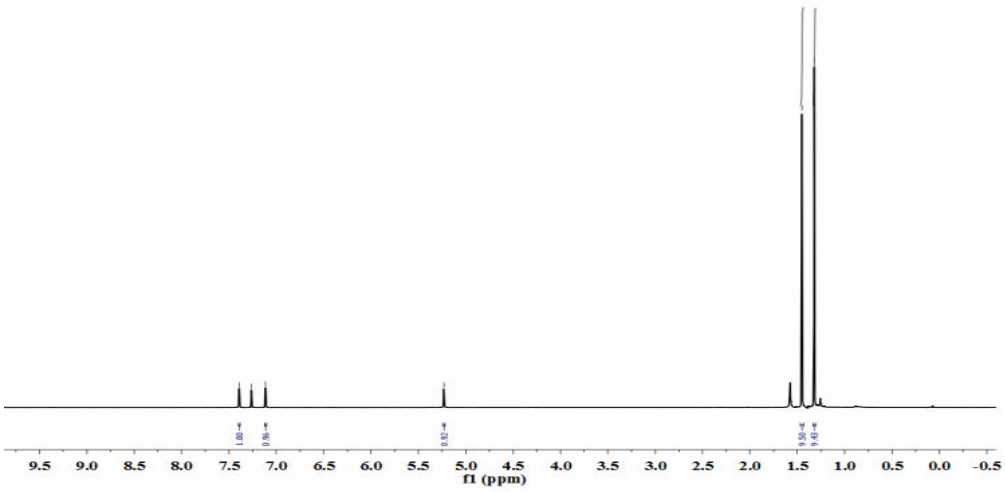

Figure A1.17. ^{1}H-NMR spectrum of 2,2′-dihydroxy-3,3′,5,5′-tetra-*tert*-butylbiphenol in $CDCl_3$.

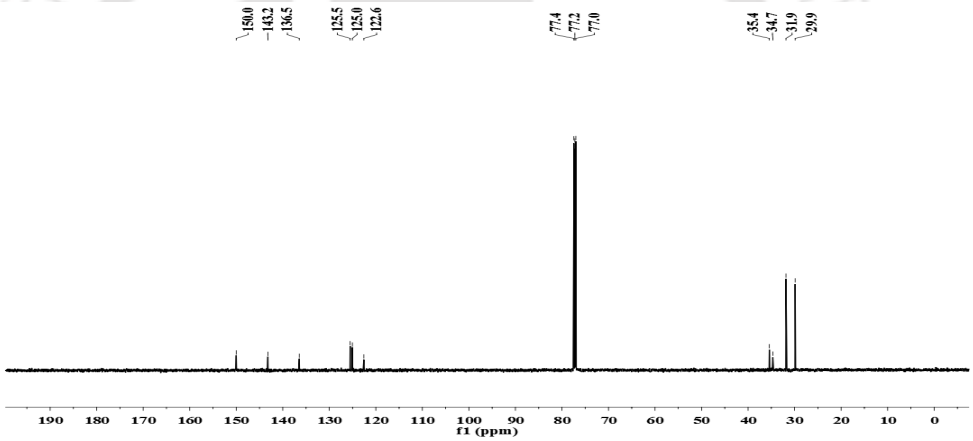

Figure A1.18. ^{13}C-NMR spectrum of 2,2′-dihydroxy-3,3′,5,5′-tetra-*tert*-butylbiphenol in $CDCl_3$.

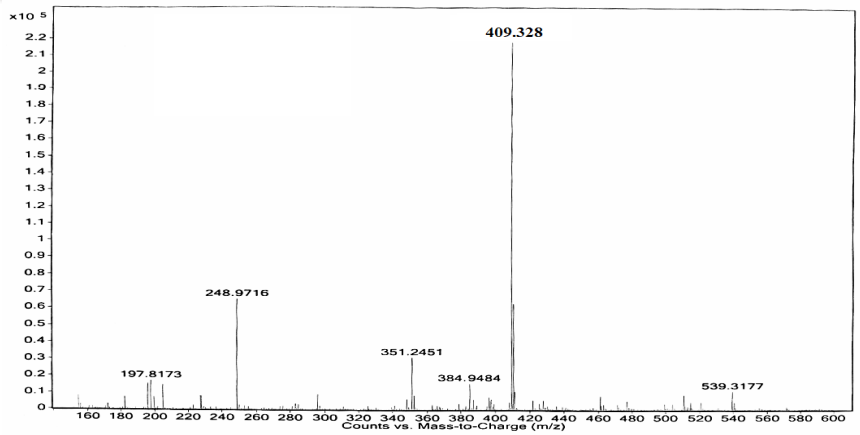

Figure A1.19. ESI-mass spectrum of 2,2′-dihydroxy-3,3′,5,5′-tetra-*tert*-butylbiphenol in methanol. (Negative mode).

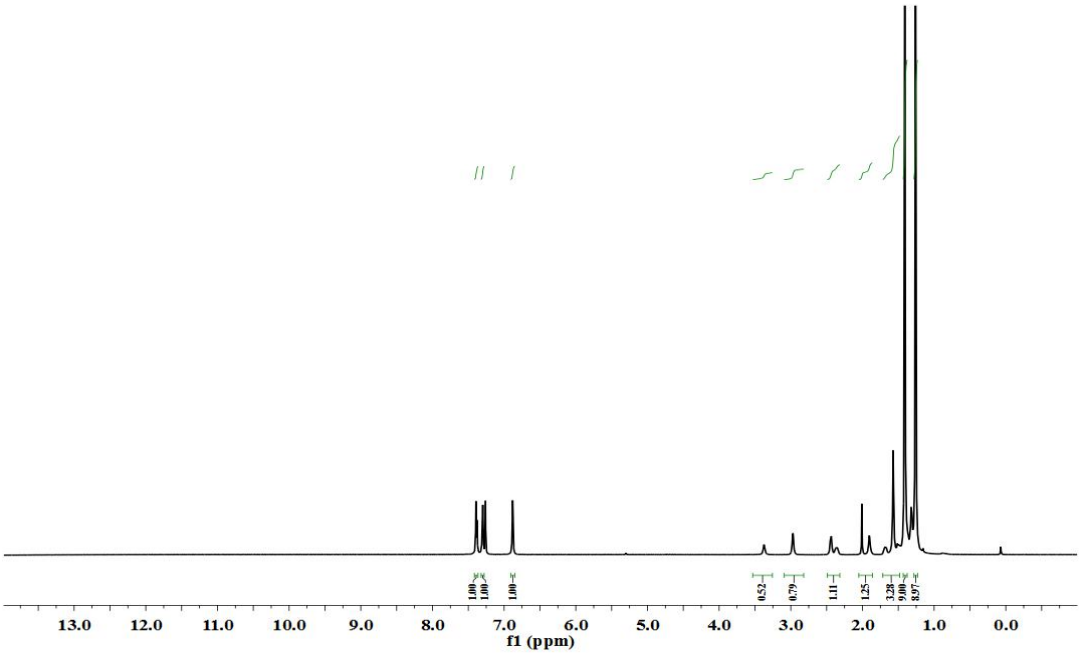

Figure A1.20. ^{1}H-NMR spectrum of ligand complex **2.3** in $CDCl_3$

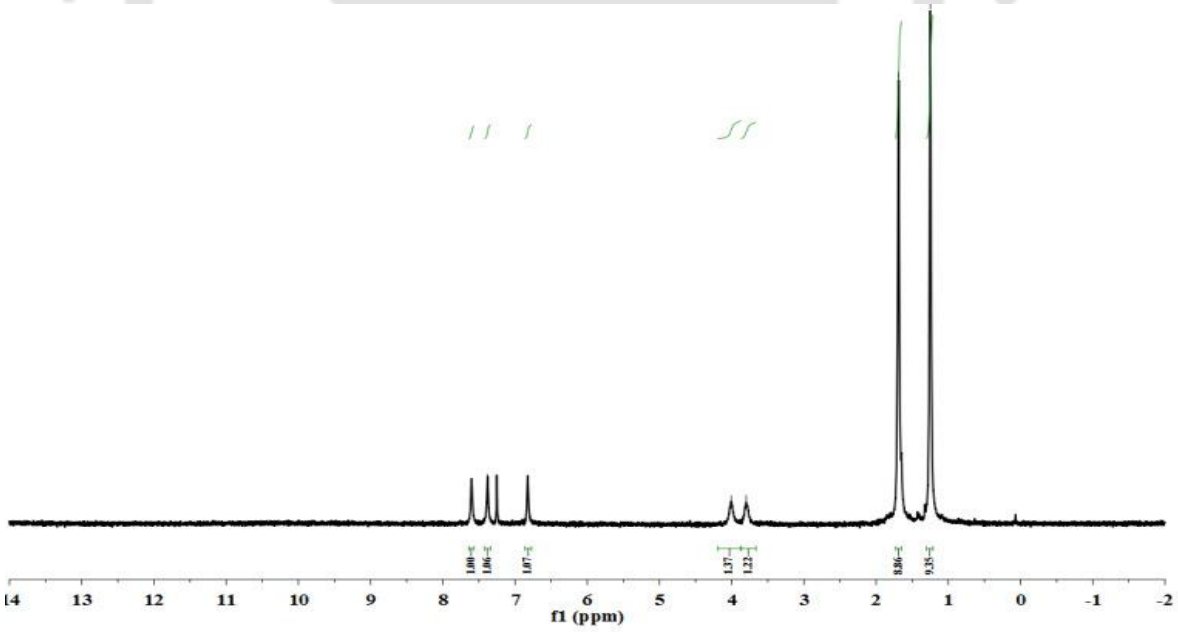

Figure A1.21. ^{1}H-NMR spectrum of ligand complex **2.4** in $CDCl_3$

Appendix II

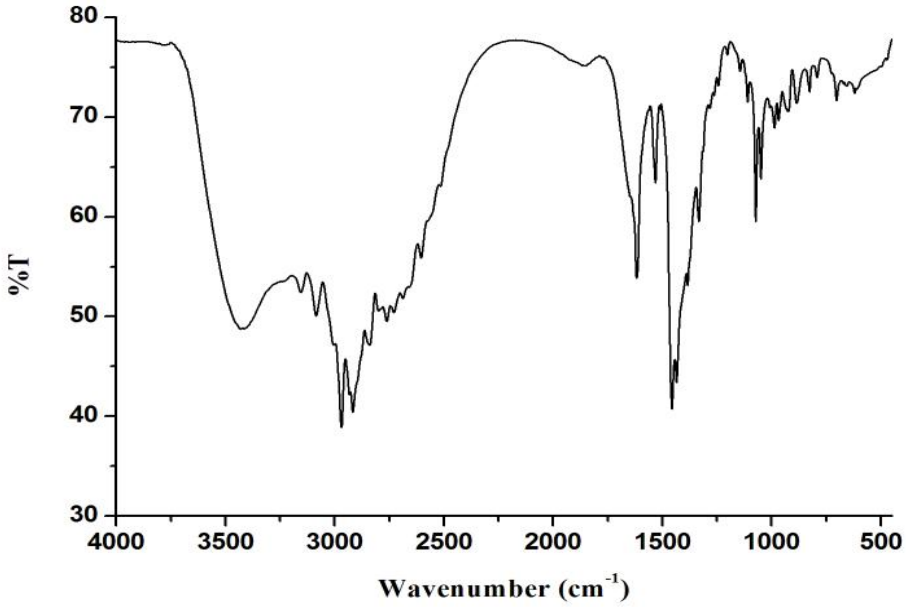

Figure A2.1. FT-IR spectrum of **L3** in KBr.

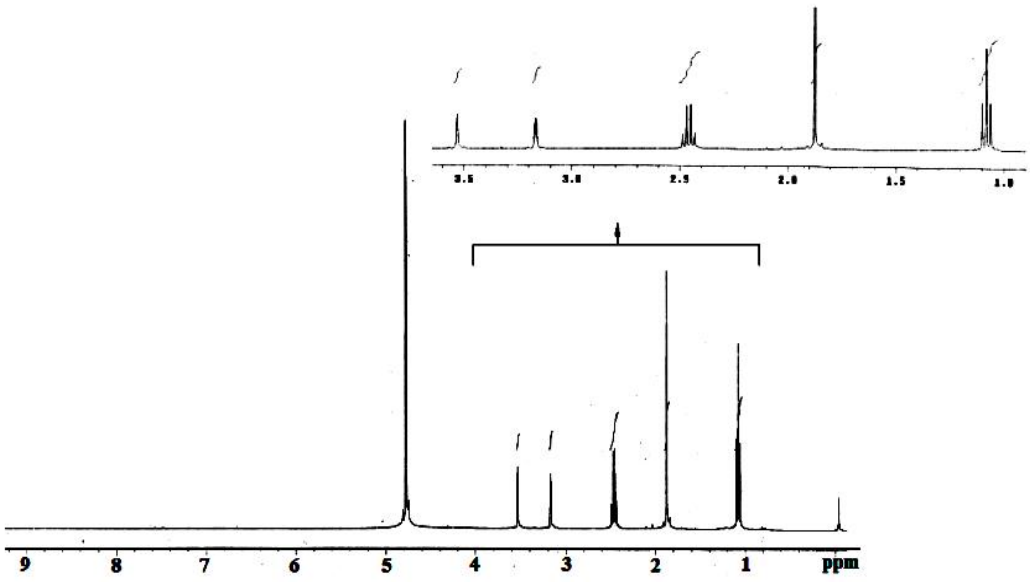

Figure A2.2. ^{1}H-NMR spectrum of **L3** in CD_3OD.

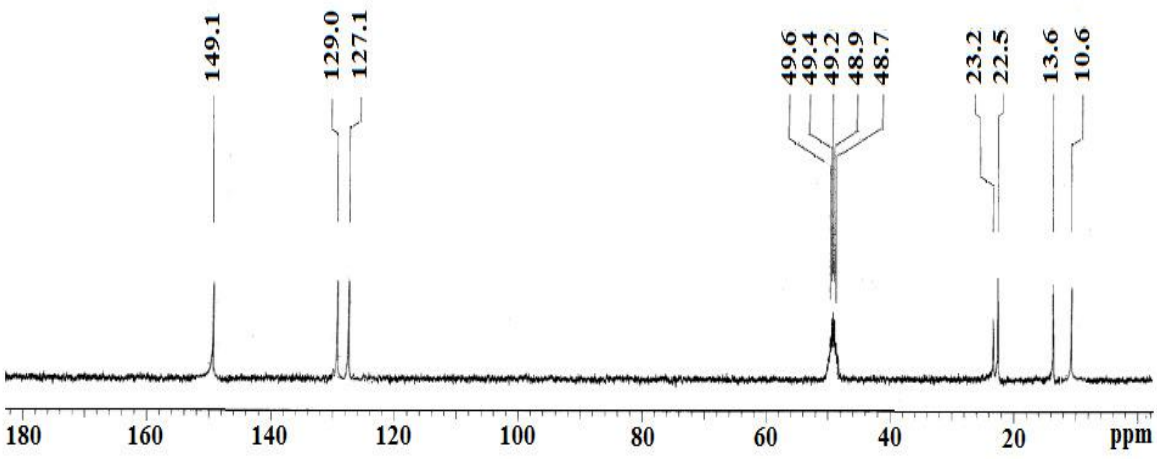

Figure A2.3. ^{13}C-NMR spectrum of **L3** in CD_3OD.

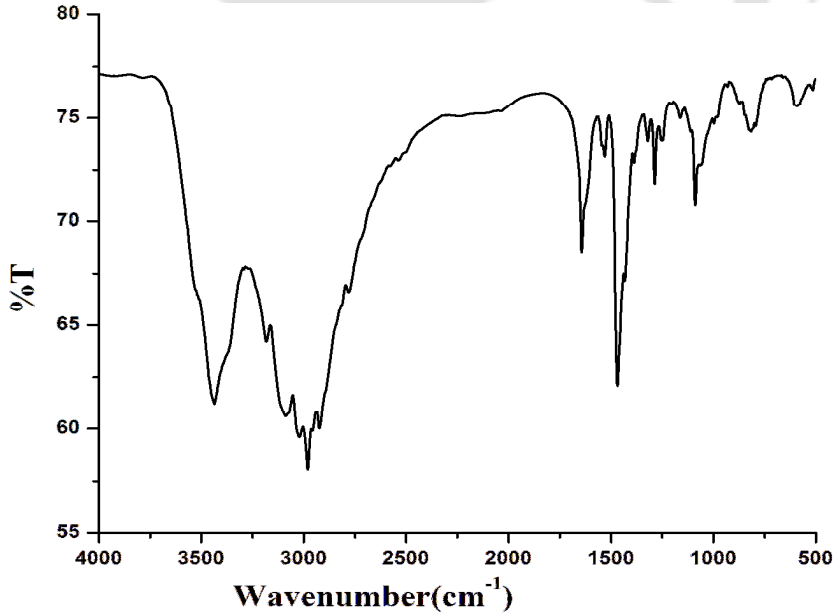

Figure A2.4. FT-IR spectrum of complex **3.1** in KBr.

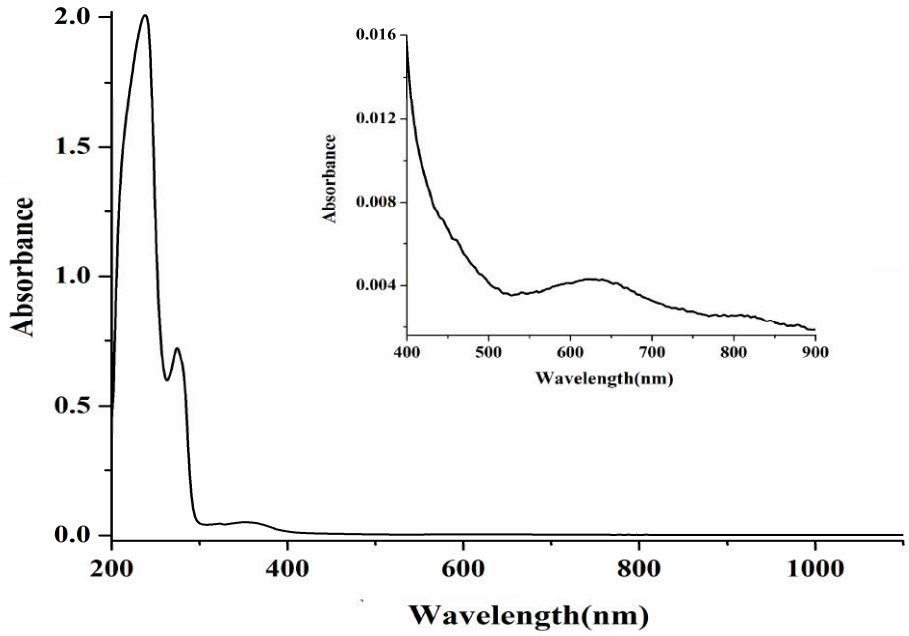

Figure A2.5. UV-visible Spectrum of complex **3.1** in dry methanol.

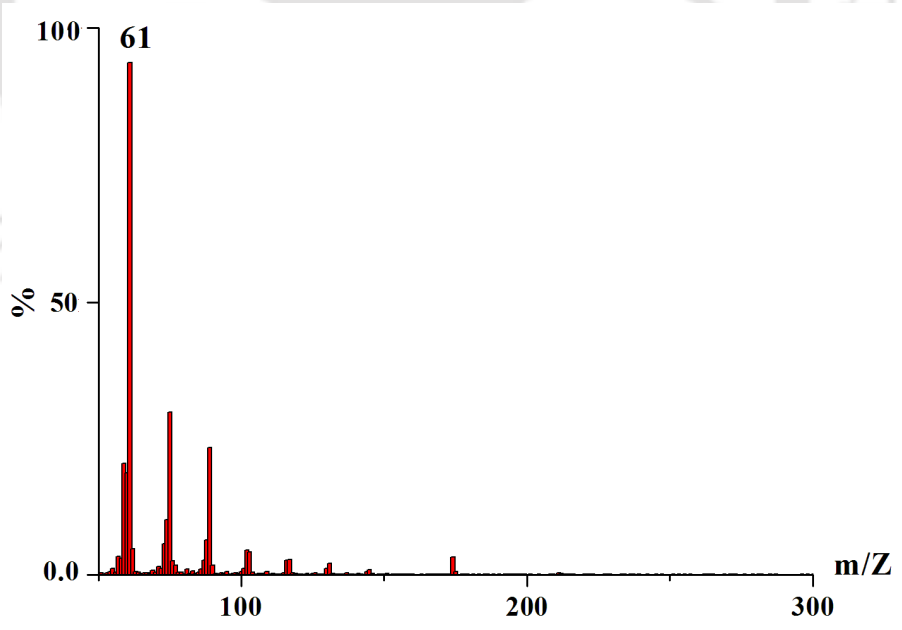

Figure A2.6. GC-mass spectra of methyl nitrite.

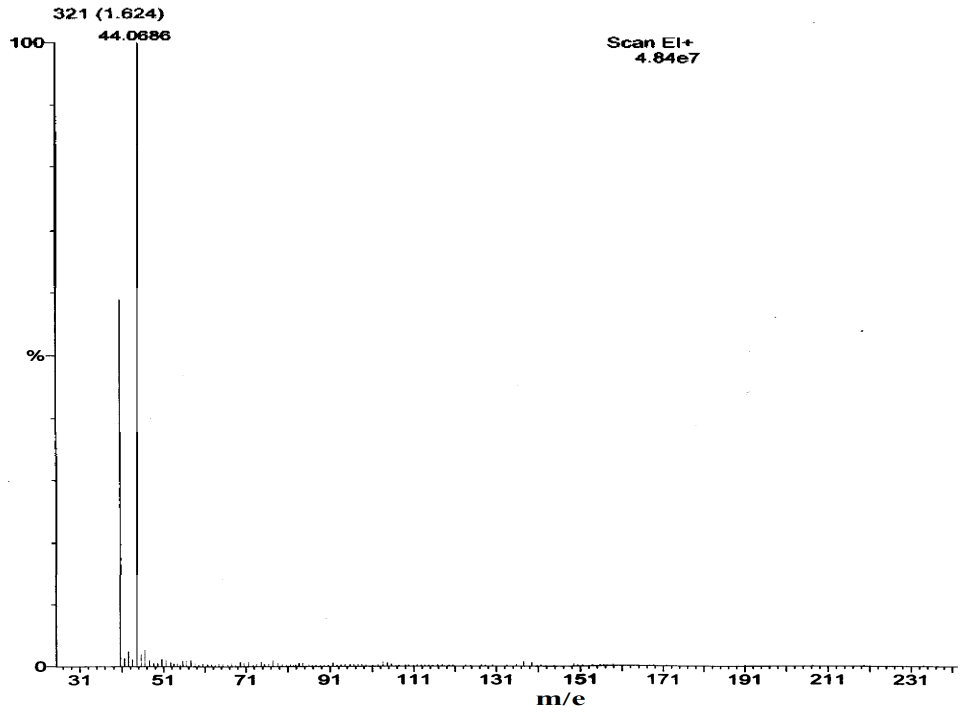

Figure A2.7. GC-mass spectra of N_2O, gas taken from the head space of the reaction mixture.

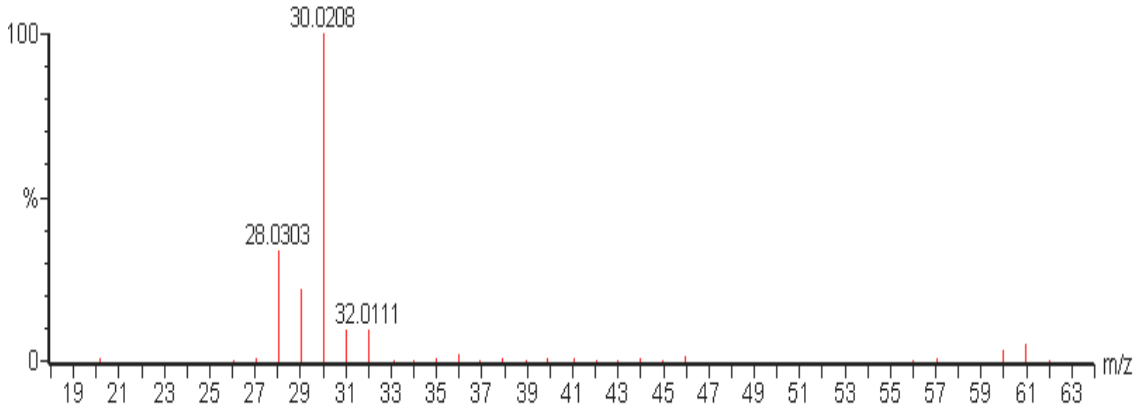

Figure A2.8. GC-mass spectrum of the head space gas taken from the round bottom flask containing dry MeOH and $NO_{(g)}$ purged into it (This suggests that N_2O does not form in the absence of the metal complex).

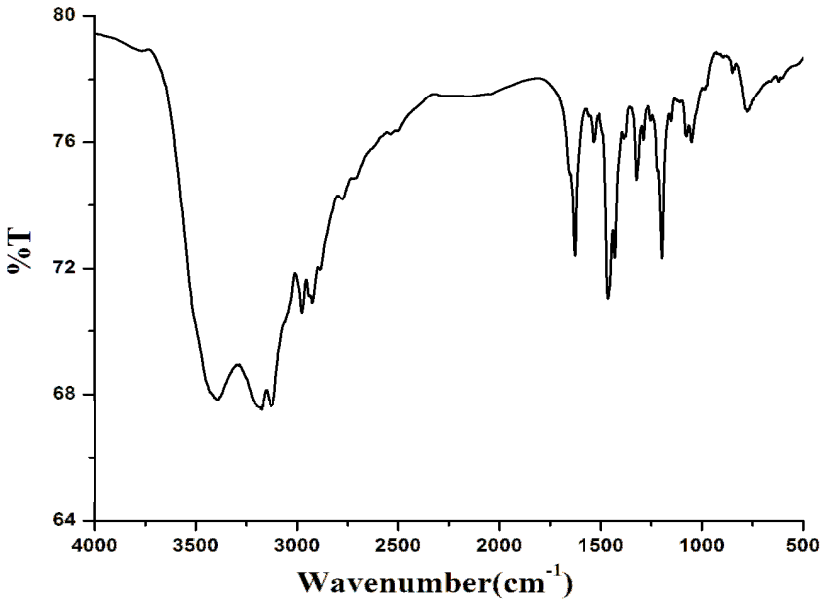

Figure A2.9. FT-IR spectrum of complex **3.2** in KBr.

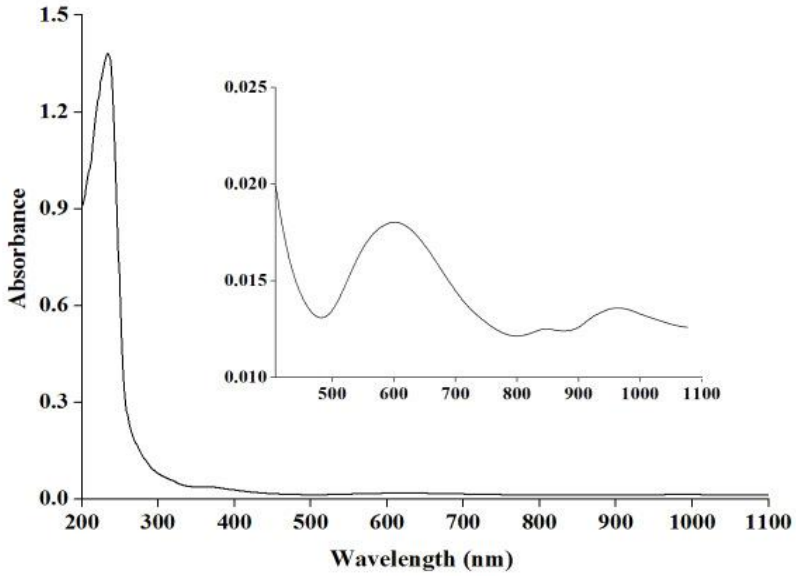

Figure A2.10. UV-visible spectrum of complex **3.2** in dry methanol.

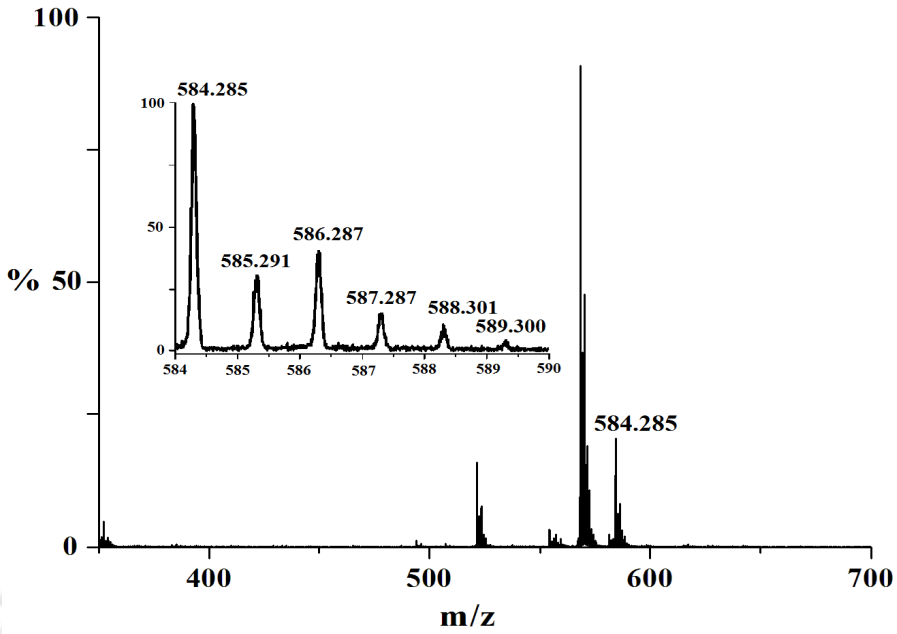

Figure A2.11. ESI-mass spectrum of $[(L3)_2Ni(I)\text{-}NO(CH_3OH)]^+$ in methanol (isotopic distribution pattern is shown inset).

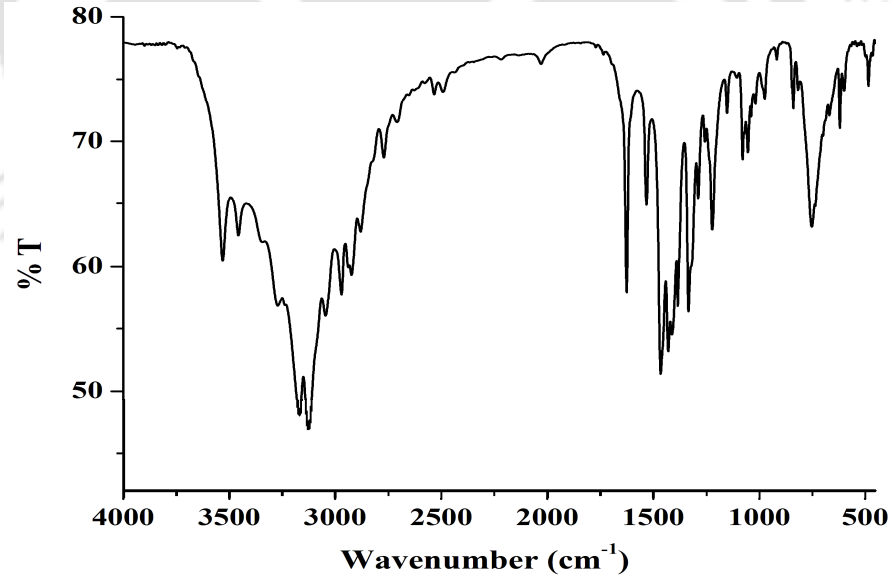

Figure A2.12. FT-IR spectrum of complex **3.3** in KBr.

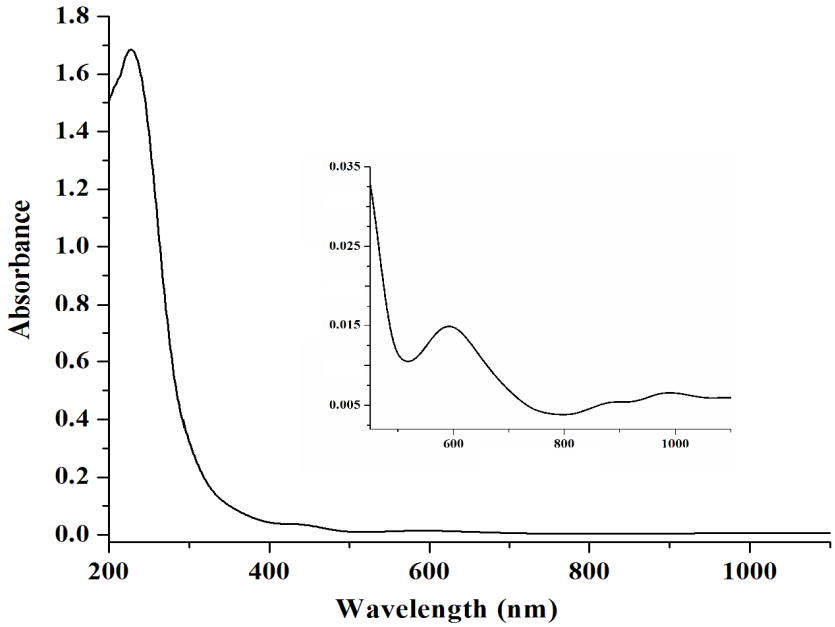

Figure A2.13. UV-visible Spectrum of complex **3.3** in dry methanol.

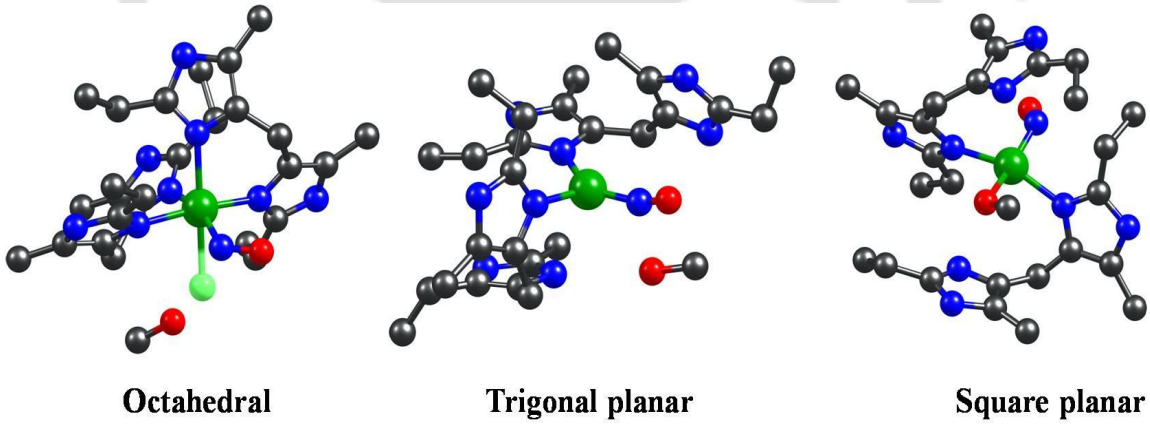

Figure A2.14. The possible structures corresponding to the proposed intermediate; the color scheme is as follows: nickel: green, chlorine: light green, carbon: black, oxygen: red, nitrogen: blue and hydrogen: white; the hydrogens have been removed for the purpose of clarity.

Table A2.1

Cartesian coordinates for DFT optimized structure

C -1.827 13.900 4.460	C -1.552 11.407 0.081	H 0.346 7.981 0.944
C -2.206 12.606 4.180	C 1.236 10.468 -2.105	H 1.790 8.652 0.163
N -1.310 12.035 3.286	C 0.952 8.898 0.830	H 3.919 8.816 0.922
C -0.390 12.963 3.013	C 1.479 9.329 2.166	H 4.641 8.377 2.488
N -0.680 14.099 3.711	N 0.609 9.754 3.162	H 4.726 10.059 1.910
C -3.343 11.808 4.738	C 1.356 10.151 4.191	H 1.335 11.748 5.588
C -2.848 10.537 5.349	N 2.674 9.969 3.885	H -0.195 10.887 5.394
N -2.142 9.630 4.575	C 2.780 9.457 2.601	H 0.785 8.893 6.628
C -1.820 8.600 5.359	C -2.783 12.190 0.375	H 0.857 10.372 7.620
N -2.303 8.834 6.612	C -2.567 13.711 0.365	H 2.325 9.769 6.813
C -2.958 10.055 6.634	C 0.887 10.745 5.476	H -4.428 9.947 8.202
Ni -1.455 9.999 2.697	C 1.236 9.892 6.706	H -4.049 11.588 7.625
N -2.367 8.556 2.150	C 4.085 9.163 1.951	H -2.900 10.727 8.678
O -2.245 7.988 1.087	O -4.808 7.733 3.269	H -4.060 11.563 3.931
C -3.616 10.604 7.850	C -5.158 8.202 4.574	H -3.887 12.402 5.486
C -1.089 7.366 4.959	H -1.844 14.005 1.139	H -3.297 14.546 5.858
C 0.775 12.863 2.089	H -3.517 14.228 0.564	H -2.708 15.839 4.785
C 2.077 13.405 2.696	H -2.191 14.055 -0.610	H -1.685 15.259 6.123
C -2.406 14.942 5.351	H -3.130 11.856 1.363	H 0.895 11.812 1.813
N -0.998 10.481 0.863	H -3.563 11.923 -0.358	H 0.546 13.411 1.157
C 0.105 9.961 0.199	H 0.765 10.161 -3.052	H 1.997 14.473 2.952
C 0.236 10.601 -1.012	H 1.982 9.708 -1.835	H 2.902 13.294 1.978
N -0.818 11.501 -1.061	H 1.766 11.418 -2.284	H 2.340 12.851 3.610

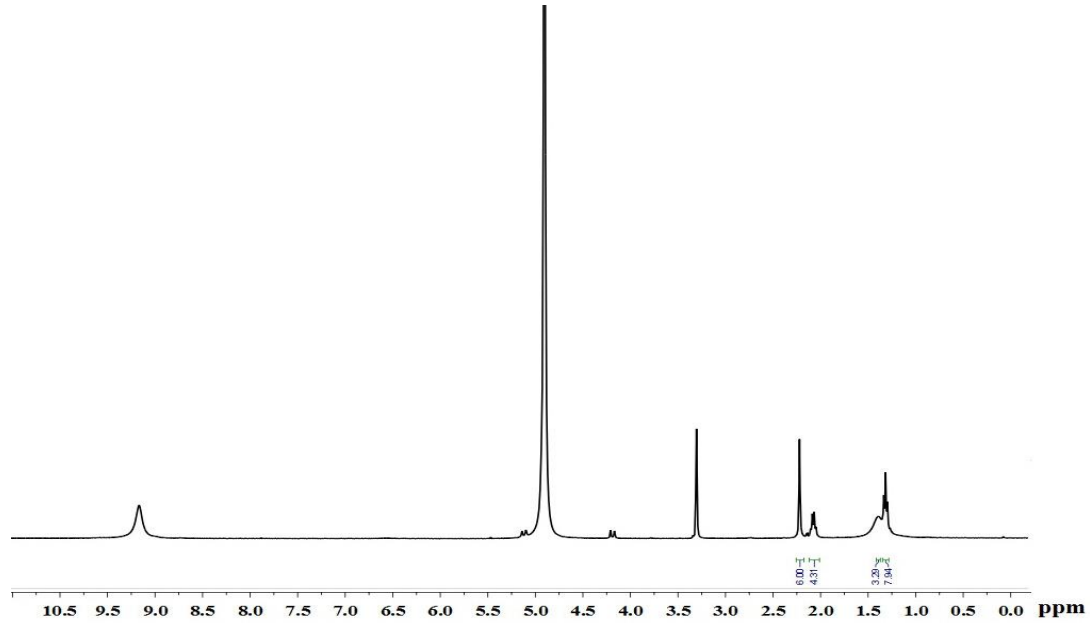

Figure A2.15. ^{1}H-NMR spectrum of complex **3.1** in CD_3OD.

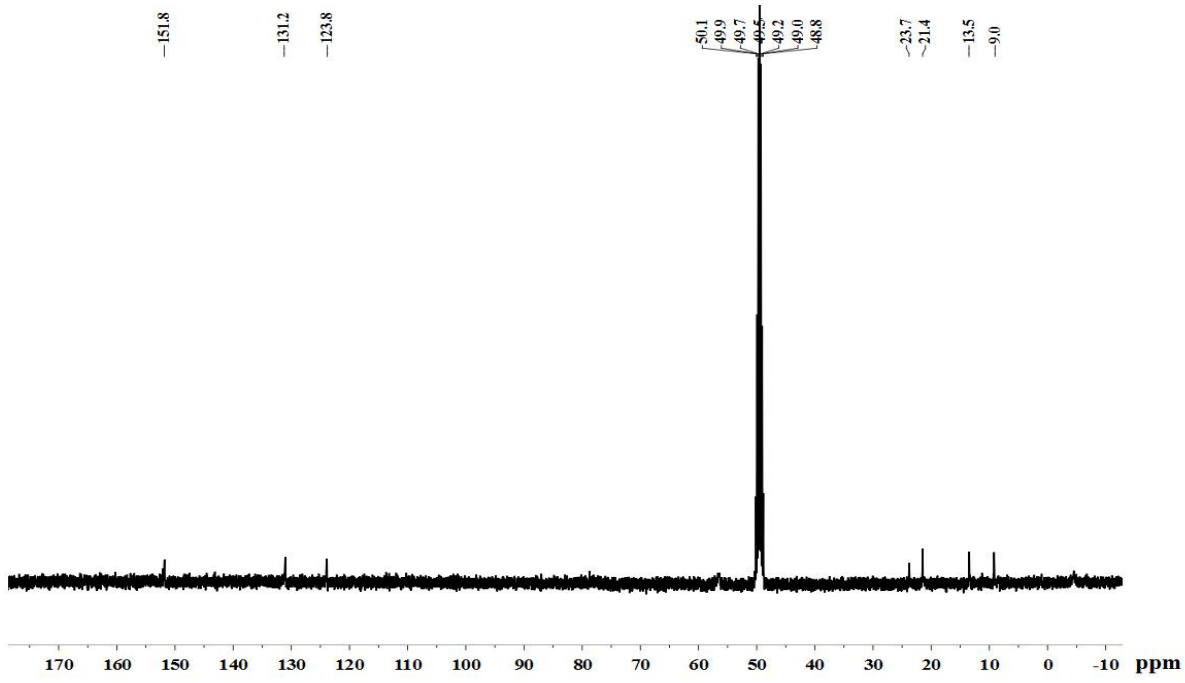

Figure A2.16. ^{13}C-NMR spectrum of complex **3.1** in CD_3OD.

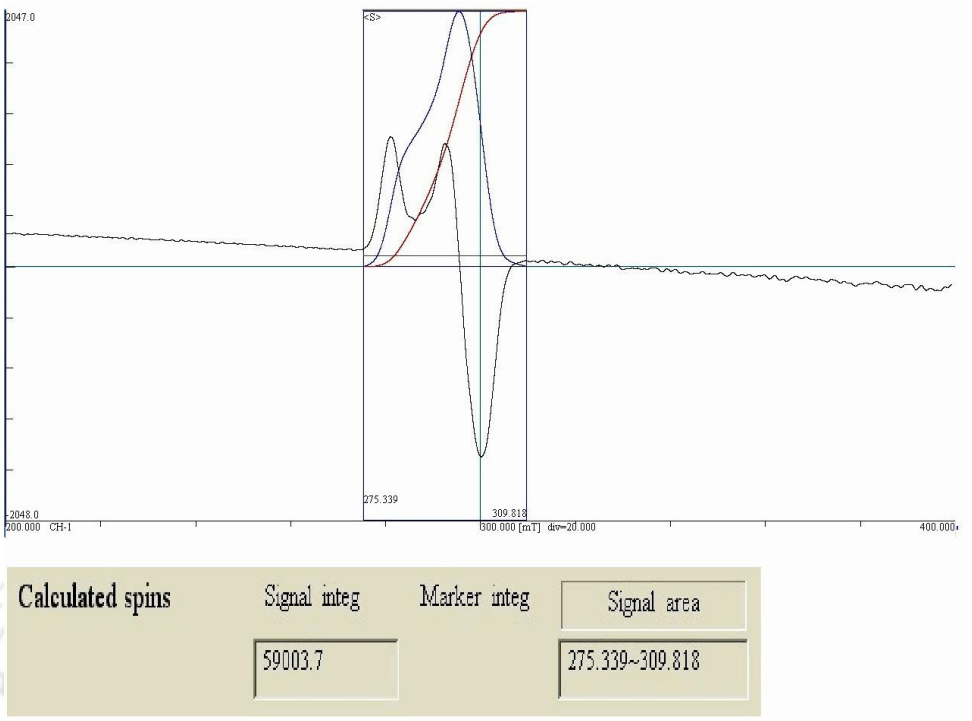

Figure A2.17. Double integration of EPR spectrum of Ni(I) species (concentration, 0.7 mmol) in methanol at 77K.

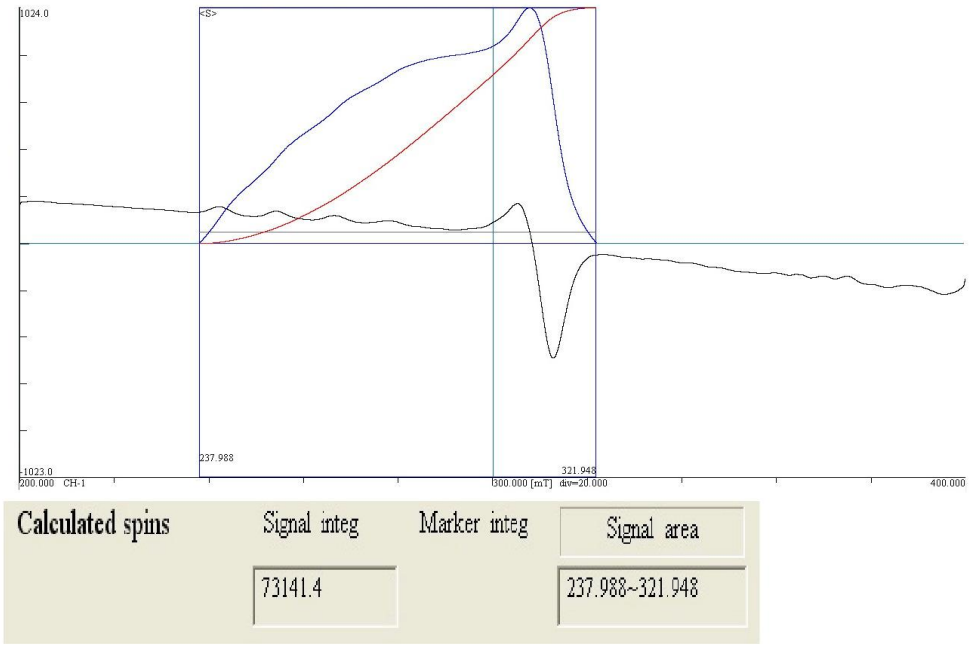

Figure A2.18. Double integration of standard $CuSO_4 \cdot 5H_2O$ (concentration, 0.7 mmol) solution in methanol at 77K.

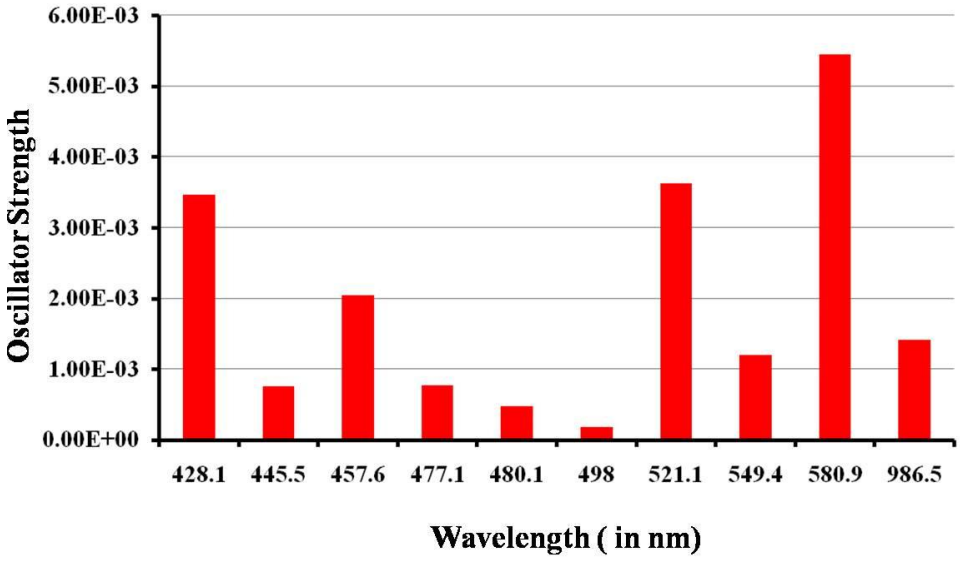

Figure A2.19. Plot of Oscillator strength *vs* Wavelength for intermediate $\{NiNO\}^{10}$ complex in methanol (ten excitations has been considered) using TD-DFT calculations at PBE/TZVP level of theory.

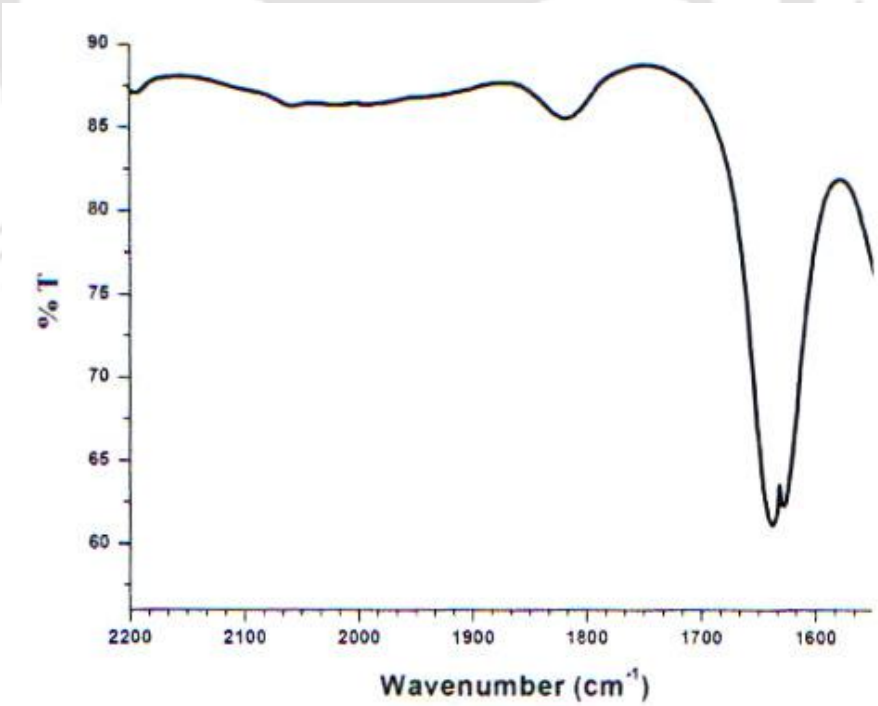

Figure A2.20. Solution FT-IR spectrum of $[(L3)_2Ni(NO)(CH_3OH)]^+$ in methanol (with ^{15}NO; only 2200 – 1600 cm^{-1} range is shown for clarity).

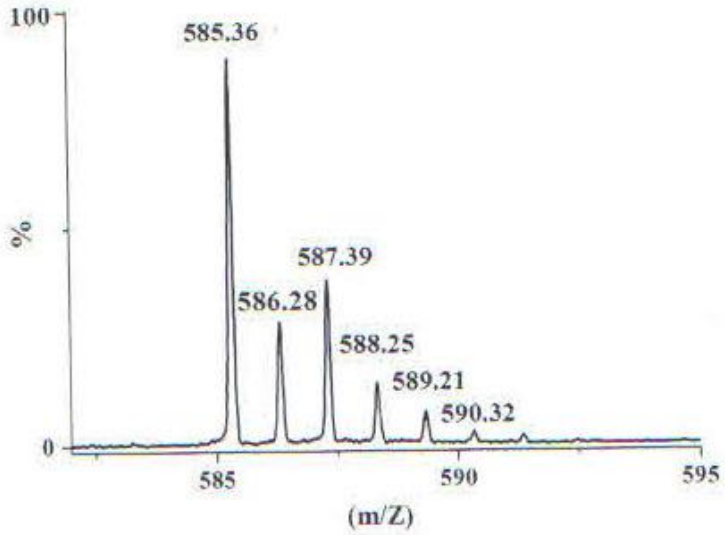

Figure A2.21. ESI-mass spectrum of $[(L3)_2Ni(NO)(CH_3OH)]^+$ in methanol (with ^{15}NO)

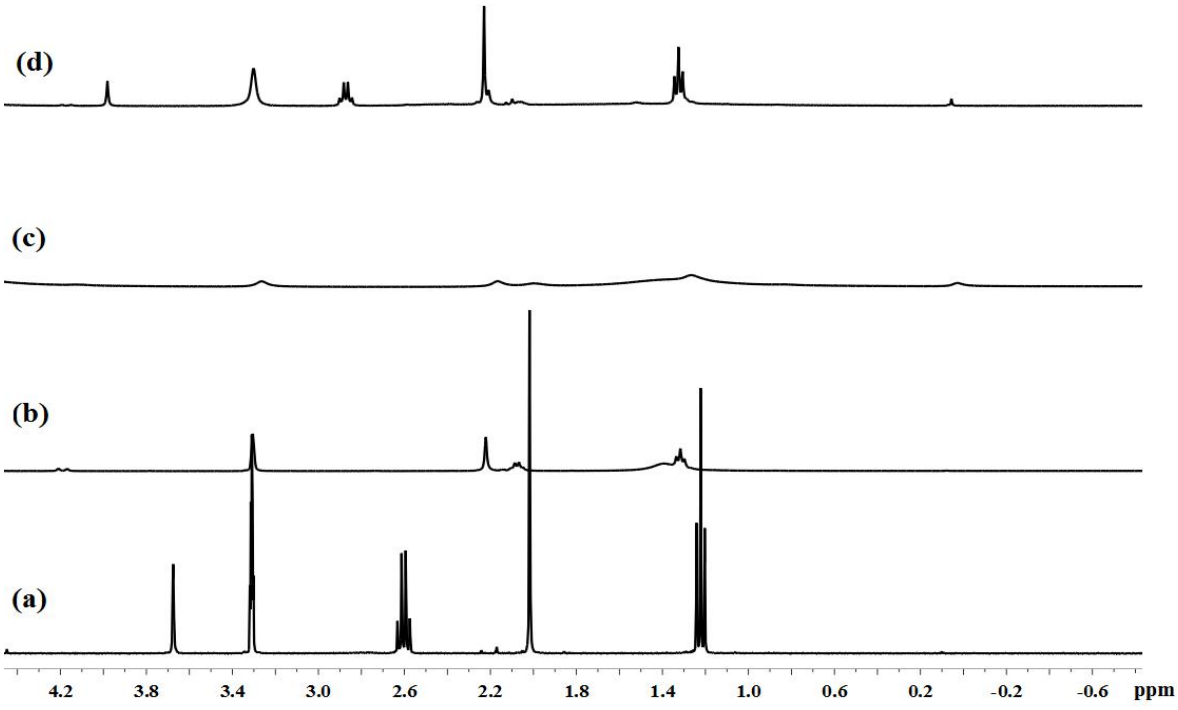

Figure A2.22. ^{1}H-NMR spectra of ligand, complex **3.1**, after purging 1 equivalent of NO in complex **3.1** and after purging 2 equivalent of NO in complex **3.1** are respectively (a), (b), (c) and (d) in CD_3OD.

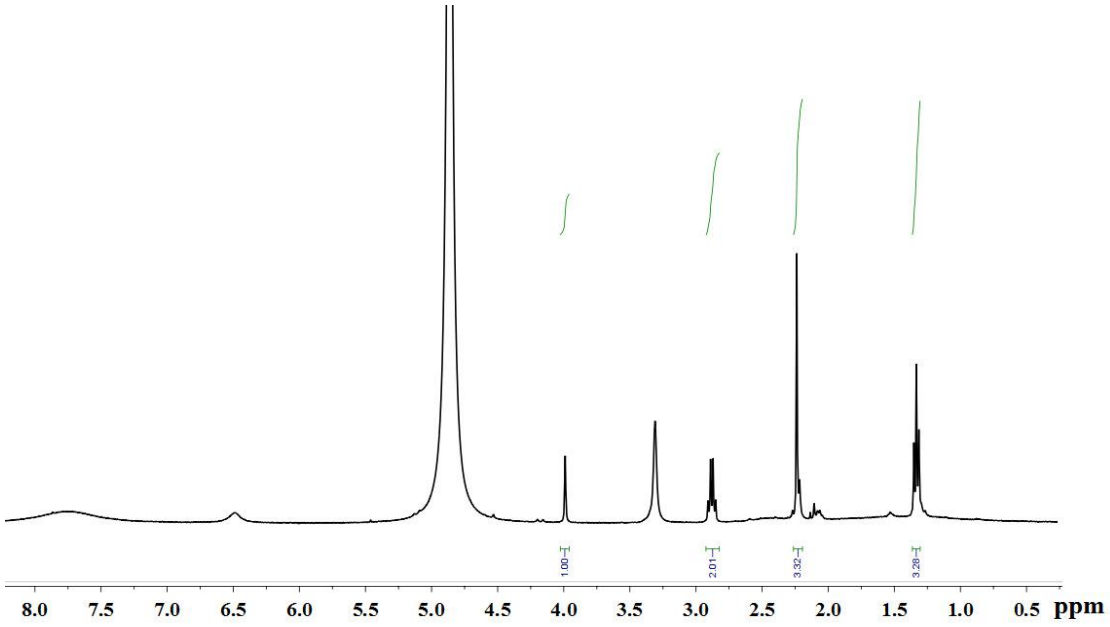

Figure A2.23. ^{1}H-NMR spectrum of complex **3.1** after purging 2 equivalent of NO, in CD_3OD.

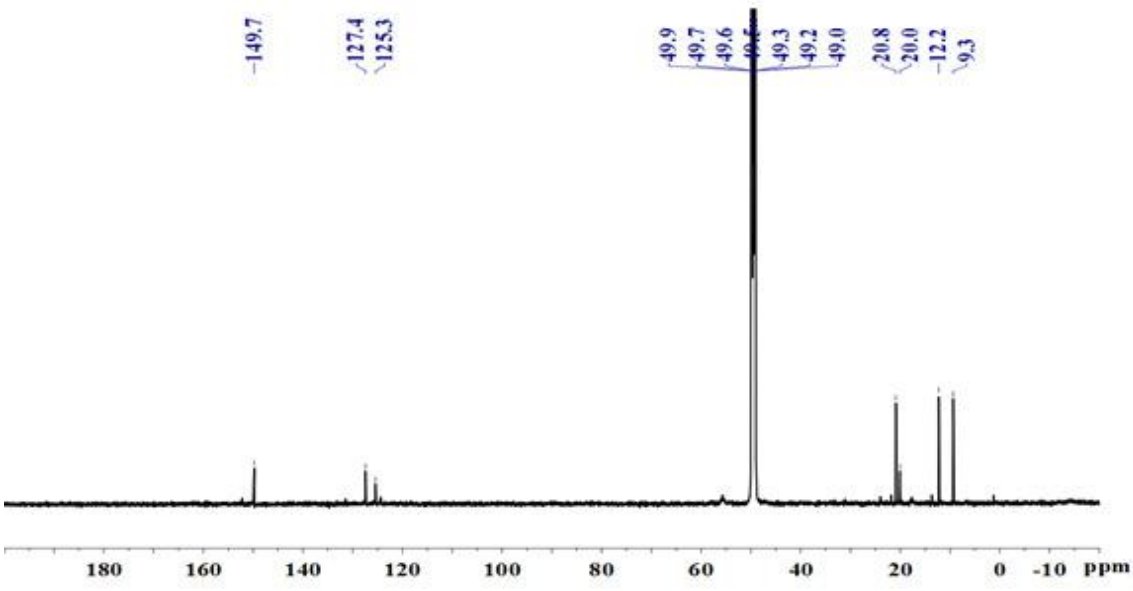

Figure A2.24. ^{13}C-NMR spectrum of complex **3.1** after purging 2 equivalent of NO, in CD_3OD.

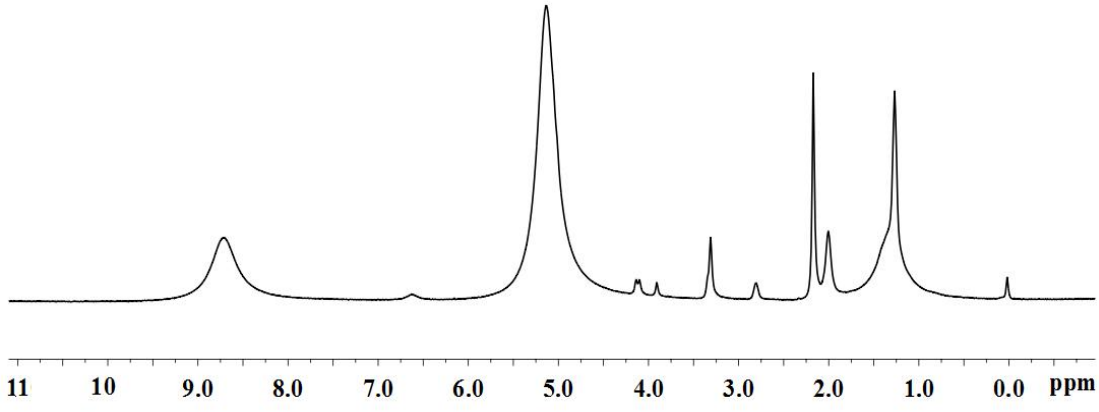

Figure A2.25. ^{1}H-NMR spectra of complex **3.2** in CD_3OD.

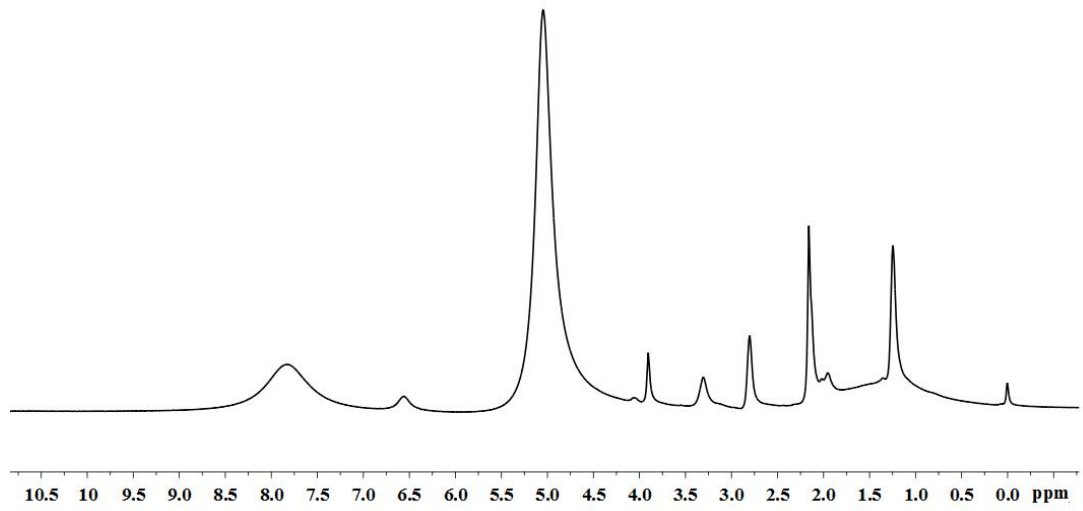

Figure A2.26. ^{1}H-NMR spectra of complex **3.3** in CD_3OD.

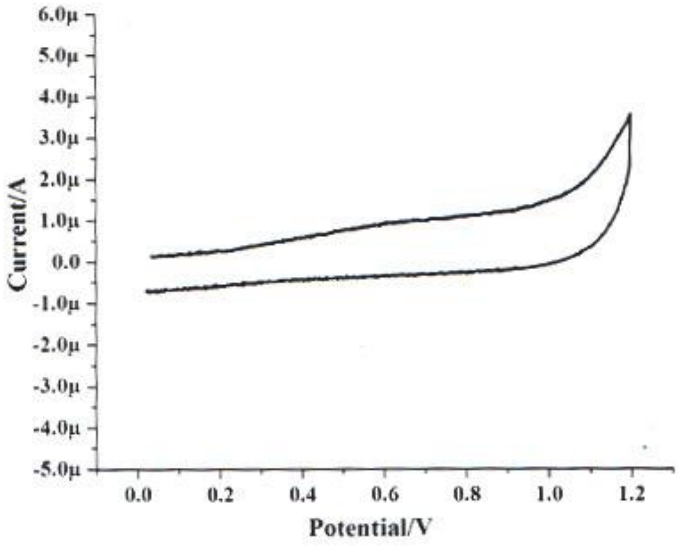

Figure A2.27. Cyclic voltammogram of complex **3.1** in methanol solvent. Working electrode, Glassy-carbon; Reference electrode, Ag/AgCl; TBAP supporting electrolyte; scan rate 50 mV/s.

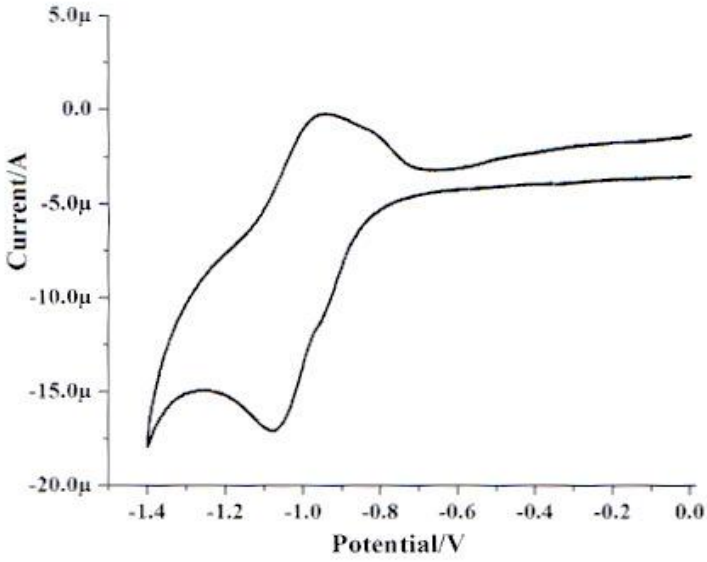

Figure A2.28. Cyclic voltammogram of complex **3.1** in methanol solvent. Working electrode, Glassy-carbon; Reference electrode, Ag/AgCl; TBAP supporting electrolyte; scan rate 50 mV/s.

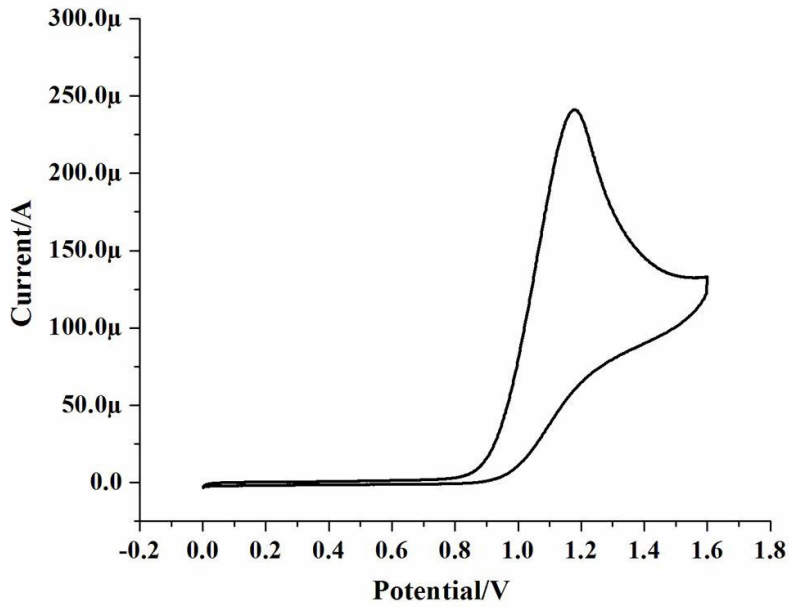

Figure A2.29. Cyclic voltammogram of NO in methanol solvent; Working electrode, Glassycarbon; Reference electrode, Ag/AgCl; TBAP supporting electrolyte; scan rate 50 mV/s.

Appendix III

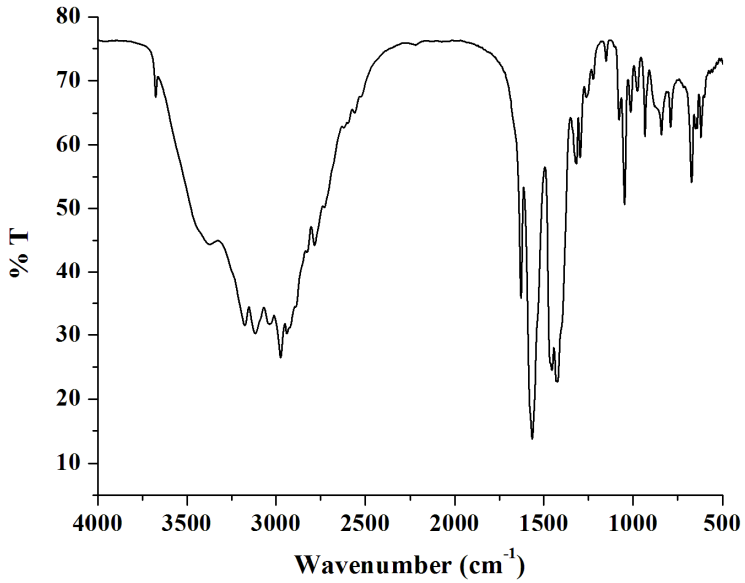

Figure A3.1. FT-IR spectrum of complex **4.1** in KBr.

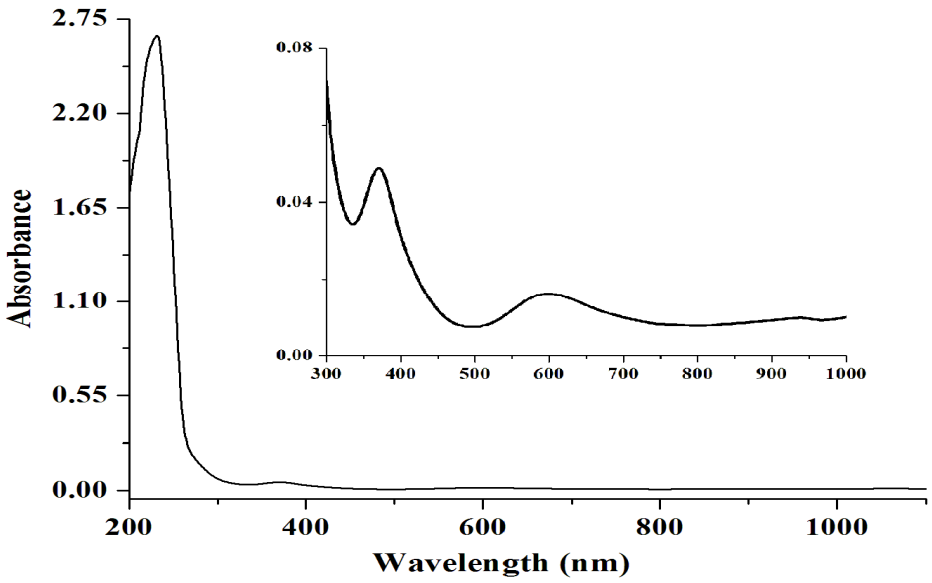

Figure A3.2. UV-visible spectrum of complex **4.1** in dry methanol.

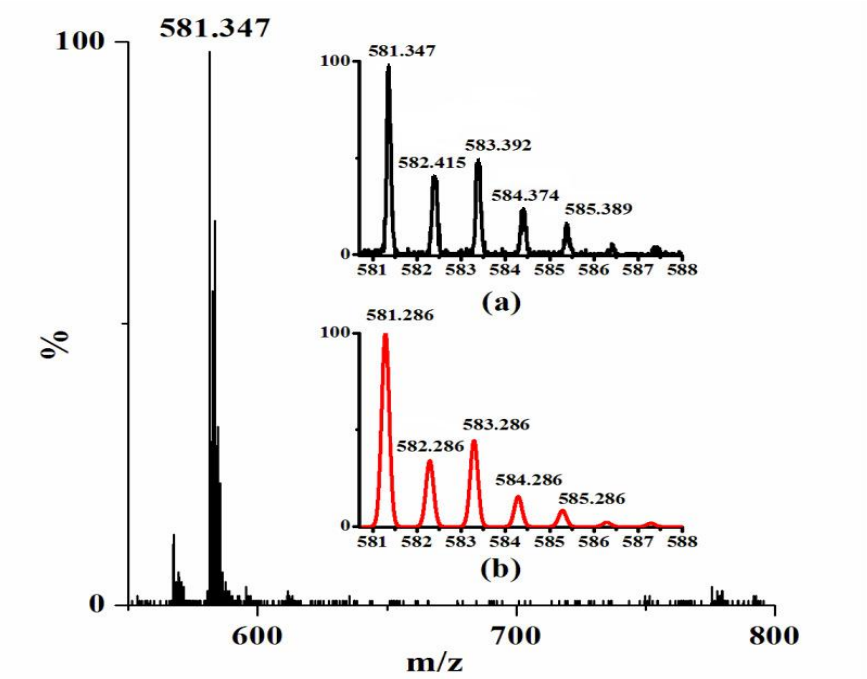

Figure A3.3. ESI- mass spectrum of complex **4.1** ($[(L3)_2Ni(OAc)]^+$) with isotopic distribution (a) experimental, (b) simulated in methanol.

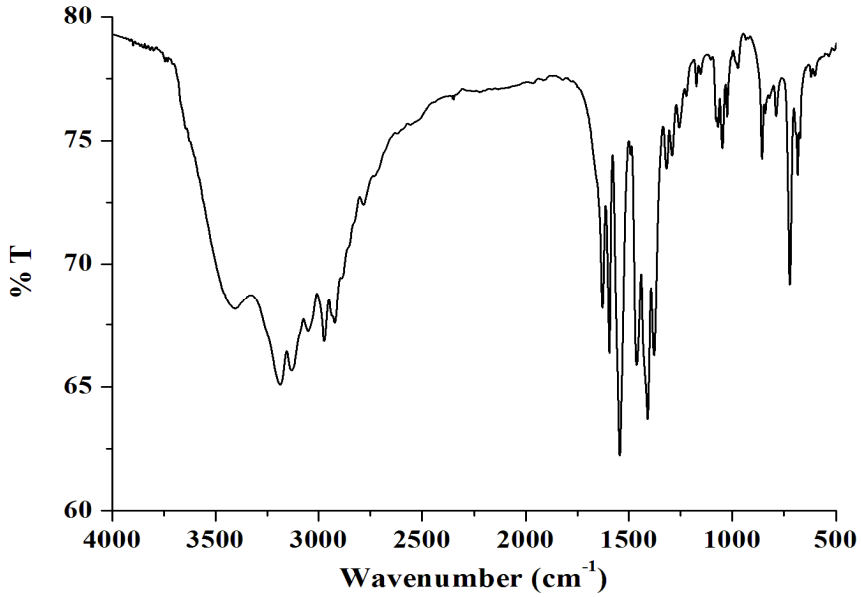

Figure A3.4. FT-IR spectrum of complex **4.2** in KBr.

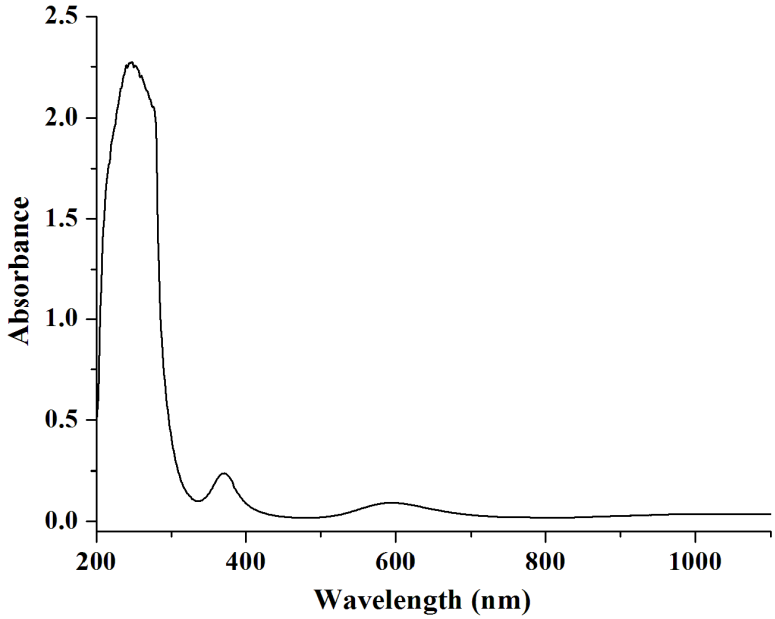

Figure A3.5. UV-visible spectrum of complex **4.2** in dry methanol.

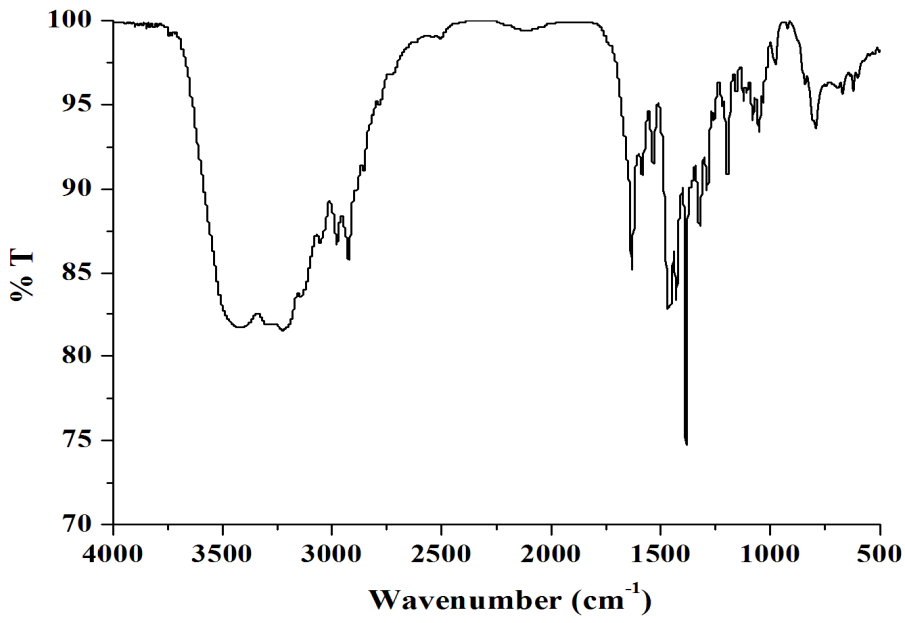

Figure A3.6. FT-IR spectrum of complex **4.3** in KBr.

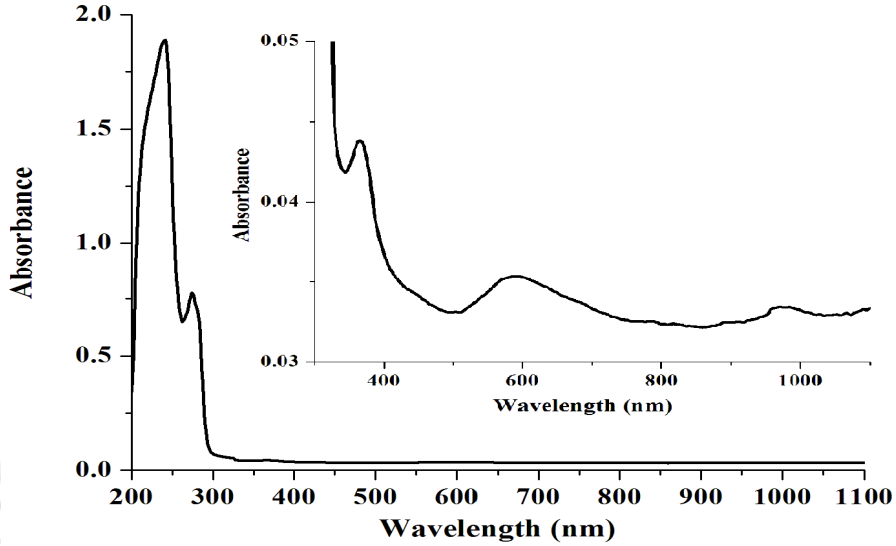

Figure A3.7. UV-visible Spectrum of complex **4.3** in dry methanol.

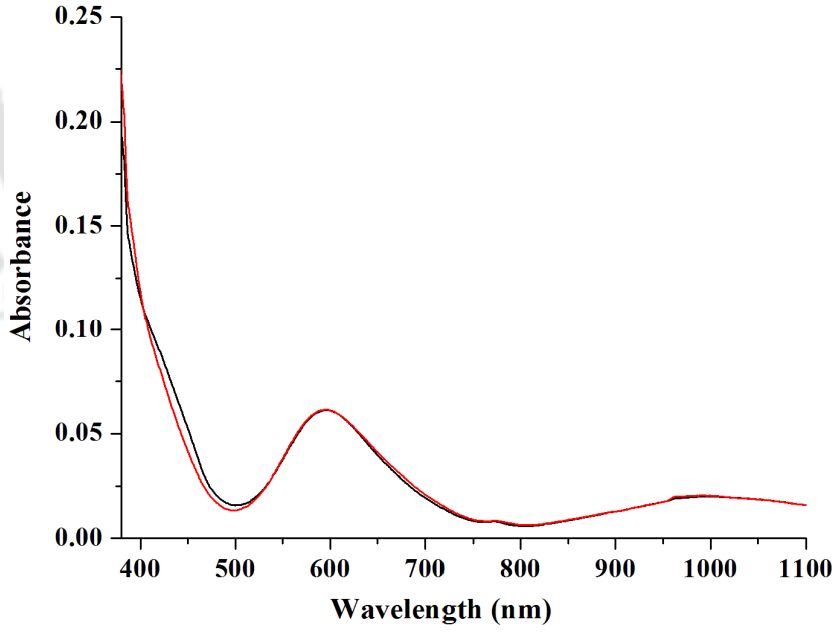

Figure A3.8. UV-visible spectra of complex **4.1**(black), after purging of NO (red) in dry methanol at room temperature.

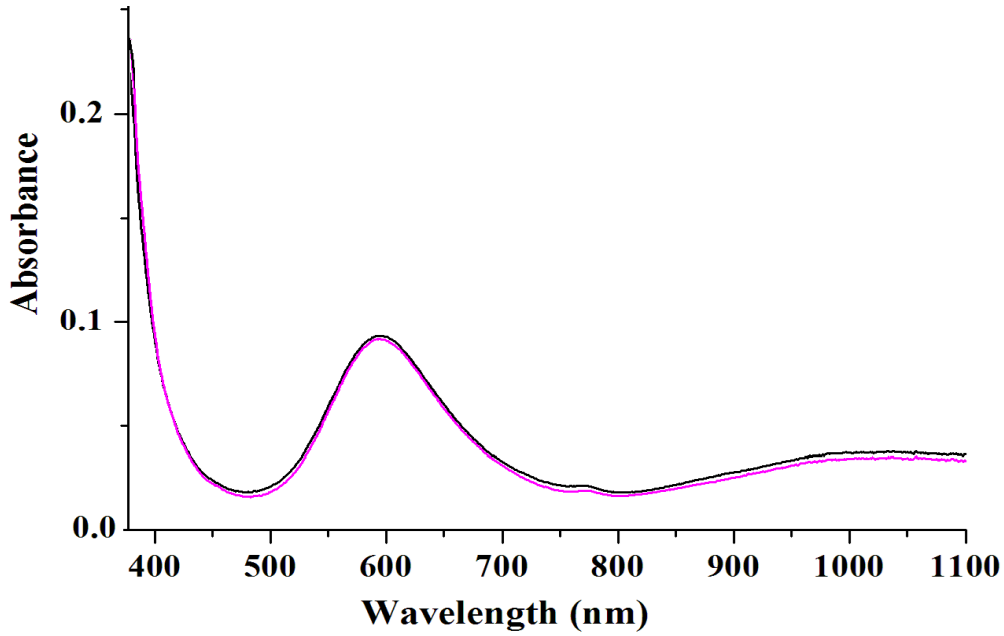

Figure A3.9. UV-visible spectra of complex **4.2**(black), after purging of NO (purple) in dry methanol at room temperature.

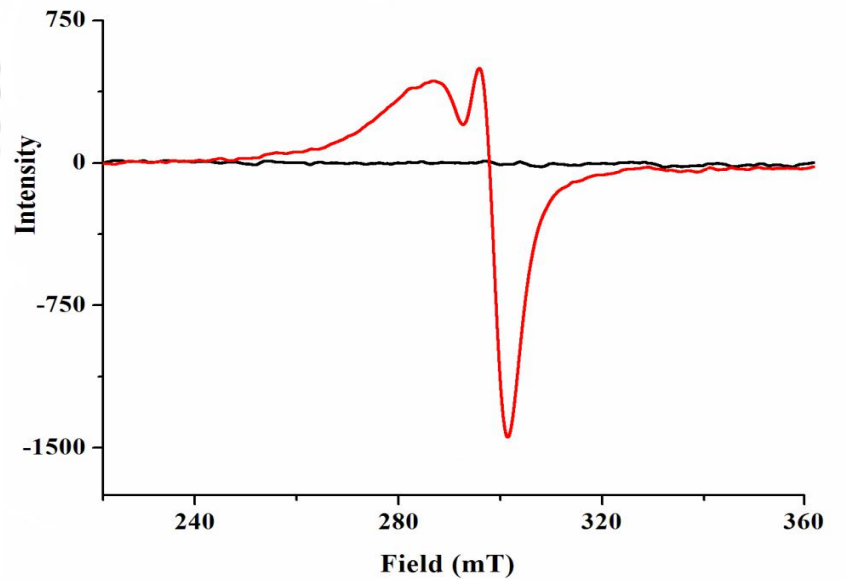

Figure A3.10. X-band EPR spectra of complex **4.1**(black), complex **4.3**(red, ($g_{\parallel}$, 2.168, $g_{\perp}$, 2.269) in dry methanol at room temperature.

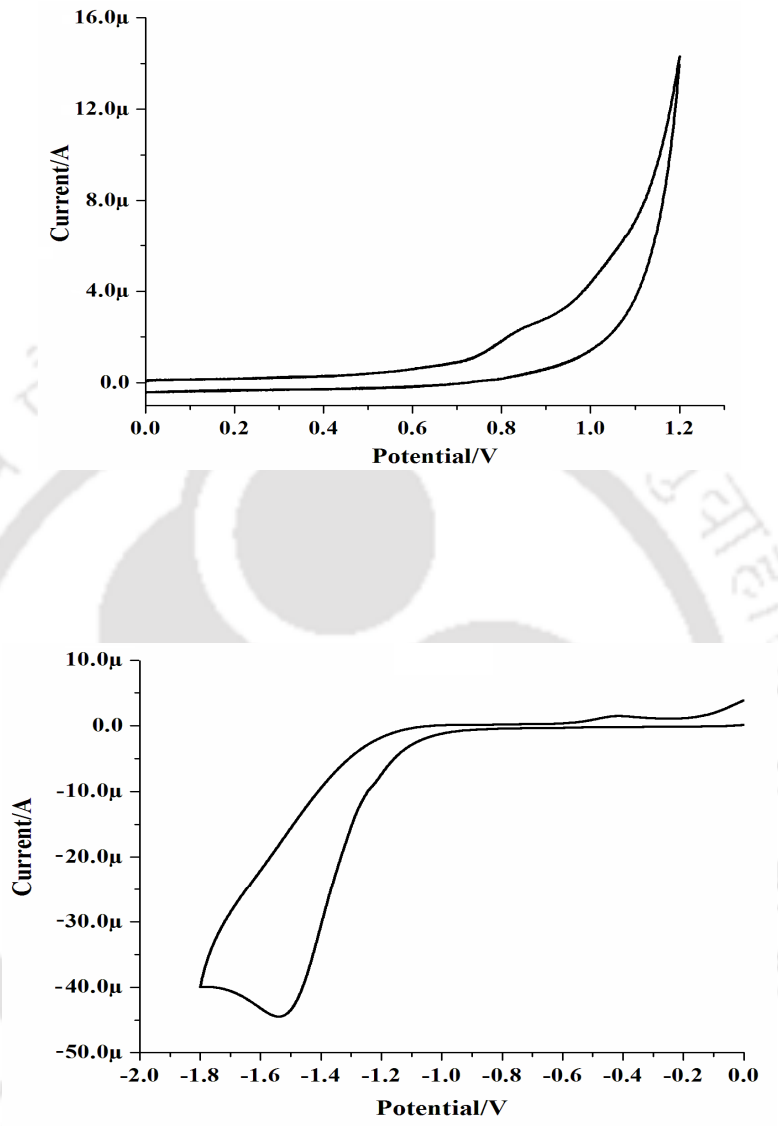

Figure A3.11. Cyclic voltammogram of complex **4.1** in methanol solvent. Working electrode, Glassy-carbon; Reference electrode, Ag/AgCl; TBAP supporting electrolyte; scan rate 50 mV/s.

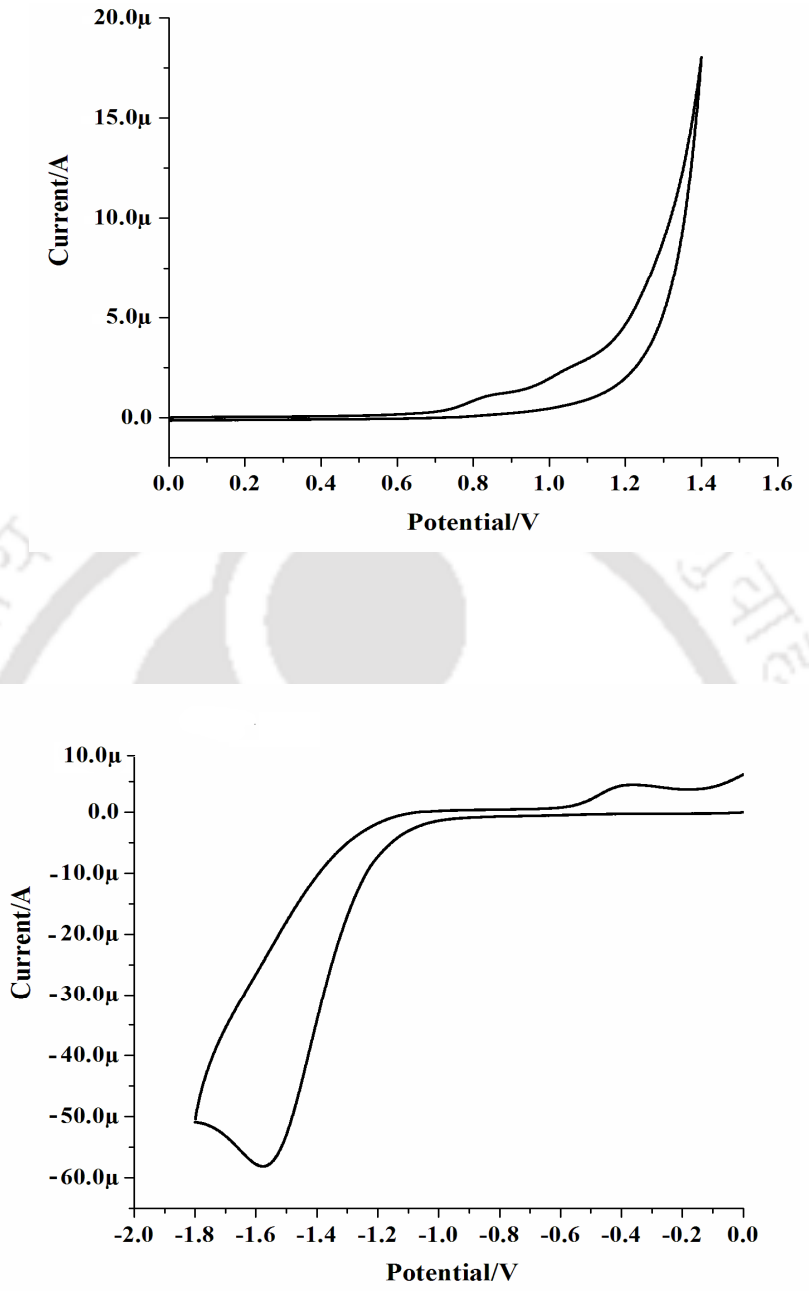

Figure A3.12. Cyclic voltammogram of complex **4.2** in methanol solvent. Working electrode, Glassy-carbon; Reference electrode, Ag/AgCl; TBAP supporting electrolyte; scan rate 50 mV/s.

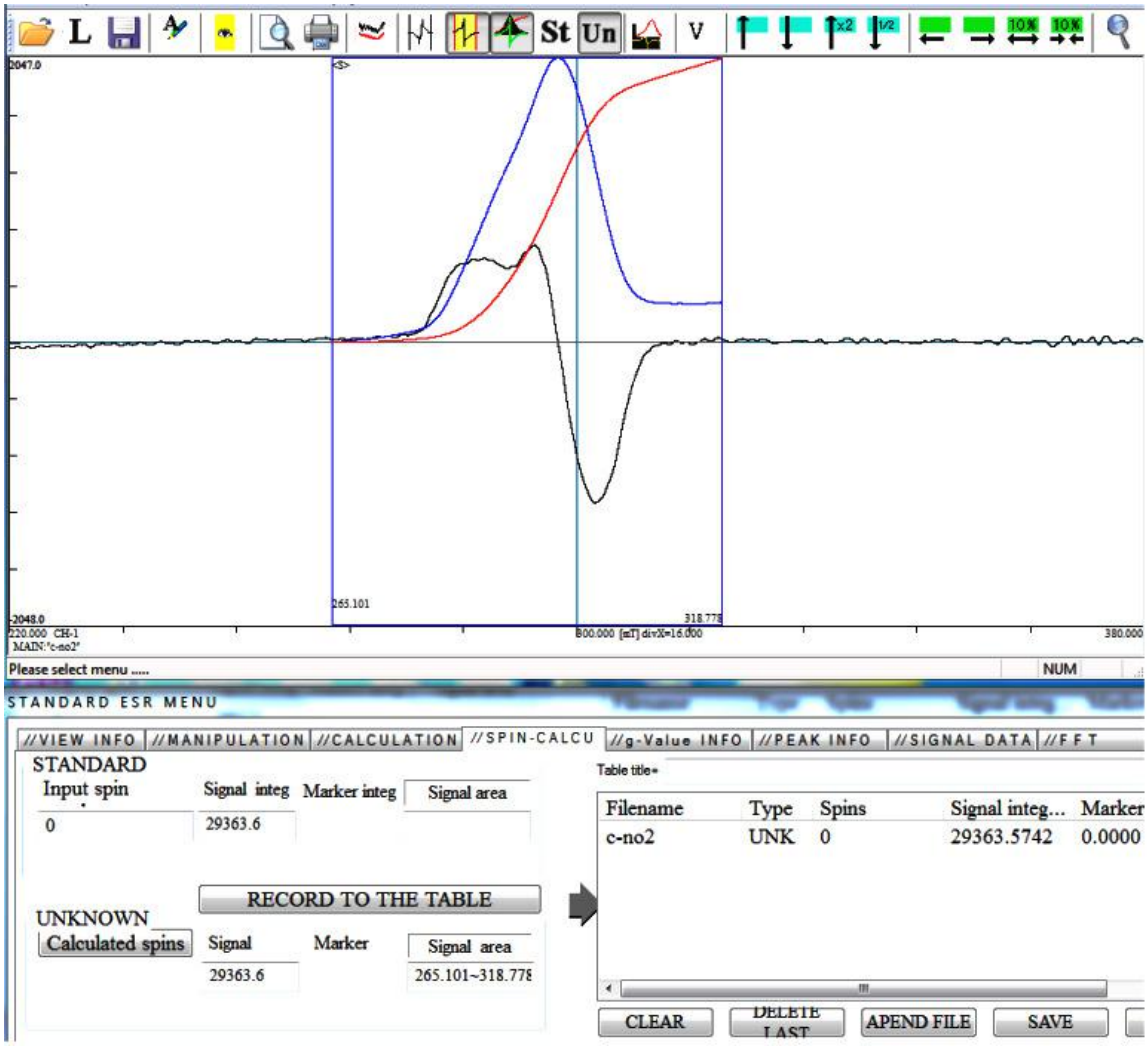

Figure A3.13. Double integration of EPR spectrum of Ni(I) species obtained from complex **4.1** (concentration, 0.3 mmol) in methanol at 77K.

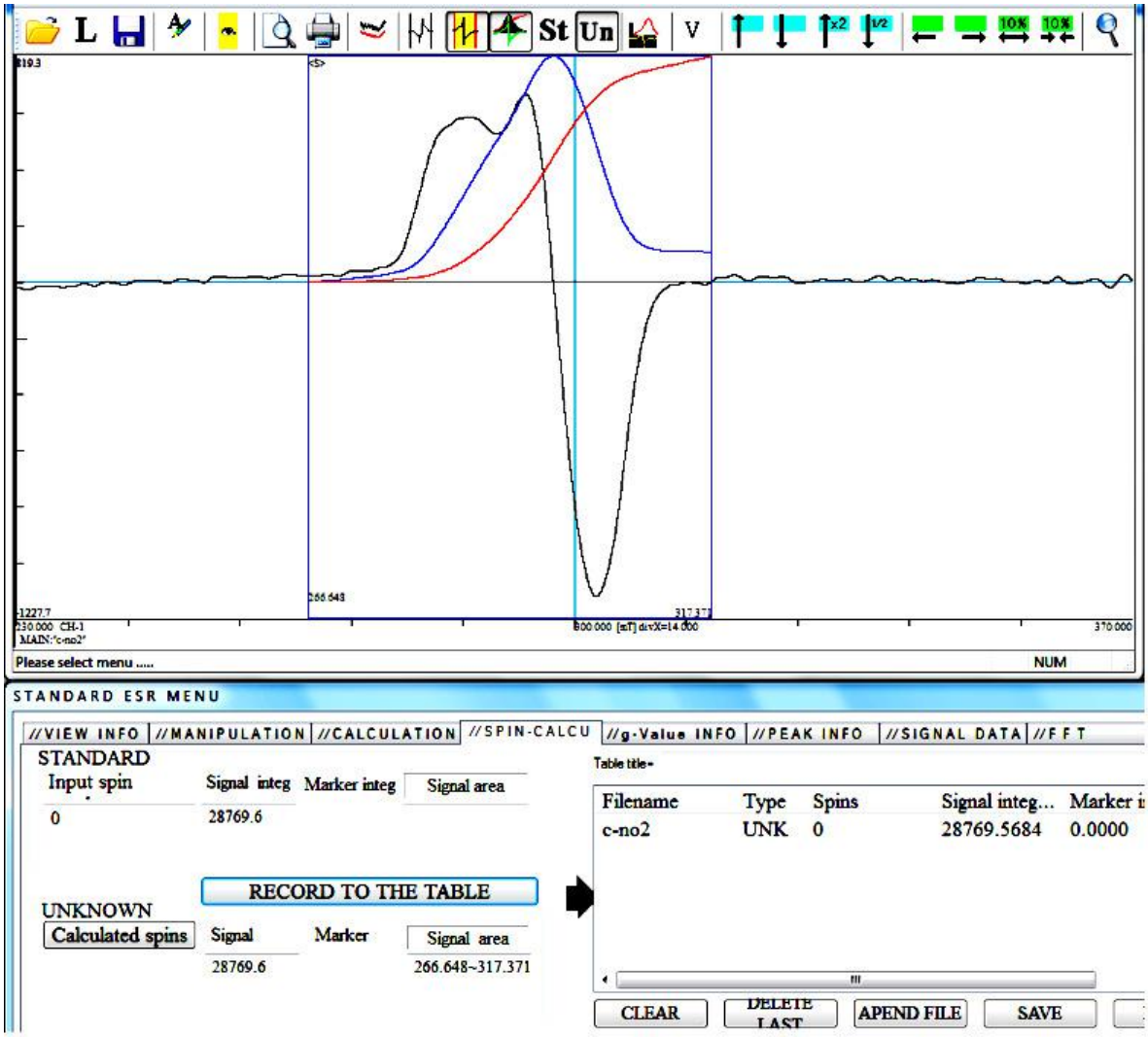

Figure A3.14. Double integration of EPR spectrum of Ni(I) species obtained from complex **4.2** (concentration, 0.3 mmol) in methanol at 77K.

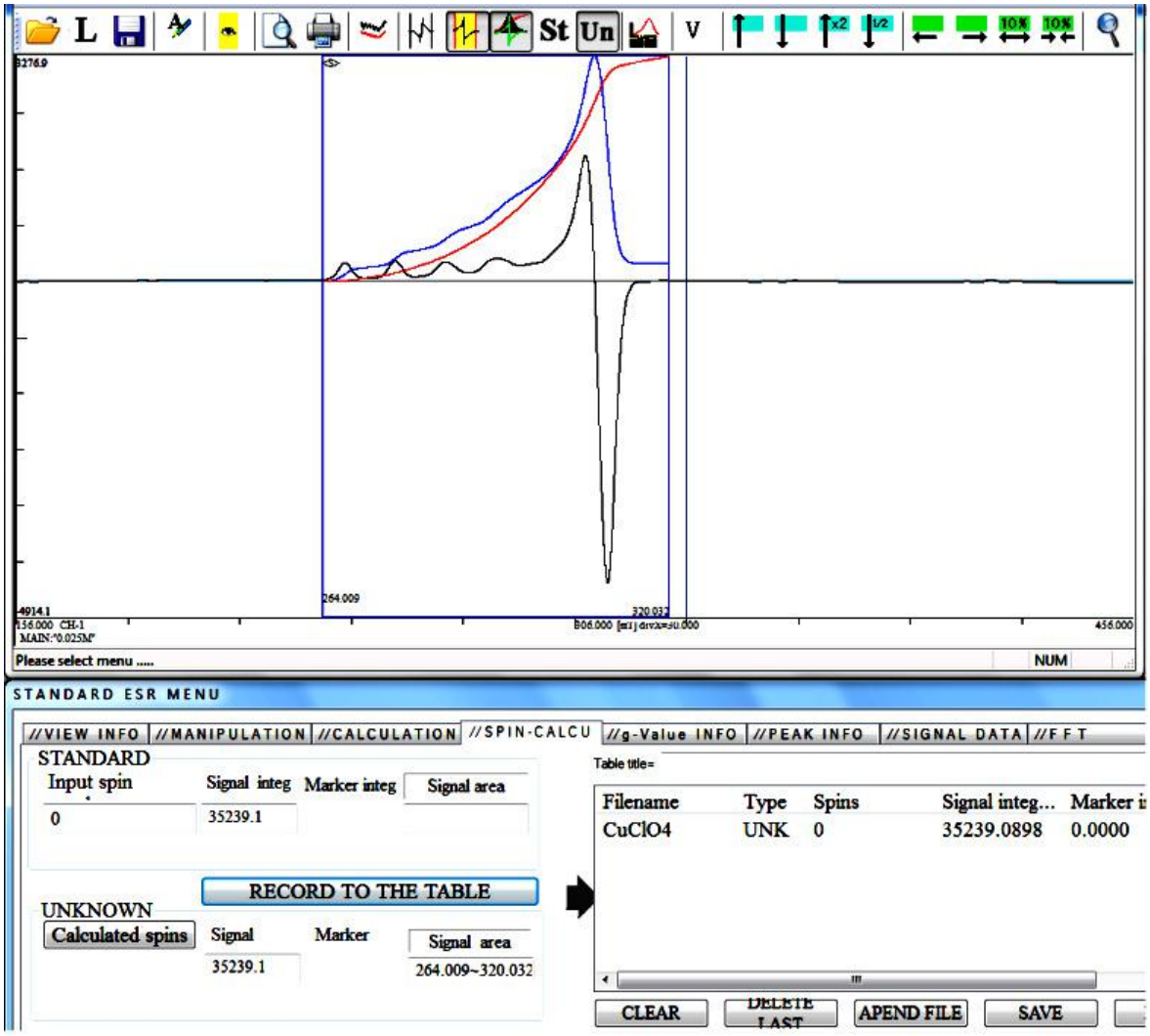

Figure A3.15. Double integration of standard $Cu(ClO_4)_2 \cdot 6H_2O$ (concentration, 0.3 mmol) solution in methanol at 77K.

Appendix IV

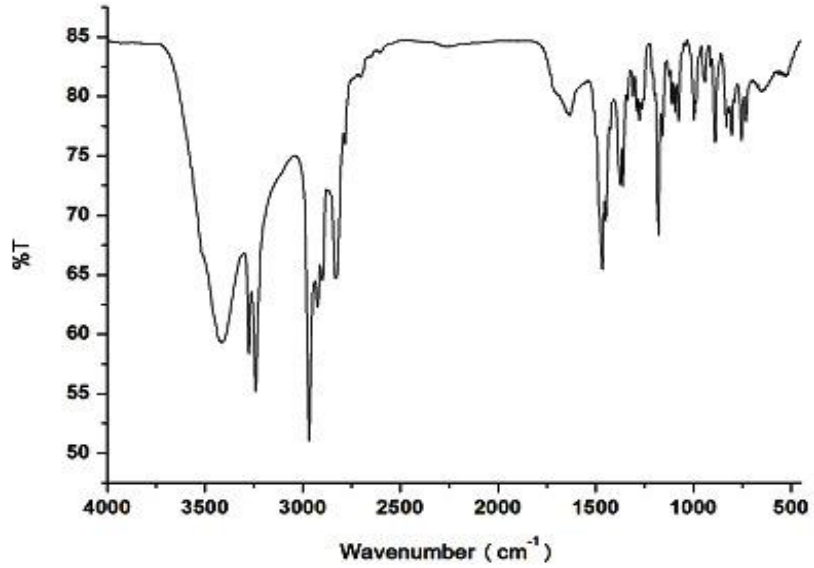

Figure A4.1. FT-IR spectrum of ligand **L4** in KBr.

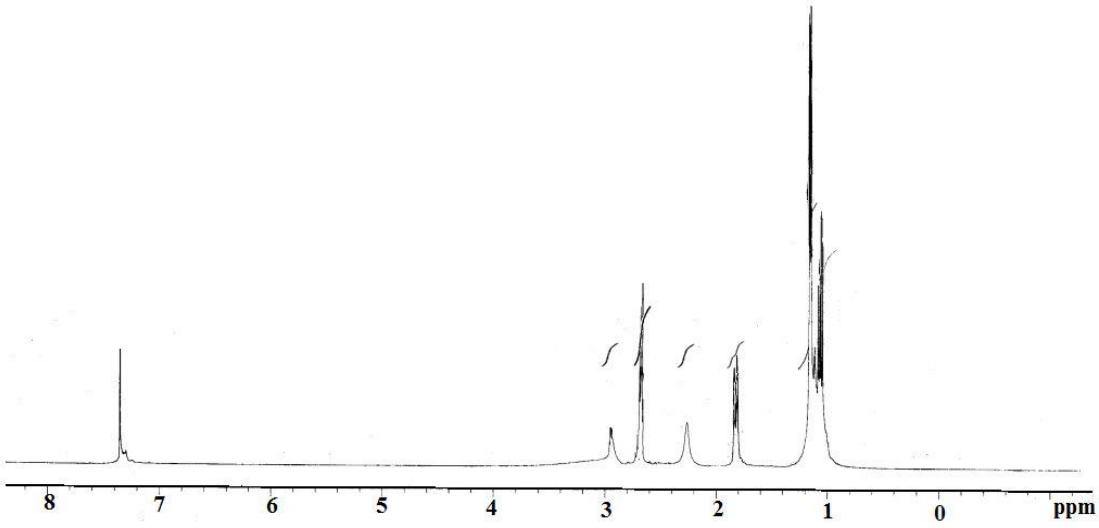

Figure A4.2. ^{1}H-NMR spectrum of ligand **L4** in $CDCl_3$.

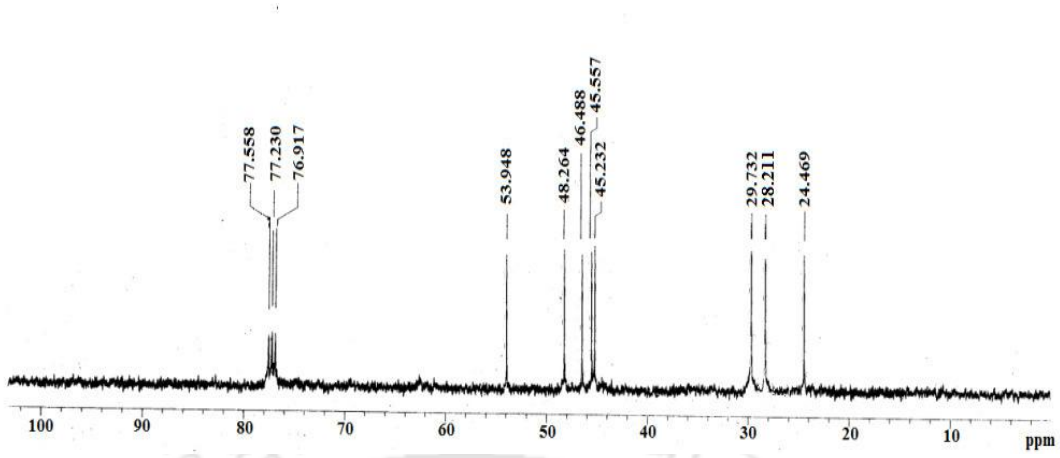

Figure A4.3. ^{13}C-NMR spectrum of ligand **L4** in $CDCl_3$.

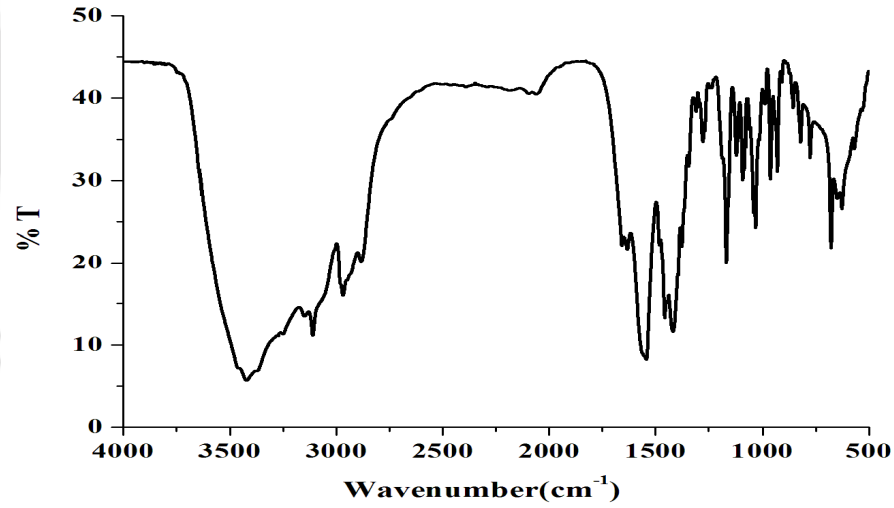

Figure A4.4. FT-IR spectrum of complex **5.1** in KBr.

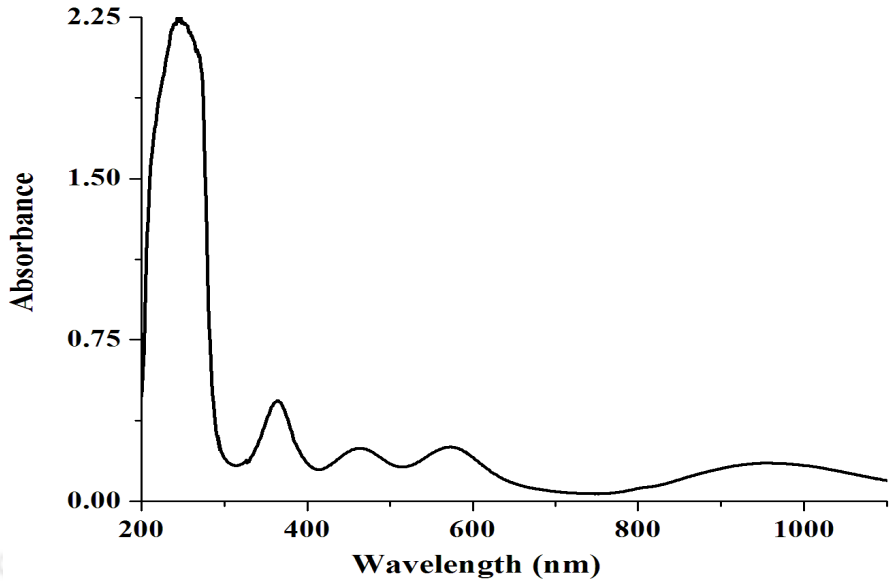

Figure A4.5. UV-visible spectrum of complex **5.1** in methanol at room temperature.

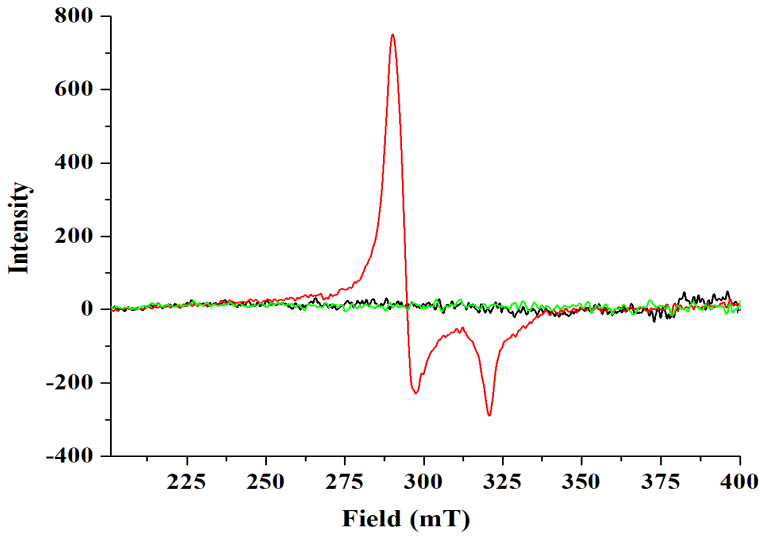

Figure A4.6. X-band EPR of complex **5.1** (black line), after purging of equivalent amount of NO_2 (red line) and further addition of equivalent of NO_2 (green line) in methanol at 77 K.

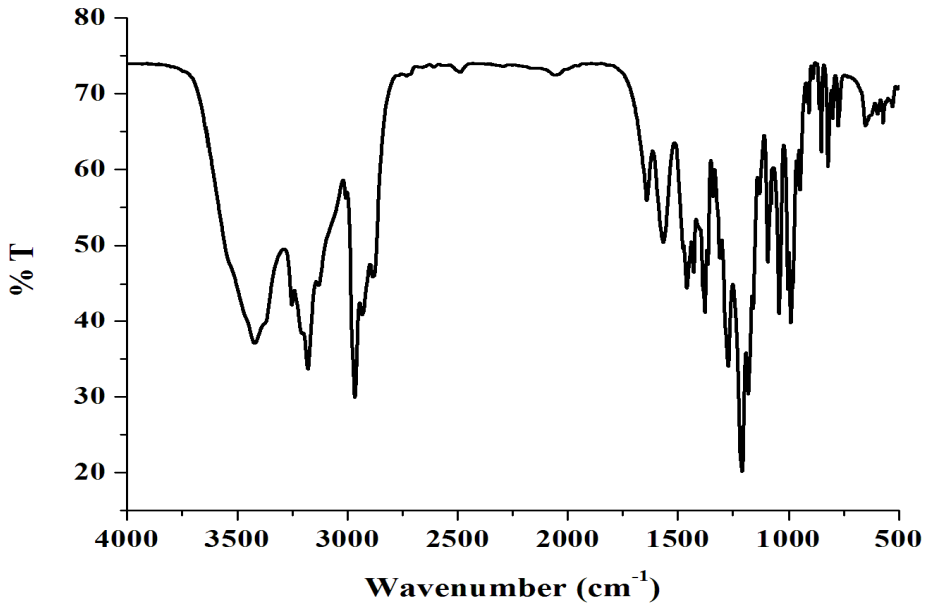

Figure A4.7. FT-IR spectrum of complex **5.2** in KBr.

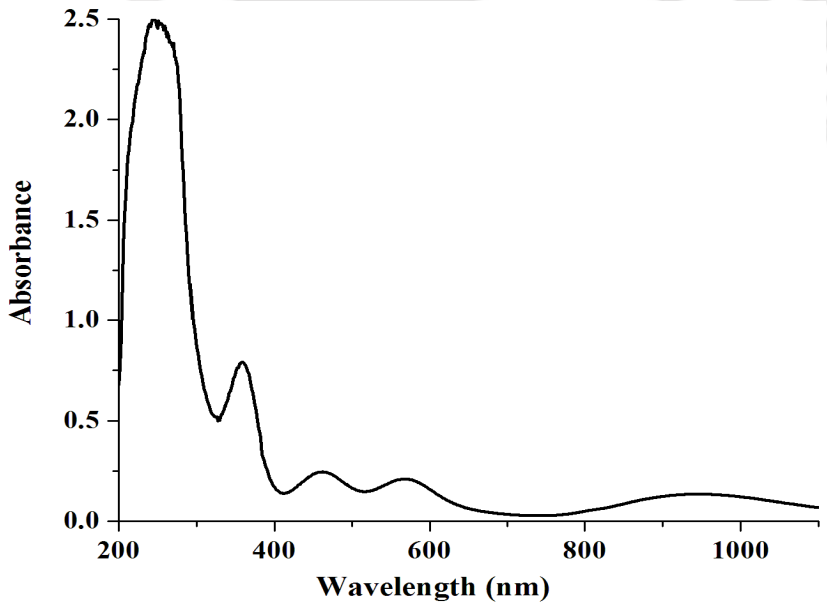

Figure A4.8. UV-visible spectrum of complex **5.2** in methanol at room temperature.

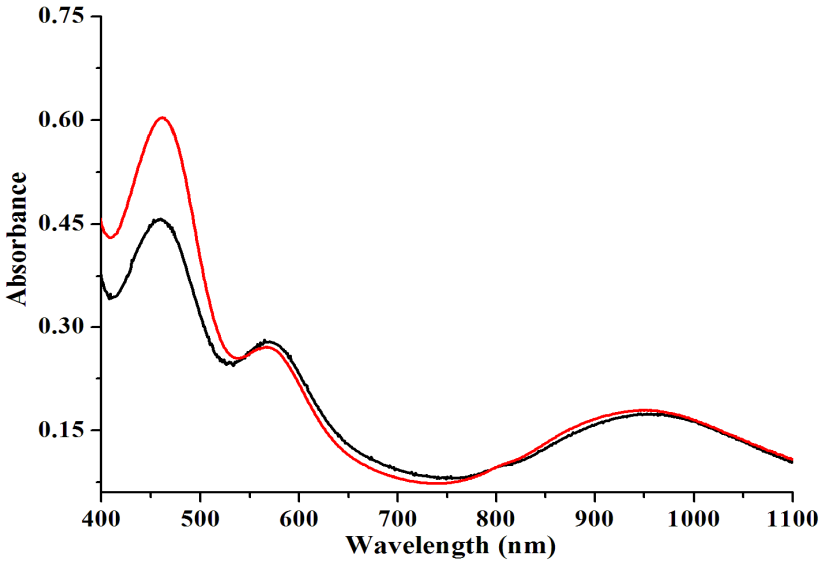

Figure A4.9. UV-visible spectrum of complex **5.2** (black), after purging NO_2 in complex **5.2** (red) in methanol at room temperature.

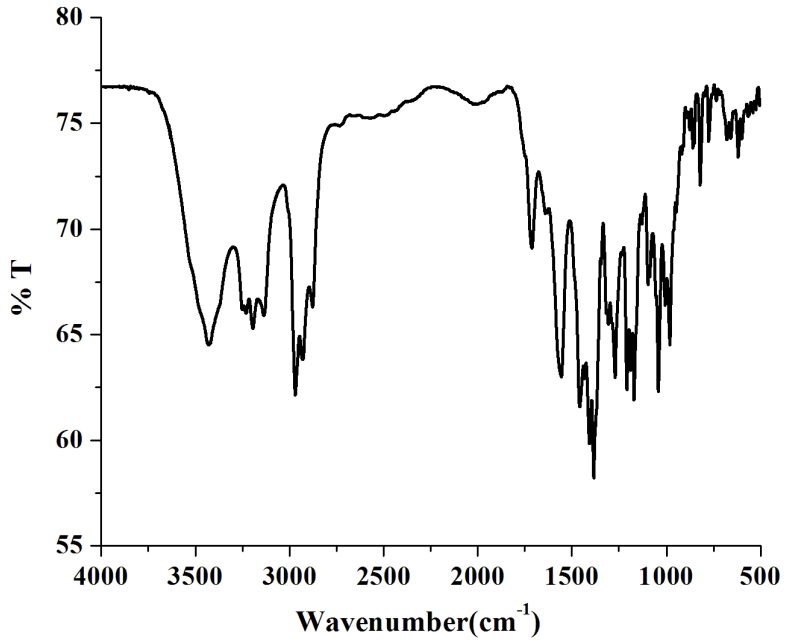

Figure A4.10. FT-IR spectrum of complex **5.3** in KBr.

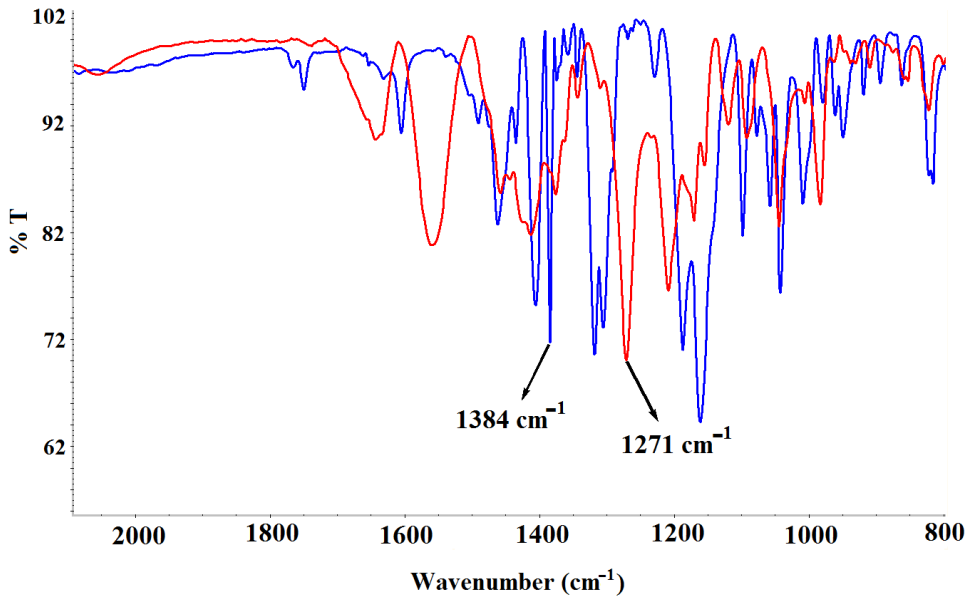

Figure A4.11. Comparison FT-IR spectra of complex **5.2** (red) and complex **5.3** (blue) in KBr.

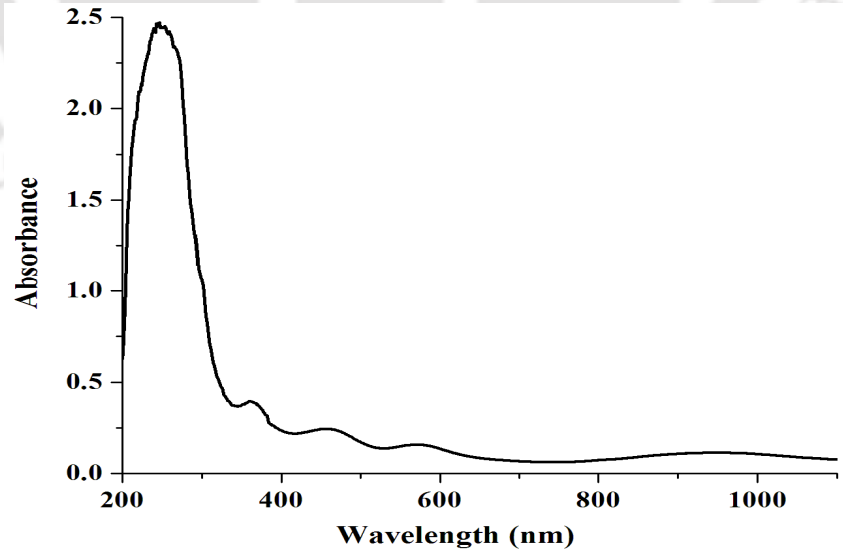

Figure A4.12. UV-visible spectrum of complex **5.3** in methanol at room temperature.

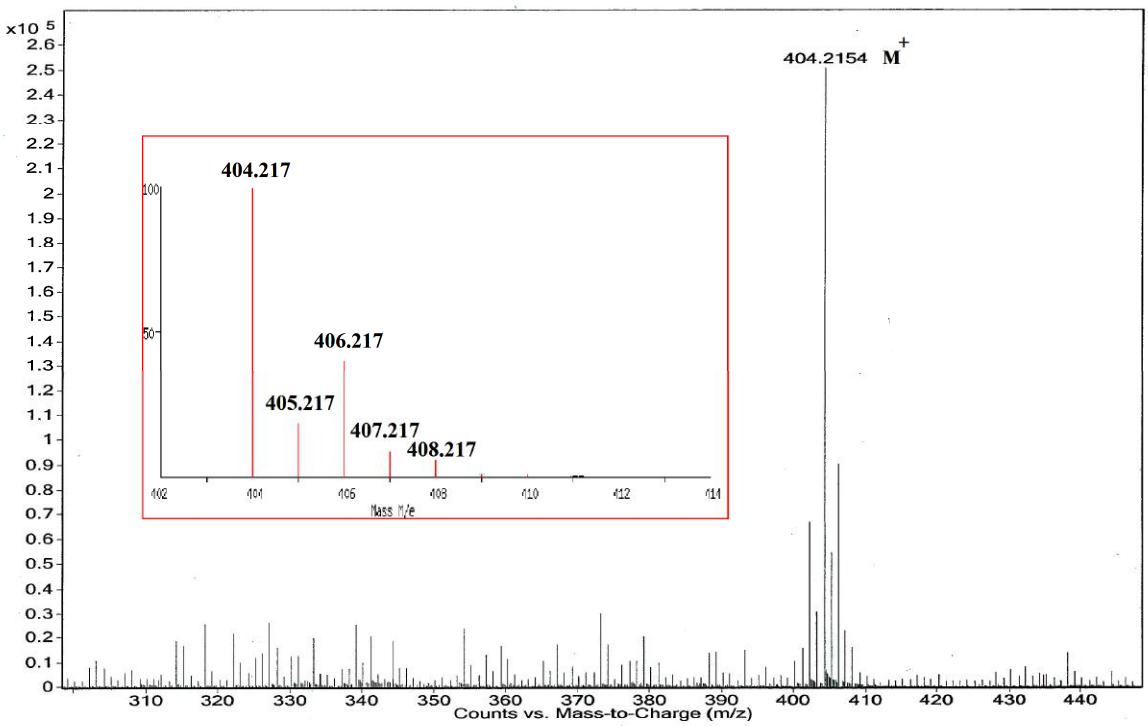

Figure A4.13. ESI- mass spectrum of complex **5.3** with isotopic distribution in methanol (Inset shows the simulated spectra).

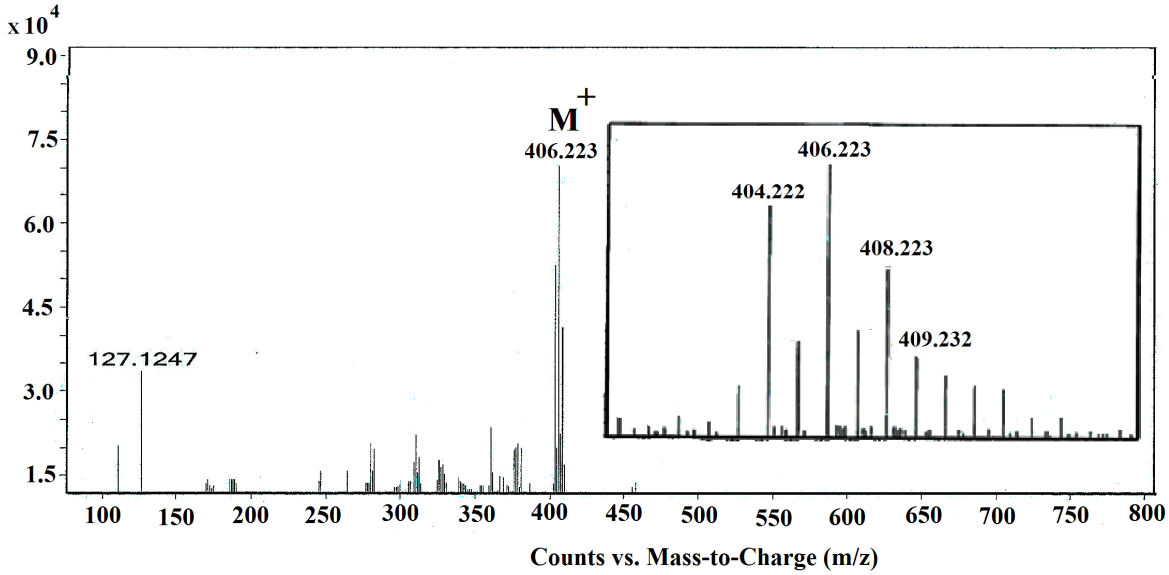

Figure A4.14. ESI- mass spectrum of complex **5.3** with isotopic distribution ($^{18}ONO_2$ as anion) in methanol.

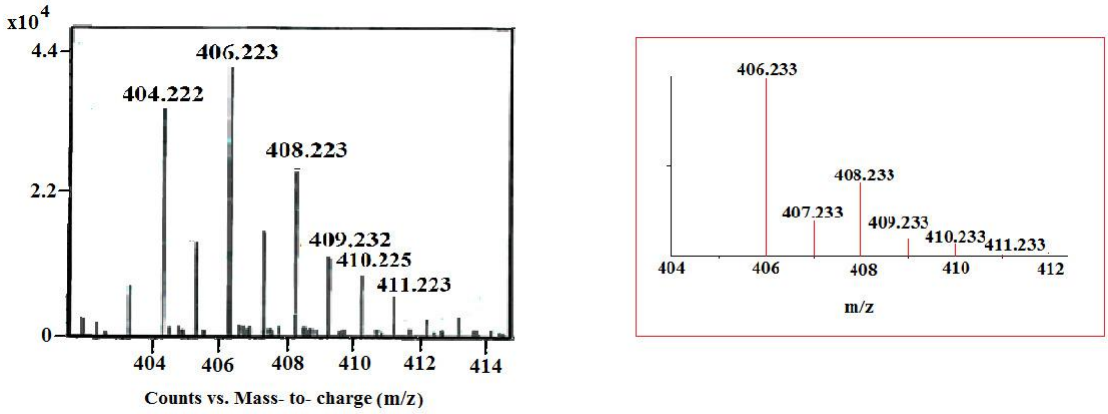

(a) (b)

Figure A4.15. ESI-mass spectrum of complex **5.3** with $^{18}ONO_2$ as anion (a) experimental and (b) simulated in methanol.

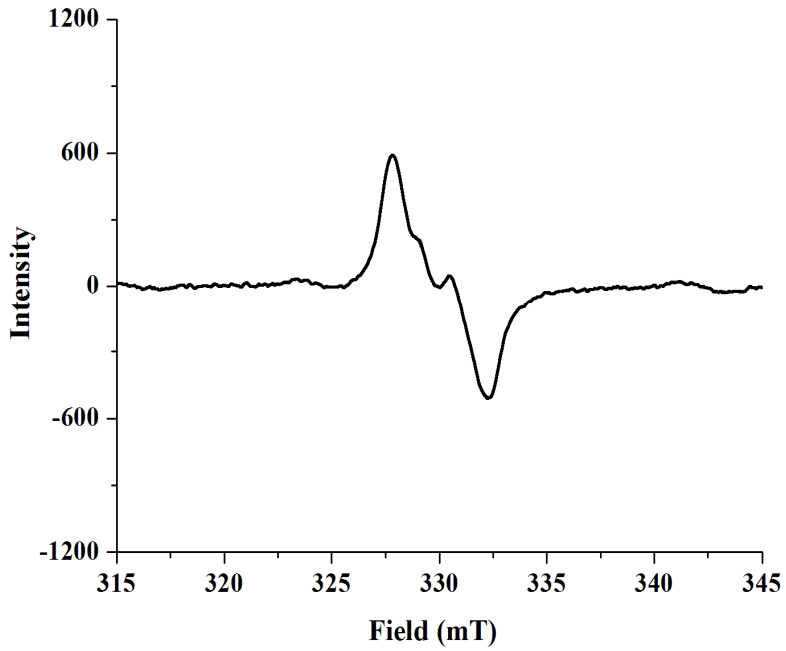

Figure A4.16. X-band EPR spectrum of $[(DTC)_2Fe^{II}]$ after reaction with NO in acetonitrile at room temperature.

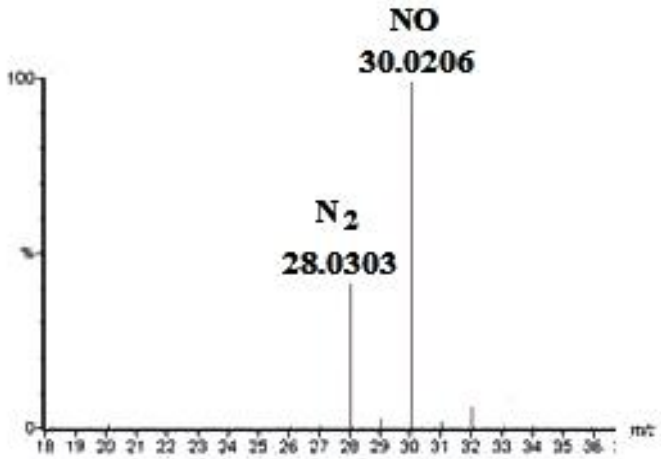

Figure A4.17. GC-mass spectrum of the head space gas from the reaction of complex **5.2** with NO_2 in acetonitrile.

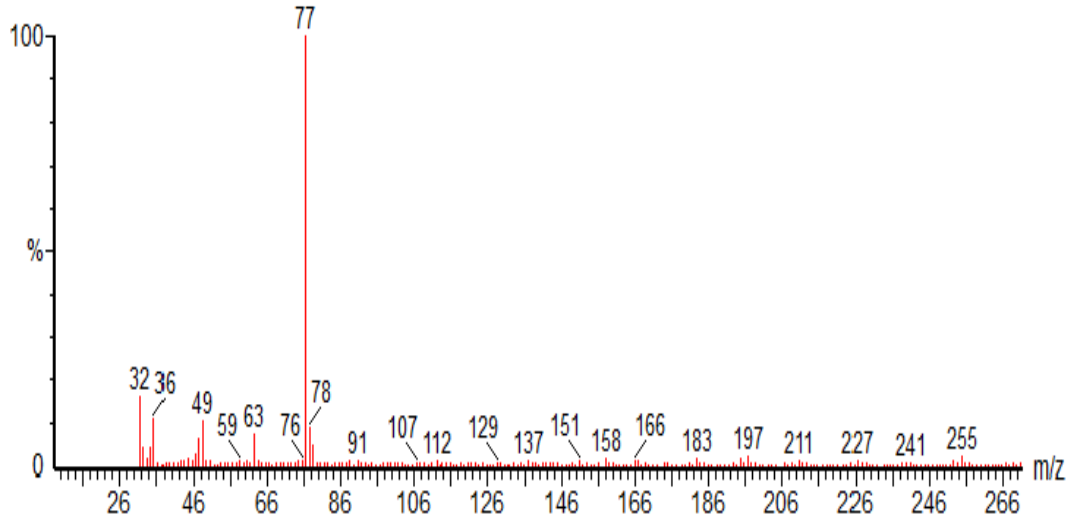

Figure A4.18. GC-mass spectrum of CH_3ONO_2 obtained by injecting the reaction mixture of complex **5.1** after purging one equivalent of NO_2.

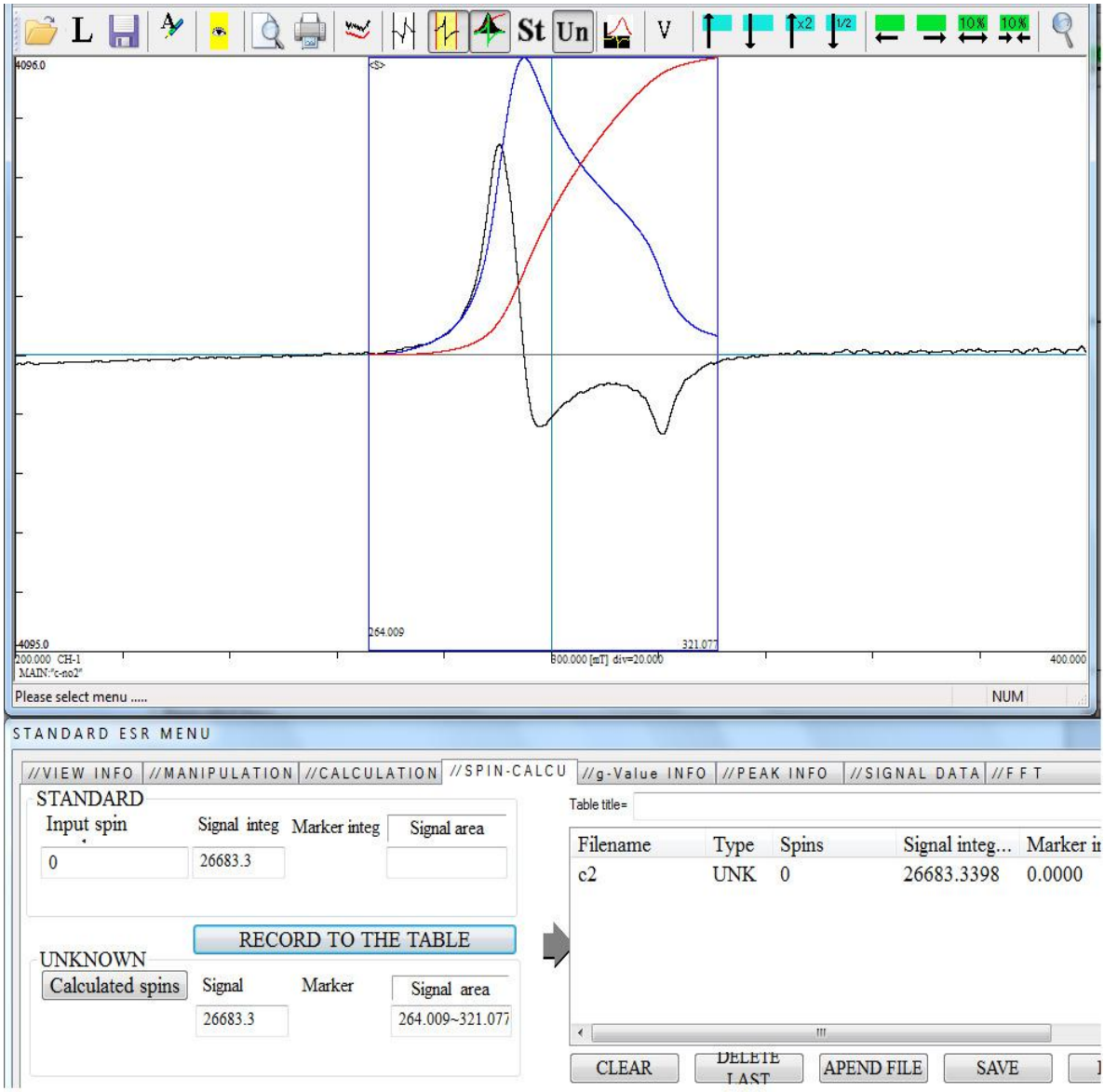

Figure A4.19. Double integration of EPR spectrum of Ni(I) species obtained from complex **5.1** (concentration, 0.3 mmol) in methanol at 77K.

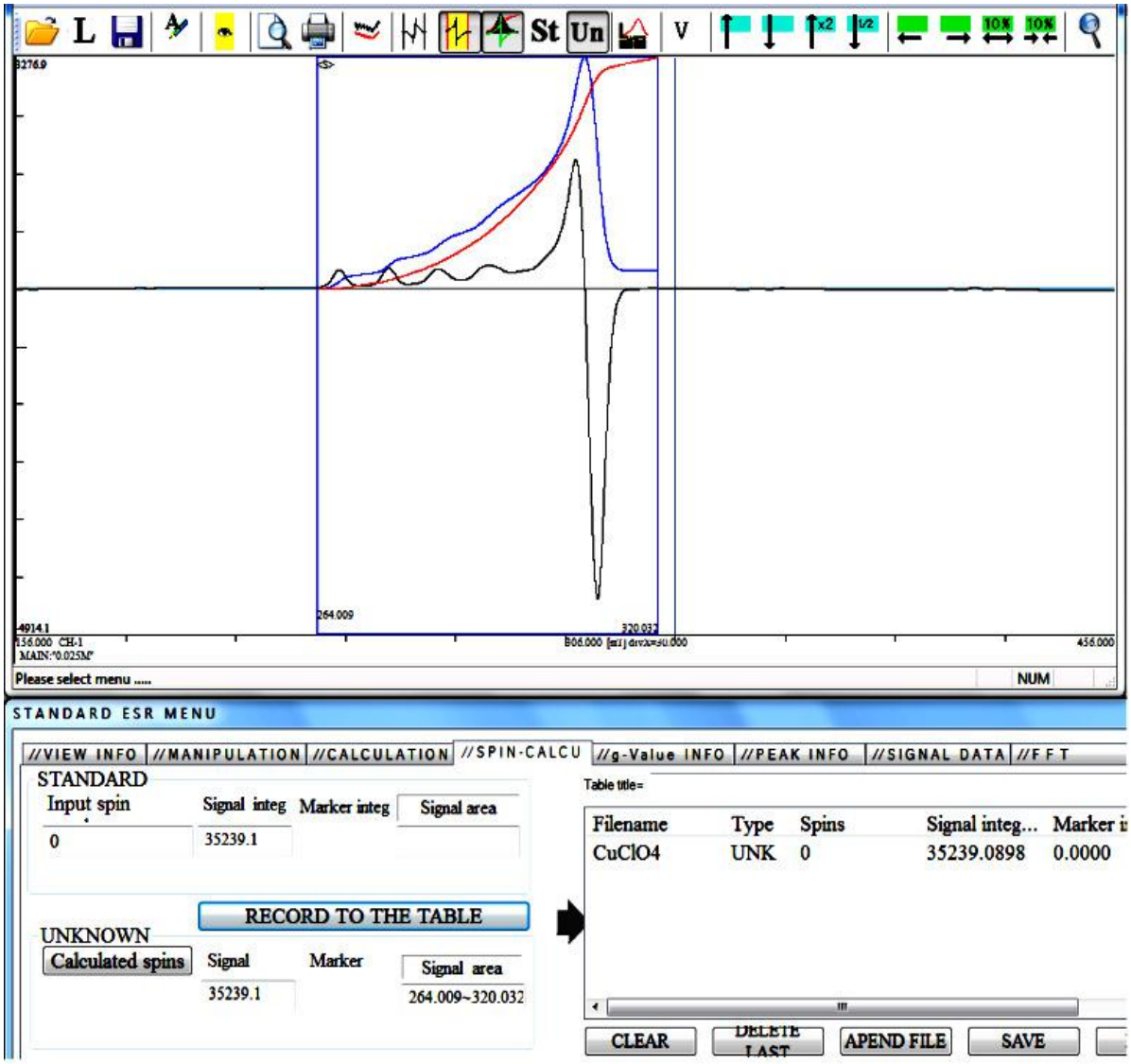

Figure A4.20. Double integration of standard $Cu(ClO_4)_2 \cdot 6H_2O$ (concentration, 0.3 mmol) solution in methanol at 77K.

List of Publications

(1) "Nitric oxide reactivity of a manganese(II) complex leading to nitrosylation of the ligand" Kalita, A.; **Ghosh, S**.; Mondal, B. *Inorg. Chem. Acta*. **2015**, *429*, 183.

(2) "Copper(II) mediated phenol ring nitration by nitrogen dioxide" Kumar, V.; **Ghosh, S.**; Saini, A. K.; Mobin, S. M.; Mondal, B. *Dalton Trans*, **2015**, 2015,**44**, 19909.

(3) "Reductive nitrosylation of nickel(II) complex by nitric oxide followed by nitrous oxide release" **Ghosh, S**.; Deka, H.; Dangat, Y. B.; Saha, S.; Gogoi, K.; Vanka, K.; Mondal, B. *Dalton Trans.* **2016,** *45*, 10200.

(4) "Effect of ligand denticity on the nitric oxide reactivity of cobalt(II) complexes" Deka, H.; **Ghosh, S**.; Saha, S.; Gogoi, K.; Mondal, B. *Dalton Trans.* **2016,** *45*, 10979.

(5) "Nitric oxide reactivity of a Cu(II) complex of an imidazole based ligand: Aromatic C-nitrosation followed by the formation of N-nitrosohydroxylaminato complex" Deka, H.; **Ghosh, S**.; Gogoi, K.; Saha, S.; Mondal, B. *Inorg. Chem.* **2017**, *56*, 5034.

(6) **"**Nitric oxide reactivity of Co(II) complexes: Formation of $\{CoNO\}^8$ and their reactivity" **Ghosh, S**.; Deka, H.; Saha, S.; Gogoi, K.; Mondal, B. (Communicated)

(7) "Nitrogen dioxide reactivity of a Ni(II) complex: Oxo transfer reaction from NO_2 to NO_2^-" **Ghosh, S**.; Deka, H.; Saha, S.; Gogoi, K.; Mondal, B. (Communicated)